HIGH FREQUENCY ABSORPTIONS, DOUBLE RELAXATION TIMES, DIPOLE MOMENTS AND MOLECULAR STRUCTURES OF SOME NONSPHERICAL POLAR AND ISOTOPOMER MOLECULES

THESIS SUBMITTED FOR THE DEGREE OF
DOCTOR OF PHILOSOPHY(SCIENCE)
OF THE
UNIVERSITY OF NORTH BENGAL, 1997

BY
SWAPAN KUMAR SIT; M.Sc.

Dedicated to my parents to whom I am indebted for what I am

ACKNOWLEDGEMENT

The works presented in the thesis entitled **"High frequency absorptions, double relaxation times, dipole moments and molecular structures of some nonspherical polar and isotopomer molecules"** have been carried out under the kind guidance and active supervision of Dr. S. Acharyya; M.Sc, D Phil (Cal), Reader, Department of Physics, Raiganj College (University College), Raiganj-733134. I am highly grateful to him for his untiring effort to make it a success.

I convey my thanks to Sri R. C. Basak . M. Sc; N. Ghosh M.Sc, B.Ed and G Dasgupta M.Sc. B.Ed; for their helpful cooperations. The author is indebted to Sri A. R. Sit; BE (Electrical) for providing the computer facilities for some calculations. The author is grateful to Dr. S. Roy, Reader of the Department of Spectroscopy, IACS, Calcutta -32 for his kind permission to perform experimental works in his laboratory. It is a pleasure on the part of the author to remember the help of Dr. S. Sahoo, Dr. (Mrs.) A. Ganguly, Dr. A. Das and Dr. K. Chatterjee of I.A.C.S, Calcutta-32 and Sri A. Chatterjee, B.Sc (Tech) in different times of this work. Finally, the author expresses his gratitude to all his family members including Mrs. Tapati Sit (wife) for their constant encouragements during the progress of the works.

Date 31.7.97.

Swapan Kumar Sit

(Swapan Kumar Sit)
Lecturer in Physics,
Raiganj Polytechnic,
Raiganj,
Dist: Uttar Dinajpur,
(WB) 733134

CONTENTS

Part A

PREFACE

Dielectric material plays an important role for its wide application in electronics and electrical technology. Scientists and research workers are mainly interested, on the other hand, in understanding the structure, shape and size of the dielectric molecules. In order to reveal the different aspects of dielectric materials the essential parameter like dipole moments, quadrupole moments, molecular polarisabilities, local fields etc. are needed to be determined. The present thesis is intended to throw much light on the structure, shape, size of a large number of nonspherical dielectric polar molecules dissolved in nonpolar solvents like C_6H_6, CCl_4, dioxane and n-heptane under high frequency electric field.

The other part of the thesis is concerned with the quantum mechanical approach to derive a formula of dipole moment of some isotopomer molecules like HD^+,HT^+ etc. The molecules are interesting because the phenomenon of photodissociation occursdue to the interaction of such molecules with photons. Photodissociation is an important photon induced process. It is of great significance in the study of photochemical reactions, in modelling the ionised atmosphere and among others in determining the vibrational population of the molecular ions.

Under the action of the electric field the centre of gravity of positive and negative charges of a molecule is little displaced producing what is known as distortion polarisation. Due to existence of several polarisability factors the predicted dipole moment does not yield better result either in the static or in low frequency electric field. This difficulty was, however, removed altogether when the static electric field is replaced by an alternating electric field of frequency in the order of $10^6 \sim 10^9$Hz. As a result all the polarisability factors other than orientational polarisation are thus eliminated.

On account of inertial effect of polarisation the molecule does not rotate immediately with the rapid reversal of the electric field, but undergoes a delay or lag in response for a certain time. When the external field is removed all types of polarisation decay exponentially with time. The time in which the polarisation is reduced to 1/e times its original value is called the relaxation time and is usually denoted by τ. The polar mol-

ecules in nonpolar solvents usually absorb energy much more strongly in the high frequency electric field of 10 GHz. Analysing the high frequency absorption relaxation data for radio and microwave regions one can easily get the relaxation time with the help of available Debye and Smyth model. This relaxation time τ is due to the molecular rotation as a whole. There is also a probability of rotation of a part of the molecule under the hf electric field. So the possible existence of multiple relaxation phenomena was proposed by Budo (1938). Bergmann et al (1960), however, considered that the polar molecules are supposed to possess two relaxation times τ_2 and τ_1, one due to whole molecular rotation (τ_2) and other, due to rotation of a part of the molecule called intramolecular relaxation time (τ_1). They used Cole - Cole (1941) plot to arrive at the desired value. Bhattacharyya et al (1970), subsequently simplified the above procedure to get two relaxation times τ_2 and τ_1 of a pure polar solute from the dielectric relaxation parameters measured at least at two different frequencies of the applied electric field. We, under such context, have been able to predict double relaxation phenomena of polar solutes in a nonpolar solvent from the values of the dielectric relaxation parameters measured under a single frequency electric field. In the Part A of the present thesis several chapters deal with the existence of double or mono-relaxation times.

Chapter III is concerned with nonspherical polar molecules like disubstituted benzenes and anilines in nonpolar solvents like C_6H_6 or CCl_4 under 9.945 GHz electric field.

Chapter IV deals with the prediction of double or single relaxation time at 22.06, 3.86 and 2.02 GHz electric field for three isomers of anisidines and toluidines.

In chapter V an attempt has been made to show that isomers of anisidines and toluidines show two relaxation times at 9.945 GHz electric field which seems to be the most effective dispersive region for such polar molecules.

In chapters VI and VII the long chain alcohols are studied at 24.33, 9.25 and 3.00 GHz electric fields only to show the fact that they always show double relaxation times at each frequency of electric field.

In chapter VIII binary aprotic polar mixtures like N, N-dimethyl formamide and dimethyl sulphoxide (DMF + DMSO) as well as single aprotic liquid DMSO and N,N

diethyl formamide (DEF) in C_6H_6 and CCl_4 are studied at 3 cm. wavelength electric field to show the different associational aspects in them.

Chapter IX deals with the experimental works performed at IACS Laboratory to show the possible occurrence of double relaxation times for the aprotic liquids like dimethyl sulphoxide (DMSO), N, N-dimethyl acetamide (DMA), N,N-dimethyl formamide (DMF), N, N-diethyl formamide (DEF), N-methyl acetamide (NMA) etc. dissolved in C_6H_6 at different temperatures. To know the actual fact measurements on ε'_{ij}, ε''_{ij}, ε_{oij} and $\varepsilon_{\infty ij}$ of them were accurately performed.

Part B of the, thesis is presented in one chapter X. It consists of estimation of dipole moments of HD^+, HT^+ etc. molecules from quantum mechanical point of view using Morse potential.

Thus the first part of the thesis beautifully explains the double relaxation phenomenon of nonspherical polar molecules in nonpolar solvents under hf electric field, in a very simple and straightforward way for the first time. It, therefore, minimizes the experimental hazards in determining dielectric relaxation parameters at more than one frequency of the electric field. From this point of view the proposed method is thought to be superior one in comparison to other existing methods.

The part B of the thesis being the last part is included in chapter X. It appears to reveal that isotopomer molecules like HD^+, HT^+ etc. are expected to obey Morse potential (1929) to yield the dipole moment μ as estimated by Saha (1974) indicating the fact that the molecules obey Morse potential.

A conclusive part is also added in the last Chapter XI of the thesis only to get a brief summary of the entire works presented in the thesis.

REFERENCES

1. A Budo; Phys. Z. **39** 706 (1938)
2. K Bergmann, D M Roberti and C P Smyth; J. Phys.Chem. **64** 665 (1960)
3. K S Cole and R H Cole; J. Chem.Phys **9** 341 (1941)
4. J Bhattacharyya, A Hasan, S B Roy and G S Kastha, J.Phys.Soc. Japan **28**, 204 (1970)
5. P Morse; Phys. Rev.**34** 57 (1929)
6. S Saha; Indian J Phys. **48** 849 (1974).

CHAPTER 1

GENERAL INTRODUCTION AND BRIEF REVIEW OF THE PREVIOUS WORKS

1.1. Polarisation and Clausius Mossotti Relation

Dielectric materials are usually divided into two classes called nonpolar and polar dielectrics. The molecules having coincident and noncoincident centres of positive and negative charges are called nonpolar and polar dielectrics respectively.

When a nonpolar molecule is placed between two charged plates the centre of gravity of positive and negative charges get displaced in order to form an electric dipole. The phenomenon of producing induced dipole moment in nonpolar molecules is known as distortion polarisation. The distortion polarisation are of three types such as electronic, atomic and interfacial polarisation. Electronic polarisation arises due to the shift of centre of gravity of electron and nuclear particles. The displacement of the atoms or ions within the molecules causes change in interatomic or ionic distances which is known as atomic or ionic polarisation. Interfacial polarisation comes into play due to inhomogeneous constituents of materials which vary from layer to layer. All the above three polarisations are induced polarisation. Besides these, due to existence of dipolar nature of molecule which arises due to asymmetry of the molecules as in the case of polar molecules, the permanent polarisation is also present.

Therefore, total polarisation

$$P_t = P_i + P_p \qquad \text{.....(1.1)}$$

where P_i = induced polarisation and P_p = Permanent polarisation.

If $\vec{p}$ be the induced dipole moment on each dielectric molecule due to the external electric field $\vec{E}$ which in its turn is modified called $\vec{E}_{loc}$, the local field or internal electric field within the dielectric.

Let $\vec{p} \propto \vec{E}_{loc}$ for a homogeneous or isotropic dielectric.

or, $$\vec{p} = \alpha \vec{E}_{loc} \qquad \text{.....(1.2)}$$

where α is the proportionality constant called molecular polarisability. Now, in order to calculate $\vec{E}_{loc}$ we assume that

$$\vec{E}_{loc} = \vec{F}_1 + \vec{F}_2 + \vec{F}_3 \qquad \text{.....(1.3)}$$

where $\vec{F}_1$ is the uniform electric field intensity at a point due to distribution of charges between condenser plates and $\vec{F}_1 = 4\pi\sigma$, σ being charge density on the plates. $\vec{F}_2$ is the electric field intensity produced due to polarisation of atoms or molecules as well as distortion of electrical lines of force.

Thus $\vec{F}_2 = \vec{F}_2' + \vec{F}_2''$ .....(1.4)

$$= -4\pi \vec{P} + \frac{4}{3}\pi \vec{P}$$

where $\vec{P}$ is the charge exerted at any point outside the sphere placed at the centre of the molecule under consideration.

Now, $\vec{E}_{loc} = \vec{F}_1 + \vec{F}_2' + \vec{F}_2'' + \vec{F}_3$

$$= 4\pi\sigma + (-4\pi \vec{P}) + \frac{4}{3}\pi \vec{P} + \vec{F}_3 \qquad \text{.....(1.5)}$$

For homogeneous dielectric as well as for cubic crystal solids, $\vec{F}_3 = 0$

So, $\vec{E}_{loc} = 4\pi\sigma - 4\pi \vec{P} + \frac{4}{3}\pi \vec{P}$

$$= \vec{D} - 4\pi \vec{P} + \frac{4}{3}\pi \vec{P}$$

$$= \vec{E} + \frac{4}{3}\pi \vec{P} \qquad \text{.....(1.6)}$$

Now, the dielectric displacement vector $\vec{D}$ is $\vec{D} = \varepsilon \vec{E}$ where ε = dielectric constant of the dielectric material.

So eq (1.2) can be written as

$$\vec{p} = \alpha \vec{E}_{loc} = \alpha\left(\vec{E} + \frac{4}{3}\pi \vec{P}\right)$$

or, $\vec{P} = n\vec{p} = n\alpha\left(\vec{E} + \frac{4}{3}\pi \vec{P}\right)$ .....(1.7)

where n = number of molecules per unit volume. $\vec{P}$ = dipole moment per unit volume = polarisation vector.

Again, $\vec{D} = \vec{E} + 4\pi \vec{P}$ and $\vec{D} = \varepsilon \vec{E}$

or, $$\vec{P} = \frac{(\varepsilon - 1)\vec{E}}{4\pi} \qquad \text{.....(1.8)}$$

From eqs. (1.7) and (1.8) one can have.

$$\frac{(\varepsilon - 1)}{(\varepsilon + 2)} \frac{M}{\rho} = \frac{4}{3} \pi N \alpha \qquad \text{.....(1.9)}$$

Where M is the molecular weight, ρ is the density of the dielectric material and N= Avogadro's number respectively. The relation (1.9) is known as Clausius-Mossotti relation.

1.2. Debye Equation

When a polar dielectric is placed in an uniform electric field the permanent electric moment $\vec{\mu}$ associated with each polar molecule tends to orient along external field direction $\vec{E}$. The average dipole moment of each molecule be $\bar{m}$ shown to be $\frac{\mu^2 E}{3kT}$

Since $\frac{\bar{m}}{E} = \alpha_o$ = orientational polarisability = $\frac{\mu^2}{3kT}$

Thus the total polarisability $\alpha_T = \alpha_d + \alpha_o \qquad = \alpha + \frac{\mu^2}{3kT}$

Equation (1.9) becomes

$$\frac{\varepsilon - 1}{\varepsilon + 2} \frac{M}{\rho} = \frac{4}{3} \pi N \left(\alpha + \frac{\mu^2}{3kT}\right) \qquad \text{.....(1.10)}$$

Equation (1.10) is known as Debye [1)] equation for polar dielectric when it is placed in an uniform electric field.

1.3. Onsager's Theory under Static Electric Field

Onsager [2] considered the polar liquid as a polarisable point dipole at the centre of a spherical cavity of molecular dimensions surrounded by an unpolarised medium. The field within the cavity consists of the cavity field $\vec{G}$, arising due to external charges. The cavity field $\vec{R}$ arises due to polarisation of the environment medium by the field of dipoles. The two fields are given by :

$$\vec{G} = \frac{3\varepsilon_0}{2\varepsilon_0 + 1}\vec{E} \qquad \text{..... (1.11)}$$

$$\text{and } \vec{R} = \frac{2(\varepsilon_0 - 1)}{(2\varepsilon_0 + 1)a^3}\vec{\mu} \qquad \text{.....(1.12)}$$

Where 'a' is the radius of the spherical cavity, ε_0 is the static dielectric constant of the surrounding medium, $\vec{\mu}$ is the dipole moment in the cavity under the uniform macroscopic field $\vec{E}$ outside the cavity. Thus the total field acting upon a spherical polar molecule in a polarised dielectric medium is given by:

$$\vec{F} = \vec{G} + \vec{R} = \frac{3\varepsilon_0}{2\varepsilon_0 + 1}\vec{E} + \frac{2(\varepsilon_0 - 1)}{(2\varepsilon_0 + 1)a^3}\vec{\mu} \qquad \text{.....(1.13)}$$

Onsager [2] equation for static dielectric constant in case of polar liquids is thus obtained in the following form:

$$\frac{\varepsilon_0 - 1}{\varepsilon_0 + 2} - \frac{\varepsilon_\infty - 1}{\varepsilon_\infty + 2} = \frac{\rho}{M}\left[\frac{3\varepsilon_0(\varepsilon_\infty + 2)}{(2\varepsilon_0 + \varepsilon_\infty)(\varepsilon_0 + 2)}\right]\frac{4\pi N\mu^2}{9kT} \qquad \text{..... (1.14)}$$

This equation becomes Debye equation when the factor. $\left[\frac{3\varepsilon_0(\varepsilon_\infty + 2)}{(2\varepsilon_0 + \varepsilon_\infty)(\varepsilon_0 + 2)}\right]$ approaches to unity as ε_0 tends to ε_∞ for infinitely dilute polar solute in a nonpolar solvent.

The approximate validity of Onsager's equation is found in case of large number of unassociated liquids, but the experimental results deviate largely from the theoretical ones

for associated liquids like water, alcohol and liquid ammonia. The discrepancies may be because of the following reasons:

a) In associated liquids short range forces arise due to ordered array of neighbouring molecules which play an important role.

b) Molecules should be spherical in form.

c) The environment of the molecule is treated as homogeneous continum and the local saturation effects are neglected

1.4. Kirkwood's Theory

The efffect of the short range forces was first considered by Kirkwood [3]. By taking into accounts the sum of the molecular dipole moment and the moment induced as a result of the hindered rotation in the spherical region surrounding the molecules, Kirkwood has derived following relation:

$$\frac{\varepsilon_0 - 1}{\varepsilon_0 + 2} - \frac{\varepsilon_\infty - 1}{\varepsilon_\infty + 2} = \frac{\rho}{M}\left[\frac{3\,\varepsilon_0\,(\varepsilon_\infty + 2)}{(2\,\varepsilon_0 + \varepsilon_\infty)\,(\varepsilon_0 + 2)}\right]\frac{4\,\pi\,N\mu^2\,g}{9\,k\,T} \qquad \text{.....(1.15)}$$

Where g is a correlation parameter which characterises the intermolecular interaction and short range forces. Kirkwood has pointed out that the departure of g from unity is a measure of hindered relative molecular rotation arising from short range intermolecular forces. Thus the unassociated liquids show the value of g approximately unity, while for associated liquids g's are sufficiently apart from unity. Moreover, like Onsager's equation the Kirkwood's equation also contains the approximation involved in treating the polar molecules as spherical.

1.5. Fröhlich's Theory

Kirkwood Theory has been modified by Fröhlich[4] by considering a dipolar dielectric with a number of polarizable units of the same kind within a large spherical region. Each unit has various dipole moment $\vec{\mu}$ in different directions due to thermal fluctuation with a certain probability. The average moment $\vec{\mu}^*$ due to such unit within

the spherical region is different from $\vec{\mu}$ because of the short range interactions between the polarizable units and the deviation of the shape of the molecules from a sphere. An equation for low intensity field has been derived on above line as:

$$\varepsilon_0 - 1 = \frac{3\varepsilon_0}{2\varepsilon_0 + 1} \frac{4\pi N_0}{3} \frac{\vec{\mu}\,\vec{\mu}^*}{kT} \qquad \text{..... (1.16)}$$

where No = number of units per unit volume. The difficulties in Fröhlich's theory are associated with the evaluation of energy of the interaction of the sample with the surrounding medium.

However, as indicated above there are experimental limitations in determining the required parameters involved in various theories lead to Onsager's equation for unassociated liquids when short range forces are absent. So one can safely use Onsager's equation for analysing the experimental data to determine the dipole moment of a polar liquid.

1.6. The Dielectric Behaviour at High Frequencies

In the case of static or low frequency electric field the dielectric is in equilibrium with the applied electric field. When the frequency of the applied electric field exceeds a certain critical value, the permanent electric dipole can not follow the exact alternations of the electric field without measurable lag. The critical value of frequency depends on the chemical compositions, the structure of the dielectrics and on the temperature. In most of the cases this critical value is higher than 3×10^6 Sec^{-1}. This lag is commonly referred to relaxation which is defined as the lag in the response of a system to change in the forces to which it is subjected.

The polarisation acquires a components out of phase with the field and the displacement current acquires a conductance component in phase with the field resulting in thermal dissipation of energy.

In such cases it is usual to relate the displacement vector $\vec{D}$ and the electric field vector $\vec{E}$ by a complex dielectric constant as:

$$\varepsilon^* = \varepsilon' - j\varepsilon'' \qquad \text{.....(1.17)}$$

where ε' is the real part of the dielectric constant and ε'' is the dielectric loss factor. So loss tangent tan δ is given by:

$$\tan \delta = \frac{\varepsilon''}{\varepsilon'} \qquad \text{.....(1.18)}$$

Debye[1] was the first to give a relation between dielectric polarisation and the frequency of the alternating field by:

$$\frac{\varepsilon^* - 1}{\varepsilon^* + 2} = \frac{\varepsilon_\infty - 1}{\varepsilon_\infty + 2} + \left[\frac{\varepsilon_0 - 1}{\varepsilon_\infty + 2} - \frac{\varepsilon_\infty - 1}{\varepsilon_\infty + 2}\right] \frac{1}{1 + j\omega\tau_0} \qquad \text{.....(1.19)}$$

where τ_0 is the molecular relaxation time and ω is the angular frequency of the applied electric field. Solving the eqs (1.17) and (1.19) for ε^* and separating real and imaginary parts, one gets.

$$\varepsilon' = \varepsilon_\infty + \frac{\varepsilon_0 - \varepsilon_\infty}{1 + X^2} \qquad \text{.....(1.20)}$$

$$\varepsilon'' = \frac{\varepsilon_0 - \varepsilon_\infty}{1 + X^2} X \qquad \text{..... (1.21)}$$

where $X = \frac{\varepsilon_0 + 2}{\varepsilon_\infty + 2} \omega \tau_0$

1.7. Macroscopic & Microscopic Relaxation Time

Fröhlich[5] has derived the Debye's equation by assuming that in the constant external field equilibrium is attained exponentially with time and has the decay function f(t) as:

$$f(t) \alpha e^{-t/\tau} \qquad \text{.....(1.22)}$$

where τ is independent of time, but depends on temperature. With an electric field E (t) which is dependent on time, a field E (u) which is applied during a time interval between u and u+du a corresponding electric displacement D(t) can be written as:

$$D(t) = \varepsilon_\infty E(t) + \int_{-\infty}^{t} E(u)\, f(t-u)\, du \qquad \text{.....(1.23)}$$

The first term on the right hand side of above equation is the instantaneous displacement while the second term is absorptive term. The calculation of the Fröhlich finally leads to following relation:

$$\varepsilon^* = \varepsilon_\infty + \frac{\varepsilon_0 - \varepsilon_\infty}{1 + j\omega\tau} \qquad \text{.....(1.24)}$$

Separating the real and the imaginary parts one gets:

$$\varepsilon' = \varepsilon_\infty + \frac{\varepsilon_0 - \varepsilon_\infty}{1 + \omega^2\tau^2} \qquad \text{.....(1.25)}$$

and $$\varepsilon'' = \frac{\varepsilon_0 - \varepsilon_\infty}{1 + \omega^2\tau^2}\,\omega\tau \qquad \text{.....(1.26)}$$

It is clear from (1.26) that ε'' has a maximum value for $\omega\tau = 1$ and approaches zero both for small and large values of $\omega\tau$ as shown in Fig (1.1). The variation of ε' with $\omega\tau$ is shown in Fig (1.2). The eqs (1.25) and (1.26) differ from the Debye eqs (1.20) and (1.21) only in that the Debye equation contains the quantity $\tau_0(\varepsilon_{0+2})/(\varepsilon_{\infty+2})$ instead of τ. Comparing, the two equations a relation between macroscopic relaxation time τ and the microscopic relaxation time τ_0 is obtained like.

$$\tau = \frac{\varepsilon_0 + 2}{\varepsilon_\infty + 2}\,\tau_0 \qquad \text{.....(1.27)}$$

Since Onsager's equation is an advancement over the Debye's equation, one can change Onsager's equation to be used for complex dielectric constant. For that μ^2 has to be replaced by $\frac{\mu^2}{1 + j\omega\tau_0}$ and ε_0 by ε^*. Thus the resulting expression is found to be quadratic in ε^* as:

$$\frac{\varepsilon^* - 1}{\varepsilon^* + 2} - \frac{\varepsilon_\infty - 1}{\varepsilon_\infty + 2} = \frac{\rho}{M}\left[\frac{3\varepsilon^*(\varepsilon_\infty + 2)}{(2\varepsilon^* + \varepsilon_\infty)(\varepsilon^* + 2)}\right]\frac{4\pi N}{9kT}\,\frac{\mu^2}{1 + j\omega\tau_0} \qquad \text{.....(1.28)}$$

Cole [6] has shown that the factor $\frac{3\varepsilon_0}{2\varepsilon_0 + \varepsilon_\infty}$ can be put approximately equal to 3/2 for higher values of ε_0. Then the resulting expression is :

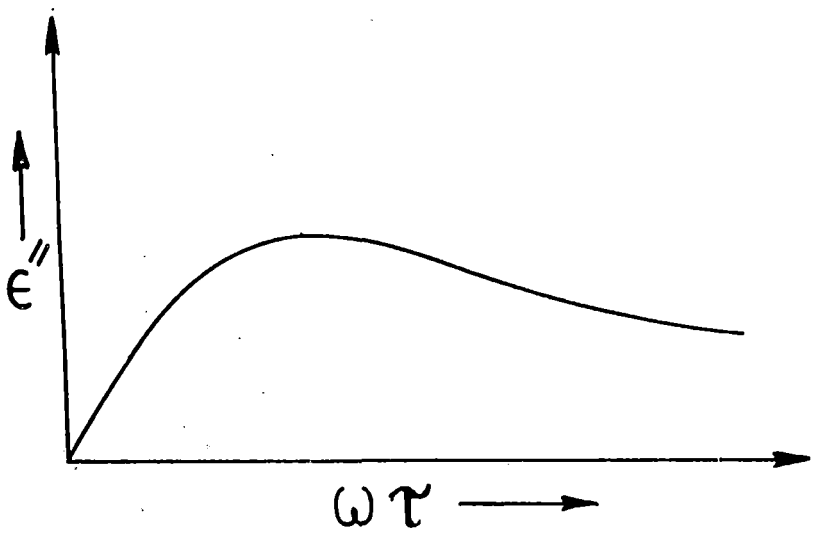

Figure 1.1 Variation of imaginary parts of dielectric constant with $\omega\tau$

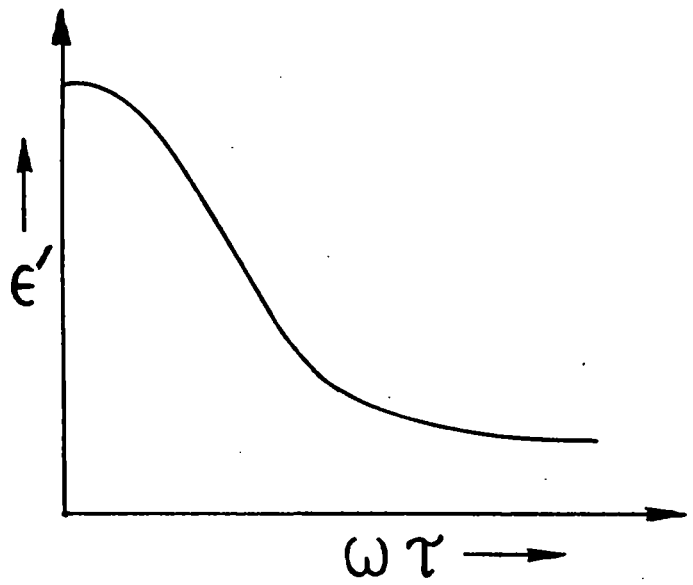

Figure 1.2 Variation of real parts of dielectric constant with ωτ

$$\frac{\varepsilon^* - \varepsilon_\infty}{\varepsilon_0 - \varepsilon_\infty} = \frac{1}{1 + j\omega\tau_0} \qquad \text{.....(1.29)}$$

which is similar to Fröhlich equation.

The above equation shows that the microscopic and macroscopic relaxation times are equal. Various workers[7-9] had roughly examined and modified the Onsager's equation, but none of them could give the satisfactory conclusion. O'Dwyer and Sack [10] had obtained a relation between macroscopic and microscopic relaxation times as a second order approximation

$$\tau_0 = \frac{3\varepsilon_\infty \varepsilon_0 (2\varepsilon_0 + \varepsilon_\infty)}{3\varepsilon_0^3 + \varepsilon_\infty^3} \tau \qquad \text{.....(1.30)}$$

Powles [11] had also tried to solve the problems in a different way. He has defined a time dependent field $\vec{H}$, which reduces to cavity field $\vec{G}$ in the static case, so that

$$\frac{\vec{H}}{\vec{E}} = \frac{3\varepsilon_\infty}{2\varepsilon_\infty + 1} + \left(\frac{3\varepsilon_0}{2\varepsilon_0 + 1} - \frac{3\varepsilon_\infty}{2\varepsilon_\infty + 1}\right) \frac{1}{1 + j\omega\tau} \qquad \text{.....(1.31)}$$

Powles[11] had shown that the comparison of eq (1.31) with that of Debye leads to a relation between τ and τ_0 like.

$$\tau = \frac{3\varepsilon_0}{2\varepsilon_0 + \varepsilon_\infty} \tau \qquad \text{.....(1.32)}$$

1.8. Distribution of Relaxation Time

To check the validity of eqs (1.25) and (1.26), the experimental results are usually represented by plotting ε' and ε'' against logarithm of frequency or wavelength of the electric field. The curves obtained (ε'vs.logω) and (ε'' vs.logω) as shown in Figs (1.3) and (1.4) are called the dispersion and absorption curves respectively. Another method of examining the equations, proposed by Cole-Cole is to construct an Argand diagram or complex plane locus in which the imaginary part ε'' of complex dielectric constant ε^* is

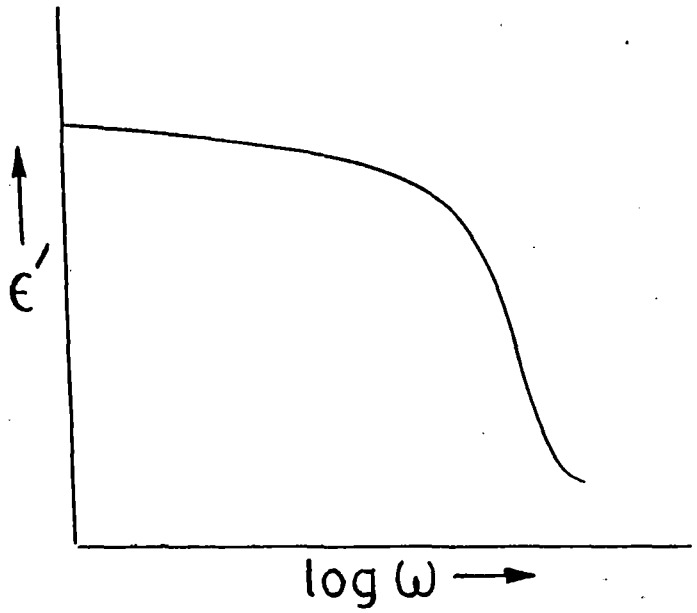

Figure 1.3 Frequency dependence of real part of dielectric constant

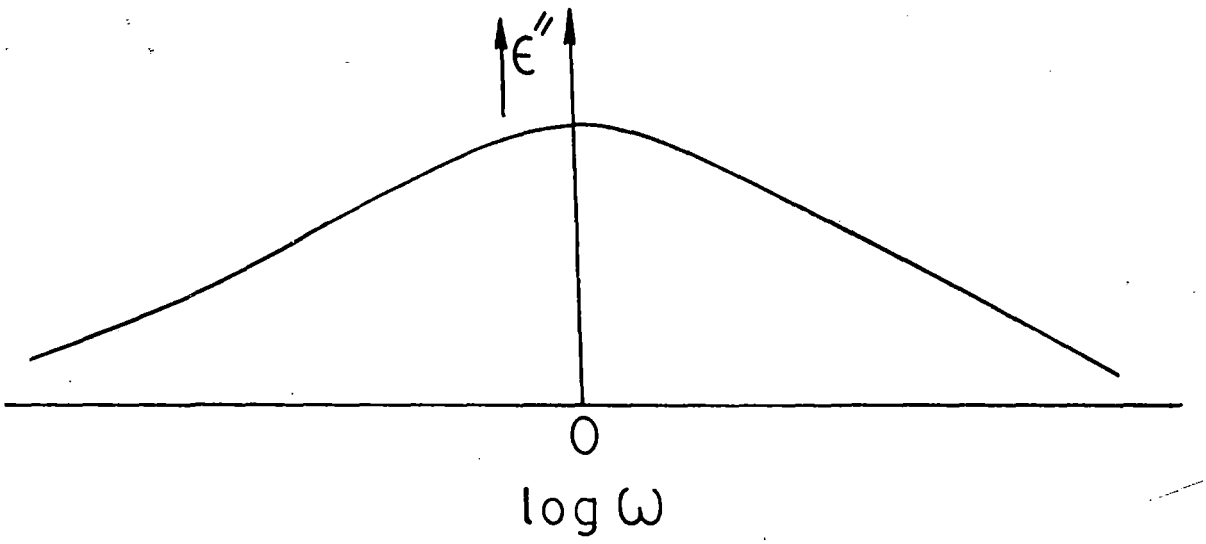

Figure 1.4 Frequency dependence of imaginary part of dielectric constant

plotted against ε′, the real part. Each point corresponds to one frequency. Combining the eqs (1.25) and (1.26) one gets:

$$\left(\varepsilon' - \frac{\varepsilon_0 + \varepsilon_\infty}{2}\right)^2 + \varepsilon''^2 = \left(\frac{\varepsilon_0 - \varepsilon_\infty}{2}\right)^2 \qquad \text{.....(1.33)}$$

Thus by plotting ε″ against ε′, as shown in Fig (1.5), semicircle must be obtained with radius $\frac{\varepsilon_0 - \varepsilon_\infty}{2}$ and centre lying on the abscissa at a distance $\frac{\varepsilon_0 + \varepsilon_\infty}{2}$ from the origin. The intersection points with the abscissa are given by $\varepsilon' = \varepsilon_\infty$ and $\varepsilon' = \varepsilon_0$. It has been found that only on exceptional cases the experimental results satisfy the above mentioned equation. Generally, the dispersion curve is found to be flatter and extends over a wide range of frequency while the absorption curve is broader and the maximum value of ε″ is smaller than the value given by $\varepsilon_m'' = \frac{\varepsilon_0 + \varepsilon_\infty}{2}$. However, the curves are still symmetrical.

1.8 a) Cole-Cole Plot

Generally, the behaviour of a dielectric can not be described by single relaxation time. Cole-Cole [12] showed that if a dielectric system has a distribution of relaxation times, then the complex plane locus, obtained by plotting ε″ vs. ε′, is generally an arc of a circle intersecting the abscissa axis at the values ε_∞ and ε_0 and having its centre lying below the abscissa axis. The diameter drawn through the centre from ε_∞ makes an angle $\alpha\ \pi/2$ with the ε′ axis as shown in Fig (1.6). α is the symmetric distribution parameter determined from the plot. The empirical formula used by Cole-Cole can be represented as :

$$\frac{\varepsilon^* - \varepsilon_\infty}{\varepsilon_0 - \varepsilon_\infty} = \frac{1}{1 + (j\omega\tau_0)^{1-\alpha}} \qquad \text{.....(1.34)}$$

1.8b) Cole - Davidson Plot

Davidson and Cole [13] had obtained an skewed arc indicating an asymmetric distribution of relaxation times in Glycerol and Glycol. The variation of ε″ with ε′ at low

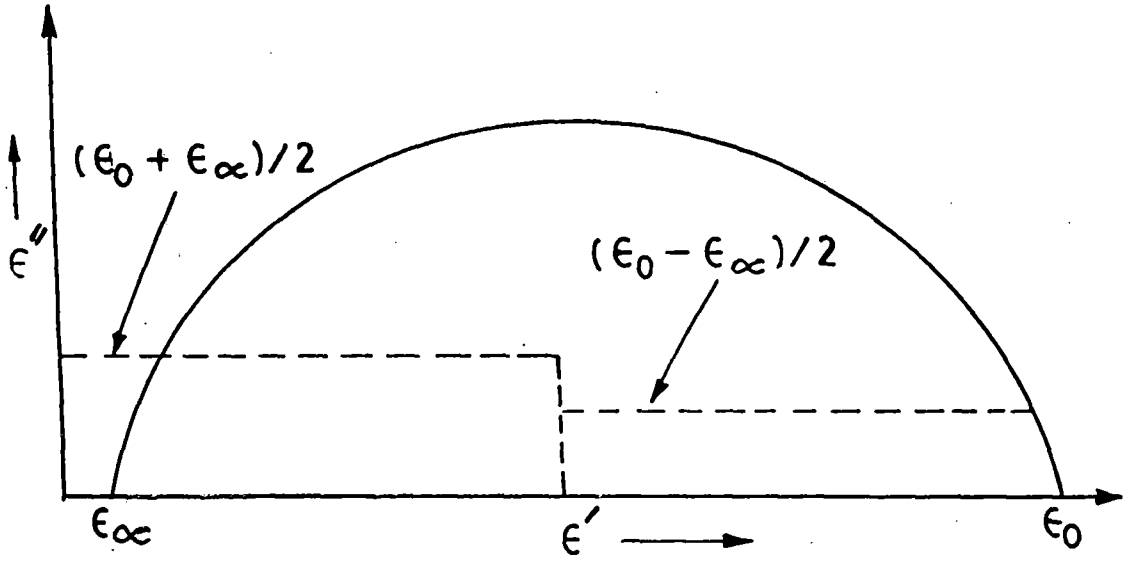

Figure 1.5 **Plot of ε″against ε′ at different frequency**

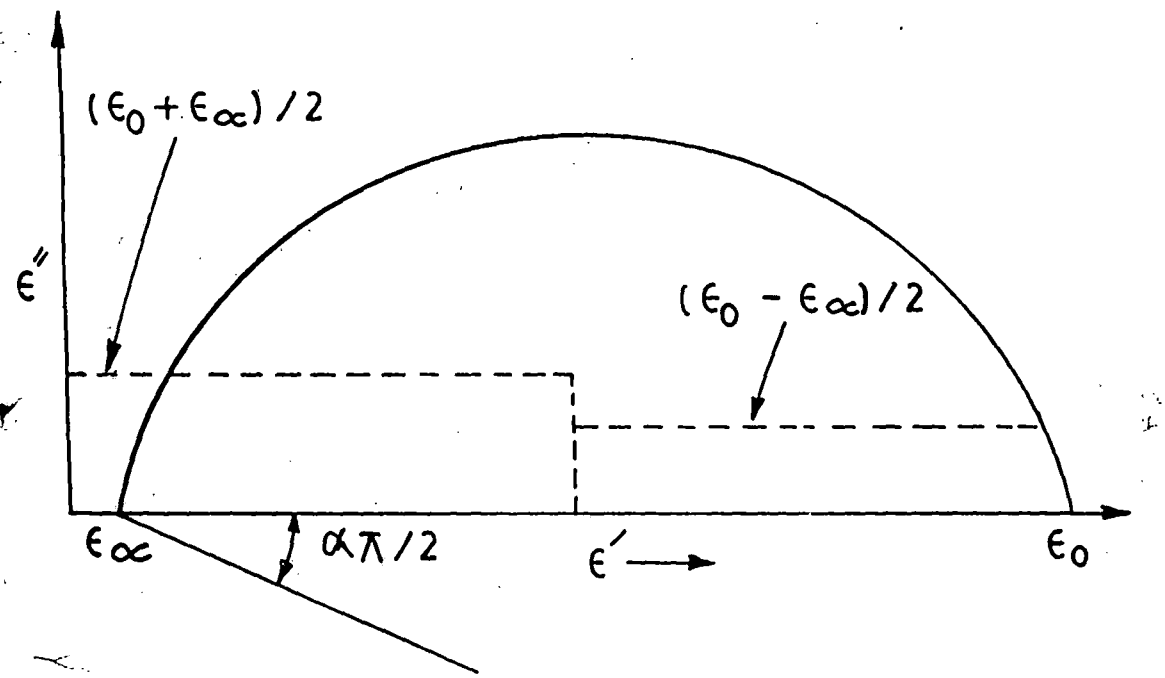

Figure 1.6 **Cole-Cole plot of ε'' vs ε'**

frequency end of this plot as seen in Fig (1.7) resembles with that found for a single relaxation time. At high frequency end, however, the locus approaches the X axis at an angle less than 90°. The corresponding form for complex dielectric constant ε^* and the asymmetric distribution parameter β can be written as:

$$\frac{\varepsilon^* - \varepsilon_\infty}{\varepsilon_0 - \varepsilon_\infty} = \frac{1}{(1 + j\omega\tau_0)^\beta} \qquad \text{.....(1.35)}$$

It is obvious that the distribution is asymmetric having a low frequency cut off at τ_0. β is a measure of the angle at which the complex plane locus intersects the ε' axis.

Although, many experimental results were found to satisfy the Cole-Cole and Cole-Davidson relation, but they have the disadvantage that a theoretical explanation has not yet been given.

The reason why in liquids the experimental curve deviates from the normal curve is that the model used in their derivations is too simple. The following three types of behaviours are generally obtained in variety of the systems in addition to semi-circular behaviour of Debye.

i) A circular arc with centres lying below the abscissa shows, the symmetric distribution of relaxation time.

ii) An skewed arc is obtained, indicating an asymmetric distribution of relaxation times.

iii) A curve which can be supposed to be made up of a number of circular arc plots, showing multiple relaxation times.

For such a distribution of relaxation times, the Debye equation must be extended to:

$$\varepsilon^* = \varepsilon_\infty + (\varepsilon_0 - \varepsilon_\infty) \int_0^\infty \frac{G(\tau)}{1 + j\omega\tau}\, d\tau \qquad \text{.....(1.36)}$$

where $G(\tau)$ is the distribution function of the relaxation times. $G(\tau)\, d\tau$ is the fraction of the molecules associated at a given instant with relaxation times between τ and $\tau + d\tau$. Thus $G(\tau)$ satisfies the normalisation condition:

$$\int_0^\infty G(\tau)\, d\tau = 1 \qquad \text{.....(1.37)}$$

The original equation of Debye can be written as:

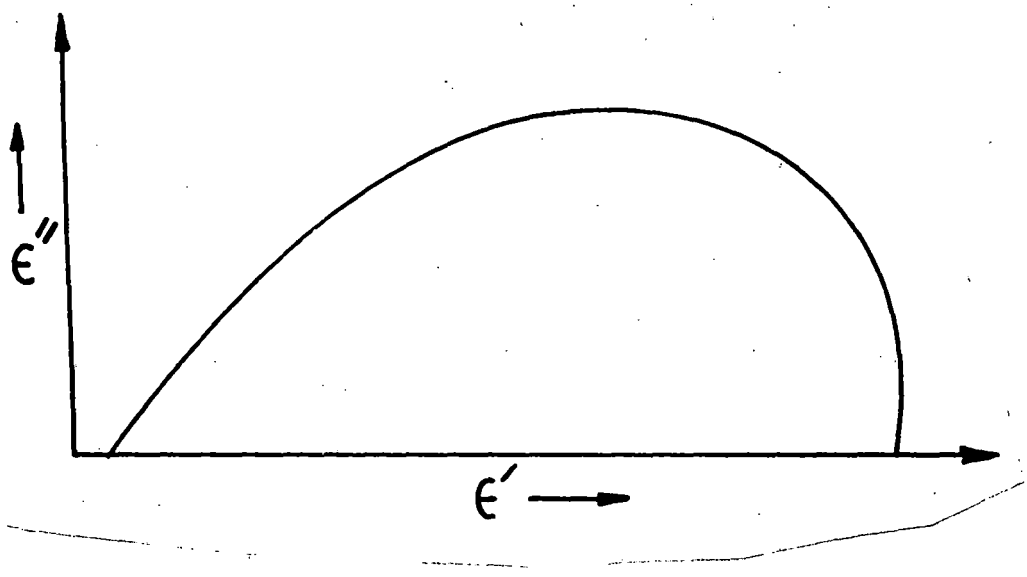

Figure 1.7 **Cole - Davidson plot of ε″ vs ε′**

$$\varepsilon' = \varepsilon_\infty + (\varepsilon_0 - \varepsilon_\infty) \int_0^\infty \frac{G(\tau)\, d\tau}{1 + \omega^2 \tau^2} \qquad \text{.....(1.38)}$$

$$\text{and } \varepsilon'' = (\varepsilon_0 - \varepsilon_\infty) \int_0^\infty \frac{\omega \tau\, G(\tau)\, d\tau}{1 + \omega^2 \tau^2} \qquad \text{.....(1.39)}$$

1.9 Calculation of Distribution Function

A large number of relations connecting the distribution functions has been given by various workers. Wagner [14] and Yager [15] had shown that the Gaussian probability distribution is

$$G(\tau)\, d\tau = \frac{b}{\sqrt{\pi}} \exp(-b^2 y^2)\, dy \qquad \text{.....(1.40)}$$

which can be used to explain the experimental results. Here b is a constant determining breadth of the distribution and y is

$$y = \ln(\tau/\tau_0) \qquad \text{.....(1.41)}$$

where τ_0 is the most probable relaxation time. $G(\tau)\, d\tau$ gives the probability of finding a relaxation time τ such that $\ln(\tau/\tau_0)$ lies between y and y + dy.

In long chain polar molecules, such as polymers there are many possibilities of internal rotations, bending and twisting each with a corresponding characteristic relaxation time. In averaging to the macroscopic condition a distribution of relaxation times will result. For long chain polymers Kirkwood and Fouss [16] derived:

$$G(\tau) = \frac{1}{2 \cosh y + 2} \qquad \text{.....(1.42)}$$

where $y = \ln(\tau/\tau_0)$.

This formula is not found in agreement with the experimental results. Fouss and Kirkwood [17] further suggested that the experimental data should be represented by empirical relation:

$$\varepsilon'' = \varepsilon''_m \operatorname{sech}\left[\beta \ln \frac{\omega}{\omega_m}\right] \qquad \text{.....(1.43)}$$

where β is a distribution parameter and ω_m is the angular frequency corresponding to the maximum value ε''_m of ε''. The corresponding distribution function is given by.

$$G(\tau) = \frac{\beta}{\pi} \frac{\cos\left(\frac{\beta\pi}{2}\right)\cosh(\beta y)}{\cos^2\left(\frac{\beta\pi}{2}\right) + \sinh^2(\beta y)} \qquad \text{.....(1.44)}$$

where $y = \log \frac{\omega}{\omega_m}$

Another distribution function of Cole-Cole eq (1.34) is given by:

$$G(\tau) = \frac{\sin \alpha\pi}{2\pi} \left[\cosh\left\{(1-\alpha)\ln\left(\frac{\tau}{\tau_0}\right)\right\} - \cos \alpha\pi\right]^{-1} \qquad \text{.....(1.45)}$$

where α is known as the distribution parameter and is measured by the width of the distribution. Fröhlich[5] derived the distribution function for a molecular mechanism which leads to a distribution of relaxation time between two limiting values τ_0 and $\tau_1 = \tau_0 \exp(v_0/kT)$. The distribution function is:

$$G(\tau) = (\varepsilon_0 - \varepsilon_\infty) \frac{kT}{v_0} \frac{1}{\tau} \text{ if } \tau_0 \le \tau \le \tau_1 = \tau_0 \exp\left(\frac{v_0}{kT}\right)$$

$$G(\tau) = 0 \text{ if } \tau < \tau_0 \text{ and } \tau > \tau_1 \qquad \text{.....(1.46)}$$

Davidson and Cole [13] showed that the molecules possess distribution of relaxation times given by

$$G(\tau) = \frac{\sin \beta\pi}{\pi} \left(\frac{\tau}{\tau_0 - \tau}\right)^{\beta} \text{ for } \tau < \tau_0$$

$$= 0 \text{ for } \tau > \tau_0 \qquad \text{.....(1.47)}$$

where the interpretation of β and τ_0 have been given in eq (1.35).

Higasi et al [18] gave the distribution function $y(\tau)$ which is similar to that of Fröhlich like.

$$y(\tau) = \frac{1}{A\tau} \text{ if } \tau_1 < \tau < \tau_2$$

$$= 0 \text{ if } \tau < \tau_1 \text{ and } \tau > \tau_2 \qquad \text{.....(1.48)}$$

A more general distribution function has been described by Matsumoto and Higasi [19] as:

$$y(\tau) = \frac{1}{A\tau^n} \text{ where } 0 < n < \infty \text{ if } \tau_1 < \tau < \tau_2$$

$$\text{and } y(\tau) = 0 \text{ if } \tau < \tau_1 \text{ and } \tau > \tau_2 \qquad \text{.....(1.49)}$$

1.10 Double Relaxation Phenomenon of Polar Molecules

If two distinct relaxation processes occur simultaneously, the mutually independent relaxation times τ_1 and τ_2 can be represented by following equations [20]:

$$\frac{\varepsilon' - \varepsilon_\infty}{\varepsilon_0 - \varepsilon_\infty} = \frac{c_1}{1 + (\omega\tau_1)^2} + \frac{c_2}{1 + (\omega\tau_2)^2} \qquad \text{.....(1.50)}$$

$$\frac{\varepsilon''}{\varepsilon_0 - \varepsilon_\infty} = c_1 \frac{\omega\tau_1}{1 + (\omega\tau_1)^2} + c_2 \frac{\omega\tau_2}{1 + (\omega\tau_2)^2} \qquad \text{.....(1.51)}$$

where c_1 and c_2 are the relative weights of each relaxation term and $c_1 + c_2 = 1$. If the probabilities of occurrence of two processes are equal, then.

$$\frac{c_1}{c_2} = \frac{\mu_1^2}{\mu_2^2} \qquad \text{.....(1.52)}$$

where μ_1, μ_2 are effective dipole moments which are relaxing.

1.11. High Frequency Conductivity

The conductivity K, due to displacement current of a dielectric material under alternating electric field $E = E_0 e^{j\omega t}$ is given by

$$K = \frac{1}{E}\frac{dq}{dt} \qquad \text{.....(1.53)}$$

Again, $D = 4\pi q = \varepsilon E$ and $E = \frac{V}{d}$ we have

$$\frac{dq}{dt} = \frac{1}{4\pi}\frac{dD}{dt} = \frac{\varepsilon}{4\pi d}\frac{dv}{dt} = I$$

Because of alternating nature of the electric field, the potential difference V is also given by

$$V = Vo\, e^{j\omega t} \qquad \text{.....(1.54)}$$

where V_0 is the amplitude. So the expression for the displacement current I is given by

$$I = \frac{dq}{dt} = \frac{\varepsilon^*}{4\pi d}\frac{dV}{dt} \qquad \text{.....(1.55)}$$

Substituting the values of ε^* and V from eqs (1.17) and (1.54) one gets

$$I = \frac{\varepsilon' - j\varepsilon''}{4\pi d} j\omega V_0 e^{j\omega t}$$

$$= \left(\frac{\omega\varepsilon''}{4\pi} + j\frac{\omega\varepsilon'}{4\pi}\right) E_0 e^{j\omega t} \qquad \text{.....(1.56)}$$

According to Ohm's law we again write

$$I = K E_0 e^{j\omega t} \qquad \text{.....(1.57)}$$

Comparing eqs (1.56) and (1.57) one gets

$$K = K' + jK'' \qquad \text{.....(1.58)}$$

Thus K' = the real part of the conductivity = $\frac{\omega\varepsilon''}{4\pi}$ and K'' = the imaginary part of conductivity = $\frac{\omega\varepsilon'}{4\pi}$. The above equation is known as Murphy and Morgan [21] relation.

The magnitude of the total high frequency conductivity is, however, given by the relation:

$$K = \frac{\omega}{4\pi}\sqrt{\varepsilon'^2 + \varepsilon''^2} \qquad \text{..... (1.59)}$$

By using the Debye's eqs (1.25) and (1.26), the expressions for conductivities are, therefore, be written as

$$K' = \frac{1}{4\pi}\frac{\varepsilon_0 - \varepsilon_\infty}{1 + \omega^2\tau^2}\omega^2\tau \qquad \text{.....(1.60)}$$

and $$K'' = \frac{\omega}{4\pi}\left[\varepsilon_\infty + \frac{\varepsilon_0 - \varepsilon_\infty}{(1 + \omega^2\tau^2)}\right] \qquad \text{.....(1.61)}$$

In the above considerations, it is assumed that there are no free ions or electrons in the dielectrics and the displacement current is the only factor to contribute to the total conductivity. When an electric field is set up across a dielectric, the total heat produced in the dielectric is not only due to dielectric loss, but due to Joule's heating also. So

conduction through polar dielectrics is due to the combined effect of the displacement current and the conduction current.

1.12. Dielectric Relaxation in Dilute Solution of Polar Molecules in Nonpolar Solvents under High Frequency Electric Field

When a trace amount of polar solute (j) is dissolved in a nonpolar solvent (i), the mixture becomes a dilute solution (ij) of polar nonpolar mixture.

Let n_i and n_j being the number of the ith and the jth molecules of molecular weights M_i and M_j are mixed per c.c to get a form of solution of certain concentration c_j. Then from Debye eq (1.10) we can write.

$$\frac{\varepsilon_{0ij} - 1}{\varepsilon_{0ij} + 2} \frac{f_i M_i + f_j M_j}{\rho_{ij}} = \frac{4}{3} \pi N \left(f_i \alpha_i + f_j \alpha_j + f_j \frac{\mu^2}{3 k T}\right) \quad \text{.....(1.62)}$$

and

$$\frac{\varepsilon_{\infty ij} - 1}{\varepsilon_{\infty ij} + 2} \frac{f_i M_i + f_j M_j}{\rho_{ij}} = \frac{4}{3} \pi N \left(f_i \alpha_i + f_j \alpha_j\right) \quad \text{.....(1.63)}$$

where $\varepsilon_{\infty ij}$ and ε_{oij} are the dielectric constants of the solution at infinite or optical frequency and the static dielectric constant respectively. f_i and f_j are the mole fractions of solvent and solute defined by:

$$f_i = \frac{n_i}{n_i + n_j} \text{ and } f_j = \frac{n_j}{n_i + n_j}$$

respectively. α being the distortional polarisability of respective molecules. Now, rearranging eqs (1.62) and (1.63) one can write:

$$(\varepsilon_{0ij} - \varepsilon_{\infty ij}) = \frac{4 \pi N \mu_j^2}{27 k T} \cdot \frac{\rho_{ij} f_j}{f_i M_i + f_j M_j} (\varepsilon_{0ij} + 2)(\varepsilon_{\infty ij} + 2) \quad \text{.....(1.64)}$$

Again, c_j the concentration of solute molecules per unit volume is given by:

$$c_j = \frac{\rho_{ij} \omega_j}{M_j} \quad \text{.....(1.65)}$$

where ω_j = weight fraction of jth solute can be written as:

$$\omega_j = \frac{f_j M_j}{f_i M_i + f_j M_j} \qquad \text{.....(1.66)}$$

So Debye eq (1.26) can now be written with the help of eq (1.65) as:

$$\varepsilon''_{ij} = \frac{4\pi N c_j \mu_j^2 (\varepsilon_{\infty ij} + 2)(\varepsilon_{0ij} + 2)}{27 k T} \frac{\omega \tau}{1 + \omega^2 \tau^2} \qquad \text{.....(1.67)}$$

In a dilute polar nonpolar mixture it is assumed that $\varepsilon_{0ij} \approx \varepsilon_{\infty ij} \approx \varepsilon'_{ij}$. Thus eq (1.67) becomes:

$$\varepsilon''_{ij} = \left(\frac{\varepsilon'_{ij} + 2}{3}\right)^2 \cdot \frac{4\pi N \rho_{ij} \mu_j^2}{3 M_j k T} \left(\frac{\omega \tau}{1 + \omega^2 \tau^2}\right) \omega_j \qquad \text{.....(1.68)}$$

The above equation reveals the linear behaviour of ε''_{ij} with ω_j for very dilute mixture of polar solute in nonpolar solvent. Now in case of infinite dilute solution i.e as $\omega_j \rightarrow 0$, $\varepsilon'_{ij} \rightarrow \varepsilon_{oi}$ and eq (1.68) becomes:

$$(\varepsilon''_{ij})_{\omega_j \rightarrow 0} = \frac{4\pi N \rho_i \mu_j^2}{3 M_j k T} \left(\frac{\varepsilon_{oi} + 2}{3}\right)^2 \left(\frac{\omega \tau}{1 + \omega^2 \tau^2}\right) \omega_j \qquad \text{.....(1.69)}$$

The real part of hf conductivity is thus given by eqs (1.58) and (1.68) as:

$$K'_{ij} = \frac{\omega}{4\pi} \varepsilon''_{ij} = \frac{\omega}{4\pi} \frac{4\pi N \rho_{ij} \mu_j^2}{3 M_j k T} \left(\frac{\varepsilon'_{ij} + 2}{3}\right)^2 \cdot \left(\frac{\omega \tau}{1 + \omega^2 \tau^2}\right) \omega_j$$

$$= \frac{N \rho_{ij} \mu_j^2}{3 M_j k T} \left(\frac{\varepsilon'_{ij} + 2}{3}\right)^2 \left(\frac{\omega^2 \tau}{1 + \omega^2 \tau^2}\right) \qquad \text{.....(1.70)}$$

The K''_{ij} is, however, written with the help of eqs (1.58) and (1.25) as:

$$K''_{ij} = \frac{\omega}{4\pi} \left(\varepsilon_{\infty ij} + \frac{\varepsilon_{0ij} - \varepsilon_{\infty ij}}{1 + \omega^2 \tau^2}\right)$$

$$= \frac{\omega}{4\pi}\left[\varepsilon_{\infty ij} + \frac{1}{\omega\tau}\,\frac{(\varepsilon_{0ij} - \varepsilon_{\infty ij})}{1+\omega^2\tau^2}\,.\,\omega\tau\right]$$

$$= \frac{\omega}{4\pi}\left(\varepsilon_{\infty ij} + \frac{1}{\omega\tau}\,\varepsilon''_{ij}\right)$$

$$= \frac{\omega}{4\pi}\,\varepsilon_{\infty ij} + \frac{1}{\omega\tau}\,\frac{\omega}{4\pi}\,\varepsilon''_{ij}$$

$$= K_{\infty ij} + \frac{1}{\omega\tau}\,K'_{ij} \qquad \text{.....(1.71)}$$

Since $\varepsilon'_{ij} >> \varepsilon''_{ij}$, so imaginary part of conductivity of eq (1.71) can be written as total hf conductivity

$$K_{ij} = K_{\infty ij} + \frac{1}{\omega\tau}\,K'_{ij} \qquad \text{.....(1.72)}$$

The eqs (1.70), (1.71) and (1.72) as presented in this chapter have been used in the present thesis to estimate relaxation time τ as well as dipole moment μ_j of a polar solute.

1.13. Eyring's Rate Theory

The study of dielectric relaxation mechanism from the stand point of chemical rate processes has been first pointed out by Eyring et al [22]. According to this theory, the dielectric relaxation mechanism may be explained by treating the dipole orientation as a rate process in which the polar molecules rotate from one equilibrium position to another. This process of rotation requires an activation energy sufficient to overcome the energy barrier separating the two mean equilibrium positions. The average time required for single rotation is known as relaxation time τ_s is given by:

$$\tau_s = \frac{h}{kT}\exp(\Delta F_\tau / RT) \qquad \text{.....(1.73)}$$

where ΔF_τ is the free energy of activation. Now, from thermodynamics one can write.

$$\Delta F_\tau = \Delta H_\tau - T\,\Delta S_\tau \qquad \text{.....(1.74)}$$

where ΔH_τ and ΔS_τ are the enthalpy and entropy of activation respectively. Eq (1.73) can now be written as:

$$\tau_S = \frac{h}{kT} \exp(-\Delta S_\tau / R) \exp(\Delta H_\tau / RT) \quad \text{.....(1.75)}$$

$$\text{or, } \ln(\tau_s T) = \ln A + \frac{\Delta H_\tau}{RT} \quad \text{.....(1.76)}$$

where $A = \frac{h}{k} \exp(-\Delta S_\tau / R)$.

Thus ΔH_τ is calculated from the slope of linear relation of ln ($\tau_s T$) vs. 1/T. Knowing ΔH_τ and τ one can easily calculate ΔS_τ and ΔF_τ by using eqs (1.75) and (1.74) respectively.

Like dielectric relaxation process; the viscous flow of the liquids may also be considered as rate process. Viscous flow is involved with the translational as well as rotational motion of molecules with an activation energy to pass over a potential barrier. If η is the co-efficient of viscosity of the medium then according to Eyring et al [22] we can write:

$$\eta = \frac{hV}{N} \exp(\Delta F_\eta / RT) \quad \text{.....(1.77)}$$

where h is the Planck's constant, N is the Avogadro's number, V is the molar volume and ΔF_η is the free energy of activation for viscous flow given by:

$$\Delta F_\eta = \Delta H_\eta - T \Delta S_\eta \quad \text{.....(1.78)}$$

Again, η of eq (1.77)can be written with the help of eq (1.78) as:

$$\eta = \frac{hV}{N} \exp(-\Delta S_\eta / R) \exp(\Delta H_\eta / RT) \quad \text{.....(1.79)}$$

$$= A \exp(\Delta H_\eta / RT) \quad \text{.....(1.80)}$$

where ΔH_η and ΔS_η are the enthalpy and entropy of activation for viscous flow. ΔH_η can be calculated from the fitted linear equation of ln η with 1/T which is subsequently used to get ΔS_η and ΔF_η from eqs. (1.79) and (1.78) respectively.

The approximate linearity of ln ($\tau_s T$) against 1/T as presented in eq (1.76) has been used in this thesis in many places to estimate thermodynamic energy parameters of a polar solute in a nonpolar solvent to get an information of the molecular associations among the molecules under investigation.

1.14 A Brief Review of Early Works

The theory of the dielectric relaxation of polar liquids and polar nonpolar liquid mixtures goes back to the time when P Debye [1] published a monograph on polar molecules in the Year 1929. After Debye a significant improvement in this field till date is as follows:

The first quantitative verification of Debye theory was done by Mizushima [23]. He measured the dispersion phenomena of some alcohols and ketones for a wide range of temperature in molecular radii as calculated by him were found to be almost of the right order in glycerin.

Fischer[24] measured the relaxation times of a number of liquid compounds in dilute solutions as well as in pure liquids. He observed that for long chain aliphatic alcohols τ is decreased in the sequence as halogenides, ketones and alcohols. The absolute value of τ can be evaluated by introducing molecular viscosity which is smaller than the macroscopic viscosity. Although, general theory becomes unable to explain the behaviour of alcohols, but the results of acetone, nitrobenzene and monochlorobenzene in pure state are in agreement with Debye theory.

τ 's of some polar molecules in benzene and paraffin were calculated by Jackson and Powles [25] and observed that the values are found to increase by 4 to 7 times for an increase in viscosity of eight fold.

An excellent method for the determination of dipole moment and relaxation time of a polar molecule in a nonpolar solvent was offered by Gopalakrishna [26] in 1957 without the prior knowledge of density of solution.

Higasi et al [18] analysed the experimental data of n-alkyl bromide in liquid state in terms of distribution of relaxation time between two limits as suggested by Fröhlich[5]. The lower values of τ were associated with the relaxation time of internal rotation of CH_2 Br group while the larger one due to the end-over end rotation of whole molecule.

Bergmann et al [20] using a graphical method analysed the systems like diphenyl ether, dibenzyl ether, anisol and o-dimethoxy benzene in terms of two relaxation times. The results are consistent with the interpretation of a larger relaxation time due to

molecular rotation and a smaller relaxation time due to intramolecular motion of a polar molecule.

By using Cole-Cole plot Kalman and Smyth [27] calculated the most probable relaxation times and the distribution parameters for the solutes like d,l-camphor, isoquinoline and 4-bromobiphenyl dissolved in a viscous oil or acridine. The effect of viscosity on relaxation time increases from the slight viscosity dependence of spherical camphor molecule to a considerable dependence for the elongated molecules.

Matsumoto and Higasi [19] observed that the plot of complex dielectric constants of supercooled, branched alkyl halides obeys skewed arc expression of Davidson and Cole. Besides this, dielectric properties of a great majority of straight chain alkyl halides at room temperature are in fair accord with the circular arc plot of Cole and Cole.

In order to solve Fröhlich's expression for complex dielectric constant at microwave frequencies Mansingh and Kumar [28] proposed a graphical technique to evaluate the minimum and maximum dielectric relaxation times τ_1 and τ_2 of a polar solute. Calculations were also made at three frequencies for ethyl bromide and butyl bromide at 25°C and dibenzyl ether at 20°, 40° and 60°C. It was found that the results were affected considerably by the inaccuracy of measurements and by the nonapplicability of Fröhlich distribution.

Higasi [29] observed that the dielectric relaxation data from dilute solutions consists of two slopes a′ and a" as defined by $\varepsilon' = \varepsilon'_1 + a'c_2$ and $\varepsilon'' = a''c_2$. In this article it was seen that the Debye equations for dilute solutions can be described by the use of a' and a". The equations were obtained by replacing ε' and ε" in Debye's equations by a' and a" for polar liquids.

Sinha, Roy and Kastha [30] showed the temperature dependence of relaxation times and dipole moments of a number of polar molecules in nonpolar solvents. They also observed the viscosity dependence of τ with T is represented as $\tau\, T/\eta^{\gamma}$ = constant, where γ is the ratio of the enthalpies of activation for dielectric relaxation and viscous flow.

The dielectric relaxation data of pure phenetole, aniline and orthochloro aniline in terms of two relaxation times for molecular and intramolecular rotations was analysed by

Bhattacharyya et al [31] using the modified relation of Bergmann et al [20] for at least two different electric field frequencies of GHz range.

ε′ and ε″ of six isomeric octyl alcohols at 25°C in n-heptane solution for various wavelengths of electric fields were measured by Crossley et al [32]. For these isomers in which —CH_3 group is attached to the same carbon atom as the — OH group or to the adjacent carbon, the dielectric absorption may be characterised by two τ's at all concentrations employed. The isomers containing relatively less shielded—OH group exhibit an additional low frequency τ at higher alcohol concentration.

Higasi et al [33] used the four Debye equations for dilute solutions of a non-rigid polar-nonpolar mixture to calculate the crude values of τ_2 and τ_1 for molecular and intramolecular rotations of the solute molecules under a single frequency electric field.

Glasser et al [34] measured dielectric relaxation parameters of four normal alcohols at 25°C in n-heptane solution under various electric fields. According to them, at lower concentration, the dielectric absorption may be characterised by two relaxation times. In higher concentration, another long relaxation time appears which is strongly concentration dependent.

Dielectric relaxation parameters like ε′ and ε″ of some long chain para compounds in dilute solution of dioxane under 3 cm wavelength electric field were measured by Dhar et al [35]. The data thus obtained were utilised to study the dipole orientation and viscous flow process by using Eyring's rate theory. It was observed that the dipole orientation was contributed by both molecular and intramolecular rotation. The comparatively higher τ's are, however, attributed to the intermolecular hydrogen bonding between solute and solvent molecules.

Purohit et al [36] measured molar polarisation of trifluoro ethanol and trifluoro acetic acid in benzene at 25°C. Measurements were performed on ε′ and ε″ at 9.83 GHz. The dielectric behaviour of the molecules has been studied by plotting tan δ - concentration curves and their behaviour in respect of hydrogen bonding has been explained .

Measurements of ε' and ε'' of chloral and ethyl trichloro acetate dissolved in nonpolar solvents like benzene, n-heptane and n-hexane were made by Srivastava and Srivastava [37] at three different microwave electric fields. The data were analysed by Cole-Cole plot and Gopalakrishna's single frequency method. The values of τ and μ suggest some type of association or interaction between polar-nonpolar mixture.

Jai Prakash [38] examined different existing methods for the determination of dipole moment of a polar solute in nonpolar solvent. It has been observed that the Palit's method in its suggested form with the weight faction as the concentration unit is most suitable.

The dielectric relaxation data of fluorobenzene, o-chlorobenzene and o-chlorotoluene and their binary mixtures were measured by Gupta et al [39] under 3 cm wavelength electric field in the temperature range 20°C to 60°C to estimate τ and thermodynamic energy parameters of them using Gopalakrishna's method. The results were explained on the basis of different molecular parameters.

Khameshara and Sisodia [40] measured the ε', ε'', ε_0 and n_D of some disubstituted anilines in benzene solution under X-band electric filed. τ's were determined following the methods of Higasi et al, Gopalakrishna and Higasi. The values of τ and distribution parameter α show the existence of more than two relaxation mechanism.

In 1982 Dhull and Sharma [41] measured the ε' and ε'' of N, N-dimethyl formamide (DMF) at 9.987 GHz for a range of temperature to estimate τ and μ of DMF in different nonpolar solvents. The energy parameters were also estimated to infer the monomer associations in nonpolar solvents.

Acharyya and Chatterjee [42] used the slope of the curve of the variation of the microwave conductivity with concentration at infinite dilution to get dipole moments of some substituted benzotrifluorides in benzene at 35°C under microwave electric field. The estimated data are in excellent agreement with the reported ones suggesting the uniqueness of the method adopted.

Using the dielectric absorption data of isobutyl methacrylate, allyl methacrylate and their mixtures in benzene solution Gandhi and Sharma[43] estimated most probable

relaxation time τ_o, molecular and intramolecular relaxation times τ_2 and τ_1 as well as distribution parameters of polar solutes. The results indicate that the properties of single polar solute are also retained in mixtures, too.

Onsager's equation was used to calculate dipole moments of five liquids in nonpolar solvents by Makosz [44] assuming ellipsoidal shape of the molecules.

A least square fit method was suggested to determine the dipole moment and relaxation time of polar-nonpolar liquid mixture by Suryavanshi and Mehrotra [45].

Using uhf conductivity method; Chatterjee et al [46] estimated the dipole moments of some binary protic polar mixtures under Giga hertz range electric field for a wide range of temperature. The result indicates the existence of monomer and dimer formations in such liquid mixtures under uhf electric filed.

Saha and Acharyya [47] estimated the dipole moments of monomer and dimer of binary protic polar liquids under 3 cm wavelength electric field from the concentration variation of ultra-high frequency conductivity. The results showed the solute-solute molecular associations in benzene solution, too.

In terms of measured relaxation parameters of polar nonpolar mixture Sit et al [48] estimated the double relaxation times of mono-substituted anilines dissolved in nonpolar solvents from the measured relaxation parameters under a single Giga Hertz electric field. The data also predict relative weight factors of two relaxations.

Sit and Acharyya [49], however, showed that monosubstituted anilines exhibit the double relaxation behaviours under an electric field of nearly 10 GHz which is the most prominent dispersive region for such liquids in benzene solutions.

REFERENCES

1. P Debye, Polar Molecules; (Chemical Catalogue; New-York) (1929)
2. L Onsager; J. Amer. Chem. Soc, **58** 1486 (1936)
3. J G Kirkwood; J.Amer. Phys, 7 911 (1939)
4. H Fröhlich ; Trans. Faraday Soc., **44** 238 (1948)

5. H Fröhlich; Theory of Dielectric, (Oxford University Press) (1949)
6. R. H Cole; J. Chem. Phys. 6 385 (1938)
7. S. C. Bolton; J. Chem. Phys. **16** 486 (1948)
8. J Ph Poley; Appl. Sci. Res, **B4** 337 (1954)
9. M Mandel; Bull. Sci. Res. Belges, **60** 301 (1951)
10. J J O'Dwyer and R Sack; Australian J. Sci. Res. **A5** 647 (1952)
11. J G Powles; J. Chem. Phys. **21** 633 (1953)
12. K S Cole and R H Cole; J. Chem.Phys. 9 341 (1941)
13. D W Davidson and R H Cole; J. Chem. Phys. **19** 1484 (1951)
14. K W Wagner; Ann.Phys. **40** 814 (1913)
15. W A Yager; Physics 7 434 (1936)
16. J G Kirkwood and R M Fouss; J. Chem.Phys, 9 329 (1941)
17. R M Fouss and J G Kirkwood; J. Amer. Chem. Soc. **63** 385 (1941)
18. K Higasi, K Bergmann and C P Smyth; J. Phy. Chem. **64** 880 (1960)
19. A Matsumoto and K Higasi; J. Chem. Phys. **36** 1776 (1962)
20. K Bergmann, D M Roberti and C P Smyth; J.Phy.Chem. **64** 665 (1960)
21. F J Murphy and S O Morgan, Bull. Syst. Techn. J. **18** 502 (1939)
22. H Eyring, S Glasstone and K J Laidler, The Theory of Rate Process, (McGraw Hill, New York) (1941)
23. S I Mizushima, Phys. Z, **28** 418 (1926)
24. E Fischer and F C Frank, Physik Z **40** 345 (1939)
25. W Jackson and J G Powles; Trans. Faraday Soc; **42A** 101 (1946)
26. K V Gopalakrishna; Trans. Faraday. Soc.**53** 767 (1957)
27. O F Kalman and C P Smyth; J. Amer. Chem. Soc, **82** 783 (1960)
28. A Mansing and P Kumar, J. Phys. Chem **69** 4197 (1965)
29. K Higasi, Bull Chem.Soc.Japan **39** 2157 (1966)
30. B Sinha, S B Roy and G S Kastha; Indian J.Phys. **41** 183 (1967)
31. J Bhattacharyya, A Hasan, S B Roy G S Kastha; J.Phy.Soc.Japan, **28** 204 (1970)
32. J Crossley, L Glasser and C P Smyth; J.Chem.Phys. **55** 2197 (1971)
33. K Higasi, Y Koga and M Nakamura; Bull.Chem.Soc.Japan **44** 988 (1971)

34. L Glasser, J Crossley and C P Smyth, J.Chem.Phys. **57** 3977 (1972)

35. R L Dhar, A Mathur, J P Shukla and M C Saxena; Indian J. Pure & Appl. Phys; **11** 568 (1973)

36. H D Purohit, H S Sharma and A D Vyas; Indian J. Pure & Appl.Phys; **12** 273 (1974).

37. S K Srivastava and S L Srivastava; Indian J. Pure & Appl. Phys, **13** 179 (1975)

38. Jai Prakash; Indian J.Pure & Appl.Phys, **14** 571 (1976)

39. P C Gupta, M L Arrawatia and M L Sisodia; Indian J. Pure & Appl. Phys, **16** 707 (1978)

40. S M Khameshara and M L Sisodia; Indian J. Pure & Appl. Phys, **18** 110 (1980)

41. J S Dhull and D R Sharma; J. Phys. D: Appl. Phys, **15** 2307 (1982)

42. S Acharyya and A K Chatterjee Indian J. Pure & Appl.Phys; **23** 484 (1985)

43. J M Gandhi and G L Sharma; J Mol. Liquid (Netherlands), **38** 23 (1988)

44. J J Makosz; Acta Phys. Pol; **A78** 907 (1990)

45. B M Suryavanshi and S C Mehrotra; Indian J Pure & Appl. Phys; **28** 67 (1990)

46. A K Chatterjee, U Saha, N Nandi, R C Basak and S Acharyya; Indian J.Phys **66B** 291 (1992)

47. U Saha and S Acharyya; Indian J Pure & Appl.Phys., **31** 181 (1993)

48. S K Sit, R C Basak, U Saha and S Acharyya; J. Phys. D: Appl.Phys.(London), **27** 2194 (1994)

49. S K Sit and S Acharyya; Indian J. Pure & Appl.Phys; **34** 255 (1996)

CHAPTER 2

THE SCOPE AND THE OBJECTIVE OF THE PRESENT WORKS

2.1 INTRODUCTION

It is a well known fact that Debye's theory is applicable to a rigid spherical polar molecule having one relaxation time τ. The nonrigid molecules, on the other hand, usually possess more than one relaxation time i.e., a distribution of relaxation times existing between two extreme values. In such cases an average macroscopic τ is always obtained with this theory. A large number of workers tried to estimate average τ_0 and other molecular relaxation parameters with the help of Cole-Cole and Cole-Davidson plots. In order to predict the double relaxation behaviour of nonspherical polar liquids it is, therefore, desirable to formulate a new theoretical technique derived on the basis of Debye and Smyth model. In this section a method is, however, suggested to estimate the molecular and intramolecular relaxation times τ_2 and τ_1 of a polar liquid dissolved in nonpolar solvents from the measured dielectric relaxation data under a single frequency electric field of GHz range.

Let $y(\tau)\, d\tau$ be the contribution to the static dielectric constant of a group of dipoles having individual relaxation times in the range τ to $\tau + d\tau$. Since in dilute solution polar-polar interaction is almost absent, the contribution to ε_0 by various groups superpose linearly. The total contribution to static dielectric constant is, therefore, given by

$$\varepsilon_0 - \varepsilon_\infty = \int_0^\infty y(\tau)\, d\tau \qquad \text{.....(2.1)}$$

where $y(\tau)$ is the distribution function associated with the relaxation times.

To obtain the complex dielectric constant ε^*, we first consider the decay function $\alpha(t)$.The dipoles with relaxation times τ to $\tau + d\tau$ make a contribution to $\alpha(t)$ which is proportional to $\exp(-t/\tau)$ and $y(\tau)\frac{d\tau}{\tau}$. Therefore, the total contribution of all the dipoles is given by

$$\alpha(t) = \int_0^\infty e^{-t/\tau}\, y(\tau)\, \frac{d\tau}{\tau} \qquad \text{.....(2.2)}$$

The complex dielectric constant ε^* is now obtained as

$$\varepsilon^* - \varepsilon_\infty = \int_0^\infty \alpha(x)\, e^{-i\omega x} dx$$

$$= \int_0^\infty \left[e^{-i\omega x} \int_0^\infty \frac{d\tau}{\tau} e^{-x/\tau} y(\tau) \right] dx$$

$$= \int_0^\infty \frac{y(\tau)}{\tau} d\tau \int_0^\infty e^{-i\omega x - \frac{x}{\tau}} dx \qquad \text{.....(2.3)}$$

Let $I = \int_0^\infty e^{-i\omega x} e^{-x/\tau} dx$ which becomes as follows with integration by parts.

$$I = -\frac{1}{i\omega}\left[e^{-x/\tau} \cdot e^{-i\omega x} \right]_0^\infty - \frac{1}{i\omega\tau} \int_0^\infty e^{-x/\tau} e^{-i\omega x} dx$$

$$\text{or, } I = \frac{1}{i\omega} - \frac{1}{i\omega\tau} I$$

$$\text{or, } I = \frac{\tau}{1 + i\omega\tau}$$

so eq (2.3) can be written as

$$\varepsilon^* - \varepsilon_\infty = \int_0^\infty \frac{y(\tau)\, d\tau}{1 + i\omega\tau} \qquad \text{..... (2.4)}$$

Substituting the value of ε^* from eq (1.17) and replacing the complex number 'i' one can write eq. (2.4) into the form:

$$\varepsilon' - j\varepsilon'' - \varepsilon_\infty = \int_0^\infty \frac{y(\tau)\, d\tau}{(1 + j\omega\tau)}$$

$$= \int_0^\infty \frac{y(\tau)\, d\tau}{(1 + \omega^2\tau^2)} (1 - j\omega\tau)$$

$$= \int_0^\infty \frac{y(\tau)\, d\tau}{1 + \omega^2\tau^2} - j \int_0^\infty \frac{y(\tau)\, \omega\tau}{1 + \omega^2\tau^2} d\tau$$

Equating the real and the imaginary parts from both sides of the above equation we have

$$\varepsilon' - \varepsilon_\infty = \int_0^\infty \frac{y(\tau)}{1 + \omega^2\tau^2} d\tau \qquad \text{.....(2.5)}$$

$$\varepsilon'' = \int_0^{\infty} \frac{y(\tau)\,\omega\tau}{1 + \omega^2\tau^2}\,d\tau \qquad \text{.....(2.6)}$$

For a detailed discussion of relations (2.5) and (2.6) the knowledge of distribution function y (τ) is to be known. Let us consider a model in which each molecule has two equilibrium positions with opposite dipolar directions and with equal energy in the ground level. The potential barrier between the two positions has different heights for each molecule. Let the heights H of the potential barriers are distributed equally over a range between H_o and $H_o + v_0$, i.e.

$$H = H_0 + v,\ 0 \le v \le v_0 \qquad \text{.....(2.7)}$$

Thus if No is the total number of dipoles per unit volume.

$$N_0 \frac{dv}{v_0} \qquad \text{..... (2.8)}$$

is the fraction with H-values in a range dv near $H_o + v$.

For dilute solutions interaction between dipoles can be neglected. Therefore, the contribution of a dipolar molecule to ε_0 is the same for all molecules given by

$$\frac{\varepsilon_0 - \varepsilon_\infty}{N_0} \text{ per molecule} \qquad \text{.....(2.9)}$$

The individual relaxation time τ, therefore, depends on H and covers the range $\tau_1 \le \tau \le \tau_2$

$$\text{where } \tau_2 = \tau_1 e^{\frac{v_0}{kT}} \qquad \text{.....(2.10)}$$

To determine the distribution function y (τ), we note that y (τ) = 0 outside the range of eq. (2.10).. Now considering τ as a function of v, eq (2.1)can be written as

$$\varepsilon_0 - \varepsilon_\infty = \int_{\tau_1}^{\tau_2} y(\tau)\,d\tau$$

$$= \frac{1}{KT} \int_0^{v_0} y(\tau)\,\tau(v)\,dv \qquad \text{.....(2.11)}$$

The contribution to ε_o of the molecules in the range of dv is

$$\frac{y(\tau)\,\tau\,dv}{kT} \qquad \text{..... (2.12)}$$

Eq. (2.12) can be written with the help of eqs (2.8) and (2.9) as

$$\frac{y(\tau)\tau\, dv}{kT} = \frac{\varepsilon_0 - \varepsilon_\infty}{N_0} \cdot \frac{N_0\, dv}{v_0}$$

$$\text{or, } y(\tau) = (\varepsilon_0 - \varepsilon_\infty)\frac{kT}{v_0} \cdot \frac{1}{\tau} \text{ if } \tau_1 \le \tau \le \tau_2 = \tau_1 e^{\frac{v_0}{kT}}$$

$$= 0 \text{ if } \tau < \tau_1 \text{ and } \tau > \tau_2 \qquad \text{.....(2.13)}$$

The dielectric constant ε' and ε'' can now be obtained from eq. (2.5) as

$$\frac{\varepsilon' - \varepsilon_\infty}{\varepsilon_0 - \varepsilon_\infty} = \frac{kT}{v_0}\int_{\tau_1}^{\tau_2} \frac{d\tau}{\tau(1 + \omega^2\tau^2)} \qquad \text{.....(2.14)}$$

$$\frac{\varepsilon''}{\varepsilon_0 - \varepsilon_\infty} = \frac{kT}{v_0}\int_{\tau_1}^{\tau_2} \frac{\omega d\tau}{1 + \omega^2\tau^2} \qquad \text{.....(2.15)}$$

Let $1 + \omega^2\tau^2 = Z$, eq. (2.14) can be written as :

$$\frac{\varepsilon' - \varepsilon_\infty}{\varepsilon_0 - \varepsilon_\infty} = \frac{kT}{2v_0}\int_{1+\omega^2\tau_1^2}^{1+\omega^2\tau_2^2} \frac{dZ}{Z(Z-1)}$$

$$= -\frac{kT}{2v_0}\left\{\ln\left(\frac{1+\omega^2\tau_2^2}{1+\omega^2\tau_1^2}\right) - \ln\frac{\omega^2\tau_2^2}{\omega^2\tau_1^2}\right\}$$

$$= \frac{kT}{2v_0}\left\{\ln\frac{\tau_1^2\, e^{\frac{2v_0}{kT}}(1 + \omega^2\tau_1^2)}{\tau_1^2(1 + \omega^2\tau_2^2)}\right\} \qquad \text{.....(2.16)}$$

Substituting $\tau_2 = \tau_1 e^{\frac{v_0}{kT}}$ in the R.H.S of the above eq. (2.16) one gets

$$\frac{\varepsilon' - \varepsilon_\infty}{\varepsilon_0 - \varepsilon_\infty} = 1 - \frac{1}{\frac{2v_0}{kT}} \ln \left(\frac{1 + \omega^2 \tau_1^2 \, e^{\frac{2v_0}{kT}}}{1 + \omega^2 \tau_1^2} \right)$$

$$= 1 - \frac{1}{2A} \ln \frac{1 + \omega^2 \tau_s^2 \, e^{2A}}{1 + \omega^2 \tau_s^2} \qquad \text{.....(2.17)}$$

where τ_s is the small limiting relaxation time = τ_1 and A = Fröhlich parameter = $\frac{v_0}{kT}$ = $\ln(\tau_2/\tau_1)$.

let us now put $\omega\tau = Z$ on the R.H.S of eq. (2.15) which after simplication yields :

$$\frac{\varepsilon''}{\varepsilon_0 - \varepsilon_\infty} = \frac{kT}{v_0} \int_{\omega\tau_1}^{\omega\tau_2} \frac{dZ}{1 + Z^2}$$

$$= \frac{1}{\frac{v_0}{kT}} \left[\tan^{-1}(\omega\tau_2) - \tan^{-1}(\omega\tau_1) \right]$$

$$= \frac{1}{A} \left[\tan^{-1}(e^A \, \omega\tau_s) - \tan^{-1}(\omega\tau_s) \right] \qquad \text{.....(2.18)}$$

In case of a polar solute (j) dissolved in a nonpolar solvent (i) eqs. (2.17) and (2.18) are finally written as :

$$\frac{\varepsilon'_{ij} - \varepsilon_{\infty ij}}{\varepsilon_{0ij} - \varepsilon_{\infty ij}} = x = 1 - \frac{1}{2A} \ln \frac{1 + \omega^2 \tau_s^2 \, e^{2A}}{1 + \omega^2 \tau_s^2} \qquad \text{.....(2.19)}$$

and $\frac{\varepsilon''_{ij}}{\varepsilon_{0ij} - \varepsilon_{\infty ij}} = y = \frac{1}{A} \left[\tan^{-1}(e^A \omega\tau_s) - \tan^{-1}(\omega\tau_s) \right]$ ..... (2.20)

These two formulae have already been used to find out relative contributions c_1 and c_2 towards dielectric relaxations in terms of τ_1 and τ_2 as estimated in our method discussed in detail in the latter parts of this thesis.

2.2 Multiple Relaxation Mechanism

The concept of existence of more than one relaxation time in a polar molecule was put forward by many workers. In 1938 Budo[1], however, proposed a relation:

$$\frac{\varepsilon^* - \varepsilon_\infty}{\varepsilon_0 - \varepsilon_\infty} = \sum_j \frac{c_j}{1 + i\omega\tau_j} \qquad \text{.....(2.21)}$$

to represent the complex dielectric constant ε^* as the sum of a number of noninteracting Debye type dispersions. The term c_j is the weight factor of the j th type relaxation mechanism; provided $\sum c_j = 1$

2.3 Double Relaxations

Bergmann et al[2] analysed the dielectric relaxation mechanism of some pure polar liquids from the measured relaxation data at different hf electric field of GHz range in terms of two Debye type dispersions. The larger and the smaller relaxation times τ_2 and τ_1 are, however, associated with molecular and intramolecular rotations of the molecule which follow the equations:

$$\frac{\varepsilon' - \varepsilon_\infty}{\varepsilon_0 - \varepsilon_\infty} = c_1 \frac{1}{1 + \omega^2\tau_1^2} + c_2 \frac{1}{1 + \omega^2\tau_2^2} \qquad \text{.....(2.22)}$$

$$\frac{\varepsilon''}{\varepsilon_0 - \varepsilon_\infty} = c_1 \frac{\omega\tau_1}{1 + \omega^2\tau_1^2} + c_2 \frac{\omega\tau_2}{1 + \omega^2\tau_2^2} \qquad \text{.....(2.23)}$$

The terms c_1 and c_2 are the relative contributions due to τ_1 and τ_2. Both c_1 and c_2 are related by

$$c_1 + c_2 = 1 \qquad \text{.....(2.24)}$$

Putting the eqs. (2.22) and (2.23) in the following form:

$$Y = c_1 Y_1 + c_2 Y_2 \qquad \text{.....(2.25)}$$

$$Z = c_1 Z_1 + c_2 Z_2 \qquad \text{.....(2.26)}$$

where $Y = \dfrac{\varepsilon''}{\varepsilon_0 - \varepsilon_\infty}$; $Z = \dfrac{\varepsilon' - \varepsilon_\infty}{\varepsilon_0 - \varepsilon_\infty}$

$$Y_1 = \frac{\omega \tau_1}{1 + \omega^2 \tau_1^2} \; ; \; Z_1 = \frac{1}{1 + \omega^2 \tau_1^2}$$

$$Y_2 = \frac{\omega \tau_2}{1 + \omega^2 \tau_2^2} \; ; \; Z_2 = \frac{1}{1 + \omega^2 \tau_2^2}$$

A graphical analysis was, however, made by Bergmann et al [2] in order to estimate τ_1, τ_2 and c_1, c_2 which consists of plotting the normalised experimental points on a complex plane as shown in Fig 2.1. A number of chords were then drawn through the experimental points to obtain a set of parameters which is consistent for all the experimental points for a suitable value of ε_∞. A point (Y,Z) was, however, selected between the points (Y_1,Z_1) and (Y_2, Z_2) of the normalised Debye semi-circle dividing the chord in the ratio $b/a = c_1/c_2$. From the known values of c_1 and c_2 one gets τ_1 and τ_2 from the appropriate values of ε', ε'', ε_0 and ε_∞ measured at different frequencies of GHz range.

2.4. Double Relaxations Measured under Two Different Frequencies

A polar molecule capable of rotation about its axis under a microwave electric field of angular frequency ω at a given temperature is presented by Bhattacharyya et al[3]

$$\frac{\varepsilon^* - \varepsilon_\infty}{\varepsilon_0 - \varepsilon_\infty} \cdot \frac{\varepsilon_0 + 2}{\varepsilon^* + 2} = a - i\,b \qquad \text{.....(2.27)}$$

$$\text{where } a = \frac{c_1}{1 + \omega^2 \tau_1^2} + \frac{c_2}{1 + \omega^2 \tau_2^2}$$

$$\text{and } \quad b = c_1 \frac{\omega \tau_1}{1 + \omega^2 \tau_1^2} + c_2 \frac{\omega \tau_2}{1 + \omega^2 \tau_2^2} \qquad \text{.....(2.28)}$$

The terms τ_1, τ_2 and c_1, c_2 carry usual meanings of eq (2.24).

Eq (2.27) after simplification for ε^* yields:

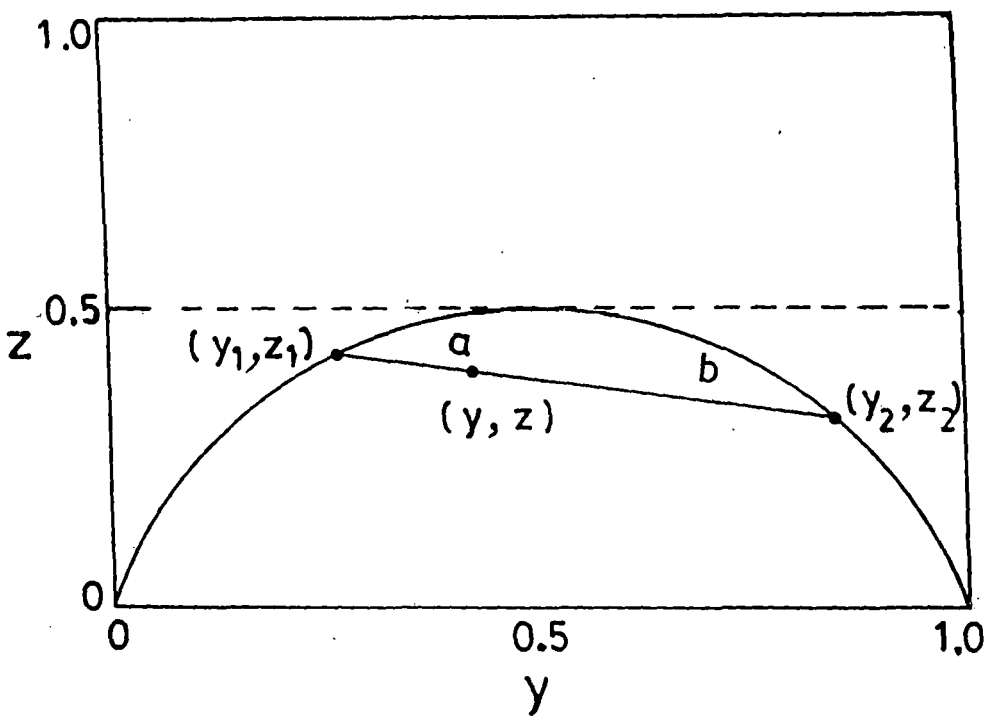

Figure 2.1 The graphical resolution of two independent Debye absorptions

$$\varepsilon^* = \frac{2\alpha(a - ib) + \varepsilon_\infty}{1 - \alpha(a - ib)}$$

$$\text{or, } \varepsilon^* - \varepsilon_\infty = \frac{\alpha(a - ib)(\varepsilon_\infty + 2)}{1 - \alpha(a - ib)}$$

$$\text{or, } \frac{\varepsilon^* - \varepsilon_\infty}{\varepsilon_0 - \varepsilon_\infty} = \frac{\alpha(a - ib)(\varepsilon_\infty + 2)}{(\varepsilon_0 - \varepsilon_\infty)\{1 - \alpha(a - ib)\}} \quad \text{..... (2.29)}$$

$$\text{where } \alpha = \frac{\varepsilon_0 - \varepsilon_\infty}{\varepsilon_0 + 2}$$

Separating the real and the imaginary parts from both sides of eq.(2.29) one gets:

$$\frac{\varepsilon' - \varepsilon_\infty}{\varepsilon_0 - \varepsilon_\infty} = \frac{a\beta - (a^2 + b^2)(\beta - 1)}{\beta^2 - 2a\beta(\beta - 1) + (a^2 + b^2)(\beta - 1)^2}$$

.....(2.30)

$$\text{and } \frac{\varepsilon''}{\varepsilon_0 - \varepsilon_\infty} = \frac{b\beta}{\beta^2 - 2a\beta(\beta - 1) + (a^2 + b^2)(\beta - 1)^2}$$

$$\text{where } \beta = \frac{\varepsilon_0 + 2}{\varepsilon_\infty + 2} = \frac{1}{1 - \alpha}$$

The terms a and b are given by:

$$a = \frac{\varepsilon_0 + 2}{\varepsilon_0 - \varepsilon_\infty}\left[\frac{(\varepsilon' - \varepsilon_\infty)(\varepsilon' + 2) + \varepsilon''^2}{(\varepsilon' + 2)^2 + \varepsilon''^2}\right]$$

& $$b = \frac{\varepsilon_0 + 2}{\varepsilon_0 - \varepsilon_\infty}\left[\frac{\varepsilon''(\varepsilon_\infty + 2)}{(\varepsilon' + 2)^2 + \varepsilon''^2}\right] \qquad \text{.....(2.31)}$$

In case of pure polar liquids if $\varepsilon_0 \approx \varepsilon' \approx \varepsilon_\infty$ and ε'' is very small, eq (2.30) is reduced to

$$\frac{\varepsilon' - \varepsilon_\infty}{\varepsilon_0 - \varepsilon_\infty} = a \text{ and } b = \frac{\varepsilon''}{\varepsilon_0 - \varepsilon_\infty}$$

which are similar like eqs (2.22) and (2.23) respectively. Putting $x_1 = \omega\tau_1$ and $x_2 = \omega\tau_2$ and using the abbreviations $\xi = 1/(1 + x^2)$ and $\eta = x/(1+x^2)$, eqs (2.28) are finally written as

$$a = c_1 \xi_1 + c_2 \xi_2$$

and $$b = c_1 \eta_1 + c_2 \eta_2 \qquad \text{.....(2.32)}$$

From equs (2.32) one gets (for $x_2 - x_1 \neq 0$ and $x_2 > x_1$)

$$c_1 = \frac{(a x_2 - b)(1 + x_1^2)}{x_2 - x_1}$$

$$c_2 = \frac{(b - a x_1)(1 + x_2^2)}{x_2 - x_1} \qquad \text{.....(2.33)}$$

Using the relation $c_1 + c_2 = 1$, eq (2.33) yields:

$$\frac{1 - a}{b} = (x_1 + x_2) - \frac{a}{b} x_1 x_2$$

or, $$\frac{1 - a}{b\omega} = (\tau_1 + \tau_2) - \frac{a\omega}{b} \tau_1 \tau_2 \qquad \text{.....(2.34)}$$

when ε', ε'', ε_0 and ε_∞ at two different frequencies ω_1 and ω_2 of the electric fields are measured at any given temperature, eq (2.34) becomes

$$\frac{1 - a_1}{b_1\omega_1} = (\tau_1 + \tau_2) - \frac{a_1}{b_1}\omega_1\tau_1\tau_2$$

and $$\frac{1 - a_2}{b_2\omega_2} = (\tau_1 + \tau_2) - \frac{a_2}{b_2}\omega_2\tau_1\tau_2$$

From the above two equations τ_1 , τ_2 and hence c_1, c_2 from eqs. (2.33) are usually estimated. In order to test the theoretical formulations described above, Bhattacharyya et al[3] used the polar liquid like phenetole, aniline and orthochloro aniline to get τ_1 , τ_2 and c_1, c_2 respectively from the measured relaxation data under 3.58 cm and 1.64 cm wavelength electric field at 45°, 60° and 75°C respectively. The data thus reported were of reasonable values.

2.5. Double Relaxation Phenomena of Polar- Nonpolar liquid Mixture under Single Frequency Electric Field.

The existing method of Bhattacharyya et al[3] although provides one with the significant improvement over the other[2] still both of them within the framework of Debye and Smyth model [23] suffer from the following inherent approximations:

i) polar-polar interactions in a pure polar liquid can not be avoided.

ii) the approximations of the equalities of $\varepsilon_0 \approx \varepsilon_\infty \approx \varepsilon'$ and $\varepsilon_0 = 0$ are not true because the dielectric relaxation parameters are usually found to be different experimentally

iii) the eq (2.27) of Bhattacharyya et al [3] seems to be complicated and is reduced to Bergmann's equations under the above approximations only and

iv) the estimated values of τ_2 and τ_1 were supposed to be constant at two different frequencies, but really they are little affected by the frequencies of the electric field of GHz range.

We, under such context proposed a very simple technique to get molecular and intra-molecular relaxation times τ_2 and τ_1 in terms of slopes and intercepts of a derived straight line equation. The equation is based on the solution data like real ε'_{ij}, imaginary ε''_{ij} parts of complex dielectric constant ε^*_{ij} as well as static ε_{0ij} and hf dielectric constant $\varepsilon_{\infty ij}$ of a solute (j) dissolved in a nonpolar solvent (i) measured under a single frequency electric field of GHz range at a given temperature. If a polar solute possesses two distinct Debye type dispersions each with a characteristic relaxation time, the eqs (2.22) and (2.23) can now be written as:

$$\frac{\varepsilon'_{ij} - \varepsilon_{\infty ij}}{\varepsilon_{0ij} - \varepsilon_{\infty ij}} = \frac{c_1}{1 + \omega^2\tau_1^2} + \frac{c_2}{1 + \omega^2\tau_2^2} \qquad \text{.....(2.35)}$$

$$\frac{\varepsilon''_{ij}}{\varepsilon_{0ij} - \varepsilon_{\infty ij}} = c_1 \frac{\omega\tau_1}{1 + \omega^2\tau_1^2} + c_2 \frac{\omega\tau_2}{1 + \omega^2\tau_2^2} \qquad \text{.....(2.36)}$$

Here, τ_1, τ_2 and c_1, c_2 carry usual significance[3] provided $c_1 + c_2 = 1$.

Substituting $\frac{\varepsilon'_{ij} - \varepsilon_{\infty ij}}{\varepsilon_{0ij} - \varepsilon_{\infty ij}} = x$ and $\frac{\varepsilon''_{ij}}{\varepsilon_{0ij} - \varepsilon_{\infty ij}} = y$

with $\omega\tau = \alpha$ in the eqs (2.35) and (2.36) one gets:

$$x = c_1a_1 + c_2a_2 \qquad \text{.....(2.37)}$$

$$y = c_1b_1 + c_2b_2 \qquad \text{.....(2.38)}$$

where $a = 1/1 + \alpha^2$ and $b = \alpha/1 + \alpha^2$

The suffices 1 and 2 with a and b are, however, related. to τ_1 and τ_2 respectively. From eqs (2.37) and (2.38) since $\alpha_2 \neq \alpha_1$, we have

$$c_1 = \frac{(x\alpha_2 - y)(1 + \alpha_1^2)}{\alpha_2 - \alpha_1} \qquad \text{.....(2.39)}$$

$$c_2 = \frac{(y - x\alpha_1)(1 + \alpha_2^2)}{\alpha_2 - \alpha_1} \qquad \text{.....(2.40)}$$

Now, using the relation $c_1 + c_2 = 1$, one can easily get the following equation with the help of eqs (2.39) and (2.40):

$$\frac{1 - x}{y} = (\alpha_1 + \alpha_2) - \frac{x}{y}\alpha_1\alpha_2 \qquad \text{.....(2.41)}$$

Substituting the values of x,y and α in the above expression we have

$$\frac{\varepsilon_{0ij} - \varepsilon'_{ij}}{\varepsilon'_{ij} - \varepsilon_{\infty ij}} = \omega(\tau_1 + \tau_2)\frac{\varepsilon''_{ij}}{\varepsilon'_{ij} - \varepsilon_{\infty ij}} - \omega^2\tau_1\tau_2 \qquad \text{.....(2.42)}$$

This is simply a straight line between $(\varepsilon_{0ij} - \varepsilon'_{ij})/(\varepsilon'_{ij} - \varepsilon_{\infty ij})$ and $\varepsilon''_{ij}/(\varepsilon'_{ij} - \varepsilon_{\infty ij})$ having intercept $-\omega^2\tau_1\tau_2$ and slope $\omega(\tau_1 + \tau_2)$ respectively. Here $\omega = 2\pi f$, f being the frequency of the alternating electric field. In order to get the slope and intercept, the eq (2.42) could, however, be fitted with the data of ε'_{ij} ε''_{ij}, ε_{0ij} and $\varepsilon_{\infty ij}$ at different ω_j's measured under a single frequency electric field at a given temperature. The estimated slope and intercept are finally used to get τ_2 and τ_1 to represent molecular and intramolecular relaxation times of a polar liquid in nonpolar solvent.

The Fröhlich parameter A ($= \ln \tau_2/\tau_1$) as seen in eq.(2.17) for polar solutes exhibiting the double relaxation phenomena are used to evaluate both x and y of eqs. (2.17) and (2.18) in terms of ω and the small limiting relaxation time $\tau_s = \tau_1$. The computed values of x and y are used to obtain c_1 and c_2 from eqs (2.39) and (2.40). In the framework of Debye and Smyth model, the values of c_1 and c_2 are estimated for the fixed values of x and y at infinite dilutions. The plots of x and y against ω_j's could, however, be made. They vary usually concave and convex manner respectively in accordance with the eqs. (2.35) and (2.36). The graphs are then extrapolated to get x and y at $\omega_j \rightarrow 0$. This is really in conformity with the fixed values of τ_1 & τ_2 and c_1 & c_2 when substituted in the R.H.S of eqs. (2.35) and (2.36) for fixed x and y in the L.H.S of those eqs. (2.35) and (2.36).

2.6. Theoretical Formulation to Estimate μ_1, μ_2 in Terms of τ_1, τ_2

The hf conductivity K_{ij} for a polar nonpolar liquid mixture (ij) has already been given by Murphy and Morgan eq (1.58) which is a function of ω_j of a polar solute. In the hf electric field, although $\varepsilon''_{ij} << \varepsilon'_{ij}$, the term ε''_{ij} still offers resistance to polarisation. Thus the real part K'_{ij} of the hf conductivity of a polar nonpolar liquid mixture at T K is [4)]

$$K'_{ij} = \frac{\mu_j^2 N \rho_{ij} F_{ij}}{3 M_j k T} \left(\frac{\omega^2 \tau}{1 + \omega^2 \tau^2} \right) \omega_j \qquad \text{.....(2.43)}$$

Differentiating the eq (2.43) with respect to ω_j and for $\omega_j \rightarrow 0$ yields that

$$\left(\frac{d K'_{ij}}{d \omega_j} \right)_{\omega_j \rightarrow 0} = \frac{\mu_j^2 N \rho_i F_i}{3 M_j k T} \left(\frac{\omega^2 \tau}{1 + \omega^2 \tau^2} \right) \qquad \text{..... (2.44)}$$

where M_j is the molecular weight of a polar solute, N is the Avogadro's number, k is the Boltzmann constant, the local field $F_{ij} = 1/9\,(\varepsilon_{ij} + 2)^2$, becomes $F_i = 1/9\,(\varepsilon_i + 2)^2$ and the density $\rho_{ij} \rightarrow \rho_i$ the density of the solvent at $\omega_j \rightarrow 0$

Again, total hf conductivitity $K_{ij} = \frac{\omega}{4\pi} \varepsilon'_{ij}$ can be written as

$$K_{ij} = K_{\infty ij} + \frac{1}{\omega \tau} K'_{ij}$$

$$\text{or, } \left(\frac{d K'_{ij}}{d \omega_j} \right)_{\omega_j \rightarrow 0} = \omega \tau \left(\frac{d K_{ij}}{d \omega_j} \right)_{\omega_j \rightarrow 0} = \omega \tau \beta \qquad \text{.....(2.45)}$$

where β is the slope of the K_{ij} - ω_j curve at $\omega_j \rightarrow 0$. From eqs. (2.44) and (2.45) we thus get.

$$\mu_j = \left(\frac{27 M_j k T \beta}{N \rho_i (\varepsilon_i + 2)^2 \omega b} \right)^{\frac{1}{2}} \qquad \text{..... (2.46)}$$

as the dipole moments μ_1 and μ_2 in terms of b, where b is a dimensionless parameter given by

$$b = \frac{1}{1 + \omega^2\tau^2} \qquad \text{.....(2.47)}$$

for τ_0, τ_1 and τ_2 respectively.

2.7. A Brief Review Works

The process of derivation of dipole moments μ from hf conductivity measurements shows that the relaxation time plays a significant role in yielding the dipole moment μ of polar liquids.

Acharyya and Chatterjee[5] used the slope of the curve of the variation of the microwave conductivity with concentration at infinite dilutions to obtain μ of some substituted benzotrifluorides and benzenes at 35°C under nearly 3cm wavelength electric field. The estimated μ showed the excellent agreement with the reported ones, suggesting the uniqueness of the method adopted.

Acharyya et al [6] used the uhf conductivity K_{ijk} of N, methyl acetamide in several nonpolar solvents in the lower as well as higher concentrations to throw much light regarding constant conductivity at $\omega_j \rightarrow 0$ due to solvation effect at different temperatures.

Chatterjee et al [7] measured the concentration variation of uhf conductivity K_{ijk} of ternary solutions at 9.885 GHz electric field for different mole fractions of N, N-dimethyl formamide (DMF) with N,N tetramethyl urea (TMU) and N,N-dimethyl acetamide (DMA) at different temperatures. The mole fraction and temperature variation of μ as seen in Figs (2.2) and (2.3) indicate the very existence of solute-solvent and solute-solute molecular associations in liquids. All these facts mentioned above inspired us to study high frequency absorptions by different nonspherical polar liquids in nonpolar solvents to arrive at the definite conclusions regarding monomer and dimer formations in liquid mixture.

We [8] in the mean time developed the theoretical procedure to estimate the double relaxation times τ_1 and τ_2 of some nonspherical polar liquids in solvent benzene and carbon tetrachloride at 9.945 GHz electric field using the single frequency measured relaxation data. The hf conductivity technique had also been used to get μ_1 and μ_2 in terms of slope β of K_{ij}- ω_j curve. The close agreement of computed μ_2 with the μ's in literature inidicates the correctness of the method suggested. This is beautifully presented and displayed in Chapter III of this thesis.

The Chapter IV is concerned with the use of the single frequency measurement technique on the dielectric relaxation parameters to measure τ_2 and τ_1 of some monosubstituted anilines for three different electric field frequencies of GHz range at 35°C. The o-and m-anisidine like p-toluidines exhibit double relaxation phenomena at 3.86 and 22.06 GHz. o-and m-toluidines show the same effect at 2.02 and 3.86 GHz respectively. p-anisidine alone shows the monorelaxation behaviour at all frequencies. The relative contributions c_1 and c_2 towards dielectric relaxations are calculated in terms of x,y and τ_1, τ_2. The dipole moments μ_1, μ_2 were also calculated in terms of slopes β's of concentration variation of their conductivity curves in order to compare with those from bond angles and bond moments of the molecules concerned.

An attempt has been made in Chapter V to show the fact that monosubstituted anilines exhibit double relaxation times at 9.945 GHz electric field which seems to be the most effective dispersive region for such molecules. All the anilines also possess symmetric distribution of relaxation behaviour at nearly 10 GHz electric field.

2.8. Symmetric Distribution of Relaxation Times

Cole and Cole [9] presented a relation:

$$\frac{\varepsilon^*_{ij} - \varepsilon_{\infty ij}}{\varepsilon_{0ij} - \varepsilon_{\infty ij}} = \frac{1}{1 + (j\omega\tau_s)^{1-\gamma}} \qquad \text{.....(2.48)}$$

in order to represent the symmetric distribution behaviour of nonrigid molecules. Here,

γ = symmetric distribution parameter associated with symmetric relaxation times τ_s

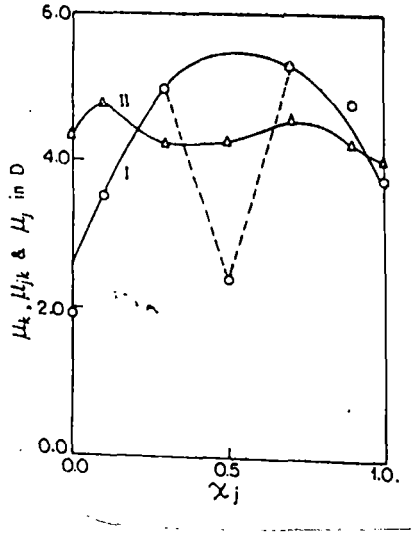

Figure 2.2 Variation of experimentally observed dipole moments μ_k, μ_{jk} and μ_j with mole fraction of DMF in (DMF+TMU) and (DMF+DMA) mixtures at 15°C (-o- for DMF+TMU and -Δ- for DMF+DMA)

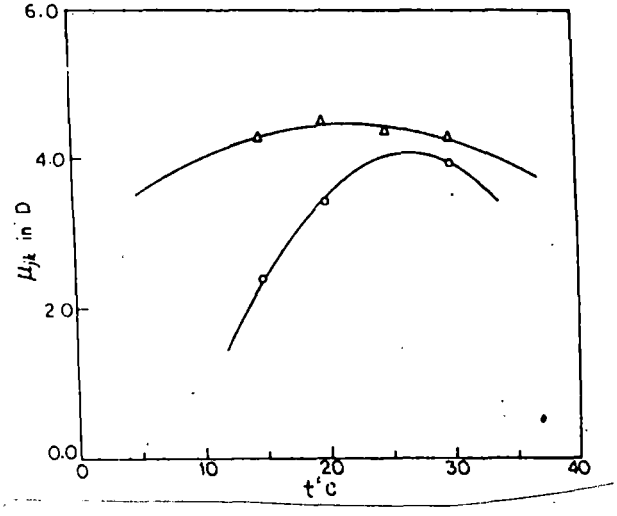

Figure 2.3 Variation of experimentally observed dipole moments with temperature in °C for DMF+TMU and DMF+DMA in 1:1 mixtures at 15°C (-o- for DMF+TMU and -Δ- for DMF+DMA)

$$\text{or, } \frac{\varepsilon^*_{ij} - \varepsilon_{\infty ij}}{\varepsilon_{0ij} - \varepsilon_{\infty ij}} = \frac{1}{1 + j\left[\cos\left(\frac{\gamma\pi}{2}\right) - j\sin\left(\frac{\gamma\pi}{2}\right)\right](\omega\tau_s)^{1-\gamma}}$$

$$= \frac{1 + (\omega\tau_s)^{1-\gamma}\sin\left(\frac{\gamma\pi}{2}\right) - j(\omega\tau_s)^{1-\gamma}\cos\left(\frac{\gamma\pi}{2}\right)}{1 + 2(\omega\tau_s)^{1-\gamma}\sin\left(\frac{\gamma\pi}{2}\right) + (\omega\tau_s)^{2(1-\gamma)}}$$

Separating real and imaginary parts from both sides one gets

$$\frac{\varepsilon'_{ij} - \varepsilon_{\infty ij}}{\varepsilon_{0ij} - \varepsilon_{\infty ij}} = x = \frac{1 + (\omega\tau_s)^{1-\gamma}\sin\left(\frac{\gamma\pi}{2}\right)}{1 + 2(\omega\tau_s)^{1-\gamma}\sin\left(\frac{\gamma\pi}{2}\right) + (\omega\tau_s)^{2(1-\gamma)}}$$

$$\frac{\varepsilon''_{ij}}{\varepsilon_{0ij} - \varepsilon_{\infty ij}} = y = \frac{(\omega\tau_s)^{1-\gamma}\cos\left(\frac{\gamma\pi}{2}\right)}{1 + 2(\omega\tau_s)^{1-\gamma}\sin\left(\frac{\gamma\pi}{2}\right) + (\omega\tau_s)^{2(1-\gamma)}} \quad \text{.....(2.49)}$$

The symmetric distribution parameter γ and relaxation time τ_s can be given by the relations:

$$\gamma = \frac{2}{\pi}\tan^{-1}\left[(1 - x)\frac{x}{y} - y\right] \quad \text{.....(2.50)}$$

$$\tau_s = \frac{1}{\omega}\left\{\frac{1}{\left[\frac{x}{y}\cos\left(\frac{\gamma\pi}{2}\right) - \sin\left(\frac{\gamma\pi}{2}\right)\right]}\right\}^{\frac{1}{1-\gamma}} \quad \text{..... (2.51)}$$

where x and y are the fixed estimated values at $\omega_j \rightarrow 0$ as obtained from graphical plot of eqs (2.35) and (2.36).

2.9. Asymmetric Distribution of Relaxation Times

Davidson and Cole[10] showed the following relation for the molecules possessing asymmetric distribution of relaxation times as:

$$\frac{\varepsilon^*_{ij} - \varepsilon_{\infty ij}}{\varepsilon_{0ij} - \varepsilon_{\infty ij}} = \frac{1}{(1 + j\,\omega\,\tau_{cs})^{\delta}} \qquad \text{.....(2.52)}$$

where δ = asymmetric distribution parameter associated with characteristic relaxation time τ_{cs}. Let $\omega\tau_{cs} = \tan\phi$. On substitution in eq (2.52) and after simplification one can write.

$$\frac{\varepsilon^*_{ij} - \varepsilon_{\infty ij}}{\varepsilon_{0ij} - \varepsilon_{\infty ij}} = \frac{(\cos\phi)^{\delta}}{\cos\delta\phi + j \sin\delta\phi}$$

$$= (\cos\phi)^{\delta} \cos(\delta\phi) - j\,(\cos\phi)^{\delta} \sin\delta\phi$$

Separating real and imaginary parts yields

$$\frac{\varepsilon'_{ij} - \varepsilon_{\infty ij}}{\varepsilon_{0ij} - \varepsilon_{\infty ij}} = x = (\cos\phi)^{\delta} \cos(\delta\phi) \qquad \text{.....(2.53)}$$

$$\frac{\varepsilon''_{ij}}{\varepsilon_{0ij} - \varepsilon_{\infty ij}} = y = (\cos\phi)^{\delta} \sin(\delta\phi) \qquad \text{.....(2.54)}$$

Similarly, δ and τ_{cs} can be had in terms of x and y at $\omega_j \rightarrow 0$ as.

$$\tan(\delta\phi) = \frac{y}{x} \qquad \text{.....(2.55)}$$

and $$\tan\phi = \omega\,\tau_{cs} \qquad \text{.....(2.56)}$$

As the values of ϕ can not be estimated directly we draw a theoretical curve for log (cos $\phi)^{\frac{1}{\phi}}$ against ϕ from which

$$\log (\cos \phi)^{\frac{1}{\phi}} = \frac{\log \frac{x}{\cos(\delta\phi)}}{\delta\phi} \qquad \text{.....(2.57)}$$

can be known. With the known ϕ one can estimate τ_{cs} and δ from eqs (2.56) and (2.55) respectively. On comparison the symmetric and asymmetric distribution behaviours it is found that all the mono-substituted anilines show the symmetric distribution of relaxation times. This has been discussed in Chapter V of the thesis.

The double relaxation behaviours of several normal and isomeric octyl alchohols dissolved in n-heptane under 24.33, 9.25 and 3.00 GHz electric fields at 25°C have been studied using single frequency measurement technique of dielectric relaxation parameters. The results are, however, presented in Chapter VI for normal alcohols and Chapter VII for isomeric octyl alcohols respectively.

It is interesting to note that all the alcohols show double relaxation times at each frequency with the exception of methanol in C_6H_6 at 9.84 GHz electric field. Although, Onsager's equation may be a better choice for such polymeric long chain molecules, but our method seems to be very much simple and straightforward within the framework of Debye and Smyth model. The corresponding μ_1, μ_2 were also calculated from slopes of K_{ij}-ω_j curves and compared with those due to bond angles and bond moments. The conformational structures also accord with the measured data.

The structural and associational aspects of some binary and single polar solutes in nonpolar solvents are given in Chapter VIII with the use of hf conductivity measurement of solutions. The valuable information on monomer and dimer formations of polar liquids at 9.945 GHz electric field as well as the temperature dependence of mesomeric and inductive moments of the various substituent groups of such polar molecules were observed.

2.10. Experimental Techniques

It is clear from the above chapters that the relaxation data of polar-nonpolar liquid mixtures under the microwave electric fields of nearly 10 GHz are expected to yield very interesting results. We, therefore, are very much tempted to perform experiments on some aprotic polar liquids like dimethyl sulphoxide (DMSO), N,N-dimethyl formamide (DMF); N,N-dimethyl acetamide (DMA) and N,N-tetra methyl urea (TMU) in C_6H_6 under 9.945 GHz electric field at different temperatures. The liquids are widely used in medicine and industry. They are already investigated in Chapter VIII to reveal their associational aspects. Thus, the purpose of the present experiment is only to observe whether they show either the double or monorelaxation behaviour at 9.945 GHz electric fields.

2.10 (a) Experimental Set up

The Block diagram of the experimental set up for the measurements of dielectric relaxation solution (ij) data is given in Fig(2.4). It consists of sample holder, temperature chamber, temperature controller and Hewlett Packard Bridge 4192A. The real ε'_{ij} and imaginary ε''_{ij} parts of complex dielectric constant ε_{ij}^* as well as static dielectric constant ε_{oij} of the polar-nonpolar mixture were measured at different temperatures at the desired electric field frequencies. The permittivity at infinite frequency $\varepsilon_{\infty ij}$ ($= n^2_{Dij}$) were, however, measured by Abbe's Refractometer.

2.10 (b) The Cell Construction and Sample Holder

A cell with a sample holder consists of two glass plates. The inner surfaces are coated with conducting layer of ITO (Indium Tin Oxide) as shown in Fig (2.5). A capacitor is thus formed with the active area of 1 cm^2. The glass plates are seperated by 40 μm apart. The connecting leads of 1m length are used for measurements. The sample for measurements is placed on the lower glass plate in contact with front edge of the upper glass plate and kept on Mettler Hot Stage FP 52. The sample is filled up by capillary action and during fill up it is essential to avoid air bubble.

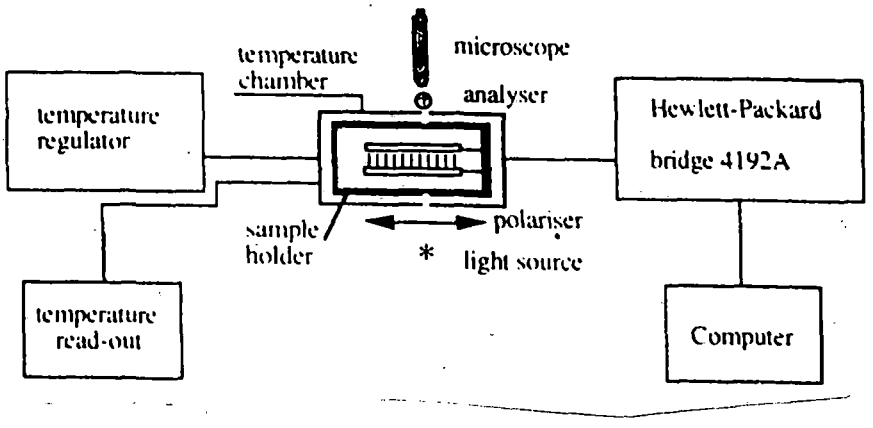

Figure 2.4 Block Diagram of the experimental set up used for dielectric measurements

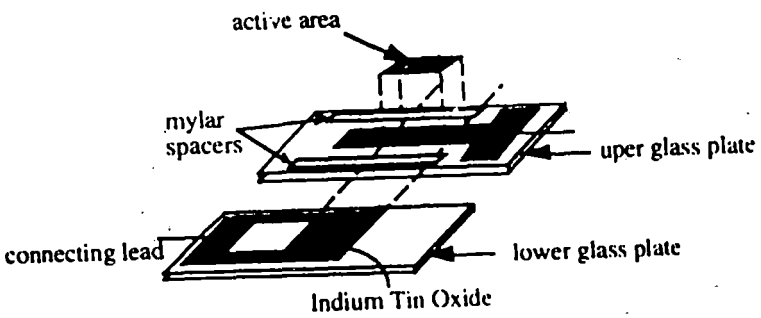

Figure 2.5 Inner surfaces of the lower and upper conducting glass plates

2.10 (c) Capacitance and Conductance Measurement by HP LF Impedence Analyser

The Block diagram of Hewlett Packard Impedence Analyser (HP 4192A) for measuring the capacitance and conductance of the cell in the frequency range of 5Hz to 13 MHz is shown in Fig (2.6). It can perform impedence measurement in the above frequency range in an almost continuous sweep. The frequency may be scanned either linearly or logarithmically. The generator generates AC signal with an amplitude variable from 5mv to 1.1 Volt. One of the disadvantage of the bridge is that its capability of impedence measurements is limited to 3 MΩ. This restricts the accuracy of the measurements at lower frequencies. However, if the capacitance of the sample is large enough, the accuracy is improved because the impedence become measurable by the bridge. When the bridge is balanced as shown in Fig (2.6), the current I_d is zero, i.e.

$$I_x = I_r \qquad \text{.....(2.58)}$$

The voltage drop across the sample is equal to that across the range resistor R_r. The complex impedence of the sample Z_x^* is given by

$$Z_x^* = R_r \frac{e_s^*}{e_r^*} \qquad \text{.....(2.59)}$$

where e_s^* and e_r^* are the complex voltages respectively. From the measurements of the complex impedence; the bridge evaluates the capacitance and conductance values.

2.10 (d) Cell Calibration

Our measurement cell consists of a parallel plate capacitor connected with relatively short leads. The cell thickness is determined by the myler spacer or glass spacer between glass plates. The measured air capacitance C_0 has a contribution from the capacitance of the active area of the plates. The stray capacitance arises from the leads and the nonhomogeneities of the field lines at the edges of the active area. The spacers do not

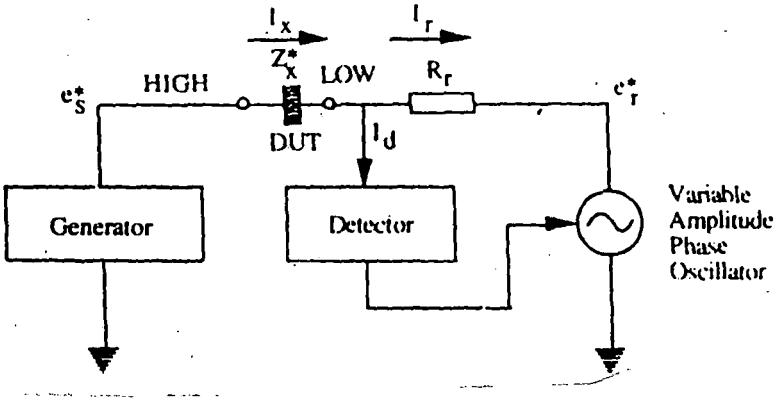

Figure 2.6 Block diagram of the HP 4192A bridge (5Hz to 13 MHz)

contribute to the capacitance because they are placed outside the active area. In this case C_0 is written as

$$C_o = C_L + C_s \qquad \text{.....(2.60)}$$

where C_L is the capacitance of the empty cell excluding the stray capacitance.To determine the stray capacitance, two standard liquids (Spec-pure benzene and para-xylene) with known dielectric permittivity were used. When the cell is filled with a liquid of known dielectric permittivity ε, the measured capacitance will be given by

$$C = \varepsilon C_L + C_s \qquad \text{.....(2.61)}$$

From the above two, eqs (2.60) and (2.61), the value of C_s is calculated. The error in measurement of C_s for standard liquids is $\pm$ 1%. The real part of the dielectric permittivity of the sample is then given by

$$\varepsilon'_{ij} = (C - C_s)/ (C_o - C_s) \qquad \text{.....(2.62)}$$

where C is the capacitance of the cell filled with the sample. The dielectric absorption for the sample is calculated from conductance measurement by

$$\varepsilon''_{ij} = G_{ij} / 2\pi f C_0 \qquad \text{.....(2.63)}$$

where G_{ij} is the conductance and f is the frequency of the electric field. In order to get the real and imaginary permittivity of the dielectric sample at 9.945 GHz,graphs were plotted with ε'_{ij} and ε''_{ij} against f for a fixed temperature and concentration of the sample. Lastly, an extrapolation procedure was adopted to get values at 9.945 GHz electric field. The findings of the experimental data are displayed column-wise in Chapter IX.

2.11. Dipole Moments of Isotopomer Molecules

The dipole moments of isotopomer molecular ions play a significant role in the photon induced dissociation process of such molecules. Photo-dissociation is used in the study of modelling the ionised atmosphere, photo chemical reactions and is, therefore, an important mechanism for destruction of inter stellar molecules. Moreover, the observed asymmetry

in the forward and backward scattering process of the fragments produced from the collision induced dissociation of heteronuclear molecular ions depends on their dipole moments.

We, in the Chaper X have calculated the dipole moments of HD^+, HT^+ molecular ions using Morse function since the diatomic molecular ions are supposed to obey the Morse potential excellently. The calculated values of μ by using Morse potential when compared with those of Saha [11] reveal the applicability of the method suggested.

Although, Morse-Kratzer [12] potential was supposed to be the most real potential for such heteronuclear molecular ions, but the calculated values did not yield better result.

In the last chapter XI, we have given the summary and concluding remarks of the whole thesis.

REFERENCES

1. A Budo, Phys. Z 39 706 (1938)
2. K Bergmann, D M Roberti and C P Smyth, J.Phys. Chem.64 665 (1960)
3. J Bhattacharyya, A Hasan, S B Roy and G S Kastha, J.Phys. Soc. Japan **28** 204(1970)
4. C P Smyth, Dielectric Behaviour and structure (McGraw Hill: New York) (1955)
5. S Acharyya and A K Chatterjee, Indian J.Pure & Appl. Phys. **23** 484 (1955)
6. C R Acharyya, A K Chatterjee, P K Sanyal and S Acharyya, Indian J Pure & Appl. Phys. **24** 234 (1986)
7. A K Chatterjee, U Saha, N Nandi, R C Basak and S Acharyya, Indian J. Phys **66B** 2921 (1992).
8. U Saha, S K Sit, R C Basak and S Acharyya, J.Phys. D: Appl. Phys.(London) **27** 596 (1994)
9. K S Cole and R H Cole ; J Chem. Phys. 9 341 (1941)
10. D W Davidson and R H Cole; J.Chem. Phys. **19** 1484 (1951)
11. S Saha; Indian J.Phys. **48** 849 (1974)
12. H N Singh and V B Singh; Indian J.Pure & Appl. Phys **31** 341 (1993)

PART A

CHAPTER 3

DOUBLE RELAXATION TIMES OF NON-SPHERICAL POLAR LIQUIDS IN NON-POLAR SOLVENT : A NEW APPROACH BASED ON SINGLE FREQUENCY MEASUREMENT

3.1. Introduction

The dielectric relaxation of polar liquids in non-polar solvents is much simpler in comparison to the case in pure polar liquids because, in dilute polar liquid solutions, the effects of the macroscopic viscosity, dipole-dipole interaction, internal field etc. are minimized. The dielectric relaxation parameters, namely the relaxation times τ_1 and τ_2, the dipole moments μ_1 and μ_2 etc. are the effective tools to investigate the molecular and intramolecular rotations, sizes, shapes and structures of polar molecules. Careful investigation of the phenomenon of dielectric relaxation in binary (Acharyya and Chatterjee 1985) and ternary (Chatterjee *et al* 1992, Saha and Acharyya 1993) solute-solvent mixtures is therefore necessary to throw much light on the structures of the polar liquids.

Khameshara and Sisodia (1980), Gupta *et al* (1978) and Arrawatia *et al* (1977) measured the static dielectric constant ε_{0ij}, the square of the refractive indices n^2_{Dij}, the real ε'_{ij} and imaginary ε''_{ij} parts of the complex dielectric constant ε^*_{ij} of five and seven disubstituted anilines and benzenes respectively in solvents benzene and carbon tetrachloride at 35°C under a single high-frequency 9.945 GHz electric field. Aniline as well as benzene derivatives are expected to absorb very strongly in the microwave electric field due to the presence of their flexible parts such as methyl or other groups. They are, therefore, expected to have more than one relaxation time because of the existence of internal rotation of these groups. Although, one should not make strong conclusions based on single frequency measurements, provided that the experimental values of ε_{0ij} and $\varepsilon_{\infty ij}$ are not accurately known. Non-spherical molecular liquids, on the other hand, are known to have non-Debye relaxation behaviour.

The existing method of Bergmann *et al* (1960) was involved in measurements of ε', ε'', ε_0 and ε_∞ of a non-spherical pure polar liquid for various frequencies at a given experimental temperature in degrees Celsius to yield τ_1 and τ_2. They actually used the Cole-Cole plot to make τ_1 and τ_2 represent the relaxation times of the smallest flexible unit attached to the parent ring and the molecule itself. Kastha *et al* (1969) subsequently

simplified the procedure of Bergmann *et al* (1960) by measuring the experimental parameters at two given frequencies of the electric field in the microwave region.

We, in this context, therefore thought to suggest an alternative method in which single frequency measurements of dielectric relaxation parameters like ε'_{ij}, ε''_{ij}, ε_{0ij} and $\varepsilon_{\infty ij}$ (Khameshara and Sisodia 1980, Gupta *et al* 1978 and Arrawatia *et al* 1977) for some highly non-spherical polar liquids like anilines and benzene derivatives in solvents benzene and carbon tetrachloride respectively are enough to estimate τ_1 and τ_2 within the framework of the Debye model (Bergmann *et al* 1960). The systems of polar-non-polar liquid mixtures under investigation are placed in the first columns of tables 3.1 - 3.3. Moreover, such rigorous studies on various types of di-or even mono-substituted polar compounds in non-polar solvents could be made in order to detect the existence of double relaxation phenomena from available data measured under a single frequency electric field in the gigahertz region. Finally, τ_1 and τ_2 thus estimated (table 3.1.) from our method on the basis of single frequency measurement, which appears to be much simpler, can be used to obtain μ_1 and μ_2 (see table 3.3. later) of the polar molecules from the slope β of the concentration variation of ultra-high-frequency conductivity K_{ij} of the solution (see figure 3.4. and table 3.3. later) in order to explore their conformations (see figure 3.5. later).

3.2. Theoretical formulations to estimate τ_1, τ_2 and c_1 and c_2

The relative contributions c_1 and c_2 towards the dielectric relaxation by the two extreme values τ_1 and τ_2 (Higasi *et al* 1960) can be given by (Bergmann *et al* 1960)

$$\frac{\varepsilon'_{ij} - \varepsilon_{\infty ij}}{\varepsilon_{0ij} - \varepsilon_{\infty ij}} = c_1 \frac{1}{1+\omega^2\tau_1^2} + c_2 \frac{1}{1+\omega^2\tau_2^2} \qquad \text{.....(3.1)}$$

$$\frac{\varepsilon''_{ij}}{\varepsilon_{0ij} - \varepsilon_{\infty ij}} = c_1 \frac{\omega\tau_1}{1+\omega^2\tau_1^2} + c_2 \frac{\omega\tau_2}{1+\omega^2\tau_2^2} \qquad \text{.....(3.2)}$$

provided that $c_1 + c_2 = 1$. The symbols used in equations (3.1) and (3.2) have their usual meanings. Let

Table 3.1 The double relaxation times τ_1 (smaller) and τ_2 (larger) estimated from intercepts and slopes of equation (3.7) with errors and correlation coefficients together with reported τ of polar liquids.

System with slope number and molecular weight M_j (g)	Intercept and slope of against $-\varepsilon''_{ij}/$	$(\varepsilon_{0ij}-\varepsilon'_{ij})/(\varepsilon'_{ij}-\varepsilon_{\infty ij})$	Correlation coefficient	Percentage error in regression technique	Estimated values of τ_1 and	τ_2 (ps).	Reported τ (ps)
(i) 4 -chloro-2-methyl aniline in benzene; $M_j = 141.52$	-1.4276	3.2169	0.9964	1.33	8.51	42.97	18.5
(ii) 3-chloro-4 -methyl aniline in benzene; $M_j = 141.52$	-0.5605	1.8913	0.9982	0.76	5.89	24.38	13.6
(iii) 5 - chloro - 2-methyl aniline in benzene; $M_j = 141.52$	-0.8107	2.0749	0.9727	3.67	8.36	24.85	16.6
(iv) 3-chloro-2-methyl aniline in benzene; $M_j = 141.52$	-0.3862	1.5960	0.9918	1.09	4.76	20.78	9.9
(v) 2-chloro-6-methyl aniline in benzene; $M_j = 141.52$	-0.3132	1.3711	0.9250	2.77	4.63	17.31	7.8
(vi) o-chloronitrobenzene in benzene; $M_j = 157.5$	-0.30.33	1.31.29	0.8170	3.77	4.79	16.22	13.5
(vii) 4-chloro-3-nitrotoluene in benzene; $M_j = 171.5$	-0.3863	1.8623	0.8776	11.90	3.81	25.99	20.9
(viii) m-nitrobenzo-trifluoride in benzene; $M_j = 191.0$	-0.6003	1.9038	0.9929	2.44	6.38	24.09	19.7
(ix) 4-chloro-3-nitrobenzotrifluride in carbon tetrachloride; $M_j = 225.5$	-0.0587	1.6634	0.9524	5.33	0.58	26.04	21.1
(x) o-nitrobenzotrifluoride in benzene; $M_j = 191.039$	-0.0620	1.0560	0.6992	4.17	0.99	15.90	13.7
(xi) 4-chloro-3-nitrotoluene in carbon tetrachloride; $M_j = 171.5$	-0.1335	2.2819	0.9771	7.51	0.96	35.56	35.0
(xii) 4-chloro-3-nitrobenzotrifluoride in benzene; $M_j = 225.5$	2.5194	-3.0302	-0.8599	13.07	—	10.87	10.2
(xiii) m-aminobenzo-trifluoride in benzene; $M_j = 161.05$	0.8445	0.0452	0.0088	11.38	—	15.07	14.5
(xiv) o-chloronitro-benzene in carbon tetrachloride; $M_j = 157.5$	0.0194	1.2973	0.9277	5.57	—	21.00	15.8
(xv) o-chlorobenzo-trifluoride in benzene; $M_j = 180.5$	0.2856	0.5696	0.14505	19.10	—	14.25	12.3

$$x = \frac{\varepsilon'_{ij} - \varepsilon_{\infty ij}}{\varepsilon_{0ij} - \varepsilon_{\infty ij}} \qquad y = \frac{\varepsilon''_{ij}}{\varepsilon_{0ij} - \varepsilon_{\infty ij}}$$

and $\omega\tau = \alpha$ Equations (3.1) and (3.2) can be written as

$$x = c_1 a_1 + c_2 a_2 \qquad \text{.....(3.3)}$$

$$y = c_1 b_1 + c_2 b_2 \qquad \text{.....(3.4)}$$

where $a = 1/(1+\alpha^2)$ and $b = \alpha/(1+\alpha^2)$. The suffixes 1 and 2 are related to τ_1 and τ_2 respectively. Solving equations (3.3) and (3.4) for c_1 and c_2, one gets

$$c_1 = \frac{(x\alpha_2 - y)(1 + \alpha_1^2)}{\alpha_2 - \alpha_1} \qquad \text{.....(3.5)}$$

$$c_2 = \frac{(y - x\alpha_1)(1+\alpha_2^2)}{\alpha_2 - \alpha_1} \qquad \text{.....(3.6)}$$

provided that $\alpha_2 > \alpha_1$. Now adding equations (3.5) and (3.6) we get, since $c_1 + c_2 = 1$,

$$\frac{1 - x}{y} = (\alpha_1 + \alpha_2) - \frac{x}{y}\alpha_1\alpha_2$$

or

$$\frac{\varepsilon_{0ij} - \varepsilon'_{ij}}{\varepsilon'_{ij} - \varepsilon_{\infty ij}} = \omega(\tau_1 + \tau_2)\frac{\varepsilon''_{ij}}{\varepsilon'_{ij} - \varepsilon_{\infty ij}} - \omega^2\tau_1\tau_2 \qquad \text{.....(3.7)}$$

which is simply a straight line between $(\varepsilon_{0ij} - \varepsilon'_{ij})/(\varepsilon'_{ij} - \varepsilon_{\infty ij})$ and $\varepsilon''_{ij}/(\varepsilon'_{ij} - \varepsilon_{\infty ij})$ having intercept $-\omega^2\tau_2\tau_2$ and slope $\omega(\tau_1 + \tau_2)$ where $\omega = 2\pi f$, f being the frequency of the applied electric field in the gigahertz region. When equation (3.7) is fitted to the experimental data ε'_{ij}, ε''_{ij}, ε_{0ij} and $\varepsilon_{\infty ij}$ for different concentrations ω_j of each of the polar molecules at 35°C, we get the intercept and slope and the corresponding values of τ_1 and τ_2 found as shown in table (3.1.) together with the reported τ. The error as well as correlation coefficient were also found for each curve of equation (3.7) and placed in table (3.1.), only to see how far they are linear as shown in figure 3.1.

The Fröhlich parameters A, where $A = \ln(\tau_2/\tau_1)$ shown in table 3.2 for all the polar compounds, are used to evaluate both x and y of equations (3.3) and (3.4) in terms of ω

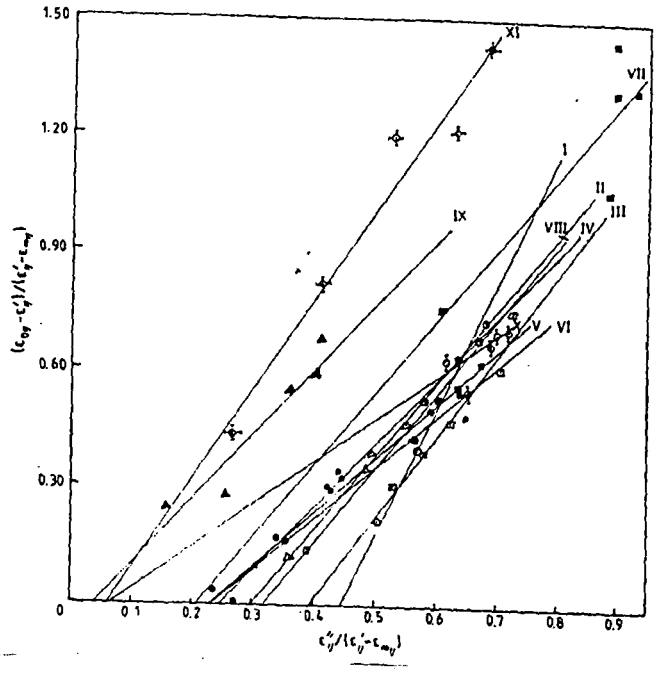

Figure 3.1 Straight line plots of $(\varepsilon_{0ij} - \varepsilon'_{ij})/(\varepsilon'_{ij} - \varepsilon_{\infty ij})$ against $\varepsilon''_{ij}/(\varepsilon'_{ij} - \varepsilon_{\infty ij})$ for the polar–non-polar liquid mixtures : (I), (II), (III), (IV), (V), of disubstituted anilines (VI), (VII), (VIII), (IX), (X) and (XI) of disubstituted benzenes respectively at 35°C (Table 3.1)

and small limiting relaxation time τ_s, where $\tau_s = \tau_1$ by the following equations (Fröhlich 1949):

$$\frac{\varepsilon'_{ij} - \varepsilon_{\infty ij}}{\varepsilon_{0ij} - \varepsilon_{\infty ij}} = 1 - \frac{1}{2A} \ln \left(\frac{1 + e^{2A\omega^2\tau_s^2}}{1+\omega^2\tau_s^2} \right) \qquad \text{.....(3.8)}$$

$$\frac{\varepsilon''_{ij}}{\varepsilon_{0ij} - \varepsilon_{\infty ij}} = \frac{1}{A} \left[\tan^{-1} (e^A \omega\tau_s) - \tan^{-1} (\omega\tau_s) \right] \qquad \text{..... (3.9)}$$

The computed values of x and y from the above equations and the corresponding c_1 and c_2 from equations (3.1) and (3.2) are presented in table 3.2. Again the left hand sides of equations (3.1) and (3.2) are obviously the functions of ω_j of the solute in a given solvent, as is evident from the plots of x and y against ω_j in figures 3.2 and 3.3 respectively. This at once prompted us to get the fixed values of x and y when $\omega_j \rightarrow 0$ from figures 3.2 and 3.3 to estimate c_1 and c_2, which are shown in table 3.2 for comparison with those of Fröhlich (1949). This is really in conformity with the fixed estimated values of τ_1 and τ_2 from the slope and intercept of equation (3.7) for each compound when substituted on the right-hand sides of equations (3.1) and (3.2).

3.3 Mathematical formulations to estimate μ_1 and μ_2

According to Murphy and Morgan (1939) the ultra-high-frequency (UHF) conductivity K_{ij} as given by

$$K_{ij} = \frac{\omega}{4\pi} (\varepsilon'^2_{ij} + \varepsilon''^2_{ij})^{1/2} \qquad \text{.....(3.10)}$$

is a function of ω_j of a polar solute. Even in the high-frequency (HF) electric field $\varepsilon''_{ij} << \varepsilon'_{ij}$, ε''_{ij} is responsible for offering resistance to polarization. Hence the real part K'_{ij} of the HF conductivity of a polar-non-polar liquid mixture at a given temperature T K is given by (Smyth 1955)

$$K'_{ij} = \frac{\mu_j^2 N \rho_{ij} F_{ij}}{3M_j kT} \left(\frac{\omega^2\tau}{1+\omega^2\tau^2} \right) \omega_j \qquad \text{.....(3.11)}$$

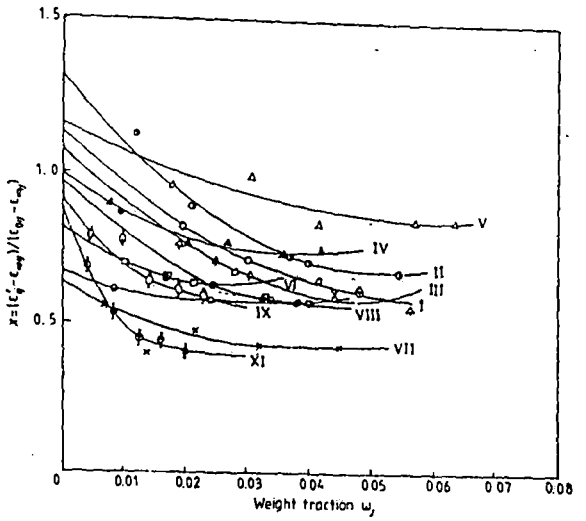

Figure 3.2 Variation of $(\varepsilon'_{ij} - \varepsilon_{\infty ij})/(\varepsilon_{oij} - \varepsilon_{\infty ij})$ against weight fraction ω_j of polar solutes in dilute solutions at 35°C (Table 3.2): (I), (II), (III), (IV), (V), of disubstituted anilines, (VI), (VII), (VIII), (IX), (X) and (XI) of disubstituted benzenes respectively

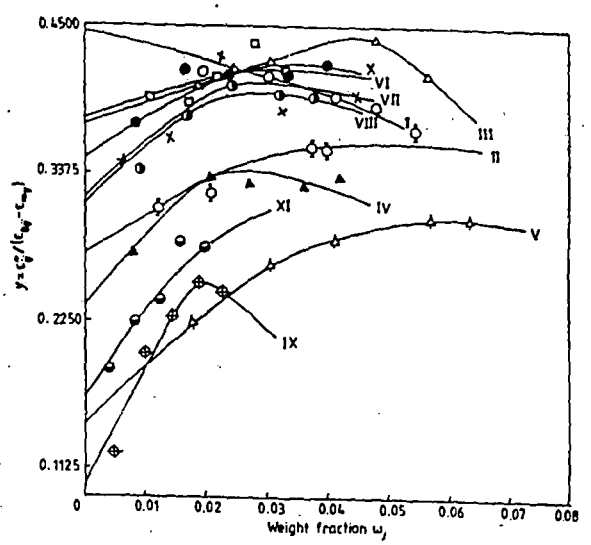

Figure 3.3 Variation of $\varepsilon''_{ij}/(\varepsilon_{oij} - \varepsilon_{\infty ij})$ against weight fraction ω_j of polar solutes in dilute solutions at 35°C (Table 3.2): (I), (II), (III), (IV), (V), of disubstituted anilines, (VI), (VII), (VIII), (IX), (X) and (XI) of disubstituted benzenes respectively

Table 3.2 Reported Fröhlich parameter A, relative contributions c_1 and c_2 towards dielectric relaxations with estimated values of x and y due to Fröhlich equation (3.8) and (3.9) and those by our method.

System with slope number and molecular weight M_j (g)	Fröhlich parameter A $= \ln(\tau_2/\tau_1)$	Theoretical x and y equations (3.9)	values of using (3.8) and	Theoretical c_1 and	values of c_2	Estimated $x = \left(\frac{\varepsilon' - \varepsilon_\infty}{\varepsilon_0 - \varepsilon_\infty}\right)_{\omega_j \to 0}$	values of $y = \left(\frac{\varepsilon''}{\varepsilon_0 - \varepsilon_\infty}\right)_{\omega_j \to 0}$	Estima values c_1 and	ted of c_2
(i) 4-chloro-2-methyl aniline in benzene; $M_j = 141.52$	1.6193	0.4269	0.4478	0.4159	0.8418	1.14	0.4455	i.5577	-0.6112
(ii) 3-chloro-4-methyl aniline in benzene ; $M_j = 141.52$	1.4205	0.8448	0.4483	0.8239	0.3953	1.32	0.2745	1.7061	-0.6065
(iii) 5-chloro-2-methyl aniline in benzene; $M_j = 141.52$	1.0894	0.5478	0.4745	0.4642	0.6239	1.08	0.3758	1.6069	-0.6227
(iv) 3-chloro-2-methyl aniline in benzene ; $M_j = 141.52$	1.4737	0.6937	0.4241	0.5180	0.5845	0.99	0.2385	1.1382	-0.1497
(v) 2-chloro-6-methyl aniline in benzene; $M_j = 141.52$	1.3187	0.7369	0.4114	0.5272	0.5430	1.17	0.1440	1.5339	-0.5334
(vi) o-chloro nitrobenzene in benzene; $M_j = 157.5$	1.2197	0.7456	0.4107	0.5259	0.5326	0.82	0.3803	0.6874	0.3832
(vii) 4-chloro-3-nitrotoluene in benzene; $M_j = 171.5$	1.9201	0.6783	0.4086	0.5282	0.6486	0.64	0.3173	0.5504	0.4328
(viii) m-nitrobenzotrifluoride in benzene; $M_j = 191.0$	132.86	0.6103	0.4551	0.4852	0.6252	0.97	0.3128	1.2013	-0.2176
(ix) 4-chloro-3-nitrobenzo-trifluoride in carbon tetrachloride; $M_j = 225.5$	3.8044	0.8302	0.2583	0.6876	0.5231	0.91	0.1012	0.8682	0.1565
(x) o-nitrobenzotrifluoride in benzene; $M_j = 191.039$	2.7764	0.8771	0.2592	0.6595	0.4371	0.67	0.3487	0.3413	0.6554
(xi) 4-chloro-3-nitrotoluene in carbontetrachloride $M_j = 171.5$	3.6120	0.7540	0.3010	0.6379	0.7022	0.88	0.1642	0.8314	0.3061

where M_j is the molecular weight of polar solute, N is Avogadro's number, k is the Boltzmann constant and F_{ij} ($= [(\varepsilon_{ij} + 2)/3]^2$) is the local field. The total HF Conductivity $K_{ij} = \omega \varepsilon''_{ij}/ 4\pi$ can be represented by

$$K_{ij} = K_{ij\infty} + K'_{ij}/\omega\tau$$

$$\text{or} \quad \left(\frac{dK'_{ij}}{d\omega_j}\right)_{\omega_j \to 0} = \omega\tau \left(\frac{dK_{ij}}{d\omega_j}\right)_{\omega_j \to 0} = \omega\,\tau\,\beta \qquad \text{.....(3.12)}$$

where β is the slope of the K_{ij} - ω_j curve at $\omega_j \to 0$.

Equation (3.11), on being differentiated with respect to ω_j and for $\omega_j \to 0$, becomes

$$\left(\frac{dK'_{ij}}{d\omega_j}\right)_{\omega_j \to 0} = \frac{\mu_j^2\, N \rho_i\, F_i}{3M_j k\, T} \left(\frac{\omega^2\tau}{1 + \omega^2\tau^2}\right) \qquad \text{.....(3.13)}$$

because $\rho_{ij} \to \rho_i$, the density of the solvent $F_{ij} \to F_i$, the local field of the solvent, in the limit $\omega_j = 0$. Using equations (3.12) and (3.13) we finally get

$$\mu_j = \left(\frac{3\, M_j\, k\, T\, \beta}{N \rho_i\, F_i\, \omega b}\right)^{1/2} \qquad \text{.....(3.14)}$$

to evaluate μ_1 and μ_2 in terms of b, where b is a dimensionless parameter given by

$$b = \frac{1}{1 + \omega^2\tau^2} \qquad \text{.....(3.15)}$$

for τ_1 and τ_2 respectively. The values of b as well as μ_1 and μ_2 thus computed from equations (3.14) and (3.15) are placed in table 3.3.

3. 4. Results and discussion

Figure 3.1 represents the linear relationship of $(\varepsilon_{0ij} - \varepsilon'_{ij})/(\varepsilon'_{ij} - \varepsilon_{\infty ij})$ to $\varepsilon''_{ij}/(\varepsilon'_{ij} - \varepsilon_{\infty ij})$ satisfying equation (3.7) having intercepts and slopes presented in table 3.1. with the experimental points placed on each curve for 11 systems possessing double

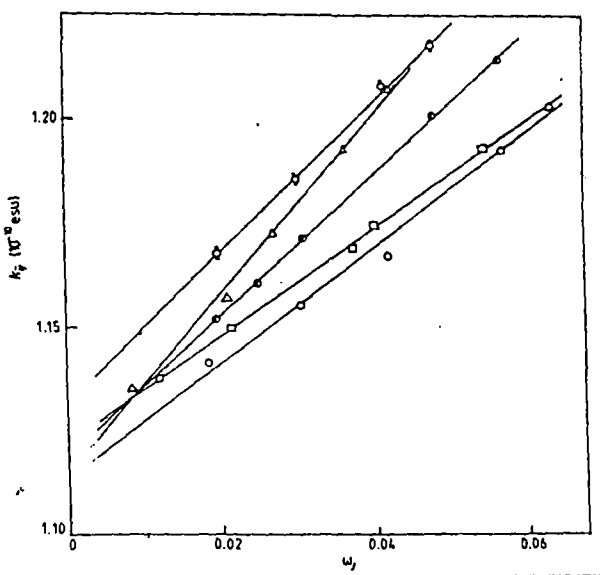

Figure 3.4 Concentration variation of microwave conductivity K_{ij} of five disubstituted anilines at 35°C

Table 3.3 Reports of the estimated intercepts and slopes of the concentration variation of UHF conductivity, dimensionless parameter b, dipole moments μ_1 and μ_2 in Debye (D) for the flexible part and the end-over-end rotation of a polar molecule, reported μ_1 and μ_2 in D due to existing methods, the theoretical μ values from the bond length and bond moments

	Intercepts and slopes of K_{ij} against ω_j		Dimensionless parameters b		Estimated dipolemoment		Reported μ (D)		Theore tical μ (D)	Experimental μ_1 (D)
Slope number and systems	α (10^{-10} esu)	β (10^{-10} esu)	$b_1 = \frac{1}{1+\omega^2\tau_1^2}$	$b_2 = \frac{1}{1+\omega^2\tau_2^2}$	μ_1 (D)	μ_2 (D)	Guggen -heim	Higasi *et al*	from bond length and bond moments	Using $\mu_1 = \mu_2 (c_1 / c_2)^{1/2}$
(i) 4-chloro-2-methyl aniline in C_6H_6	1.1323	1.7863	0.7797	0.1219	2.51	6.36	3.28	3.12	3.06	4.47
(ii) 3-chloro-4 -methyl aniline in C_6H_6	1.1220	1.2865	0.8808	0.3014	2.01	3.43	2.61	2.43	2.20	4.95
(iii) 5 - chloro - 2-methyl aniline in C_6H_6	1.1189	1.6848	0.7858	0.2934	2.43	3.98	3.10	2.92	2.83	3.43
(iv) 3-chloro-2-methyl aniline in C_6H_6	1.1144	2.1490	0.9188	0.3725	2.54	3.99	3.02	2.86	2.48	3.75
(v) 2-chloro-6-methyl aniline in C_6H_6	1.1135	1.3766	0.9228	0.4611	2.03	2.87	2.32	2.20	1.85	2.83
(vi) o-chloronitro benzene in C_6H_6	1.1265	4.0539	0.9178	0.4935	3.68	5.02	4.35	4.43	5.28	4.99
(vii) 4-chloro-3-nitroto-luene in C_6H_6	1.1250	2.8594	0.9464	0.2751	3.18	5.89	4.49	4.59	5.58	5.31
(viii) m-nitrobenzotri- fluoride in C_6H_6	1.1262	1.7747	0.8630	0.3064	2.77	4.64	3.67	3.80	3.74	4.08
(ix) 4-chloro-3-nitroben zotriflouride in CCl_4	1.0999	1.5781	0.9987	0.2744	1.99	3.79	3.17	3.15	3.78	4.34
(x) o-nitrobenzotri- fluoride in C_6H_6	1.1169	4.1557	0.9962	0.5035	3.94	5.54	4.96	5.07	6.18	6.80
(xi) 4-chloro-3-nitrotoluene in CCl_4	1.1044	3.2769	0.9964	0.1686	2.50	6.07	4.68	4.63	5.58	5.78
(xii) 4-chloro-3-nitro- benzotrifluoride in C_6H_6	1.1286	1.1894	—	0.6845	—	2.76	2.97	2.98	3.78	—
(xiii) m-aminoben zotrifluoride in C_6H_6	1.1106	2.3536	—	0.5303	—	3.73	3.51	3.60	2.48	—
(xiv) o-chloronitro- benzene in CCl_4	1.0973	5.4508	—	0.3676	—	5.08	4.19	4.13	5.28	—
(xv) o-chlorobenzo- trifluoride in C_6H_6	1.1199	2.0159	—	0.5580	—	3.57	3.38	3.49	3.98	—

relaxation phenomena. The error involved in such regressions as well as the correlation coefficients for all the curves were also calculated and placed in table 3.1 in order to test their linearity and to assess the errors introduced in τ values, which may normally be claimed to be accurate up to $\pm$ 10%. Attempts were made to measure the double relaxation times of the molecules as mentioned in tables 3.1 -3.3 in order to calculate μ_1 and μ_2 of the flexible parts as well as the whole molecules. they are shown in tables 3.1 and 3.3 respectively. In 11 systems out of 15, nevertheless, double relaxation phenomena were found by showing the lower as well as higher values of τ_1 and τ_2 respectively. As shown in table 3.1, eight molecules, namely all the disubstituted anilines and three benzene derivatives namely o-chloronitrobenzene, 4-chloro-3-nitrotoluene and m-nitrobenzotrifluoride, all in C_6H_6, show considerably larger values of τ_1 in their relaxation behaviours. This is perhaps due to the fact that the flexible —CH_3 group in aniline, and those attached to the benzene rings mentioned above, absorb energy much more strongly in the microwave electric field and thereby yield large values of τ_1. 4-chloro-3-nitrobenzotrifluoride in CCl_4, o-nitrobenzotrifluoride in C_6H_6 and 4-chloro-3-nitrotoluene in CCl_4 have their τ_1 much smaller, presumably due to the fact that their flexible parts are comparatively rigidly fixed to the parent ones (table 3.1). It is, however, interesting to note that the last four systems of table 3.1 show single relaxation processes, probably owing to their rigid attachment to the flexible parts. The slopes and intercepts of equation (3.7) yield τ_1 with negative sign for the aforesaid molecules.

Again, o-chloronitrobenzene shows a double relaxation phenomenon in C_6H_6 but a single relaxation process in CCl_4. The reverse case, however, occurs in 4-chloro-3-nitrobenzotrifluoride, which shows a low value of τ_1 in CCl_4 and a single relaxation process in C_6H_6. This may perhaps be attributed to solvent effects upon the polar molecules. So a firm conclusion on solvent effects seems to be of utmost importance if measurements are to be performed on a single polar molecule in different non-polar solvents.

Table 3.2 reports the relative contributions c_1 and c_2 due to τ_1 and τ_2 (table 3.1) towards relaxation as computed from Fröhlich's equations (3.8) and (3.9) for x and y as

well as by our graphical technique (figures 3.2 and 3.3). In total, c_2 values calculated for six polar molecules are negative although they fulfil the condition $c_1 + c_2 \simeq 1$. The disagreements in c_1 and c_2 with those of Fröhlich (1949) indicate that their flexible parts are loosely bound. In HF electric field the contribution by the rest of the molecule towards relaxation could not be in accord with the flexible one, due to inertia.

The variation of HF conductivities K_{ij} of five disubstituted anilines with respect to ω_j of polar solutes is shown in figure 3.4. The intercept α and slope β are placed in table 3.3 to compute μ_1 and μ_2 using relaxation times τ_1 and τ_2 of table 3.1 from equations (3.14) and (3.15). The values of b_1 and b_2 are also placed in the fourth and fifth columns of table 3.3. The corresponding μ_1 and μ_2 from equation (3.14) are shown in table 3.3. They are compared with μ values of Guggenheim (1949) and Higasi *et al* (1952). The disubstituted benzenes had already been studied by Acharyya and Chatterjee (1985) by the conductivity method. The theoretical μ_{theo} from bond lengths and bond angles had also previously been studied. The same data, with those of disubstituted anilines are shown again in table 3.3 for comparison only.

In figure 3.5 the bond moments of $CH_3 \rightarrow C$ and $C \rightarrow Cl$ are 0.37 D and 1.69 D respectively. The bond moment 1.48 D of $C \rightarrow NH_2$ makes an angle 142° with the bond axis. The component along the bond axis in these molecules becomes 1.166 D. With these preferred conformational structures of the disubstituted. anilines, the theoretical μ_{theo} were computed by the vector addition method and are placed in table 3.3. The close agreement of these μ_{theo} with our experimental μ_2 values suggests their correct conformational structures as shown in figure 3.5

The values of μ_1 may also be obtained from $\mu_1 = \mu_2(c_1/c_2)^{1/2}$ when the two relaxation phenomena are equally probable (Fröhlich 1949). However, the present investigation finds that μ_1 values as calculated from the above relation are larger for c_1 and c_2 due to Fröhlich's equations. The τ values gradually decrease due to various conformations of the disubstituted anilines (figure 3.5 and table 3.1), probably due to decrease in the effective radii of the rotating units under HF electric field. Although, the molecules are in the same environment and their molecular weights are the same, the most

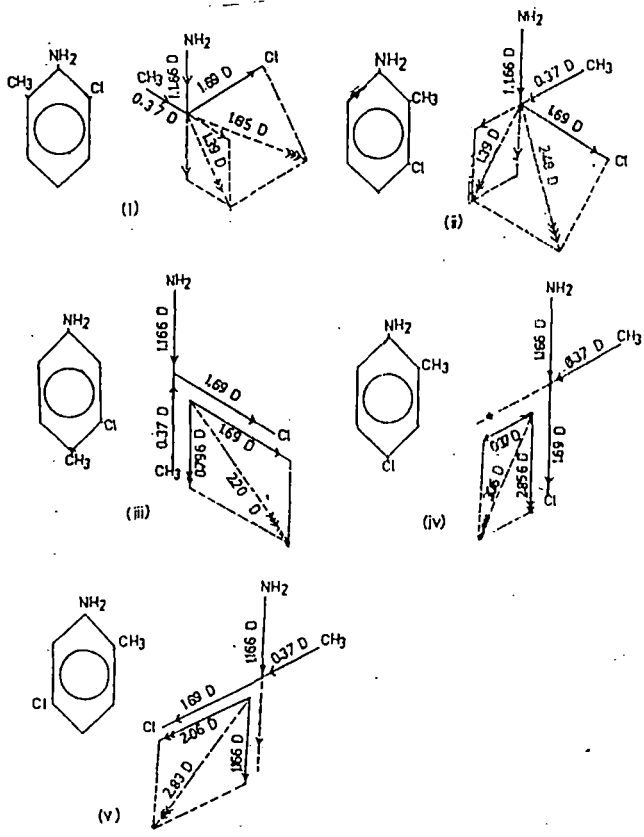

Figure 3·5 Conformations of five disubstituted anilines showing the orientation of the bond axes and bond moments and dipole moments.

probable relaxation time due to Higasi (1966) and Guggenheim (1957) also show a trend similar to ours as shown in table 3.1.

3.5 Conclusions

The close agreement of μ_2 values with literature values at once suggests that our new approach can justifiably be claimed to be a simple, straightforward and useful one. The method of single frequency measurements of dielectric relaxation data at a given temperature is comparatively easy to perform. It requires only easy and time-saving calculations, unlike other existing methods, to detect the very existence of double relaxation phenomena in polar nonpolar liquid mixture. Thus the present procedure offers a significant improvement for derivation of τ_1 and τ_2 and μ_1 and μ_2 because it allows one to find not only an estimate of the errors, but also the correlation coefficients between the desired values generated from the dielectric relaxation.

Acknowledgments

The authors are grateful to Mr. S N Roy MA, Principal and Mr. Amal Bhattacharya MSc of Raiganj University college for their kind interest in this work.

References

Acharyya S and Chatterjee A K 1985 Indian J. Pure Appl. Phys. **23** 484

Arrawatia M L, Gupta P C and Sisodia M L 1977 Indian J. Pure Appl. Phys. **15** 770

Bergmann K, Roberti D M and Smyth C P 1960 J. Phys. Chem. **64** 665

Bhattacharyya J, Sinha B, Roy S B and Kastha G S 1964 Indian J. Phys. **38** 413

Chatterjee A K, Saha U, Nandi N, Basak R C and Acharyya S 1992 Indian J. Phys. **66** 291

Fröhlich H 1949 Theory of Dielectrics (Oxford: Oxford University Press)p 94

Guggenheim E A 1949 Trans. Faraday Soc. **45** 714

Gupta P C, Arrawatia M L and Sisodia M L 1978 Indian J. Pure Appl. Phys. **16** 934

Higasi K 1952 Denaki Kenkyusho Iho 4 231

Higasi K 1966 Bull. Chem. Soc. Japan **39** 2157

Higasi K, Bergmann K and Smyth C P 1960 J. Phys. Chem. **64** 880

Kastha G S, Dutta B, Bhattacharyya J and Roy S B 1969 Indian J. Phys. **43** 14

Khameshara S M and Sisodia M L 1980 Indian J. Pure Appl. Phys. **18** 110

Murphy F J and Morgan S O 1939 Bell. Syst. Tech. J. **18** 502

Saha U and Acharyya S 1993 Indian J. Pure Appl. Phys. **31** 181

Smyth C P 1955 Dielectric Behaviour and Structure (New York: McGraw-Hill)

CHAPTER 4

SINGLE FREQUENCY MEASUREMENT OF DOUBLE-RELAXATION TIMES OF MONO-SUBSTITUTED ANILINES IN BENZENE

4.1. Introduction

In recent years the dielectric relaxation phenomena of polar-non-polar liquid mixtures under ultra-high-frequency (UHF) electric fields have gradually gained the attention of a large number of workers [1-3] as they reveal significant information on various types of molecular associations. There exist several methods [4-6] of estimating the relaxation time τ_s as well as the dipole moment μ_j of a polar liquid within the framework of the Debye and Smyth model. We [7], however, observe that the imaginary K''_{ij} and real K'_{ij} of the complex UHF conductivity K^*_{ij} of a polar-non-polar liquid mixture vary linearly and independently in the low-concentration region. The relaxation time, which is the lag in response to the alternation of the electric field, could, however, be estimated from their slopes.

Bergmann *et al* [8] devised a graphical technique in order to obtain τ_1 and τ_2 to represent relaxation times of the flexible part attached to the parent molecule and the molecule itself respectively. The corresponding contributions c_1 and c_2 towards dielectric relaxations in terms of τ_1 and τ_2 were also found for some complex molecules. The method is based on plotting the normalized experimental points involved with the measured data of the real ε', the imaginary ε'' of the complex dielectric constant ε^*, the static dielectric constant ε_0 and the optical dielectric constant ε_∞ at various frequencies ω on a semicircle in a complex plane. A point was then selected on the chord through the two fixed points on the semicircle in consistency with all the experimental points. Bhattacharyya *et al* [9] subsequently modified the above procedure to get τ_1, τ_2, c_1 and c_2 with the experimental values measured at two different frequencies.

Under such conditions, an alternative procedure [10] has recently been suggested to determine τ_1 and τ_2 based on a single-frequency measurement of dielectric relaxation parameters like ε'_{ij}, ε''_{ij}, and $\varepsilon_{\infty ij}$ of a polar molecule (j) for different weight fractions ω_j in a non-polar solvent (i) at a given temperature in degrees Celsius. They are, however, estimated from the slope and intercept of the straight line equation between $(\varepsilon_{0ij} - \varepsilon'_{ij})/(\varepsilon'_{ij} - \varepsilon_{\infty ij})$ and $\varepsilon''_{ij}/(\varepsilon'_{ij} - \varepsilon_{\infty ij})$. This is derived from the dielectric relaxation data for different ω_j of a polar solute measured under a single-frequency electric

field in the GHz region. The correlation coefficient r, could also be calculated because of the linear behaviour of the derived parameters. This helps one find out the percentage error introduced in the obtained results, too.

The corresponding contributions c_1 and c_2 towards dielectric relaxation in terms of estimated τ_1 and τ_2 can, however, be calculated from x and y where

$$x = \frac{\varepsilon'_{ij} - \varepsilon_{\infty ij}}{\varepsilon_{0ij} - \varepsilon_{\infty ij}}; \qquad y = \frac{\varepsilon''_{ij}}{\varepsilon_{0ij} - \varepsilon_{\infty ij}}$$

in Fröhlich's equations [11]. The variations of x and y with ω_j of a polar solute in a system of a polar-non-polar liquid mixture are found to obey the equations of Bergmann *et al* [8] almost exactly. c_1 and c_2 can also be calculated by the graphical technique suggested by Saha *et al* [10], which consists of plotting those experimental values at different ω_j's with a view to getting x and y at infinite dilution. The UHF electrical conductivity K_{ij} of a polar-non-polar liquid mixture, on the other hand, is thought to be a sensitive tool in ascertaining the dipole moment μ_j of a polar liquid in terms of τ_s.

Some of the disubstituted aniline and benzene derivatives had already been studied in detail by the new approach suggested by Saha *et* al [10]. Ten out of 12 highly non-spherical disubstituted anilines and benzenes were found to exhibit the double-relaxation phenomena as their flexible parts are not rigidly fixed in relation to the parent ones.

We, therefore, thought to study the available solution data of ε'_{ij}, ε''_{ij}, ε_{0ij} and $\varepsilon_{\infty ij}$ of mono-substituted anilines like anisidines and toluidines in their *ortho, meta* and *para* forms for their various concentrations as measured by Srivastava and Suresh Chandra [12] at different frequencies of 2.02, 3.86 and 22.06 GHz electric fields at 35°C to obtain τ_1 and τ_2 based on the new approach of Saha *et al* [10]. Highly non-spherical molecules like mono-substituted anilines are also expected to possess the double-relaxation phenomena by showing τ_1 and τ_2. Although they are strongly of non-Debye type in their relaxation behaviour, it is found, in the present investigation, that they do not exhibit the effect of double-relaxation phenomena at all frequencies of the electric field. When the available data [12] were extended to 9.945 GHz (about 3 cm wavelength), which is supposed to be the most effective dispersive region for such polar molecules all

Table 4.1 The dielectric relaxation parameters like ε'_{ij}, ε''_{ij}, ε_{0ij} and $\varepsilon_{\infty ij}$ of three isomers of anisidines and toluidines in benzene under different weight fractions ω_j's of solutes at 35°C from high frequency absorption measurements

System	Weight fraction (ω_j) of solute	ε_{0ij} at 450 KHz	ε'_{ij} at 2.02 GHz	ε''_{ij}	ε'_{ij} at 3.86 GHz	ε''_{ij}	ε'_{ij} at 22.06 GHz	ε''_{ij}	$\varepsilon_{\infty ij} = n^2_{Dij}$
	0.0326	2.336	2.33	0.005	2.32	0.011	2.31	0.015	2.239
o-anisidine	0.0604	2.404	2.39	0.009	2.37	0.021	2.36	0.026	2.247
in benzene	0.0884	2.459	2.45	0.013	2.44	0.029	2.40	0.041	2.255
	0.1135	2.538	2.50	0.018	2.49	0.033	2.42	0.053	2.262
	0.1361	2.588	2.57	0.027	2.53	0.041	2.56	0.065	2.267
m-anisidine	0.0160	2.315	2.30	0.006	2.31	0.018	2.29	0.021	2.235
in benzene	0.0336	2.384	2.37	0.010	2.25	0.026	2.32	0.038	2.241
	0.0579	2.477	2.44	0.017	2.43	0.043	2.36	0.068	2.246
	0.0823	2.553	2.52	0.037	2.51	0.059	2.40	0.080	2.253
	0.1109	2.675	2.62	0.047	2.61	0.084	2.43	0.115	2.261
p-anisidine	0.0319	2.373	2.36	0.008	2.34	0.014	2.31	0.031	2.237
in benzene	0.0597	2.442	2.46	0.015	2.43	0.027	2.38	0.069	2.246
	0.0848	2.539	2.52	0.022	2.52	0.042	2.44	0.088	2.250
	0.1106	2.638	2.63	0.031	2.60	0.061	2.48	0.105	2.262
	0.1396	2.745	2.72	0.042	2.70	0.082	2.54	0.146	2.269
o-toluidine	0.0137	2.301	2.30	0.005	2.29	0.008	2.27	0.026	2.241
in benzene	0.0332	2.334	2.36	0.010	2.35	0.020	2.30	0.042	2.247
	0.0459	2.392	2.38	0.013	2.38	0.023	2.32	0.069	2.250
	0.0622	2.457	2.42	0.015	2.42	0.029	2.34	0.079	2.255
	0.1048	2.577	2.55	0.022	2.55	0.061	2.42	0.096	2.264
m-toluidine	0.0264	2.337	2.32	0.005	2.31	0.007	2.29	0.020	2.243
in benzene	0.0538	2.413	2.38	0.006	2.37	0.016	2.33	0.040	2.248
	0.0781	2.470	2.42	0.010	2.44	0.024	2.37	0.053	2.252
	0.1015	2.526	2.50	0.017	2.39	0.036	2.40	0.081	2.258
	0.1225	2.591	2.54	0.023	2.54	0.045	2.45	0.095	2.262
p-toluidine	0.0213	2.319	2.31	0.010	2.31	0.010	2.31	0.009	2.237
in benzene	0.0428	2.367	2.35	0.012	2.32	0.016	2.33	0.020	2.244
	0.0616	2.413	2.37	0.013	2.38	0.018	2.36	0.033	2.249
	0.0916	2.483	2.43	0.018	2.46	0.029	2.40	0.046	2.254
	0.1048	2.523	2.46	0.026	2.48	0.046	2.44	0.058	2.260

of them, on the other hand, showed the double-relaxation phenomena of reasonable τ_1 and τ_2 [13]. However, out of 18 systems, as shown in tables and figures, eight systems like o- and- m-anisidine and p-toluidine at 3.86 and 22.06 GHz together with o- and m-toluidine at 2.02 and 3.86 GHz are found to show τ_1 and τ_2. Only p-anisidine is an exception. It shows mono-relaxation behaviour at all frequencies. This sort of mono-relaxation behaviour may equally well be explained by considering a distribution of relaxation times, namely a single broad dispersion. Only τ_2 values of the compounds showing mono-relaxation are, however, obtained from the slopes of the straight line equations (such as (4.15), see later) of $(\varepsilon_{0ij} - \varepsilon'_{ij})/(\varepsilon'_{ij} - \varepsilon_{\infty ij})$ with $\varepsilon''_{ij}/(\varepsilon'_{ij} - \varepsilon_{\infty ij})$ having zero intercepts.

The relaxation times τ, since accurate values for mono-substituted anilines are not available, are also estimated from the slopes of K''_{ij} versus K'_{ij}. They may be called the most probable relaxation time τ_0 of the three isomers of anisidine and toluidine. τ_0 is often given by $\tau_0 = (\tau_1\tau_2)^{1/2}$ where τ_1 and τ_2 convey their usual meanings. c_1 and c_2 in terms of τ_1 and τ_2 are also calculated from Fröhlich's equation [11] as well as by our graphical technique. The dipole moments μ_1 and μ_2 of these three isomers of anisidine and toluidine are finally estimated from the slope β of their concentration variation of UHF conductivities K_{ij} at $\omega_j \rightarrow 0$ and in terms of the estimated τ_1 and τ_2 in order to establish the conformational structures of those compounds under investigation

4.2. Theoretical formulations of c_1 and c_2 in terms of τ_1 and τ_2 based on the single-frequency method

When the complex dielectric constants ε^*_{ij} is represented as the sum of two non-interacting Debye-type dispersions; the dielectric relaxation by the two extreme values of τ, τ_1 and τ_2, their relative contributions c_1 and c_2 can, however, be expressed for a polar-non-polar liquid mixture [8] by

$$\frac{\varepsilon'_{ij} - \varepsilon_{\infty ij}}{\varepsilon_{0ij} - \varepsilon_{\infty ij}} = c_1 \frac{1}{1 + \omega^2\tau_1^2} + c_2 \frac{1}{1 + \omega^2\tau_2^2} \qquad \text{.....(4.1)}$$

$$\frac{\varepsilon''_{ij}}{\varepsilon_{0ij} - \varepsilon_{\infty ij}} = c_1 \frac{\omega \tau_1}{1 + \omega^2 \tau_1^2} + c_2 \frac{\omega \tau_2}{1 + \omega^2 \tau_2^2} \qquad \text{.....(4.2)}$$

Such that $c_1 + c_2 = 1$. All the symbols used are of their usual significance. Putting

$$\frac{\varepsilon'_{ij} - \varepsilon_{\infty ij}}{\varepsilon_{0ij} - \varepsilon_{\infty ij}} = x \qquad \frac{\varepsilon''_{ij}}{\varepsilon_{0ij} - \varepsilon_{\infty ij}} = y$$

with $\omega\tau = \alpha$ and using the abbreviations $a = 1/(1 + \alpha^2)$ and $b = \alpha/(1 + \alpha^2)$ the above equations (4.1) and (4.2) can be written as

$$x = c_1 a_1 + c_2 a_2 \qquad \text{.....(4.3)}$$

$$y = c_1 b_1 + c_2 b_2 \qquad \text{.....(4.4)}$$

where suffices 1 and 2 with a and b are related to τ_1 and τ_2 respectively.

From equations (4.3) and (4.4), since $\alpha_2 - \alpha_1 \neq 0$ and $\alpha_2 > \alpha_1$ we have

$$c_1 = \frac{(x\alpha_2 - y)(1 + \alpha_1^2)}{\alpha_2 - \alpha_1} \qquad \text{.....(4.5)}$$

$$c_2 = \frac{(y - x\alpha_1)(1 + \alpha_2^2)}{\alpha_2 - \alpha_1} \qquad \text{.....(4.6)}$$

Now, using the relation $c_1 + c_2 = 1$; one can easily get the following equation with the help of equations (4.5) and (4.6):

$$\frac{1 - x}{y} = (\alpha_1 + \alpha_2) - \frac{x}{y} \alpha_1 \alpha_2$$

which, on substitution of the values of x, y and α, becomes

$$\frac{\varepsilon_{0ij} - \varepsilon'_{ij}}{\varepsilon'_{ij} - \varepsilon_{\infty ij}} = \omega(\tau_1 + \tau_2) \frac{\varepsilon''_{ij}}{\varepsilon'_{ij} - \varepsilon_{\infty ij}} - \omega^2 \tau_1 \tau_2 \qquad \text{.....(4.7)}$$

Equation (4.7) is simply a straight line relation between $(\varepsilon_{0ij} - \varepsilon'_{ij})/(\varepsilon'_{ij} - \varepsilon_{\infty ij})$ and $\varepsilon''_{ij}/(\varepsilon'_{ij} - \varepsilon_{\infty ij})$ having slope $\omega(\tau_1 + \tau_2)$ and intercept $-\omega^2\tau_1\tau_2$ respectively. Here $\omega = 2\pi f$, f being the frequency of the alternating electric field in gigahertz. When equation (4.7) is fitted with the measured data of ε'_{ij}, ε''_{ij}, ε_{0ij} and $\varepsilon_{\infty ij}$ for different weight fractions ω_1 (table 4.1) of ortho, meta and para anisidines and toluidines in benzene at 35°C [12] we

get slopes and intercepts as shown in (table. 4.2) to determine τ_1 and τ_2 for each single frequency of 2.02, 3.86 and 22.06 GHz electric fields respectively. The error as well as the correlation coefficient were also found out for each curve of equation (4.7) and placed in table 4.2 only to verify their linearity as illustrated graphically in figure 4.1 together with the experimental points upon them.

The Fröhlich parameter A as shown in table 4.3 for polar solutes exhibiting the double-relaxation phenomena are used to evaluate both x and y of equations (4.3) and (4.4) in terms of ω and the small limiting relaxation time $\tau_s = \tau_1$ by the following equations [11]:

$$\frac{\varepsilon'_{ij} - \varepsilon_{\infty ij}}{\varepsilon_{0ij} - \varepsilon_{\infty ij}} = 1 - \frac{1}{2A} \ln\left(\frac{1 + e^{2A\omega^2\tau_s^2}}{1 + \omega^2\tau_s^2}\right) \qquad \text{.....(4.8)}$$

$$\frac{\varepsilon''_{ij}}{\varepsilon_{0ij} - \varepsilon_{\infty ij}} = \frac{1}{A}\left[\tan^{-1}(e^{A\omega\tau_s}) - \tan^{-1}(\omega\tau_s)\right] \qquad \text{.....(4.9)}$$

where $A = \ln(\tau_2/\tau_1)$. The computed values of x and y are placed in table 4.3 to obtain c_1 and c_2 from equations (4.5) and (4.6). The latter are also shown in table 4.3. The left-hand sides of equations (4.1) and (4.2) are really the function of ω_j of the solutes in a given solvent as shown from the plots of x and y against ω_j in figures (4.2) and (4.3) respectively. The fixed values of x and y when $\omega_j \rightarrow 0$ for each system, as shown in table (4.3), can then be used to estimate c_1 and c_2 from equations (4.5) and (4.6) in order to compare them with those of Fröhlich [11]. The τ_1 and τ_2 values estimated from the slope and intercept of equation (4.7) for each solute, when substituted on the right-hand sides of equations (4.1) and (4.2), suggest the limiting values of x and y as obtained from figures 4.2 and (4.3) at infinite dilution.

4.3. Estimated μ_1 and μ_2 from UHF conductivity K_{ij} in terms of τ_1 and τ_2

The UHF conductivity K_{ij} is given by Murphy and Morgan [14] as

$$K_{ij} = \frac{\omega}{4\pi}(\varepsilon''^2_{ij} + \varepsilon'^2_{ij})^{1/2} \qquad \text{.....(4.10)}$$

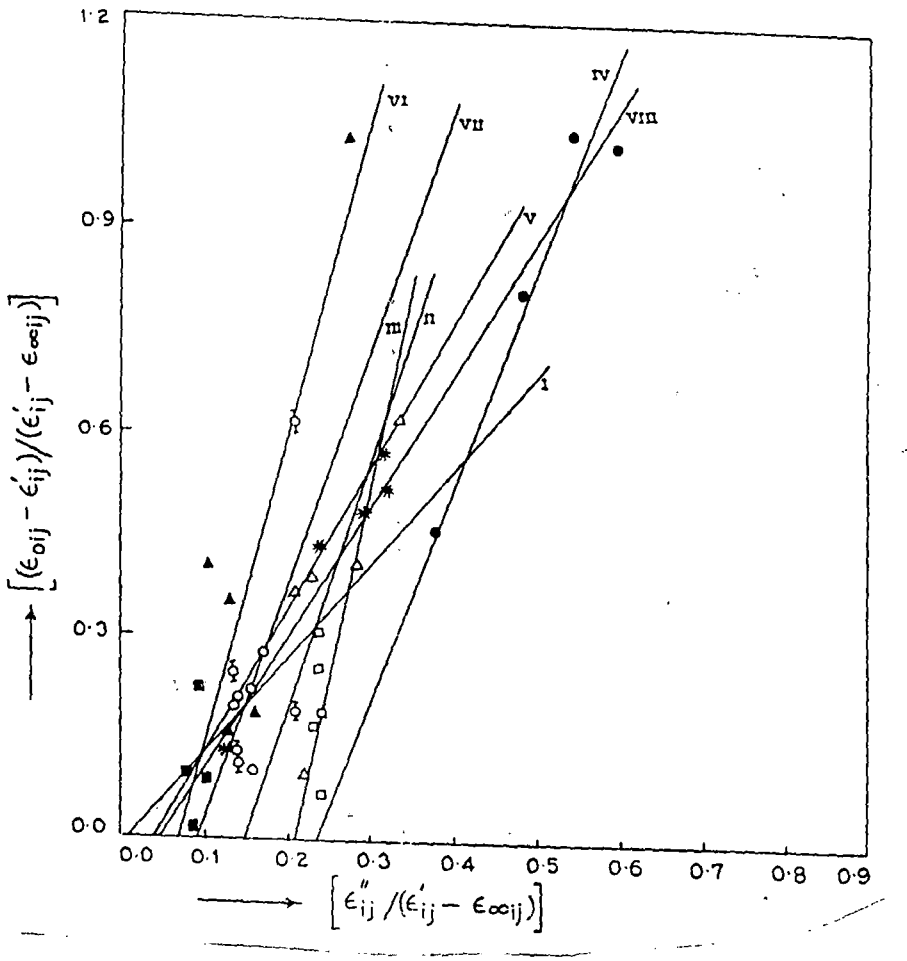

Figure 4.1 Variation of $(\varepsilon_{0ij} - \varepsilon'_{ij})/(\varepsilon'_{ij} - \varepsilon_{\infty ij})$ against $\varepsilon''/(\varepsilon'_{ij} - \varepsilon_{\infty ij})$ at 35°C for different weight fraction ω_j for the polar-non-polar liquid mixture at (table 4.2): (I) o-anisidine at 3.86 GHz (o); (II) o-anisidine at 22.06 GHz (Δ); (III) m-anisidine at 3.86 GHz (□); (IV) m-anisidine at 22.06 GHz (●); (V) o-toluidine at 2.02 GHz (■); (VI) m-toluidine at 3.86 GHz (▲); (VII) p-toluidine at 3.86 GHz (O); and (VIII) p-toluidine at 22.06 GHz (*).

Table 4.2 The intercepts and the slopes of the straight line curves of $(\varepsilon_{0ij}-\varepsilon'_{ij})/(\varepsilon'_{ij}-\varepsilon_{\infty ij})$ against $\varepsilon''_{ij}/(\varepsilon'_{ij}-\varepsilon_{\infty ij})$ of anisidines and toluidines at 35°C to estimate the relaxation times τ_1 (smaller) and τ_2 (larger) with respective errors and correlation coefficients involved in the calculations as well as their estimated τ_s'.

System with molecular wt M_j in gm.	Frequency f in GHz	Intercept and slope of $(\varepsilon_{0ij}-\varepsilon'_{ij})/(\varepsilon'_{ij}-\varepsilon_{\infty ij})$ versus $-\varepsilon''_{ij}/(\varepsilon'_{ij}-\varepsilon_{\infty ij})$ curve		Estimated relaxation times $\tau_1 \times 10^{12}$ s & $\tau_2 \times 10^{12}$ s		Correlation coefficient r	% error involved in calculation	Estimated relaxation time $\tau_0 \times 10^{12}$ s	$\tau_2 \times 10^{12}$ due to single broad dispersion
o-anisidine	2.02	-0.0596	0.3759	—	39.10	0.1082	29.81	6.02	96.83
$M_j = 123$	3.86	0.0179	1.4360	0.52	58.72	0.3021	27.41	5.89	—
	22.06	0.5406	3.6741	1.11	25.41	0.8274	9.52	1.61	—
m-anisidine	2.02	-0.2109	-0.4703	—	22.13	-0.2588	28.14	11.87	120.9
$M_j = 123$	3.86	-1.1404	5.5485	8.82	220.07	-0.9999	0	8.46	—
	22.06	0.7318	3.1447	1.83	20.87	0.9805	1.16	3.88	—
p-anisidine	2.02	-0.2406	-2.1899	—	8.27	-0.7375	13.75	6.64	61.63
$M_j = 123$	3.86	-0.4927	-2.2136	—	8.41	-0.4782	23.27	6.53	34.31
	22.06	-1.2868	-1.2818	—	4.77	-0.3395	26.69	3.15	9.91
o-toluidine	2.02	0.0773	2.0910	2.97	161.86	0.0743	33.54	5.01	—
$M_j = 107$	3.86	-0.5925	-2.3787	—	9.38	-0.6779	16.30	6.84	35.94
	2206	-0.4603	0.6684	—	7.87	0.3732	25.96	4.06	8.76
m-toluidine	2.02	-0.4062	-3.0101	—	10.20	-0.5757	20.17	8.70	258.61
$M_j = 107$	3.86	0.2938	4.5092	2.73	183.29	0.8469	8.53	6.78	—
	22.06	-1.2064	-0.6295	—	5.98	-0.3213	27.05	3.42	13.31
p-toluidine	2.02	-0.6655	-3.5127	—	14.21	-0.5101	22.31	4.08	167.73
$M_j = 107$	3.86	0.3149	3.4446	3.88	138.22	0.6477	17.51	5.15	—
	22.06	0.0821	1.9151	0.32	13.51	0.9408	3.47	2.91	—

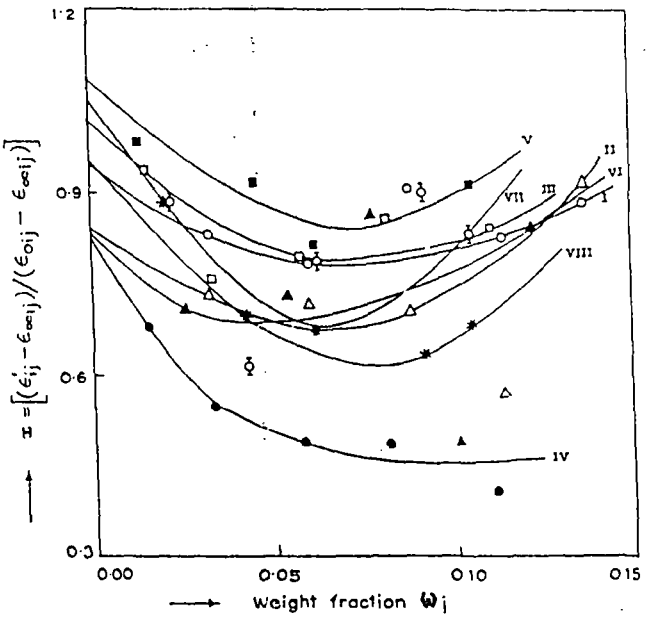

Figure 4.2 Plot of $(\varepsilon'_{ij} - \varepsilon_{\infty ij}) / (\varepsilon_{0ij} - \varepsilon_{\infty ij})$ against weight fraction ω_j for the polar-non-polar liquid mixture at 35°C (table 4.3): (I) o-anisidine at 3.86 GHz (o); (II) o-anisidine at 22.06 GHz (Δ); (III) m-anisidine at 3.86 GHz (□); (IV) m-anisidine at 22.06 GHz (●); (V) o-toluidine at 2.02 GHz (■); (VI) m-toluidine at 3.86 GHz (▲); (VII) p-toluidine at 3.86 GHz (⊽); and (VIII) p-toluidine at 22.06 GHz (*).

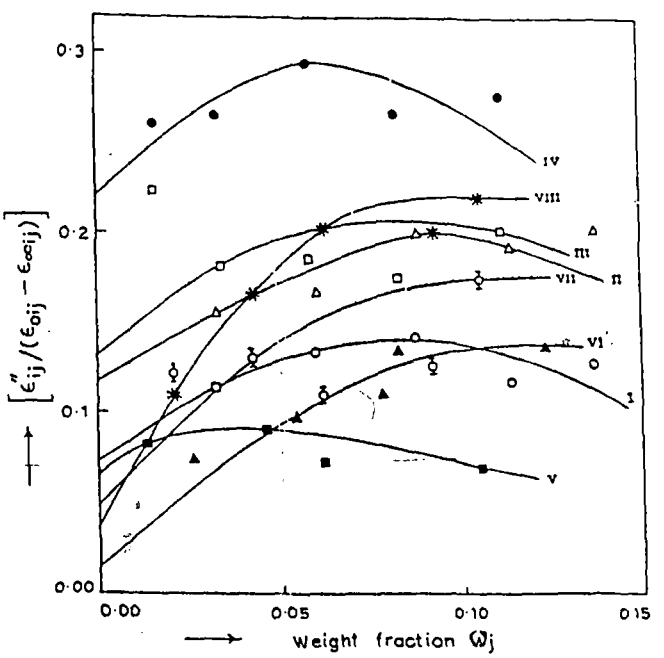

Figure 4.3 Plot of $\varepsilon''_{ij} / (\varepsilon_{0ij} - \varepsilon_{\infty ij})$ against weight fraction ω_j for the polar-non-polar liquid mixture at 35°C (table 4.3): (I) o-anisidine at 3.86 GHz (o); (II) o-anisidine at 22.06 GHz (Δ); (III) m-anisidine at 3.86 GHz (□); (IV) m-anisidine at 22.06 GHz (●); (V) o-toluidine at 2.02 GHz (■); (VI) m-toluidine at 3.86 GHz (▲); (VII) p-toluidine at 3.86 GHz (⊽); and (VIII) p-toluidine at 22.06 GHz (*)

Table 4.3 The relative contributions c_1 and c_2 towars dielectric relaxation, Fröhlich parameters A (= ln (τ_2 / τ_1) together with the estimatd values of x and y due to Fröhlich equations (equations (4.8) and (4.9) and those by our graphical techniques (figures 4.2 and 4.3)

Sl. No.	System with	Frequency in GHz	Fröhlich parameter A = ln (τ_2 / τ_1)	Theoretical values of x and y using equations (4.8) and (4.9)		Theoretical values c_1 and c_2		Estimated values of $x = \left(\frac{\varepsilon' - \varepsilon_\infty}{\varepsilon_0 - \varepsilon_\infty}\right)_{\omega_1 \to 0}$ $y = (\varepsilon''/\varepsilon_0 - \varepsilon_\infty)_{\omega_1 \to 0}$		Estimated values of c_1 and c_2 from figures 4.2 and 4.3	
										c_1	and c_2
1	o-anisidine	3.86	4.7267	0.8829	0.1999	0.7491	0.4051	0.942	0.072	0.8995	0.1278
2	o-anisidine	22.06	3.1308	0.5894	0.3645	0.5200	1.0893	0.840	0.117	0.8636	-0.0484
3	m-anisidine	3.86	3.2169	0.4811	0.3650	0.4496	1.5081	1.017	0.132	1.081	-0.4915
4	m-anisidine	22.06	2.4340	0.5534	0.4063	0.4816	0.9439	0.828	0.221	0.8767	0.0393
5	o-toluidine	2.02	3.9982	0.7936	0.2699	0.6755	0.6212	1.086	0.066	1.0751	0.0649
6	m-toluidine	3.86	4.2067	0.6401	0.3049	0.5827	1.2441	0.834	0.014	0.8471	-0.1952
7	p-toluidine	3.86	3.5730	0.6509	0.3320	0.5727	1.0167	1.050	0.048	1.0750	-0.1905
8	p-toluidine	22.06	3.7428	0.7992	0.2766	0.6685	0.5943	0.948	0.036	0.9532	-0.0149

namely as a function of ω_j of a polar solute. In the UHF electric field, although $\varepsilon''_{ij} << \varepsilon'_{ij}$, the ε''_{ij} term still offers resistance to polarization. Thus the real part K'_{ij} of the UHF conductivity of a polar-non-polar liquid mixture at T K is [15]

$$K'_{ij} = \frac{\mu_j^2 N \rho_{ij} F_{ij}}{3 M_j kT} \left(\frac{\omega^2 \tau}{1 + \omega^2 \tau^2} \right) \omega_j$$

which on differentiation with respect to ω_j and for $\omega_j \rightarrow 0$ yields that

$$\left(\frac{d K'_{ij}}{d\omega_j} \right)_{\omega_j \rightarrow 0} = \frac{\mu_j^2 N \rho_i F_i}{3 M_j kT} \left(\frac{\omega^2 \tau}{1 + \omega^2 \tau^2} \right) \qquad \text{.....(4.11)}$$

where M_j is the molecular weight of a polar solute, N is Avogadro's number, k is the Boltzmann constant, the local field $F_{ij} = \frac{1}{9} (\varepsilon_{ij} + 2)^2$, becomes $F_i = \frac{1}{9} (\varepsilon_i + 2)^2$. and the density $\rho_{ij} \rightarrow \rho_i$ the density of the solvent at $\omega_j \rightarrow 0$.

Again the total UHF conductivity $K_{ij} = \omega \varepsilon'_{ij} / 4\pi$ can be written as

$$K_{ij} = K_{ij\,\infty} + \frac{1}{\omega\tau} K'_{ij}$$

or

$$\left(\frac{d K'_{ij}}{d \omega_j} \right)_{\omega_j \rightarrow 0} = \omega\tau \left(\frac{d K_{ij}}{d \omega_j} \right)_{\omega_j \rightarrow 0} = \omega \tau \beta \qquad \text{.....(4.12)}$$

where β is the slope of the K_{ij} - ω_j curve at $\omega_j \rightarrow 0$. From equations (4.11) and (4.12) we thus get

$$\mu_j = \left(\frac{3 M_j k T \beta}{N \rho_i F_i \omega b} \right)^{1/2} \qquad \text{.....(4.13)}$$

as the dipole moments μ_1 and μ_2 in terms of b, where b is a dimensionless parameter given by

$$b = 1/(1 + \omega^2\tau^2) \qquad \text{.....(4.14)}$$

for τ_0, τ_1 and τ_2. The computed values of μ_0, μ_1 and μ_2 with b are given in table 4.4

4.4. Results and discussion

Figure 4.1 represents the fitted straight line curves between $(\varepsilon_{0ij} - \varepsilon'_{ij})/(\varepsilon'_{ij} - \varepsilon_{\infty ij})$ and $\varepsilon''_{ij}/(\varepsilon'_{ij} - \varepsilon_{\infty ij})$ for different weight fraction ω_j of o-anisidine, m-anisidine and p-toluidine for 3.86 and 22.06 GHz, and for o-toluidine and m-toluidine at 2.02 and 3.86 GHz respectively, together with their experimental points. (table 4.1). The ω_j for the compounds in benzene were, however, calculated from the experimental mole fractions x_i and x_j of solvent and solutes of molecular weights M_i and M_j respectively by using the relation [16]

$$\omega_j = \frac{x_j M_j}{x_i M_i + x_j M_j}$$

The correlation coefficients r for each curve were also calculated to confirm their linearity. Some of the coefficients were found to be negative only due to their negative slopes, as a is evidenced from table 4.2. The percentage of error involved in the calculation was found for each curve. The slope and intercept of equation (4.7) for each straight line were, however, used to determine τ_1 and τ_2 for each compound as shown in table 4.2. Although equation (4.7) is based on assumption of the existence of τ_1 and τ_2, the mono-relaxation behaviour showing only τ_2 for some compounds at different frequencies of the electric field may be equally explained by taking into account a single braod dispersion. The resulting equation (4.7) becomes, when $\tau_1 = 0$,

$$\frac{\varepsilon_{0ij} - \varepsilon'_{ij}}{\varepsilon'_{ij} - \varepsilon_{\infty ij}} = \omega\tau_2 \frac{\varepsilon''_{ij}}{\varepsilon'_{ij} - \varepsilon_{\infty ij}} \qquad \text{.....(4.15)}$$

which may also be derived by using $c_1 = 0$ in equations (4.1) and (4.2) of section 4.2. Equation (4.15) for ten different frequencies of the electric field was then used to obtain τ_2 values, which are shown in the last column of table 4.2 for comparison. It is, however, interesting to note that the agreement is closer with τ_2 values obtained from the method of

Table 4.4 Estimated slope β of K_{ij} - ω_i equations with % of error involved, the dimensionless parameters b_0, b_1, b_2 in terms of most probable relaxation time τ_0, relaxation time due to flexible part τ_1 and the same due to end-over end rotation of the molecule τ_2; corresponding estimated dipole moments μ_0, μ_1 and μ_2 together with the theoretical values of μ_{theo} from bond angles and bond moments and estimated values of μ_1 from $\mu_1 = \mu_2 (c_1/c_2)^{1/2}$ respectively.

System	Frequency in GHz	Slope $\beta \times 10^{10}$ of K_{ij} - ω_j equations	% error involved in calculation	Dimensionless parameters $b_0 = \frac{1}{1+\omega^2\tau_0^2}$	$b_1 = \frac{1}{1+\omega^2\tau_1^2}$	$b_2 = \frac{1}{1+\omega^2\tau_2^2}$	Estimated dipole moments (in Debye) μ_0	μ_1	μ_2	Theoretical μ_1 in D from bond angle and bond moment	Estimated μ_1 in D from $\mu_1 = \mu_2 (c_1/c_2)^{1/2}$
o-anisidine	2.02	0.1620	0.40	0.9942		0.8026	1.39		1.54		
	3.86	0.1786	0.41	0.9800	0.9998	0.3119	1.06	1.05	1.88	1.02	2.56
	22.06	0.3870	1.01	0.9526	0.9769	0.0747	0.66	0.65	2.37		1.64
m-anisidine	2.02	0.3347	0.18	0.9778		0.9269	2.01		2.07		
	3.86	0.2311	2.06	0.9596	0.9563	0.0339	1.22	1.22	6.49	1.65	3.54
	22.06	2.2841	0.08	0.7758	0.9396	0.1068	1.78	1.62	4.81		3.44
p-anisidine	2.02	0.3380	0.35	0.9930		0.9891	2.01		2.01		
	3.86	0.6473	0.09	0.9756		0.9601	2.03		2.04	1.89	
	22.06	2.8513	0.31	0.8400		0.6960	1.91		2.10		
o-toluidine	2.02	0.2097	0.26	0.9960	0.9986	0.1917	1.47	1.47	3.35		3.49
	3.86	0.5507	0.37	0.9732		0.9508	1.74		1.76	1.39	
	2206	1.3618	0.09	0.7597		0.4569	1.29		1.67		
m-toluidine	2.02	0.2359	0.39	0.9879		0.9835	1.56		1.57		
	3.86	0.4889	1.82	0.9737	0.9956	0.0482	1.64	1.63	7.38	1.03	5.05
	22.06	0.9826	1.30	0.8167		0.5930	1.06		1.24		
p-toluidine	2.02	0.0906	0.21	0.9973	0.9912	0.9685	0.97		0.98		
	3.86	0.1583	0.44	0.1873	0.9980	0.0818	2.13	0.93	3.23	1.54	2.42
	22.06	1.2927	0.34	0.8602		0.2221	1.19	1.10	2.34		2.48

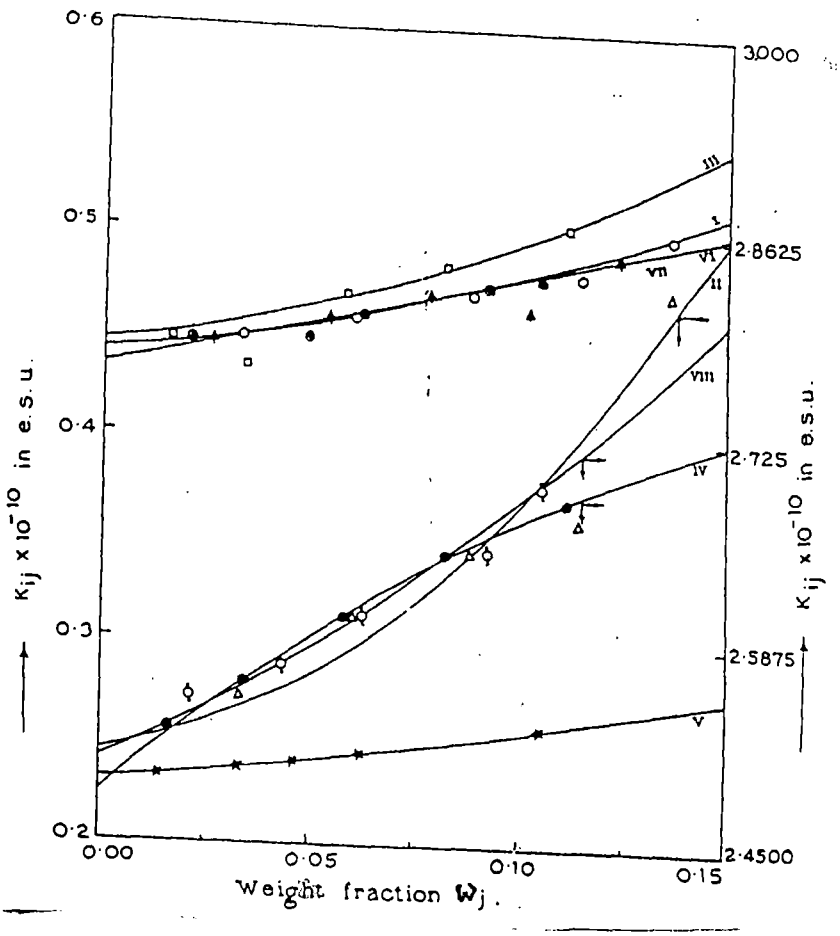

Figure 4.4 Concentration variation of ultra-high frequency conductivity K_{ij} of mono-substituted anilines at 35°C: (I) o-anisidine at 3.86 GHz (o); (II) o-anisidine at 22.06 GHz (Δ); (III) m-anisidine at 3.86 GHz (□); (IV) m-anisidine at 22.06 GHz (●); (V) o-toluidine at 2.02 GHz (*); (VI) m-toluidine at 3.86 GHz (▲); (VII) p-toluidine at 3.86 GHz (⊕); and (VIII) p-toluidine at 22.06 GHz (ϕ)

double-relaxation phenomena, as the frequency of the electric field increases from 2.02 to 22.06 GHz. The most probable relaxation time τ_0, as accurate values for these mono-substituted anilines are not available, was also calculated from the slope m of the linear plot of imaginary K''_{ij} versus the real K'_{ij} parts of the complex conductivity K^*_{ij} under UHF electric field in the relation:

$$K''_{ij} = K_{ij\,\infty} + \frac{1}{\omega\tau_S} K'_{ij} \qquad (4.16)$$

where $\tau_0 = 1/(2\pi fm)$. They are seen to correspond to the relation $\tau_0 = (\tau_1\tau_2)^{1/2}$ approximately, which gives 5.53, 5.31, 44.06, 6.18, 21.93, 22.37, 23.16 and 4.32 ps respectively for the mono-substituted anilines showing the double-relaxation phenomena at different frequencies of the applied electric field. Some of these relaxation times are reasonably good. The estimated values of τ_1, τ_2 and τ_0 are all given in table 4.2

It is found in table 4.2 that m-anisidine, m-and p-toluidines at 3.86 GHz and o-toluidine at 2.02 GHz show considerably high values of τ_1 in the range 9-3 ps; while their τ_2 values are comparatively much larger in the range 220-138 ps. This fact confirms that, under such frequencies of alternating electric field, the flexible parts are loosely bound to the parent molecules. They, therefore, require longer times to accommodate their flexible parts towards dielectric relaxation as shown by c_2 values in table 4.3 being greater than unity. The other molecules like o-anisidine at 3.86 and 22.06 GHz and m-anisidine and p-toluidine at 22.06 GHz show very small values of τ_1, often less than or equal to unity, while their τ_2 values are more or less consistent with the expected values that are often observed in the literature. However, p-anisidine shows the mono-relaxation behaviour at all frequencies by showing only τ_2 in agreement with τ_0. Hence p-anisidine unlike p-toluidine appears to be highly rigid at all the experimental frequencies. The o-and m-anisidines at 2.02 GHz, o-toluidine at 3.86 and 22.06 GHz, m-toluidine at 2.02 and 22.06 GHz and p-toluidine at 2.02 GHz exhibit the mono-relaxation behaviour in yielding τ_2 values in agreement with our τ_0 values. They indicate their rigidity at those frequencies. When the dielectric relaxation data are extended to 9.945 GHz [13] it is really interesting to note that all these mono-substituted anilines show τ_1 and τ_2 in close agreement with the expected literature values. This fact establishes that an X-band microwave electric field

is actually the most effective dispersive region for highly non-spherical polar molecules like mono-or disubstituted aniline and benzene respectively [10].

The c_1 and c_2 values were also calculated from the values of x and y in Fröhlich's equations (4.8) and (4.9) with $\tau_1 = \tau_s$ (table 4.2) and Fröhlich's parameter A. where A = ln (τ_2/ τ_1). They are given in table 4.3 together with those values obtained from the graphical technique of determination of x and y from figures 4.2 and 4.3 at infinite dilution. The experimental x and y values on the left-hand sides of equations 4.1 and 4.2 as plotted with different ω_j in figures 4.2 and 4.3 show the usual decrease in x while the latter increases with ω_j in concave and convex ways respectively indicating the values of τ_1 and τ_2 as a function of concentration [5]. τ_1 and τ_2, as obtained from the slope and intercept of equation (4.7) for a polar-non-polar liquid mixture are, therefore, fixed for a polar compound in consistency with the right-hand sides of equations (4.1) and (4.2). The values of c_1 by Fröhlich's method are found to be less than unity while c_2 values are greater than and nearly equal to unity. The graphical technique adopted here yields the opposite results by showing $c_1 \geq 1.0$ and c_2 very small, often becoming negative (table 4.3), probably due to inertia [10]. The values of c_1 and c_2 in table 4.3 suggest that the two double-relaxation phenomena are not equally probable.

The UHF K_{ij} as a function of ω_j for the following mono-substituted anilines showing τ_1 and τ_2, were, however, arrived at:

(i) o-anisidine at 3.86 GHz: $K_{ij} \times 10^{-10} = 0.4398 + 0.1786\omega_j + 1.9381\omega^2_j$

(ii) o-anisidine at 22.06 GHz: $K_{ij} \times 10^{-10} = 2.5112 + 0.3870\ \omega_j + 13.011\ \omega^2_j$

(iii) m-anisidine at 3.86 GHz: $K_{ij} \times 10^{-10} = 0.4438 + 0.2311\omega_j + 2.9354\ \omega^2_j$

(iv) m-anisidine at 22.06 GHz: $K_{ij} \times 10^{-10} = 2.4896 + 2.2841\ \omega_j - 4.7796\ \omega^2_j$

(v) o-toluidine at 2.02 GHz: $K_{ij} \times 10^{-10} = 0.2294 + 0.2097\omega_j + 0.5641\ \omega^2_j$

(vi) m- toluidine at 3.86 GHz: $K_{ij} \times 10^{-10} = 0.4326 + 0.4889\omega_j - 0.1380\omega^2_j$

(vii) p-toluidine at 3.86 GHz: $K_{ij} \times 10^{-10} = 0.4402 + 0.1583\omega_j + 2.1467\omega^2_j$ and

(viii) p-toluidine at 22.06 GHz: $K_{ij} \times 10^{-10} = 2.5063 + 1.2927\omega_j + 4.5909\omega^2_j$

which are shown graphically in figure 4.4. together with the experimental points upon the curves. The slopes of K_{ij} - ω_j curves are, however, listed in table 4.4. together with those

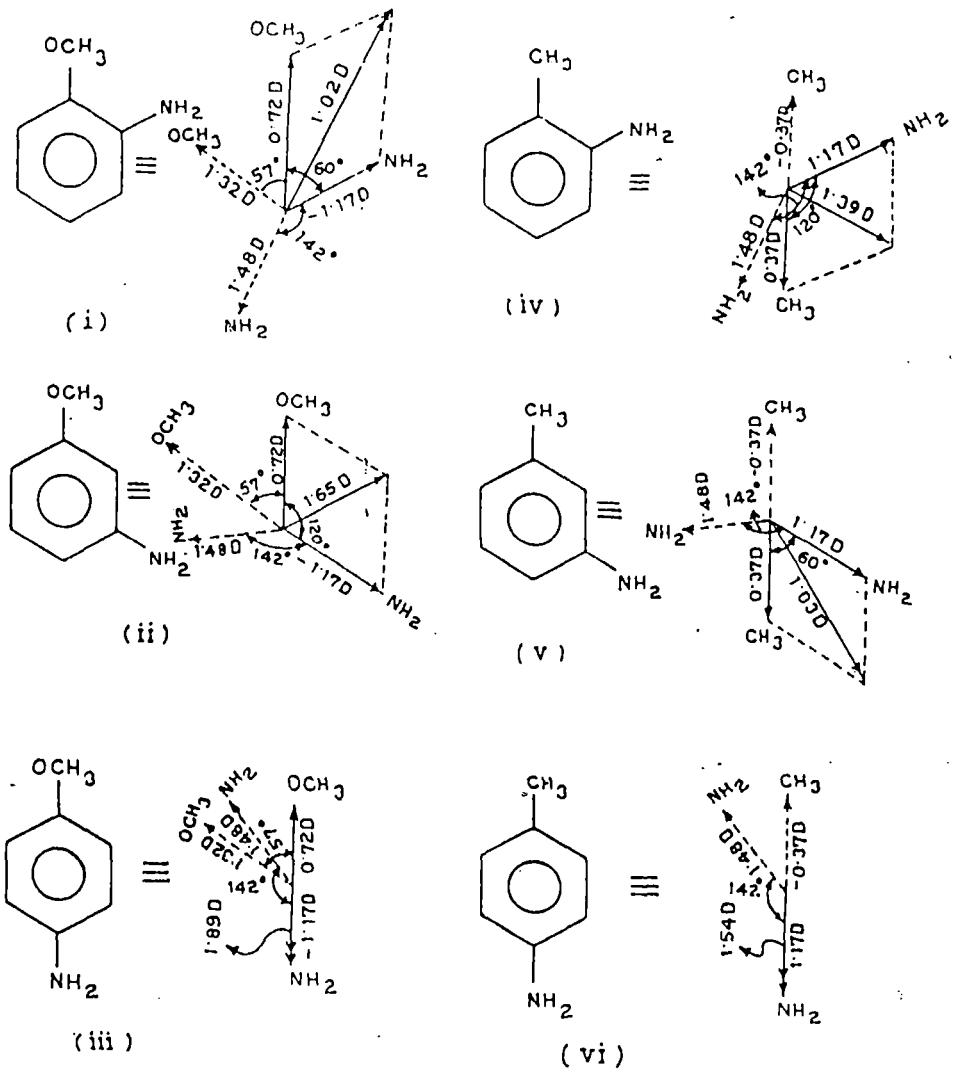

Figure 4.5 Conformational structures of anisidines and toluidines in ortho, meta and para forms: (i) o-anisidine, (ii) m-anisidine, (iii) p-anisidine, (iv) o-toluidine, (v) m-toluidine and (vi) p-toluidine.

of the other ten K_{ij}-ω_j equations showing the monorelaxation behaviour. The percentage of error in computation of K_{ij}-ω_j equations are also shown in table 4.4. The slopes β are finally used to estimate μ_1 and μ_2 from equations (4.13) and (4.14) in terms of τ_1 and τ_2 as presented in table 4.2. The dimensionless parameters b_0, b_1 and b_2 in terms of τ_0, τ_1 and τ_2 are also given in table 4.4.

An attempt was made to estimate from the available bond moments and bond angles the theoretical μ values of the polar liquids, assuming the molecules to be planar. The bond moments and bond angles of C $\rightarrow$ OCH_3 in ansidine and C $\leftarrow$ CH_3 in toluidine are 1.32 D, 0.37 D and 57°, 180° with respect to the benzene ring while those of C $\rightarrow$ NH_2 are 1.48 D and 142° respectively [17]. The conformational structures thus obtained by the vector addition method for anisidine and toluidine in their ortho, meta and para forms are displayed in figure 4.5. The estimated μ_j are given in table 4.4. with those of μ_1, where $\mu_1 = \mu_2 (c_1/c_2)^{1/2}$ assuming that the two relaxation phenomena are equally probable. The close agreement of μ values as shown in table 4.4 at once indicates that the method as suggested is a simple straightforward and unique one.

4.5 Conclusion

The determination of slope and intercept of the derived linear equation (equation 4.7) involved with a single UHF dielectric relaxation parameters of a polar-non-polar liquid mixture at different ω_j and at a given temperature in degrees Celsius is an analytical and reliable method to calculate τ_1 and τ_2 of the flexible part as well as of the whole molecule itself. The relative contributions c_1 and c_2 towards dielectric relaxations in terms of τ_1 and τ_2 can be calculated by using Fröhlich's equations. The graphical techniques used are also convenient tools to estimate c_1 and c_2. The dipole moments μ_1 and μ_2 in terms of τ_1 and τ_2, and from the slope β of the concentration variation of K_{ij} of polar-non-polar liquid mixtures, throw much light on the structural conformation of a complex polar liquid under investigation. The methodology so far advanced seems to be a significant improvement over the existing ones in that it allows estimation of correlation coefficients between the data used and the percentage of error introduced in the obtained results. The procedure is

thus simple, straightforward and required less computational work than the existing methods, in which experimental data of a pure polar liquid at two or more electric field frequencies are usually needed.

References

[1] Kastha G S, Dutta J, Bhattacharyya J and Roy S B 1969 Ind. J. Phys. **43** 14

[2] Acharyya C R, Chatterjee A K, Sanyal P K and Acharyya S 1986 Ind. J. Pure Appl. Phys. **24** 234

[3] Saha U and Acharyya S 1993 Ind. J. Pure Appl. Phys. **31** 181

[4] Gopalakrishna K V 1957 Trans. Faraday Soc. **53** 767

[5] Sen S N and Ghosh R 1972 Ind. J. Pure Appl. Phys. **10** 701

[6] Acharyya S and Chatterjee A K 1985 Ind. J. Pure Appl. Phys. **23** 484

[7] Saha U and Acharyya S 1994 Ind. J. Pure Appl. Phys. **32** 346

[8] Bergmann K, Roberti D M and Smyth C P 1960 J. Phys. Chem **64** 665

[9] Bhattacharyya J, Hasan A, Roy S B and Kastha G S 1970 J. Phys. Soc. Japan **28** 204

[10] Saha U, Sit S K, Basak R C and Acharyya S 1994 J. Phys. D: Appl. Phys. **27** 596

[11] Fröhlich H 1949 Theory of Dielectrics (Oxford: Oxford University Press) p 94

[12] Srivastava S C and Suresch Chandra 1975 Ind. J. Pure Appl. Phys. **13** 101

[13] Sit S K and Acharyya S 1996 Ind. J. Pure Appl. Phys. **34** 255

[14] Murphy F J and Morgan S O 1939 Bull. Syst. Techn. J. **18** 502

[15] Smyth C P 1955 Dielectric Behaviour and Structure (New York: McGraw-Hill)

[16] Ghosh A K and Acharyya S 1978 Ind. J. Phys. **B 52** 129

[17] Weast R C (ed) 1976-77 Handbook of Chemistry and Physics 5th edn

CHAPTER 5

DOUBLE RELAXATIONS OF MONOSUBSTITUTED ANILINES IN BENZENE UNDER EFFECTIVE DISPERSIVE REGIONS

5. 1 Introduction

The highly nonspherical molecules like mono - or di-substituted benzenes and anilines have more then one relaxation times τs' due to presence of their flexible parts attached to the parent molecule[1,2]. The study of dielectric relaxation phenomena of such polar molecules in nonpolar solvent provides one with the valuable information of various types of interactions such as monomer and dimer formations[3-5] in liquids. The polar nonpolar liquid mixtures instead of pure polar liquids deserve much more advantages as the polar - polar interactions, viscosity effect and the other factors become minimized. Moreover, much disputed ambiguity concerning the internal field correction can also be avoided.

Bergmann *et al*[6] however, devised a graphical method to obtain τ_1 and τ_2 to represent the relaxation times of the smallest flexible part as well as the whole molecule for their end-over-end rotations under an electric field of Giga hertz frequency. The respective contributions c_1 and c_2 towards dielectric relaxation were also estimated in terms of τ_1 and τ_2. The method consists of plotting the normalised experimental points involved with the measured data of the real ε',the imaginary ε'' parts of the complex dielectric constant ε*, the static dielectric constant ε_0 and the optical dielectric constant ε_∞ at different frequencies ω on a semicircle in a complex plane. A point was, however, then selected on the chord through the two fixed points lying on the said semicircle which contained all the experimental points in consistency with the measured data for various frequencies. Bhattacharyya *et al*[7] subsequently simplified the above procedure to get τ_1, τ_2 and the weighted contributions c_1 and c_2 towards dielectric relaxations with the experimental values of ε', ε'', ε_0 and ε_∞ of a pure polar liquid measured at two different frequencies in GHz regions.

The highly nonspherical polar liquid molecules like mono-or di-substituted anilines and benzenes are usually thought to absorb energy much more strongly in a high frequency electric field of nearly 10 GHz. Moreover, such type of polar liquids are supposed to be non-Debye in their relaxation behaviours, From this point of view, the study of dielectric

relaxation of polar-nonpolar liquid mixtures under the electric field of nearly 3 cm wavelength is preferable. Saha *et al*[1] and Sit *et al*[2] recently presented an alternative approach to estimate τ_1 and τ_2 from the intercept and the slope of a derived straight line equation involved with dielectric relaxation solution data like. ε'_{ij}, ε''_{ij}, ε_{0ij} and $\varepsilon_{\infty ij}$ measured under a single frequency electric field of GHz range. One could not make a strong conclusion if ε_{0ij} and $\varepsilon_{\infty ij}$ of a polar solute (*j*) dissolved in a nonpolar solvent (i) were not accurately known.

Table 5.1 The dielectric relaxation parameters like ε'_{ij}, ε''_{ij}, ε_{0ij} and $\varepsilon_{\infty ij}$ of three isomers of anisidines and toluidines in benzene for different weight fractions ω_j's of solutes at 35°C under effective dispersive region of 9.945 GHz electric field.

System	Weight fraction (ω_j) of solute	ε'_{ij}	ε''_{ij}	ε_{0ij} at 450 KHz	$\varepsilon_{\infty ij} = n^2_{D_{ij}}$
I) o-anisidine in benzene	0.0326	2.3104	0.0148	2.336	2.239
	0.0604	2.3520	0.0244	2.404	2.247
	0.0884	2.4064	0.0340	2.459	2.255
	0.1135	2.4416	0.0400	2.538	2.262
	0.1361	2.4672	0.0512	2.588	2.267
II) m- anisidine in benzene	0.0160	2.2720	0.0234	2.315	2.235
	0.0336	2.3040	0.0390	2.384	2.241
	0.0579	2.3904	0.0618	2.477	2.246
	0.0823	2.4544	0.0744	2.553	2.253
	0.1109	2.5344	0.1056	2.675	2.261
III) p- anisidine in benzene	0.0319	2.3104	0.0252	2.373	2.237
	0.0597	2.3904	0.0474	2.442	2.246
	0.0848	2.5088	0.0642	2.539	2.250
	0.1106	2.5376	0.0840	2.638	2.262
	0.1396	2.6272	0.1086	2.745	2.269
IV) o- toluidine in benzene	0.0137	2.2752	0.0162	2.301	2.241
	0.0459	2.3648	0.0408	2.392	2.250
	0.0622	2.4032	0.0570	2.457	2.255
	0.1048	2.5376	0.0900	2.577	2.264
V) m- toluidine in benzene	0.0264	2.3136	0.0150	2.337	2.243
	0.0538	2.3552	0.0342	2.413	2.248
	0.0781	2.4576	0.0402	2.470	2.252
	0.1015	2.3840	0.0618	2.526	2.258
	0.1225	2.5280	0.0732	2.591	2.262
VI) p- toluidine in benzene	0.0213	2.3100	0.0102	2.319	2.237
	0.0428	2.3040	0.0204	2.367	2.244
	0.0616	2.3904	0.0276	2.413	2.249
	0.0916	2.4704	0.0384	2.483	2.254
	0.1048	2.4960	0.0582	2.523	2.260

Disubstituted anilines and benzenes were found to possess the double relaxation phenomena[1] by showing considerable values of τ_1 and τ_2 in solvent benzene under the electric field of 9.945 GHz. Monosubstituted anilines, however, showed mono as well as often the double relaxation phenomena[2] in solvent benzene under the electric field of different frequencies of 2.02 to 22.06 GHz. We, therefore, thought to use ε'_{ij}, ε''_{ij}, ε_{0ij} and $\varepsilon_{\infty ij}$ of such monosubstituted anilines for different weight fractions ω_is' under 9.945 GHz electric field which is supposed to be the most effective dispersive region for such isomers of anisidine and toluidine. The dielectric relaxation parameters were, however, obtained at 35°C as shown in Table 5.1 from the careful graphical interpolation made by the available data measured by Srivastava and Suresh Chandra[8] at different frequencies.

The monosubstituted anilines are really found to exhibit the expected double relaxation phenomenon under 9.945 GHz electric field at 35°C by showing reasonable values of τ_1 and τ_2 as presented in Table 5.2, from the slopes and the intercepts of curves of Fig 5.1 as derived from Bergmann's equations. The relative contributions c_1 and c_2 (Table 5.3) towards dielectric relaxations in terms of estimated τ_1 and τ_2 (Table 5.2) were evaluated by the graphical method[1,2] using Figs 5.2 and 5.3 as well as by Fröhlich's equations[9] respectively. The symmetric and the asymmetric distribution parameters of such compounds under the effective dispersive region of 9.945 GHz electric field can also be judged to throw much light on their distribution behaviour (Table 5.3). In absence of the reliable τ of such isomers of anisidine and toluidine, the slope of the linear variations of the imaginary parts K''_{ij} against the real parts K'_{ij} of the complex *hf* conductivities K^*_{ij} of solutions were used to get τ as shown in Table 5.2, together with τ_0, τ_s and τ_{cs} where τ_0 is the most probable relaxation time given by $\tau_o = \sqrt{\tau_1 \tau_2}$. τ_s and τ_{cs} are called symmetric and characteristic relaxation times associated with symmetric and asymmetric distribution parameters γ and δ respectively. The respective dipole moments μ_1, μ_2 and μ_0 in terms of τ_1, τ_2 and τ_0 of these compounds as obtained from the slope β of the linear variations of total *hf* conductivities K_{ij}s' of the solutions against ω_is' of monosubstituted anilines in

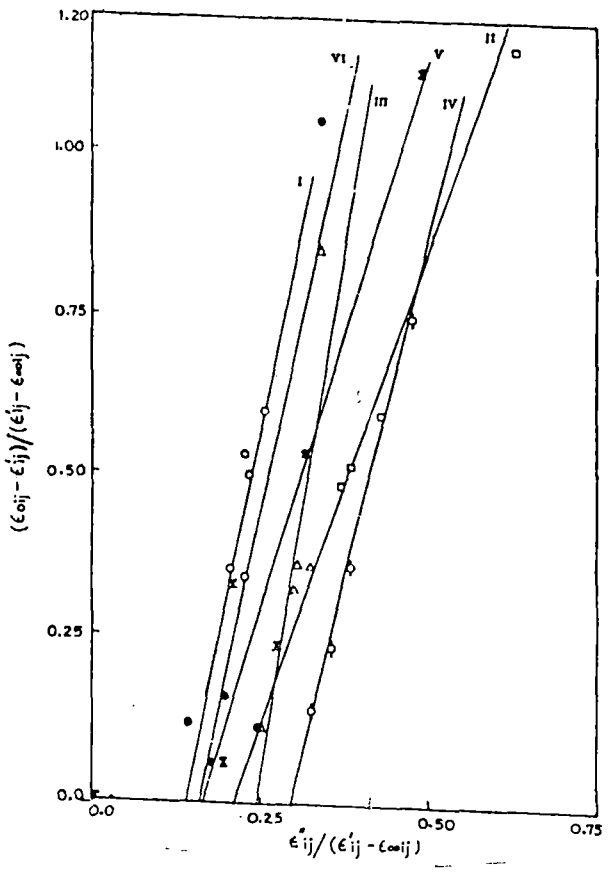

Figure 5.1 **Linear variation of** $(\varepsilon_{0ij}-\varepsilon'_{ij})/(\varepsilon'_{ij}-\varepsilon_{\infty ij})$ **against** $\varepsilon''_{ij}/(\varepsilon'_{ij}-\varepsilon_{\infty ij})$ **of mono-substituted anilines under 9.945 GHz electric field at 35°C**

System-I: *o*-**anisidine (-O-) System-II:** *m*-**anisidine (-□-)**
System-III: *p*-**anisidine (-Δ-) System-IV:** *o*-**toluidine (-◊-)**
System-V: *m*-**toluidine (-X-) System-VI:** *p*-**toluidine (-●-)**

Table 5.2 The slope and intercept of the straight lines of $[(\varepsilon_{0ij} - \varepsilon'_{ij})/(\varepsilon'_{ij} - \varepsilon_{\infty ij})]$ against $[(\varepsilon''_{ij})/(\varepsilon'_{ij} - \varepsilon_{\infty ij})]$, correlation co-efficients (r), % of error involved, relaxation times τ_1 and τ_2 of the flexible parts as well as the whole molecules, measured τ from $K''_{ij} - K'_{ij}$ equations and the most probable relaxation times τ_0 together with τ_s and τ_{as} from symmetric and asymmetric distribution parameters γ and δ of monosubstituted anilines at 35°C under 9.945 GHz electric field

System with Sl. No.	Slope and straight $[(\varepsilon_{0ij} - \varepsilon'_{ij})/$ versus $[(\varepsilon''_{ij})/$	intercept of lines Eq(5.7) $(\varepsilon'_{ij} - \varepsilon_{\infty ij})]$ $(\varepsilon'_{ij} - \varepsilon_{\infty ij})]$	Correlation Co-efficient (r)	% of error involved in Eq (5.7)	Estimated times τ_1 p	relaxation and τ_2 in sec	Most probable relaxation time $\tau_0 = (\tau_1\tau_2)^{1/2}$	Measured τ from $K''_{ij} - K'_{ij}$ Eq (5.20) in p sec	τ_s from symmetric distribution parameter γ of Eq (5.13)	τ_{as} from asymmetric distribution parameter δ of Eq (5.15)
I o-anisidine	4.9294	0.6583	0.7789	11.86	2.20	76.73	12.99	3.54	0.55	61.91
II m-anisidine	2.9043	0.6073	0.9888	0.67	3.63	42.87	12.47	4.77	14.78	86.39
III p-anisidine	6.2098	1.4923	0.8308	9.34	4.01	95.42	19.56	4.20	1.41	75.33
IV o-toluidine	4.2660	1.2707	0.9994	0.04	5.16	63.15	18.05	4.56	4.62	41.71
V m-toluidine	3.3514	0.5415	0.9622	2.24	2.73	50.94	11.79	5.52	0.64	66.69
VI p-toluidine	4.7133	0.7348	0.8684	7.41	2.58	72.88	13.71	3.57	0.66	20.13

Table 5.3 The estimated values of x [$= (\varepsilon'_{ij} - \varepsilon_{\infty ij})/(\varepsilon_{0ij} - \varepsilon_{\infty ij})$] and y [$= \varepsilon''_{ij}/(\varepsilon_{0ij} - \varepsilon_{\infty ij})$] from Fröhlich's equations and by the graphical techniques at $\omega_j \to 0$. Fröhlich's parameter A, symmetric and asymmetric distribution parameters γ and δ from x and y at $\omega_1 \to 0$ along with the relative contributions c_1 and c_2 due to Fröhlich and the graphical technique under 9.945 GHz electric field

System with Sl No.	Fröhlich's parameter $A=\ln(\tau_2/\tau_1)$	Estimated x and y from Eq (5.8) &	values of Fröhlich's (5.9)	Weighted c_1 & c_2 Eq (5.5) &	contribution from (5.6)	Esimated x & y from Fig at $\omega_1 \to 0$	values of (5.2) & (5.3)	Weighted c_1 & c_2 graphical	contributions from the technique	Symmetric & distribution γ & δ	asymmetric parameters
I o-anisidine	3.5518	0.5555	0.3457	0.5069	1.3869	0.0875	0.106	0.8946	-0.0732	0.47	0.09
II m-anisidine	2.4689	0.5848	0.4009	0.4997	0.8945	0.515	0.254	0.4825	0.4574	0.40	0.33
III p-anisidine	3.1695	0.4420	0.3655	0.4223	1.6298	0.810	0.140	0.8725	-0.4020	0.49	0.13
IV o-toluidine	2.5046	0.4594	0.4033	0.4293	1.1669	0.740	0.228	1.1326	-0.0478	0.35	0.25
V m-toluidine	2.9263	0.5933	0.3748	0.5170	1.0107	0.870	0.106	0.9097	-0.1564	0.49	0.09
VI p-toluidine	3.3410	0.5432	0.3574	0.4942	1.3351	0.950	0.084	0.9908	-0.3417	0.29	0.09

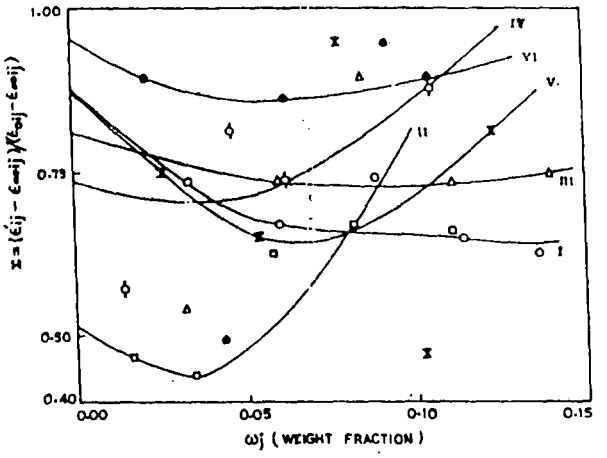

Figure 5.2 Variation of $(\varepsilon'_{ij} - \varepsilon_{\infty ij})/(\varepsilon_{0ij} - \varepsilon_{\infty ij})$ against weight fraction ω_js' of solutes under 9.945 GHz electric field at 35°C
System-I: *o*-anisidine (-O-) System-II: *m*-anisidine (-□-)
System-III: *p*-anisidine (-Δ-) System-IV: *o*-toluidine (-◊-)
System-V: *m*-toluidine (-X-) System-VI: *p*-toluidine (-●-)

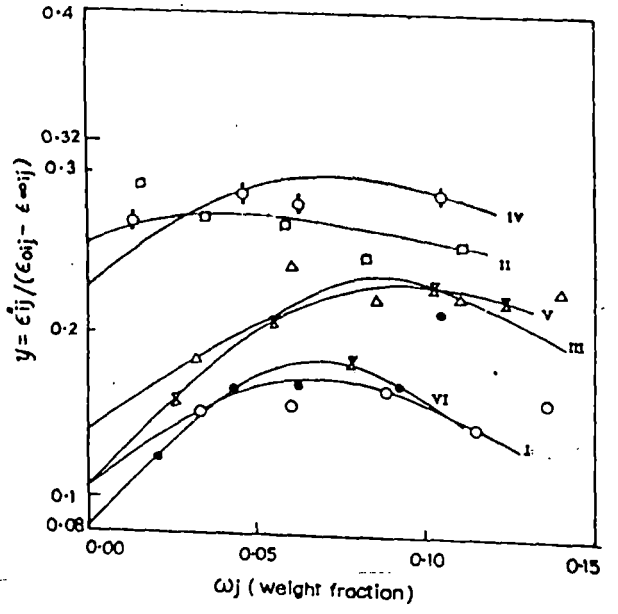

Figure 5.3 Variation of $\varepsilon''_{ij}/(\varepsilon'_{ij} - \varepsilon_{\infty ij})$ against ω_js' of isomers of anisidines and toluidines under 9.945 GHz electric field at 35°C
System-I: *o*-anisidine (-O-) System-II: *m*-anisidine (-□-)
System-III: *p*-anisidine (-Δ-) System-IV: *o*-toluidine (-◊-)
System-V: *m*-toluidine (-X-) System-VI: *p*-toluidine (-●-)

benzene (Fig 5.4) are in close agreement with the theoretical dipole moments μ_{theo}s. (Table 5.4) as computed from bond angles and bond moments of several groups in anisidines and toluidines with respect to benzene ring.

5.2 Theory and Formulation

When the polar molecule is provided with more than one relaxation times i. e., τ_1 and τ_2 Debye's equations of polar - nonpolar liquid mixture lead to Bergmann's equatons :

$$\frac{\varepsilon'_{ij}-\varepsilon_{\infty ij}}{\varepsilon_{0ij}-\varepsilon_{\infty ij}}=\frac{c_1}{1+\omega^2\tau_1^2}+\frac{c_2}{1+\omega^2\tau_2^2} \qquad \text{.....(5.1)}$$

$$\frac{\varepsilon''_{ij}}{\varepsilon_{0ij}-\varepsilon_{\infty ij}}=c_1\frac{\omega\tau_1}{1+\omega^2\tau_1^2}+c_2\frac{\omega\tau_2}{1+\omega^2\tau_2^2} \qquad \text{.....(5.2)}$$

such that $c_1 + c_2 = 1$.

The co-efficients c_1 and c_2 are the weight factors of the two Debye processes governed by τ_1 and τ_2 respectively. The symbols used in Eqs (5.1) and (5.2) convey the usual meanings:

$$\text{Let } x=\frac{\varepsilon'_{ij}-\varepsilon_{\infty ij}}{\varepsilon_{0ij}-\varepsilon_{\infty ij}}, \qquad y=\frac{\varepsilon''_{ij}}{\varepsilon_{0ij}-\varepsilon_{\infty ij}}$$

and $\omega\tau = \alpha$. Using the notations $a = 1/(1+\alpha^2)$ and $b = \alpha/(1+\alpha^2)$ the above Eqs (5.1) and (5.2) can be written as :

$$x = c_1a_1 + c_2a_2 \qquad \text{.....(5.3)}$$

$$y = c_1b_1 + c_2b_2 \qquad \text{.....(5.4)}$$

The suffices 1 and 2 with a and b are related to τ_1 and τ_2 respectively.

Evaluating c_1 and c_2 from Eqs (5.3) and (5.4) one gets:

Table 5.4 Intercepts and slope of K_{ij}-ω_j curve, dimensionless parameters bs' dipole moments μ_js' in Debye (D) together with estimated μ_1 from $\mu_1 = \mu_2 (c_1/c_2)^{1/2}$ and theoretical μ from bond angles and bond moments of isomers of anisidine and toluidine at 9.945 GHz electric field an at 35°C

System with Sl.No. & mol wt	Intercept & slope of K_{ij}-ω_j equation		Dimensionless parameter			Estimated dipole moments in Debye			μ_{theo} in D from bond angles and bond moments	Estimated μ_1 from $\mu_1 = \mu_2 (c_1/c_2)^{1/2}$ in D
	$\alpha \times 10^{-10}$ esu	$\beta \times 10^{-10}$ esu	$b_0 = \frac{1}{1+\omega^2\tau_0^2}$	$b_1 = \frac{1}{1+\omega^2\tau_1^2}$	$b_2 = \frac{1}{1+\omega^2\tau_2^2}$	μ_0 D	μ_1 D	μ_2 D		
I o-anisidine M_j = 123 gm	1.1244	0.7757	0.6030	0.9815	0.0417	2.45	1.92	9.33	1.02	5.64
II m-anisidine M_j = 123 gm	1.1039	1.4215	0.6224	0.9511	0.1224	3.27	2.264	7.37	1.65	5.51
III p-anisidine M_j = 123 gm	1.1060	1.4663	0.4012	0.9410	0.0274	4.13	2.70	15.82	1.89	8.05
IV o-toluidine M_j = 107 gm	1.1151	1.1932	0.4404	0.9059	0.0604	3.32	2.31	8.96	1.39	5.43
V m-toluidine M_j = 107 gm	1.1359	0.5788	0.6484	0.9718	0.0899	1.91	1.56	5.12	1.03	3.66
VI p-toluidine M_j = 107 gm	1.1323	0.3501	0.5770	0.9747	0.0460	1.57	1.21	5.56	1.54	3.38

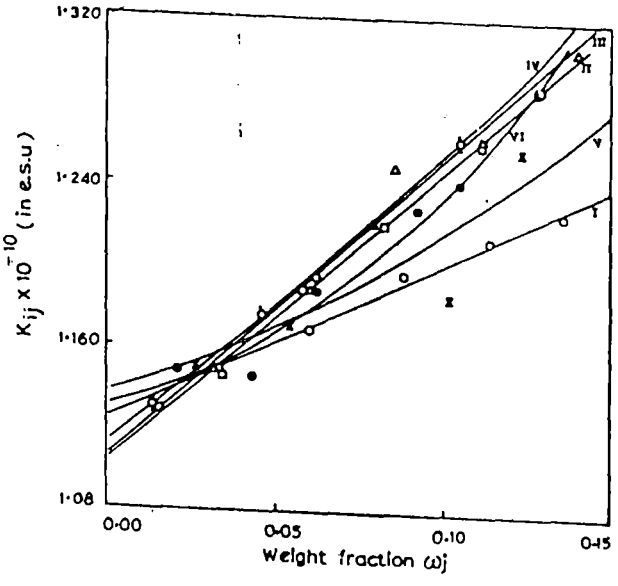

Figure 5.4 Variation of *hf* conductivity K_{ij} with different weight fractions ω_js' of solutes at 35°C and 9.945 GHz electric field
System-I: *o*-anisidine (-O-) System-II: m-anisidine (-□ -)
System-III: *p*-anisidine (-Δ-) System-IV: *o*-toluidine (-◊-)
System-V: *m*-toluidine (-X-) System-VI: *p*-toluidine (-●-)

$$c_1 = \frac{(x\alpha_2 - y)(1+\alpha_1^2)}{\alpha_2 - \alpha_1} \qquad \text{.....(5.5)}$$

and

$$c_2 = \frac{(y - x\alpha_1)(1+\alpha_2^2)}{\alpha_2 - \alpha_1} \qquad \text{.....(5.6)}$$

provided $\alpha_2 > \alpha_1$. Now adding Eqs (5.5) and (5.6) and since $c_1 + c_2 = 1$ we get :

$$\frac{1-x}{y} = (\alpha_1 + \alpha_2) - \frac{x}{y}\alpha_1\alpha_2$$

which on substitution of the values of x, y and α yields :

$$\frac{\varepsilon_{0ij} - \varepsilon'_{ij}}{\varepsilon'_{ij} - \varepsilon_{\infty ij}} = \omega(\tau_1 + \tau_2)\frac{\varepsilon''_{ij}}{\varepsilon'_{ij} - \varepsilon_{\infty ij}} - \omega^2\tau_1\tau_2 \qquad \text{.....(5.7)}$$

representing a straight line of $[(\varepsilon_{0ij} - \varepsilon'_{ij})/(\varepsilon'_{ij} - \varepsilon_{\infty ij})]$ against $[\varepsilon''_{ij}/(\varepsilon'_{ij} - \varepsilon_{\infty ij})]$ with slope $\omega(\tau_1 + \tau_2)$ and intercept $-\omega^2\tau_1\tau_2$. The slopes and intercepts of Eq. (5.7) were, however, evaluated by fitting ε'_{ij}, ε''_{ij}, ε_{0ij} and $\varepsilon_{\infty ij}$ for different ω_is' of the monosubstituted anilines, referred to Tables (5.1-5.4) and Figs (5.1-5.4) at 35°C under 9.945 GHz electric field. They are finally placed in Table 5.2. to yield, τ_1 and τ_2 respectively for them.

The weighted contributions c_1 and c_2 towards dielectric relaxation may be computed from Eqs (5.5) and (5.6) using x and y in Fröhlich's equations[9]

$$x = \frac{\varepsilon'_{ij} - \varepsilon_{\infty ij}}{\varepsilon_{0ij} - \varepsilon_{\infty ij}} = 1 - \frac{1}{2A}\ln\left(\frac{1+e^{2A}\omega^2\tau_s^2}{1+\omega^2\tau_s^2}\right) \qquad \text{.....(5.8)}$$

and

$$y = \frac{\varepsilon''_{ij}}{\varepsilon_{0ij} - \varepsilon_{\infty ij}} = \frac{1}{A}[\tan^{-1}(e^A\omega\tau_s) - \tan^{-1}(\omega\tau_s)] \qquad \text{.....(5.9)}$$

where A = Fröhlich parameter = $\ln(\tau_2/\tau_1)$ and τ_s= small limiting relaxation time = τ_1. Both c_1 and c_2 may also be calculated from Eqs (5.5) and (5.6) with the graphically extrapolated

fixed values of x and y when $\omega_j \rightarrow 0$ as shown in Figs (5.2) and (5.3). They are shown in Table 5.3.

The molecules appear to behave like nonrigid ones having either symmetric or asymmetric distribution parameters γ and δ which may be calculated from Eqs (5.10-5.11)

$$\varepsilon^{*}_{ij} = \varepsilon_{\infty ij} + \frac{\varepsilon_{oij} - \varepsilon_{\infty ij}}{1+(j\omega\tau_s)^{1-\gamma}} \qquad \text{.....(5.10)}$$

or,

$$\varepsilon^{*}_{ij} = \varepsilon_{\infty ij} + \frac{\varepsilon_{oij} - \varepsilon_{\infty ij}}{(1+j\omega\tau_{cs})^{\delta}} \qquad \text{..... (5.11)}$$

where $j = \sqrt{-1}$.

The former and the latter ones are associated with τ_s and τ_{cs} where τ_s and τ_{cs} are called the symmetric as well as the characteristic relaxation times. Separating the real and the imaginary parts of Eqs (5.10) and (5.11) and rearranging them in terms of x and y as shown in Figs (5.3) and (5.4) at $\omega_j \rightarrow 0$ we have the symmetric parameter γ from :

$$\gamma = \frac{2}{\pi}\tan^{-1}\left[(1-x)\frac{x}{y} - y\right] \qquad \text{.....(5.12)}$$

$$\tau_s = \frac{1}{\omega}\left\{\frac{1}{\left[\frac{x}{y}\cos\left(\frac{\gamma\pi}{2}\right) - \sin\left(\frac{\gamma\pi}{2}\right)\right]}\right\}^{1/(1-\gamma)} \qquad \text{.....(5.13)}$$

similarly, δ and τ_{cs} can be had from Eqs (5.11) as:

$$\tan^{-1}(\delta\phi) = \frac{y}{x} \qquad \text{.....(5.14)}$$

and

$$\tan\phi = \omega\tau_{cs} \qquad \text{..... (5.15)}$$

As the values of ϕ can not be estimated directly we draw a theoretical curve for log $(\cos\phi)^{1/\phi}$ against ϕ as shown in Fig 5.5 from which.

$$\log (\cos\phi)^{1/\phi} = \frac{\log \cos (\delta\phi)}{\delta\phi} \quad \text{.....(5.16)}$$

can be known. With the known ϕ from Fig 5.5 ; τ_{es} and δ can be estimated from Eqs (5.14) and (5.15) respectively. The τ_s and τ_{es} thus estimated are placed in Table 5.2 to compare with τ_1 and τ_2 from double relaxation method, but γ and δ are placed in Table 5.3

The complex high frequency conductivity K^*_{ij} of a dilute polar - nonpolar liquid mixture[12] is given by :

$$K^*_{ij} = K'_{ij} + jK''_{ij} \quad \text{.....(5.17)}$$

where $K'_{ij} = \frac{\omega}{4\pi}\varepsilon''_{ij}$ and $K'_{ij} = \frac{\omega}{4\pi}\varepsilon'_{ij}$.

The magnitude of the total hf conductivity is :

$$K_{ij} = \frac{\omega}{4\pi}(\varepsilon''^2_{ij} + \varepsilon'^2_{ij})^{\frac{1}{2}} \quad \text{.....(5.18)}$$

The dielectric permittivity ε'_{ij} of solution in hf region is very small and eventually equals the optical dielectric constant. The dielectric loss ε''_{ij} is responsible for the absorption of electrical energy and, therefore, offers resistance to polarisation. The K_{ij} may thus be approximated as :

$$K_{ij} = \frac{\omega}{4\pi}\varepsilon'_{ij} \text{ since } \varepsilon'_{ij} >> \varepsilon''_{ij}$$

The real part of the complex conductivity of a solution of weight - fraction ω_j of polar solute at T K is :

$$K'_{ij} = \frac{\mu_j^2 N \rho_{ij} F_{ij}}{3M_j kT}\left(\frac{\omega^2\tau}{1+\omega^2\tau^2}\right)\omega_j \quad \text{.....(5.19)}$$

where the symbols have their usual significance. But for hf region it can be shown that

$$K''_{ij} = K_{\infty ij} + \frac{K'_{ij}}{\omega\tau}$$

$$\text{or,} \quad K_{ij} = K_{\infty ij} + \frac{K'_{ij}}{\omega\tau} \quad \text{.....(5.20)}$$

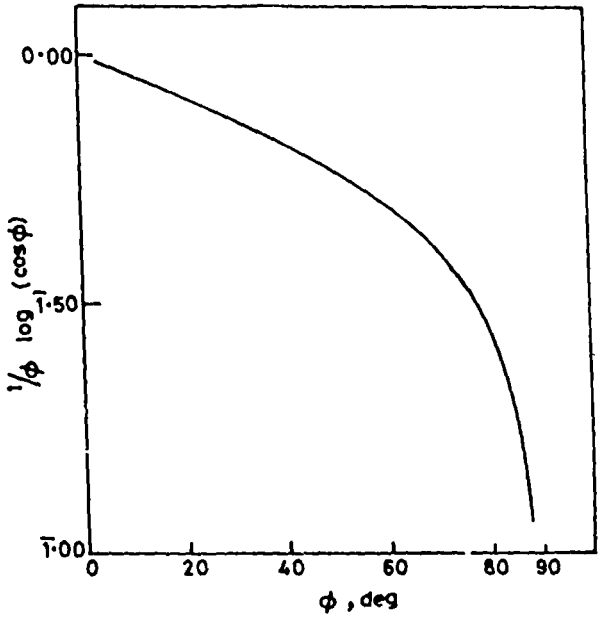

Figure 5.5 Variation of log $(\cos\phi)^{1/\phi}$ against ϕ

Since K_{ij} is a function of ω_j it can be shown at infinite dilution :

$$\left(\frac{dK'_{ij}}{d\omega_j}\right)_{\omega_j \to 0} = \omega\tau\beta \qquad \text{.....(5.21)}$$

where β is the slope of K_{ij} - ω_j curve at $\omega_j \to 0$. Eq (5.19) on being differentiated with respect to ω_j and at $\omega_j \to 0$ becomes.

$$\left(\frac{dK'_{ij}}{d\omega_j}\right)_{\omega_j \to 0} = \frac{\mu_j^2 N \rho_i F_i}{3 M_j kT}\left(\frac{\omega^2\tau}{1+\omega^2\tau^2}\right) \qquad \text{.....(5.22)}$$

because at $\omega_j \to 0$, ρ_{ij} the density of the solution becomes ρ_i, the density of the solvent and F_{ij} the local field in the solution becomes F_i, where $F_i = [(\varepsilon_i + 2)/3]^2$, ε_i, is the dielectric constant of the solvent. From Eqs. (5.21) and (5.22) we finally get :

$$\mu_j = \left(\frac{3 M_j kT\beta}{N\rho_i F_i \omega b}\right)^{1/2} \qquad \text{.....(5.23)}$$

as the dipole moment of the polar liquid in terms of *b* where

$$b = \frac{1}{1 + \omega^2\tau^2} \qquad \text{.....(5.24)}$$

which is a dimensionless parameter. The μ_1, μ_2 and μ_0 in terms of b_1, b_2 and b_0 involved with τ_1, τ_2 and τ_0 respectively were then computed with the knowledge of β. They are finally placed in Table 5.4 together with μ_{theo} obtained from bond angles and bond moments for comparison.

5.3 Results and Discussion

The values of x and y in terms of dielectric relaxation data at 9.945 GHz as shown in Table 5.1 are first estimated for different ω_js' with the available data[8] measured under 2.02, 3.86 and 22.06 GHz electric field. They are then plotted against ω_js' as shown in Figs (5.2) and (5.3) which are found to agree well with the Bergmann Eqs (5.1) and (5.2)

almost exactly. The close agreement of the curves in Figs (5.2) and (5.3), with Eqs. (5.1) and (5.2) suggests that the data (Table (5.1)) selected by graphical interpolations at 3 cm wavelength electric field are almost accurate. The dielectric relaxation parameters ε'_{ij}, ε''_{ij}, ε_{0ij}, and $\varepsilon_{\infty ij}$ thus obtained, are used to calculate the slopes and the intercepts of the fitted straight lines of Eq. (5.7) with the experimental points placed upon them as shown in Fig 5.1. The correlation coefficient r for each straight line is, however, estimated and found to lie within the range of 0.9994 to 0.7789 together with % error involved in each case. They are shown in 4th and 5th columns of Table 5.2. Table 5.2 also shows that *o*- and *p*-anisidine like *p*- toluidine exhibit errors of larger magnitudes than the other systems. This may, perhaps, be due to the uncertainty in the estimation of dielectric relaxation data for such systems. Monosubstituted anilines often showed double as well as mono relaxation behaviour as observed earlier[2]. *p*- anisidine, however, is an exception[2]. It showed the mono relaxation behaviour at 2.02, 3.86 and 22.06 GHz respectively. It is again very much interesting to note that all the anisidines and toluidines as referred to Table 5.2, nevertheless exhibit the double relaxation behaviour by showing reasonably considerable values of τ_1 (smaller) and τ_2 (larger) to represent the relaxation times for their flexible parts attached to the parent ring and the whole molecules respectively. It signifies that 9.945 GHz ($\cong$ 3 cm wavelength) electric field seems to be the most effective dispersive region for such molecule to yield τ_1 and τ_2.

The τ_2s` as observed from the slopes and the intercepts of Eq. (5.7) gradually increase from *meta*- to *ortho*- and to *para*-forms of all the anisidines and toluidines probably due to C—NH_2 groups which is highly influenced by 9.945 GHz ($\cong$ 3 cm wavelength) electric field for its different positions in them. The τ_1s`, on the other hand, increase from ortho to para for anisidines while reverse is true for toluidines. The increase in the values of $\tau_1$s` indicates the flexible parts of the molecules are more loosely bound to parent molecules[1,2].

The most probable relaxation time τ_0 as shown in the 8th column of Table 5.2, can be compared with the measured τs`from the slopes[5] of $K''_{ij}$ - $K'_{ij}$ along with symmetric $\tau_s$ and characteristic $\tau_{cs}$ from $\gamma$ and $\delta$. The $\tau$s` as shown in the 9th column of Table 5.2 agree

excellently well with τ_1. This fact indicates that the *hf* conductivity measurement of polar - nonpolar liquid mixture yields the microscopic relaxation time while the double relaxation method gives macroscopic as well as microscopic relaxation times as observed earlier[13]. τ_ss' in Table 5.2 are slightly smaller than τs', as obtained from *hf* conductivity for almost all systems besides *m*-ianisidine and *o*-toluidine whose τ_ss' agree well with τ_0 and τ respectively. The slight difference is due to different steric hindrances as a result of structural conformations. All these discussions made above, confirms τ_s to represent microscopic relaxation time. τ_{cs}s', on the other hand, are larger in magnitude and agree with τ_2 as obtained by double relaxation method. Thus τ_{cs} under the electric field of 9.945 GHz gives τ_2.

The relative contributions c_1 and c_2 towards dielectric relaxations were found out in the graphical method by using Figs 5.2 and 5.3 as well as Fröhlich's equations of $x\left[=\frac{\varepsilon'_{ij}-\varepsilon_{\infty ij}}{\varepsilon_{0ij}-\varepsilon_{\infty ij}}\right]$ and $y\left[=\frac{\varepsilon''_{ij}}{\varepsilon_{0ij}-\varepsilon_{\infty ij}}\right]$ both from Bergmann's Eqs (5.1) and (5.2) in terms of τ_1 and τ_2. The x and y in Fröhlich's Eqs (5.8) and (5.9) are related to Fröhlich parameter A which depends on the difference of the activation energies E_2 and E_1 of the rotating units and is expressed in terms of τ_2/τ_1 by $\tau_2/\tau_1 = \exp(E_2 - E_1)/RT$. The constancy of the factor $(E_2-E_1)/RT$ at a fixed temperature may be put equal to A where $A = \ln(\tau_2/\tau_1)$. The positive values of c_1 and c_2 such that $c_2 > c_1$ and $c_1+c_2 > 1$ in Fröhlich's method for all the systems are shown in the 5th and 6th columns of Table 5.3 together with the Fröhlich parameters A in the 2nd column respectively. But the graphical extrapolation technique suggested by Saha *et al*[1] and Sit *et al*[2], however, yields c_2 always negative except m-anisidine satisfying the condition that $c_1 + c_2 \cong 1$ as shown in the 9th and 10th columns of same Table 5.3. The negative sign before c_2 in the latter method signifies the lag in inertia of the whole molecules with respect to their flexible parts[1,2] under *hf* electric field.

The double relaxation times showed by all the monosubstituted anilines under 9.945 GHz electric field at 35°C indicate the nonrigidity of the molecules. This fact at once inspired us to test the symmetric as well as asymmetric distribution parameters γ and δ for

such compounds. They are calculated from Eqs (5.12) and (5.16) with the values of x and y at $\omega_j \rightarrow 0$ from Figs 5.2 and 5.3. The values of γ and δ thus obtained with the aid of the direct measurements of relaxation data seem to be accurate enough to specify the distribution parameters as placed in the last two columns of Table 5.3. It is observed from Table 5.3 that the values of γ lie in the range of $0.29 \leq \gamma \leq 0.49$ indicating thereby symmetric relaxation behaviour for such molecules under 9.945 GHz electric field. The low values of δ in the range of $0.09 \leq \delta \leq 0.33$ invariably rules out the possibility of occurrence of asymmetric dielectric distributions[14].

The dipole moments μ_1 and μ_2 of the flexible parts and the whole molecules of anisidines and toluidines are obtained from Eq. (5.23) in terms of dimensionless parameters b_1, b_2 from Eq. (5.24) involved with τ_1 and τ_2 respectively (Table 5.2) and the slope β of K_{ij} - ω_j curves in Fig 5.4 which shows the variation of K_{ij}s' with ω_js'. The intercepts and slopes of K_{ij} - ω_j equations are shown in the 2nd and 3rd columns of Table 5.4. The intercepts are of almost equal in magnitudes in all of them, but the slopes β increase slowly from *ortho*-to *para*- for anisidines and reverse in toluidines. The almost same intercepts and slopes of K_{ij} - ω_j curves in Fig 5.4 arise probably due to the identical polarity[3] of the molecules. Some of the curves in Fig 5.4 meet at a point near $\omega_j \rightarrow 0$ indicating thereby solute - solvent (monomer) or solute - solute (dimer) associations in the region $0.02 < \omega_j < 0.035$ of the concentration. Unlike toluidines the most probable dipole moments μ_0 and μ_1 gradually increase from *o*- to *p*- for anisidines as reported in 7th and 8th columns of Table 5.4. μ_2s', on the other hand, increase gradually from *m*- to *o*- with a high value in *p*- anisidine while in case of toluidines μ_2s' increase from *m*- to *p*- and *o*- configurations. The above facts, however, reveal that μ_0 as obtained from $\tau_0 = \sqrt{\tau_1 \tau_2}$ depends solely upon the group moments like μ_1 of their flexible parts. The gradual increase of μ_0 from *o*- to *p*-anisidine and from *p*- to *o*-toluidine like μ_1 is probably due to their almost same polarity as supported by the slopes βs' of K_{ij} as a function of ω_js' (Fig 5.4).

The theoretical dipole moments μ_{theo}s' from the bond angles and bond moments of C→OCH_3 in anisidines and C ←CH_3 in toluidines with C→ NH_2 with respect to the

benzene ring were already calculated elsewhere[2] and placed in the 10th column of Table 5.4. They are compared with all the μ_is' together with μ_1 from $\mu_1 = \mu_2 (c_1/c_2)^{1/2}$ assuming the two relaxation processes are equally probable.

5.4 Conclusion

The correlation coefficients r s' and hence the % of errors introduced in Eq. (5.7) with the dielectric relaxation parameters like ε'_{ij} . ε''_{ij} . ε_{0ij} and $\varepsilon_{\infty ij}$ of the polar - nonpolar liquid mixtures under 9.945 GHz electric field at 35°C (Table 5.1) as presented in Table 5.2, are within such range that τ_1 and τ_2 as obtained from the intercepts and slopes of Eq. (5.7) are of considerable accuracy because τs' are usually claimed to be accurate within ± 10%. The methodology of single frequency measurements of dielectric relaxation data at different ω_is' seems to be much simple in comparison to the existing methods where data of pure polar liquid at two or more electric field frequencies of GHz region are, usually required. The relative contributions c_1 and c_2 in terms of τ_1 and τ_2 are, however, obtained by using Fröhlich's equations as well as graphical technique which also offers a convenient method to decide either symmetric or asymmetric distribution behaviour under the electric field of given frequency. The dipole moments μ_1, μ_2 in terms of τ_1 and τ_2 and slope β of concentration variation of K_{ij} of polar - nonpolar liquid mixture provide the valuable information of the conformation of a complex polar liquid.

References

1 Saha U, Sit S. K, Basak R. C and Acharyya S, J Phys D, **27** (1994) 596.

2 Sit S. K; Basak R. C, Saha U and Acharyya S, J Phys D. **27** (1994) 2194.

3 Chatterjee A. K, Saha U, Nandi N, Basak R. C and Acharyya S, Indian J Phys **B, 66** (1992) 291.

4 Saha U and Acharyya S, Indian J Pure and Appl Phys, **31** (1993) 181.

5 Saha U and Acharyya S, Indian J Pure and Appl Phys, **32** (1994) 346.

6 Bergmann K, Roberti D. M and Smyth C. P, J Phys Chem, 64 (1960) 665.

7 Bhattacharyya J, Hasan A, Roy S. B and Kastha G. S, J Phys Soc Japan, **28** (1970) 204.

8 Srivastava S. C. and Suresh Chandra, Indian J Pure and Appl Phys, **13** (1975) 101.

9 Fröhlich H, Theory of Dielectrics (Oxford University Press, Oxford), 1949, p 94.

10 Cole K. S and Cole R. H, J Chem Phys, **9** (1941) 341.

11 Davidson D. W and Cole R. H, J Chem Phys, **19** (1951) 1484.

12 Murphy F. J and Morgan S. O, Bull syst Techn J, **18** (1939) 502.

13 Sit S. K and Acharyya S, Indian J Phys **B, 70** (1996) 19.

14 Suresh Chandra and Jai Prakash, J Phys Soc Japan, **35** (1975) 876.

CHAPTER 6

DOUBLE RELAXATION OF STRAIGHT CHAIN ALCOHOLS UNDER HIGH FREQUENCY ELECTRIC FIELD

6.1. Introduction

The dielectric relaxation phenomena of highly nonspherical polar liquids in nonpolar solvents under the ultra high frequency (uhf) electric fields have gained much attention [1,2] as they reveal various types of molecular interactions like solute - solute (dimer) and solute - solvent (monomer) formations in liquid mixtures. They also provide one with valuable information regarding sizes, shapes, structures and different thermodynamic parameters due to relaxation of the polar liquids [3].

The relaxation phenomena of pure primary alcohols are very interesting as they were found to possess three distinct low frequency Debye type processes predicting inherently the single relaxation time [4,5]. The dilution of polar alcohols with nonpolar solvents, however, increases the relative contributions towards dielectric dispersions in the hf electric field [6]. The straight chain mono - alcohols, on the other hand, are almost like polymers having $-CH_3$ and $-OH$ groups in their structures. Obviously, there exist many possibilities of internal and molecular rotations, bending, twisting etc each with a characteristic relaxation time. In averaging to the macroscopic condition, a distribution of relaxation time may also be possible. Mishra et al [7] claimed that it is not possible to resolve dielectric dispersion in three relaxation processes from the measured relaxation data under a single frequency electric field.

Again, to detect the double relaxation phenomena of a polar solute, Bergmann et al [8] proposed a technique based on measured relaxation parameters of pure polar liquid like real ε', loss ε'', of the complex dielectric constant ε^* as well as static ε_0 and the high frequency dielectric constant ε_∞ at different frequencies of the electric field. The term $\frac{\varepsilon'-\varepsilon_\infty}{\varepsilon_0-\varepsilon_\infty}$ was then plotted against $\frac{\varepsilon''}{\varepsilon_0-\varepsilon_\infty}$ following Cole - Cole semi-circle equation. A suitable chord joining the two fixed points on the semi-circle consistent with all the experimental points is then chosen to yield the relaxation time τ_1 and τ_2 of the flexible part and the whole molecule itself. Bhattacharyya et al [9] had subsequently modified the procedure of Bergmann et al [8] to get τ_1 and τ_2 of a pure polar liquid in terms of the relaxation parameters measured at two different frequencies of the electric field in the GHz range.

In such a context, we have studied the double relaxation phenomena of some straight chain aliphatic alcohols, namely 1 -butanol, 1 -hexanol, 1-heptanol and 1-decanol dissolved in n-heptane at 24.33, 9.25 and 3.00 GHz electric field together with methanol and ethanol dissolved in benzene at 9.84 GHz electric field respectively at a temperature of 25°C by the recently developed method [10]. It is usually made with the single frequency measurements of the dielectric relaxation parameters like ε'_{ij},ε''_{ij}, ε_{0ij}, and $\varepsilon_{\infty ij}$ of a polar solute (j) in a nonpolar solvent (i) for different weight frations ω_j's of the polar solute as shown in Table 6.1. τ_1 and τ_2 are then obtained from the slope and the intercept of a straight line equation containing the dielectric relaxation data of which ε_{0ij} and $\varepsilon_{\infty ij}$ should be accurately known [11]. The approach as suggested earlier [10], seems to be an effective tool to detect the double relaxation phenomena of the polar liquid in a nonpolar solvent within the framework of Debye and Smyth model. For such straight chain alcohols behaving almost like polymers, Onsager's equation may be a better choice due to the strong intermolecular force exerted by alcohols in solution owing to their high dipole moments. But the resulting expressions can not be solved so easily as has been done in [10], because of the presence of the quadratic term ε^*_{ij}. The method [10] was already applied to mono -substituted anilines [12] in benzene in order to get the frequency dependence of τ_1 and τ_2 under three different electric fields of 22.06, 3.86 and 2.02 GHz respectively, showing either the double or the mono-relaxation behaviours. p-anisidine alone shows the mono-relaxation bahaviour at all frequencies. When the data are extended to 9.945 GHz electric field, all of them, on the other hand, show the double relaxation phenomena [13]. No such rigorous study on monohydric alcohols has been made so far. So it seems worthwhile to make an extensive study on the available data of aliphatic alcohols [14] as well as ethanol and methanol [15,16] with special emphasis on possible occurrence of τ_1 and τ_2 in the hf electric field [6].

It is evident from Table 6.2 and Figure 6.1 that all the alcohols show the double relaxation phenomena in all the frequencies of GHz range except methanol at 9.84 GHz, indicating separate broad dispersions in them. Ethanol is a system with $\tau_2 >> \tau_1$ while methanol shows very high value of τ_2 only. τ_1 and τ_2 are compared with most probable

Table 6.1 Dielectric relaxation data like ε'_{ij}, ε''_{ij}, ε_{oij}, and $\varepsilon_{\infty ij}$ of some normal alcohols in n-heptane at 25°C from high frequency absorption measurements.

Weight fraction (ω_j) of solute.	frequency in GHz	ε'_{ij},	ε''_{ij},	ε_{oij}	$\varepsilon_{\infty ij}$
		System I : 1- Butanol in n-heptane			
	24.33	1.957	0.0079		
0.0292	9.25	1.963	0.0059	1.971	1.928
	3.00	1.970	0.0044		
	24.331	1.981	0.0147		
0.0451	9.25	1.985	0.0121	2.000	1.945
	3.00	1.994	0.0114		
	24.33	2.011	0.0236		
0.0697	9.25	2.015	0.0220	2.05	1.958
	3.00	2.03	0.0188		
	24.33	2.060	0.0425		
0.1163	9.25	2.066	0.0416	2.175	1.978
	3.00	2.101	0.0460		
	24.33	2.105	0.0644		
0.1652	9.25	2.121	0.0637	2.381	2.000
	3.00	2.180	0.0782		
	24.33	2.144	0.0818		
0.2072	9.25	2.172	0.0956	2.621	2.020
	3.00	2.244	0.1119		

System II :- 1-Hexanol in n-heptane.

	24.33	1.968	0.0131		
0.0459	9.25	1.970	0.0083	1.988	1.944
	3.00	1.977	0.0065		
	24.331	1.984	0.019		
0.0703	9.25	1.990	0.0121	2.015	1.952
	3.00	2.003	0.0117		
	24.33	2.001	0.0296		
0.1028	9.25	2.015	0.0226	2.064	1.970
	3.00	2.04	0.0214		
	24.33	2.037	0.0425		
0.1688	9.25	2.074	0.0454	2.196	1.989
	3.00	2.112	0.0446		
	24.33	2.088	0.0569		
0.2335	9.25	2.128	0.0688	2.36	2.002
	3.00	2.186	0.0755		
	24.33	2.134	0.0748		
0.2901	9.25	2.179	0.1000	2.580	2.018
	3.00	2.250	0.1097		

System III:- 1 - heptanol in n-heptane.

	24.33	1.975	0.0182		
0.0735	9.25	1.985	0.0129	2.008	1.945
	3.00	1.998	0.0111		
	24.33	2.007	0.0265		
0.1175	9.25	2.017	0.0232	2.066	1.957
	3.00	2.043	0.0216		
	24.33	2.076	0.0482		
0.1909	9.25	2.079	0.0438	2.195	1.989
	3.00	2.117	0.0456		
	24.33	2.097	0.0567		
0.2465	9.25	2.114	0.0609	2.315	2.002
	3.00	2.175	0.0651		
	24.33	2.126	0.0693		
0.2970	9.25	2.157	0.0774	2.464	2.008
	3.00	2.225	0.0864		

System IV:- 1 - Decanol. in n-heptane.

	24.33	1.965	0.012		
0.0572	9.25	1.968	0.009	1.976	1.94
	3.00	1.972	0.0041		
	24.33	1.979	0.0223		
0.0857	9.25	1.977	0.0146	2.003	1.952
	3.00	1.995	0.0086		
	24.33	2.003	0.0273		
0.1351	9.25	2.011	0.0228	2.05	1.964
	3.00	2.031	0.0194		
	24.33	2.036	0.0449		
0.2140	9.25	2.055	0.0386	2.147	1.990
	3.00	2.088	0.0371		
	24.33	2.064	0.0513		
0.2640	9.25	2.077	0.0484	2.220	2.008
	3.00	2.129	0.0496		
	24.33	2.097	0.0637		
0.3553	9.25	2.123	0.0656	2.346	2.03
	3.00	2.186	0.0690		

System V :- Ethanol in benzene.

0.0664		2.4500	0.008166	3.3	2.2620
0.1393		2.4833	0.012416	4.3	2.1904
0.2077	9.84	2.5000	0.020833	5.4	2.1199
0.2953		2.5500	0.029750	7.0	2.0621
0.3638		2.5666	0.034213	8.2	2.0164

System VI :- Methanol in benzene.

0.0514		2.4666	0.00822	4.8	2.2141
0.0930		2.5000	0.00833	6.5	2.1550
0.1495	9.84	2.5166	0.01677	8.6	2.0851
0.2266		2.5500	0.02975	11.4	2.0164
0.3049		2.5833	0.03875	13.7	1.9600

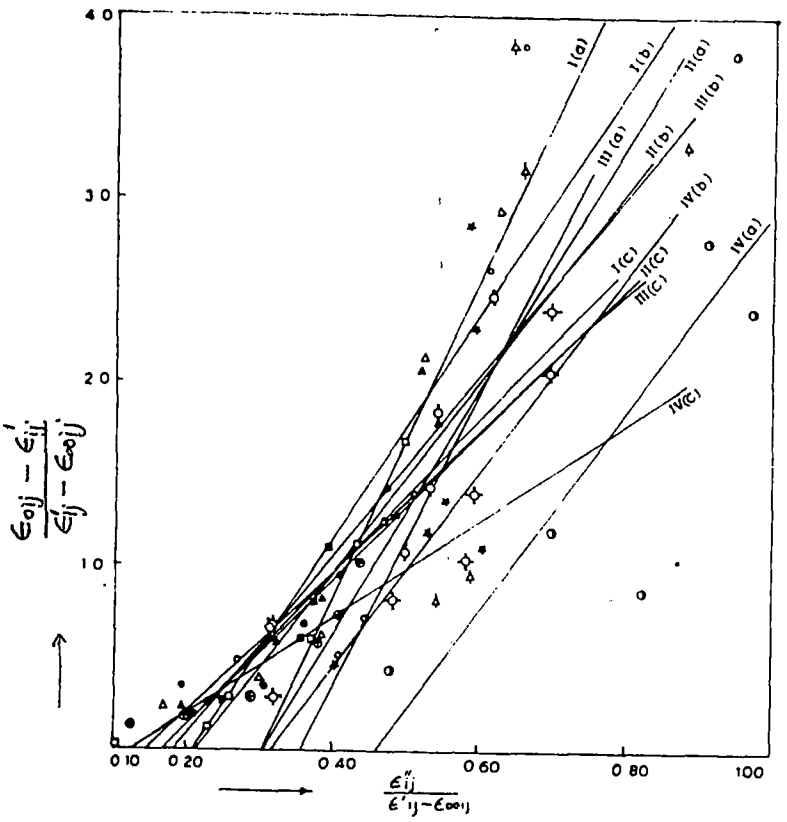

Figure 6.1 **Straight line plot of $(\varepsilon_{0ij}-\varepsilon'_{ij})/(\varepsilon'_{ij}-\varepsilon_{\infty ij})$ against $\varepsilon''_{ij}/(\varepsilon'_{ij}-\varepsilon_{\infty ij})$ of monoalcohols at 25°C under different *uhf* electric field**

System-I (a): (-O-) for 1-Butanol at 24.33 GHz
System-I (b): (-Δ-) for 1-Butanol at 9.25 GHz
System-I (c): (-□-) for 1-Butanol at 3.00 GHz

System-II (a): (-⧊-) for 1-Hexanol at 24.33 GHz
System-II (b): (-⧋-) for 1-Hexanol at 9.25 GHz
System-II (c): (-●-) for 1-Hexanol at 3.00 GHz

System-III (a): (-✱-) for 1-Heptanol at 24.33 GHz
System-III (b): (-▲-) for 1-Heptanol at 9.25 GHz
System-III (c): (-■-) for 1-Heptanol at 3.00 GHz

System-IV (a): (-◍-) for 1-Decanol at 24.33 GHz
System-IV (b): (-⧋-) for 1-Decanol at 9.25 GHz
System-IV (c): (-⊕-) for 1-Decanol at 3.00 GHz

Table 6.2 The estimated intercept and slopes of straight line equation $[(\varepsilon_{0ij} - \varepsilon'_{ij})/(\varepsilon'_{ij} - \varepsilon_{\infty ij})]$ against $[\varepsilon''_{ij}/\varepsilon'_{ij} - \varepsilon_{\infty ij})]$ with errors and correlation coefficients together with measured τ's of some normal alcohols at 25°C under different ultra high frequency (- gigahertz) electric field.

System with Sl. No. and molecular wt.	Frequency f in GHz	Intercept and slope of equation (6.8)		Correlation coefficient (r)	Percentage error in regression technique	Estimated values of τ_2 and τ_1 in p Sec		Measured τ_0 in p Sec	Most probable relaxation time $\tau_0 = \sqrt{\tau_1 \tau_2}$ in p Sec
I) I-Butanol	a) 24.33	2.6046	8.6557	0.9013	5.16	54.60	2.04	1.96	10.55
in n-heptane	b) 9.25	1.2809	6.1343	0.9347	3.47	101.87	3.73	4.30	19.49
M_j = 74 gm	c) 3.00	0.6825	4.1544	0.9328	3.57	211.41	9.10	16.98	43.86
II) I-Hexanol in	a) 24.33	2.045	6.7079	0.6195	18.58	41.81	2.10	2.74	9.37
n-heptane	b) 9.25	1.0803	5.1697	0.9163	4.42	85.24	3.76	5.86	17 90
M_j = 102 gm	c) 3.00	0.6651	4.0210	0.9308	3.67	204.26	9.17	13.14	43.28
III) I-Heptanol in	a) 24.33	2.8273	7.9933	0.6752	14.98	49.89	2.43	2.11	11.01
n-heptane	b) 9.25	0.9233	5.0147	0.9433	3.03	83.03	3.30	5.78	16.55
M_j = 116 gm	c) 3.00	0.6823	4.1075	0.9638	1.95	208.81	9.20	13.49	43.83
IV) I-Decanol in	a) 24.33	2.4813	5.4316	0.8153	9.23	32.25	3.30	2.69	10.32
n-heptane	b) 9.25	1.5735	5.1553	0.9463	2.87	83.14	5.61	5.71	21.60
Mj = 158 gm	c) 3.00	0.3316	2.6855	0.9228	4.08	135.66	6.89	14.37	30.57
V) Ethanol in benzene M_j = 46 gm	9.84	4.5211	288.7386	0.9416	3.42	4672.26	0.25	3.9	34.18
VI) Methanol in benzene M_j = 32 gm	9.84	-5.4003	198.2809	0.8952	5.99	3209.12	—	4.3	—

relaxation time τ_0 where $\tau_o = \sqrt{\tau_1 \tau_2}$ as shown in the last column of Table 6.2. In absence of accurate τ for such alcohols, τ's are estimated from the slope of the imaginary part K''_{ij} and the real part K'_{ij} of the total uhf conductivity K^*_{ij} and placed in the 9th column of Table 6.2 for comparison with τ_1, τ_2 and τ_o respectively.

The relative contributions towards the dielectric relaxation i.e. c_1 and c_2 due to τ_1 and τ_2 are estimated by using Fröhlich's equations [17] as well as graphical method (Figures 6.2 and 6.3). They are also shown in Table 6.3.

The dipole moments μ_1 and μ_2 of the flexible part as well as of the whole molecule are then estimated in terms of τ and slope β of the linear plot of K_{ij} against ω_j (Figure 6.4). They are shown in Table 6.4 in order to compare with μ_0 due to τ_o and μ_{theo} from bond angles and bond moments (Figure 6.5) respectively. The μ_1's in terms of c_1, c_2 and μ_2 are also calculated by assuming that the two relaxation processes are equally probable; and they are placed in the last column of Table 6.4 only to compare with μ_1 due to τ_1.

6.2 Theoretical formulations to estimate τ_1, τ_2; c_1, c_2 and μ_1, μ_2.

The complex dielectric constant ε^*_{ij} of a polar non-polar liquid mixture can be represented as the sum of a number of non-interacting Debye type dispersions in accordance with the Budo's [18] relation as:

$$\frac{\varepsilon^*_{ij} - \varepsilon_{\infty ij}}{\varepsilon_{0ij} - \varepsilon_{\infty ij}} = \sum_k \frac{c_k}{1 + j\omega\tau_k} \qquad \text{.....(6.1)}$$

where $j=\sqrt{-1}$ and $\sum c_k = 1$. The term c_k is the weight factor for the k-th type of relaxation mechanism. When the complex dielectric constant ε^*_{ij} consist of two non-interacting Debye type dispersions, Budo's relation reduces to Bergmann's [8] equations:

$$\frac{\varepsilon'_{ij} - \varepsilon_{\infty ij}}{\varepsilon_{0ij} - \varepsilon_{\infty ij}} = \frac{c_1}{1+\omega^2\tau_1^2} + \frac{c_2}{1+\omega^2\tau_2^2} \qquad \text{.....(6.2)}$$

and

$$\frac{\varepsilon''_{ij}}{\varepsilon_{0ij} - \varepsilon_{\infty ij}} = c_1 \frac{\omega\tau_1}{1+\omega^2\tau_1^2} + c_2 \frac{\omega\tau_2}{1+\omega^2\tau_2^2} \qquad \text{.....(6.3)}$$

such that $c_1 + c_2 = 1$, where c_1 and c_2 are the relative contributions towards dielectric relaxations due to intra-molecular relaxation time τ_1 and molecular relaxation time τ_2.

Putting $\frac{\varepsilon'_{ij} - \varepsilon_{\infty ij}}{\varepsilon_{0ij} - \varepsilon_{\infty ij}} = x$ and $\frac{\varepsilon''_{ij}}{\varepsilon_{0ij} - \varepsilon_{\infty ij}} = y$ with $\omega\tau = \alpha$ and using the abbreviations,

$a = \frac{1}{1+\alpha^2}$ and $b = \frac{\alpha}{1+\alpha^2}$, the above eqs. (6.2) and (6.3) can be written as

$$x = c_1 a_1 + c_2 a_2, \qquad \text{.....(6.4)}$$

$$y = c_1 b_1 + c_2 b_2, \qquad \text{.....(6.5)}$$

where suffices 1 and 2 with a and b are related to τ_1 and τ_2 respectively. From eqs. (6.4) and (6.5) since $\alpha_2 - \alpha_1 \neq 0$ and $\alpha_2 > \alpha_1$ we have

$$c_1 = \frac{(x\alpha_2 - y)(1 + \alpha_1^2)}{\alpha_2 - \alpha_1} \qquad \text{.....(6.6)}$$

$$c_2 = \frac{(y - x\alpha_1)(1+\alpha_2^2)}{\alpha_2 - \alpha_1} \qquad \text{.....(6.7)}$$

Now, using $c_1 + c_2 = 1$, one gets the following equation with the help of eqs. (6.6) and (6.7)

$$\frac{1-x}{y} = (\alpha_1 + \alpha_2) - \frac{x}{y}\alpha_1\alpha_2$$

which, on substitution of the values of x, y and α yields

$$\frac{\varepsilon_{0ij} - \varepsilon'_{ij}}{\varepsilon'_{ij} - \varepsilon_{\infty ij}} = \omega(\tau_1 + \tau_2)\frac{\varepsilon''_{ij}}{\varepsilon'_{ij} - \varepsilon_{\infty ij}} - \omega^2\tau_1\tau_2. \qquad \text{.....(6.8)}$$

Equation (6.8) is a straight line between $\frac{\varepsilon_{0ij} - \varepsilon'_{ij}}{\varepsilon'_{ij} - \varepsilon_{\infty ij}}$ and $\frac{\varepsilon''_{ij}}{\varepsilon'_{ij} - \varepsilon_{\infty ij}}$ with slope $\omega(\tau_1 + \tau_2)$ and intercept - $\omega^2\tau_1\tau_2$ respectively. Here, ω = angular frequency of the applied electric field of frequency f in GHz. When the eq. (6.8) is fitted with the measured dielectric relaxation data ε'_{ij}, ε''_{ij} ε_{0ij}, and $\varepsilon_{\infty ij}$ for different weight fractions ω_j's of each alcohol in

n-heptane (at 25°C under 24.33, 9.25 and 3.00 GHz electric fields) as well as of methanol and ethanol in benzene (at 9.84 GHz), we get the slopes and intercepts as shown in Table 6.2 to yield τ_1 and τ_2.

The relative contributions c_1 and c_2 towards the dielectric relaxations in terms of x,y and τ_1, τ_2 for each alcohol are found out and shown in Table 6.3. The theoretical values of x and y are, however, calculated from Fröhlich's equations [17]as

$$x = \frac{\varepsilon'_{ij} - \varepsilon_{\infty ij}}{\varepsilon_{0ij} - \varepsilon_{\infty ij}} = 1 - \frac{1}{2A} \ln \left(\frac{e^{2A} \omega^2 \tau_s^2 + 1}{1 + \omega^2 \tau_s^2} \right), \qquad \text{.....(6.9)}$$

and

$$y = \frac{\varepsilon''_{ij}}{\varepsilon_{0ij} - \varepsilon_{\infty ij}} = \frac{1}{A} \left[\tan^{-1}(e^A \omega\tau_s) - \tan^{-1}(\omega\tau_s) \right], \qquad \text{.....(6.10)}$$

where A = Fröhlich parameter = ln (τ_2/τ_1) and τ_s is called the small limiting relaxation time being given by $\tau_s = \tau_1$. A simple graphical extrapolation technique, on the other hand, has been adopted here to get the values of x and y at $\omega_j \to 0$, as illustrated graphically in Figures 6.2 and 6.3 respectively. This is really in accord with Bergmann's eqs. (6.2) and (6.3) when the once estimated τ_1 and τ_2 from eq (6.8) are substituted in the right hand sides of the above eqs. (6.2) and (6.3).

The dipole moments μ_1 and μ_2 of polar solutes in terms of τ_1 and τ_2 as obtained from the double relaxation method and slope β of the concentration variation of the experimental uhf conductivity K_{ij} are then estimated.The uhf conductivity K_{ij} is, however, given by Murphy and Morgan [19] as

$$K_{ij} = \frac{\omega}{4\pi} (\varepsilon''^2_{ij} + \varepsilon'^2_{ij})^{1/2}, \qquad \text{.....(6.11)}$$

which is a function of ω_j of polar solute. Although $\varepsilon''_{ij} < \varepsilon'_{ij}$ in the uhf electric field, still the term ε''_{ij} offers resistance to polarisation. Thus, the real part K'_{ij} of the uhf conductivity of a polar-nonpolar liquid mixture at T°K can be written according to Smyth [20] as:

Table 6.3 Fröhlich parameter A, relative contributions c_1 and c_2 due to τ_1 and τ_2, theoretical values of x and y due to Fröhlich equations (6.9) and (6.10) and those by our method at infinite dilution for monoalcohols under different uhf electric field at 25°C.

System with Sl. No. and molecular wt.	Frequency f in GHz	Fröhlich parameter $A=\ln(\tau_2/\tau_1)$	Theoretical values of x and y from eq. no. (6.9) and (6.10)		Theoretical values of c_1 and c_2 from eq. no. (6.4) and (6.5)		Estimated values of x and y at $\omega_j \to 0$ from Figs. (6.2) and (6.3)		Estimated values of c_1 and c_2 from graphical technique	
I) l-Butanol in n-heptane M_j =74gm	(a) 24.33	3.2871	0.3666	0.3495	0.3701	2.0678	0.83	0.218	0.9162	-0.3579
	(b) 9.25	3.3073	0.4651	0.3596	0.4394	1.6354	0.99	0.15	1.0483	-0.4076
	(c) 3.00	3.1455	0.5556	0.3670	0.4985	1.2024	1.11	0.13	1.1589	-0.2668
II) l-Hexanol in n-heptane M_j = 102gm	(a)24.33	2.9912	0.3924	0.3692	0.3885	1.6769	0.79	0.264	0.8694	0.0725
	(b) 9.25	3.1211	0.4885	0.3704	0.4535	1.4215	0.70	0.130	0.7385	-0.1234
	(c) 3.00	3.1035	0.5600	0.3689	0.5004	1.1707	1.005	0.078	1.0618	-0.4113
III) l-Heptanol in n-heptane M_j = 116 gm	(a) 24.33	3.0219	0.3464	0.3588	0.3580	1.8763	0.655	0.236	0.7464	-0.0586
	(b) 9.25	3.2253	0.5112	0.3647	0.4703	1.3973	0.835	0.130	0.8724	-0.1575
	(c) 3.00	3.1222	0.5560	0.3682	0.4983	1.1910	1.045	0.116	1.0942	-0.2853
IV) l-Decanol in n-heptane M_j = 158 gm	(a) 24.33	2.2796	0.3412	0.3962	0.3644	1.2809	1.11	0.29	1 4687	-1.5413
	(b) 9.25	2.6960	0.4268	0.3899	0.4105	1.3544	0.955	0.17	1.0911	-0.7627
	(c) 3.00	2.9801	0.6640	0.3585	0.5611	0.8453	1.005	0.012	1.0716	-0.3678
V) Ethanol in benzene M_j = 46 gm	9.84	9.8357	0.4240	0.1577	0.4236	43.6436	0.24	0.0099	0.2400	1.7937

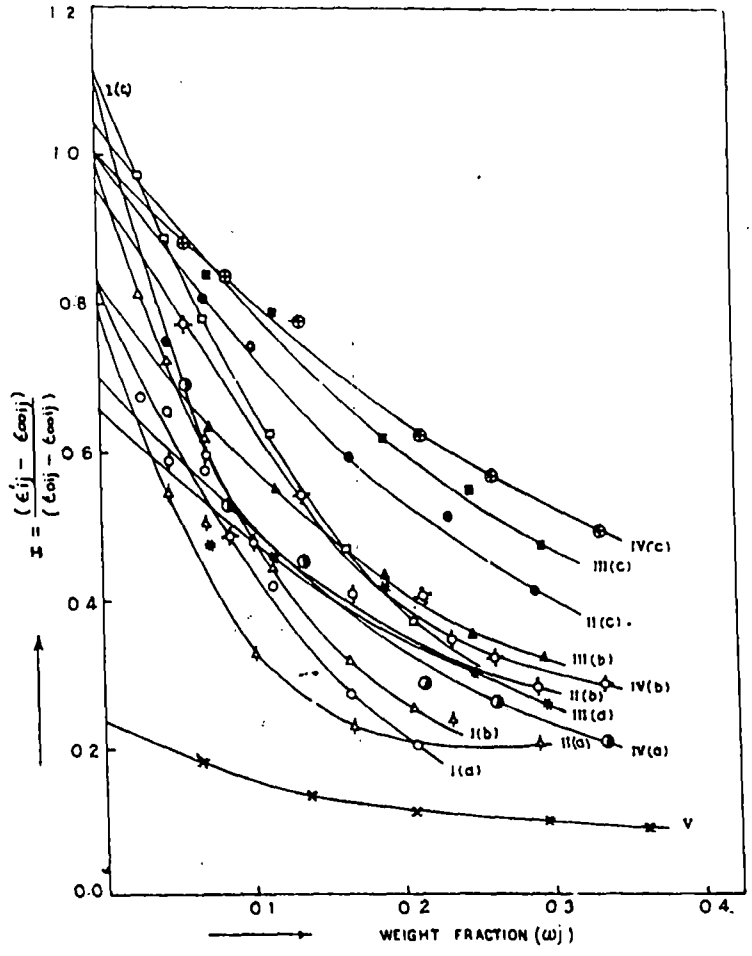

Figure 6.2 **Variation of $(\varepsilon'_{ij}-\varepsilon_{\infty ij})/(\varepsilon_{0ij}-\varepsilon_{\infty ij})$ against weight fraction ω_j for monoalcohols at different *uhf* electric field**

System-I (a): (-O-) for 1-Butanol at 24.33 GHz
System-I (b): (-Δ-) for 1-Butanol at 9.25 GHz
System-I (c): (-□-) for 1-Butanol at 3.00 GHz

System-II (a): (-Δ-) for 1-Hexanol at 24.33 GHz
System-II (b): (-Q-) for 1-Hexanol at 9.25 GHz
System-II (c): (-●-) for 1-Hexanol at 3.00 GHz

System-III (a): (-✱-) for 1-Heptanol at 24.33 GHz
System-III (b): (-▲-) for 1-Heptanol at 9.25 GHz
System-III (c): (-■-) for 1-Heptanol at 3.00 GHz

System-IV (a): (-◐-) for 1-Decanol at 24.33 GHz
System-IV (b): (-Q-) for 1-Decanol at 9.25 GHz
System-IV (c): (-⊕-) for 1-Decanol at 3.00 GHz

System-V : (-X-) for 1-Ethanol at 9.84 GHz

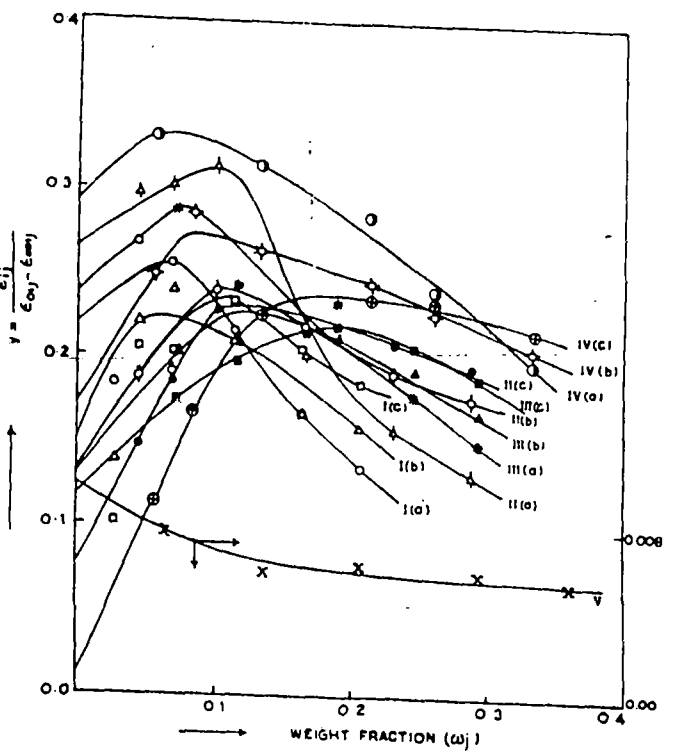

Figure 6.3 Variation of $\varepsilon''_{ij}/(\varepsilon'_{ij}-\varepsilon_{\infty ij})$ against weight fraction ω_j for monoalcohols at different *uhf* electric field

System-I (a): (-O-) for 1-Butanol at 24.33 GHz
System-I (b): (-Δ-) for 1-Butanol at 9.25 GHz
System-I (c): (-□-) for 1-Butanol at 3.00 GHz

System-II (a): (-⏃-) for 1-Hexanol at 24.33 GHz
System-II (b): (-⏀-) for 1-Hexanol at 9.25 GHz
System-II (c): (-●-) for 1-Heptanol at 3.00 GHz

System-III (a): (-✱-) for 1-Heptanol at 24.33 GHz
System-III (b): (-▲-) for 1-Heptanol at 9.25 GHz
System-III (c): (-■-) for 1-Heptanol at 3.00 GHz

System-IV (a): (-⏀-) for 1-Decanol at 24.33 GHz
System-IV (b): (-⏀-) for 1-Decanol at 9.25 GHz
System-IV (c): (-⊕-) for 1-Decanol at 3.00 GHz

System-V : (-X-) for 1-Ethanol at 9.84 GHz

$$K'_{ij} = \frac{\mu_j^2 N \rho_{ij} F_{ij}}{3M_j kT} \left(\frac{\omega^2 \tau}{1+\omega^2 \tau^2} \right) \omega_j \qquad \text{.....(6.12)}$$

Differentiating the above eq. (6.12) with respect to ω_j and for $\omega_j \rightarrow 0$, the eq (6.12) reduces to

$$\left(\frac{dK'_{ij}}{d\omega_j} \right)_{\omega_j \rightarrow 0} = \frac{\mu_j^2 N \rho_i F_i}{3M_j kT} \left(\frac{\omega^2 \tau}{1+\omega^2 \tau^2} \right), \qquad \text{.....(6.13)}$$

where, M_j is the molecular weight of a polar solute, N is the Avogadro's number, k is the Boltzman's constant, the local field $F_{ij} = \frac{1}{9}(\varepsilon_{ij}+2)^2$ becomes $F_i = \frac{1}{9}(\varepsilon_i+2)^2$ and the density $\rho_{ij} \rightarrow \rho_i$ the density of solvent at $\omega_j \rightarrow 0$.

Again, the total uhf conductivity $K_{ij} = \frac{\omega}{4\pi}\varepsilon'_{ij}$ can now be written as :

$$K_{ij} = K_{\infty ij} + \frac{1}{\omega\tau} K'_{ij}$$

or

$$\left(\frac{dK'_{ij}}{d\omega_j} \right)_{\omega_j \rightarrow 0} = \omega\tau \left(\frac{dK_{ij}}{d\omega_j} \right)_{\omega_j \rightarrow 0} = \omega\tau\beta, \qquad \text{.....(6.14)}$$

where β is the slope of K_{ij} - ω_j curve at infinite dilution, From eqs. (6.13) and (6.14) we thus get

$$\mu_j = \left(\frac{3M_j \, k \, T\beta}{N \rho_i \, F_i \, \omega b} \right)^{1/2} \qquad \text{.....(6.15)}$$

in order to obtain the dipole moment in terms of b, where b is a dimensionless parameter given by

$$b = \frac{1}{1+\omega^2\tau^2}. \qquad \text{.....(6.16)}$$

The computed μ_1, μ_2 and μ_0 together with b_1, b_2 and b_0 and β's of K_{ij} - ω_j equations for all the alcohols are given in Table. 6.4.

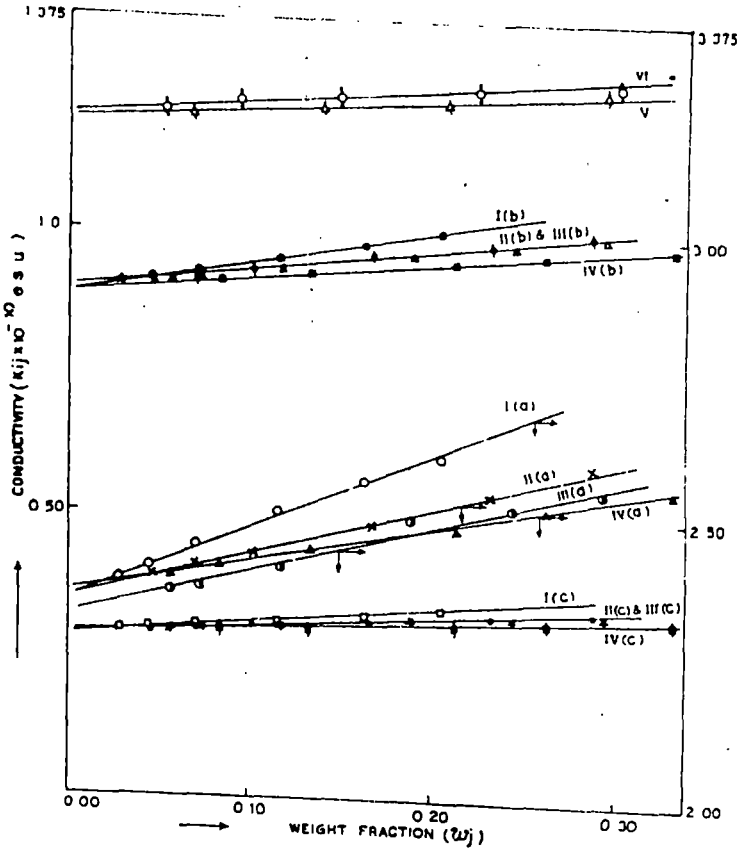

Figure 6.4 Straight line plots of K_{ij} against ω_j under different uhf electric field at 25°C

System-I (a): (-O-) for 1-Butanol at 24.33 GHz
System-I (b): (-✱-) for 1-Butanol at 9.25 GHz
System-I (c): (-□-) for 1-Butanol at 3.00 GHz

System-II (a): (-X-) for 1-Hexanol at 24.33 GHz
System-II (b): (-◆-) for 1-Hexanol at 9.25 GHz
System-II (c): (-●-) for 1-Hexanol at 3.00 GHz

System-III (a): (-◑-) for 1-Heptanol at 24.33 GHz
System-III (b): (-Δ-) for 1-Heptanol at 9.25 GHz
System-III (c): (-✱-) for 1-Heptanol at 3.00 GHz

System-IV (a): (-▲-) for 1-Decanol at 24.33 GHz
System-IV (b): (-■-) for 1-Decanol at 9.25 GHz
System-IV (c): (-■-) for 1-Decanol at 3.00 GHz

System-V : (-Δ-) for Ethanol at 9.84 GHz

System-VI : (-Q-) for Methanol at 9.84 GHz

6.3. Results and discussions

The least - square - fitted straight line equations of $(\varepsilon_{0ij} - \varepsilon'_{ij})/(\varepsilon'_{ij} - \varepsilon_{\infty ij})$ against $\varepsilon''_{ij}/(\varepsilon'_{ij} - \varepsilon_{\infty ij})$ for different weight fractions ω_j's of 1-butanol, l-hexanol, l-heptanol and l-decanol in n-heptane under alternating electric field of 24.33, 9.25 and 3.00 GHz at 25°C are shown in Figure 6.1, together with the experimental points on them as seen in Table 6.1. The straight line equations of methanol and ethanol in benzene at 9.84 GHz are:

$$\frac{\varepsilon_{0ij} - \varepsilon'_{ij}}{\varepsilon'_{ij} - \varepsilon_{\infty ij}} = 198.2809 \frac{\varepsilon''_{ij}}{\varepsilon'_{ij} - \varepsilon_{\infty ij}} + 5.4003$$

and $$\frac{\varepsilon_{0ij} - \varepsilon'_{ij}}{\varepsilon'_{ij} - \varepsilon_{\infty ij}} = 288.7386 \frac{\varepsilon''_{ij}}{\varepsilon'_{ij} - \varepsilon_{\infty ij}} - 4.5211 \text{ respectively.}$$

The experimental data of $(\varepsilon_{0ij} - \varepsilon'_{ij})/(\varepsilon'_{ij} - \varepsilon_{\infty ij})$ for methanol and ethanol are so high that they can not be plotted in Figure 6.1. In absence of reliable values of ε_{0ij} and $\varepsilon_{\infty ij}$ for methanol, it is not possible to show the applicability of simple mixing rule in determining relaxation data for this system. But the method has been applied to ethanol and it is found that the τ value is 3207.57 p Sec which is in good agreement with the measured data as presented in Table 6.2. The weight fractions ω_j's of the respective solutes have been obtained from mole fractions x_i and x_j of the solvent and solute of molecular weights M_i and M_j respectively by a relation [21]

$$\omega_j = \frac{x_j M_j}{x_i M_i + x_j M_j} \qquad \text{.....(6.17)}$$

The linearity of all the straight lines, as illustrated in Figure 6.1; is, however, tested by evaluating their correlation coefficient r. They are found to lie within the range of 0.9638 to 0.6195 as shown in Table 6.2. The corresponding percentage of errors in the fitting technique, can be had from the correlation coefficients. They are all shown in the 5-th and the 6-th columns of Table 6.2 respectively. The errors, are, however, large in magnitudes in the hf electric field of 24.33 GHz for l-hexanol, 1-heptanol and l-decanol respectively, probably due to unavoidable uncertainty in measurements of relaxation parameters for such higher frequency.

τ_1 and τ_2 for each alcohol are estimated from the slope and the intercept of straight line eq (6.8) and are placed in the 7-th and the 8-th columns of Table 6.2 respectively. All the monoalcohols show τ_1 and τ_2 at all the frequencies with an exception for methanol which exhibits the monorelaxation behaviour [12].

The monorelaxation behaviour [12] can easily be evaluated on the basis of the relaxation parameters by putting $c_1 = 0$ in eqs (6.2) and (6.3). The resulting equation becomes :

$$\frac{\varepsilon_{0ij} - \varepsilon'_{ij}}{\varepsilon'_{ij} - \varepsilon_{\infty ij}} = \omega\tau_2 \frac{\varepsilon''_{ij}}{\varepsilon'_{ij} - \varepsilon_{\infty ij}} \qquad \text{.....(6.18)}$$

τ_2 for methanol is found to be 5254.3 p Sec in approximate agreement with τ_2 as obtained by double relaxation method (Table 6.2). τ_2's and τ_1's as obtained from the double relaxation method are then compared with the most probable relaxation time τ_0 where $\tau_0 = \sqrt{\tau_1 \tau_2}$ and the measured relaxation time τ_s's from the slope of the given relation :

$$K''_{ij} = K_{\infty ij} + \frac{1}{\omega\tau_s} K'_{ij}, \qquad \text{.....(6.19)}$$

where $K_{\infty ij}$ is the constant conductivity at infinite dilution. Both τ_0 and τ_s are shown in the 10-th and the 9-th columns of Table 6.2 respectively. τ_2 and τ_1 for the double relaxation processes show low values at 24.33 GHz and increase gradually at the lower frequencies of 9.25 and 3.00 GHz respectively. This is explained on the basis of the fact that at higher frequency, the rate of hydrogen bond rupture in long chain alcohols may be maximum to reduce τ for each rotating unit. This sort of behaviour is also observed in the estimated τ_s and τ_0 respectively. Although the measured τ_s and τ_0 are smaller in magnitudes, τ_1 agrees excellently with τ_s (Table 6.2). This is perhaps due to the fact that the hf conductivity measurement always yields the average microscopic relaxation time whereas the double relaxation phenomena offers a better understanding of microscopic as well as macroscopic molecular relaxation times.

The relative contributions c_1 and c_2 towards dielectric relaxations for each alcohol have been evaluated from Bergmann's eqs. (6.2) and (6.3) for fixed values of τ_1 and τ_2 as

predicted by eqs. (6.8) with the estimated x and y from graphical technique as well as from Fröhlich's eqs. (6.9) and (6.10) respectively. c_1 and c_2 thus obtained by Fröhlich's method are placed in the 6-th and 7-th columns of Table 6.3. In the 10-th and the 11-th columns of the same Table 6.3 are shown c_1 and c_2 values with the fixed values of x and y at infinite dilutions of Figures 6.2 and 6.3. The variations of x and y with ω_j are concave and convex in nature as illustrated graphically in Figures 6.2 and 6.3 in accordance with Bergmann's eqs (6.2) and (6.3) respectively. Ethanol is an exception whose y value changes in a similar way as x. This anomaly is perhaps due to nonavailability of the accurate ε_{0ij} and $\varepsilon_{\infty ij}$ [11], and it thereby yields abnormally high τ value like methanol, although the latter one exhibits monorelaxation behaviours as shown in Table 6.2. However, the estimated value of c_2 is greater than c_1 for each alcohol, under investigation, in Fröhlich's method, while the reverse is true for the graphical method. Eventually, c_2 is -ve for most of the cases except l-hexanol at 24.33 GHz and ethanol at 9.84 GHz respectively in the latter case. This -ve value of c_2 is due to inertia of the flexible part [10]. This type of behaviour may be explained on the basis of the fact that the latter one ascertains the nature of the flexible part in comparison to Fröhlich's method. It is also interesting to note that unlike Fröhlich's method, the latter method yields $c_1 + c_2 < 1$ except for l-decanol at 24.33 GHz where $c_1 + c_2 < 0$, although $| c_1 + c_2 | > 1$ signifying more than two relaxation processes may be possible in them [14].

The dipole moments $\mu_1$and μ_2 of all the alcohols, as enlisted in Table 6.4 were estimated in terms of dimensionless parameters b_1 and b_2 and slopes β of K_{ij} versus ω_j equations by using eq (6.15). The linear variation of uhf conductivities K_{ij} of all the alcohols as a function of ω_j's are shown in Figure 6.4. The correlation coefficient r and the corresponding percentage of error in the estimation of the slope β and hence all the μ's together with b's are shown in Table 6.4. From Table 6.4, μ_2's are, however, found to be large at 24.33 GHz while in comparatively lower frequencies like 9.25 and 3.00 GHz, they are gradually smaller for each polar alcohol under our investigation. But μ_1's, on the other

hand, show the opposite trend. It is also interesting to note that the values of μ_2's for all the alcohols decrease with the increase of C-atoms in them. This type of behaviour may be explained by the fact that the long chain polymer type molecules having a large number of carbon atoms, in a nonpolar solvent, tend to break up in the hf electric field in order to reduce or even eliminate the absorption attributable to them. The proportion of smaller molecular species, on the other hand, have comparatively smaller number of C-atoms and the corresponding absorption will increase [14]. This is also confirmed by the fact that as τ decreases with increasing ω, the term $\omega^2\tau^2$ is higher and therefore, eq (6.16) yields smaller b values to increase μ's according to eq. (6.15).

μ_1, μ_2 and μ_0 are finally compared with μ_{theo} for the orientational polarisation of all the associated liquids containing a large number of dipolar groups like $H_3 \rightarrow C$, $C \leftarrow 0$ and $0 \leftarrow H$ when their individual monomeric moments are added vectorially as shown in Figure 6.5. μ_{theo} may also be inferred from Fröhlich's equation having correlation factor which bears structural information for such liquids. But to a fair approximation, the structural conformation of such liquids, as shown diagrammatically in Figure 6.5 and placed in Table 6.4, from the bond moments of $H_3 \rightarrow C$, $C \leftarrow 0$ and $0 \leftarrow H$ and the bond angle of 105° made by –OH groups with the main bond axis, have major contributions in yielding the theoretical dipole moment, μ_{theo}. All the μ's are displayed in Table 6.4 with those of μ_1, where $\mu_1 = \mu_2\left(\frac{c_1}{c_2}\right)^{1/2}$ assuming the two relaxation processes are equally probable. These μ_1's are slightly larger in magnitudes in comparison to μ_{theo}, μ_1 and μ_0 which are in close agreement among themselves.

6.4. Conclusion

The methodology so far advanced for double and single broad dispersions of the polar-nonpolar liquid mixtures seems to be much simpler, straightforward and significant one to detect the existence of double and monorelaxation behaviours of polar liquids in nonpolar solvents. The correlation coefficients between the desired parameters as given in

Table 6.4 The estimated intercept (α) and slope (β) of K_{ij}- ω_j equation with correlation coefficient (r) and percentage of error, dimensionless parameters β's and dipole moments μ_js with theoretical μ_{theo}'s and μ's calculated by using the relation $\mu_1 = \mu_2 (c_1/c_2)^{1/2}$ at 25°C of monoalcohols under different hf electric field.

System with Sl. No. and Mol. Wt. of solute	Frequency f in GHz	Intercept and slope of K_{ij} -ω_j eqn.		Correlation coeff. (r)	% of error in regre. tech.	Dimensionless para meters				Estimated dipole moments in Debye			
		$\alpha \times 10^{-10}$ in e.s.u.	$\beta \times 10^{-10}$ in e.s.u.			$b_0 = \frac{1}{1+\omega^2\tau_0^2}$	$b_2 = \frac{1}{1+\omega^2\tau_2^2}$	$b_1 = \frac{1}{1+\omega^2\tau_1^2}$	μ_0	μ_2	μ_1	μ_{theo}	$\mu_1 = \mu_2\left(\frac{c_1}{c_2}\right)^{\frac{1}{2}}$
I) l-Butanol in n-heptane M_j = 74 gm	(a) 24.33	2.3523	1.2679	0.9978	0.12	0.2777	0.0142	0.9115	1.97	8.75	1.09		3.70
	(b) 9.25	0.8941	0.5400	0.9997	0.01	0.4382	0.0278	0.9552	1.66	6.62	1.13	1.49	3.43
	(c) 3.00	0.2887	0.2338	0.9999	0.00	0.5942	0.0593	0.9715	1.65	5.23	1.29		3.37
II) l-Hexanol in n-heptane M_j = 102 gm	(a) 24.33	2.3522	0.8192	0.9961	0.21	0.3279	0.0239	0.9066	1.72	6.36	1.03		3.06
	(b) 9.25	0.8929	0.4005	0.9997	0.01	0.4804	0.0392	0.9545	1.61	5.63	1.14	1.31	3.18
	(c) 3.00	0.2889	0.1695	0.9999	0.00	0.6006	0.0633	0.9710	1.64	5.06	1.29		3.31
III) l-Heptanol in n-heptane M_j = 116 gm	(a) 24.33	2.3169	0.8276	0.9927	0.40	0.2611	0.0169	0.8788	2.06	8.10	1.12		3.54
	(b) 9.25	0.8973	0.3555	0.9993	0.04	0.5196	0.0412	0.9646	1.55	5.52	1.14	1.22	3.20
	(c) 3.00	0.2891	0.1519	0.9997	0.01	0.5946	0.0607	0.9708	1.67	5.22	1.30		3.38
IV) l-Decanol in n-heptane M_j = 158 gm	(a) 24.33	2.3575	0.5787	1.0002	0.01	0.2870	0.0396	0.7973	1.92	5.17	1.15		2.76
	(b) 9.25	0.8949	0.2609	0.9966	0.18	0.3885	0.0411	0.9040	1.79	5.52	1.18	0.95	3.04
	(c) 3.00	0.2894	0.1151	0.9997	0.01	0.7509	0.1327	0.9834	1.51	3.58	1.32		2.92
V) Ethanol in benzene M_j = 46 gm	9.84	1.1925	0.1977	0.9927	0.44	0.1831	0.00001	0.9997	1.19	147.19	0.51	1.67	14.50
VI) Methanol in benzene M_j = 32 gm	9.84	1.2058	0.2161	0.9928	0.43	--	0.00002	--	--	88.17	--	1.76	--

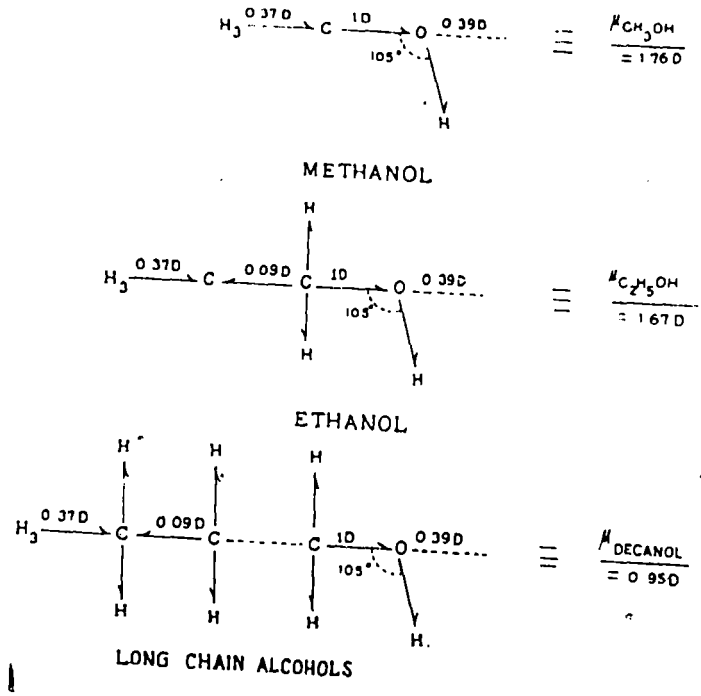

Figure 6.5 Conformational structures of methanol, ethanol and decanol

eqs. (6.8) and (6.18) could, however, be estimated to find out the percentage of errors entered in the dielectric relaxation data, to yield τ_1 and τ_2 of the polar liquids, because the relaxation times τ's are claimed to be accurate within $\pm$ 10%. The monohydric alcohols so far studied always yield, both τ_1 and τ_2 at all frequencies of the electric field. The corresponding dipole moments μ_1 and μ_2 can then be estimated from eq. (6.15) in terms of b_1 and b_2 (which are, however, related to $\tau_1$and τ_2 as estimated) to arrive at their conformations as shown in Figure 6.5

Acknowledgment

The authors are thankful to Mr. A. R. Sit, BE (Electrical) for his interest in this work.

References

[1] A.K Chatterjee, U Saha, N Nandi, R C Basak and S Acharyya Indian J. Phys. **66** 291 (1992)

[2] U Saha and S Acharyya Indian J. Pure Appl. Phys **31** 181 (1993)

[3] U Saha and S Acharyya Indian J. Pure Appl. Phys **32** 346 (1994)

[4] S K Garg and C P Smyth J. Phys Chem. **69** 1294 (1965)

[5] M Magat Hydrogen Bonding (New York : Pergamon) p 309 (1959)

[6] D J Denny and J W Ring J. Chem. Phys. **39** 1268 (1963); M Moriamez and A Lebrun Arch. Sci.(Geneva) **13** 40 (1960)

[7] R Mishra, A Sing, J P Shukla and M C Saxena Indian J. Pure Appl. Phys. **24** 536 ((1986)

[8] K Bergmann, D M Roberti and C P Smyth. J. Phys. Chem. **64** 665 (1960)

[9] J Bhattacharyya, A Hasan, S B Roy and G S Kastha J. Phys. Soc. Jpn. **28** 204 (1970)

[10] U Saha, S K Sit, R C Basak and S Acharyya J. Phys. D: Appl. Phys. **27** 596 (1994)

[11] M D Magee and S Walker J. Chem. Phys. **50** 2580 (1969)

[12] S K Sit, R C Basak, U Saha and S Acharyya J. Phys. D : Appl. Phys. **27** 2194 (1994)

[13] S K Sit and S Acharyya Indian J. Pure Appl. Phys. **34** 255 (1996)

[14] L Glasser, J Crossley and C P Smyth J. Chem. Phys. **57** 3977 (1972)

[15] H D Purohit and H S Sharma Indian J. Pure Appl. Phys. **8** 107 (1970)

[16] A K Ghosh PhD Dissertation (University of North Bengal, India) (1981)

[17] H Fröhlich Theory of Dielectrics (Oxford : Oxford University Press) p 94 (1949)

[18] A Budo Phys. Z. **39** 706 (1938)

[19] F J Murphy and S O Morgan Bull. Syst. Techn. J **18** 502 (1939)

[20] C P Smyth Dielectric Behaviour and Structure (New York : McGraw-Hill) (1955)

[21] A K Ghosh and S Acharyya Indian J. Phys. **52B** 129 (1978)

CHAPTER 7

DOUBLE RELAXATIONS OF SOME ISOMERIC OCTYL ALCOHOLS BY HIGH FREQUENCY ABSORPTION IN NONPOLAR SOLVENT

7.1 Introduction

The dielectric relaxation mechanism of a polar-nonpolar liquid mixture is a very convenient and useful tool in ascertaining the shape, size and structure of a polar molecule [1]. The process is generally involved with the estimation of dipole moment μ in terms of the relaxation time τ for a polar molecule in a nonpolar solvent under different high frequency (hf) electric field of Giga hertz (GHz) range at a fixed or different temperatures. There exist several methods to estimate τ [2] of a polar liquid in a nonpolar solvent. They offer a deep insight into the intrinsic properties of a polar molecule because of the absence of dipole-dipole interactions in polar-nonpolar liquid mixtures.

Highly nonspherical polar molecules, on the other hand, possess more than one τ in the electric field of GHz range for the rotations of different substituent groups attached to the parent molecule and the whole molecule itslef. Budo[3], however, proposed that complex dielectric constant ε^* of a polar liquid may be represented as the sum of a number of noninteracting Debye type dispersions each with a characteristic τ. The method was then made simpler by Bergmann *et al* [4] by assuming that the dielectric relaxation is the sum of two Debye type dispersions characterised by the intramolecular and molecular τ_1 and τ_2 respectively. The corresponding relative contributions c_1 and c_2 towards dielectric relaxations could then be estimated. They used a graphical analysis which consists of plotting normalised values of $(\varepsilon'-\varepsilon_\infty)/(\varepsilon_0-\varepsilon_\infty)$ against $\varepsilon''/(\varepsilon_0-\varepsilon_\infty)$ on a complex plane in terms of the measured real ε', imaginary ε'' parts of ε^*, static dielectric constant ε_0 and high frequency dielectric constant ε_∞ of a polar liquid for different frequencies of the electric field. A number of chords were then drawn through the points on the curve untill a set of parameters was found out in consistency with all the experimental points. Bhattacharyya *et al* [5] subsequently modified the above procedure to get τ_1, τ_2, c_1 and c_2 for a polar liquid from relaxation data measured at least at two different frequencies of the electric field.

We. [6] however, devised earlier a procedure to get τ_1 and τ_2 from the slope and intercept of a derived straight line equation involved with the single frequency measurements of the dielectric relaxation parameters like ε_{0ij}, $\varepsilon_{\infty ij}$, ε'_{ij}, ε''_{ij} for different

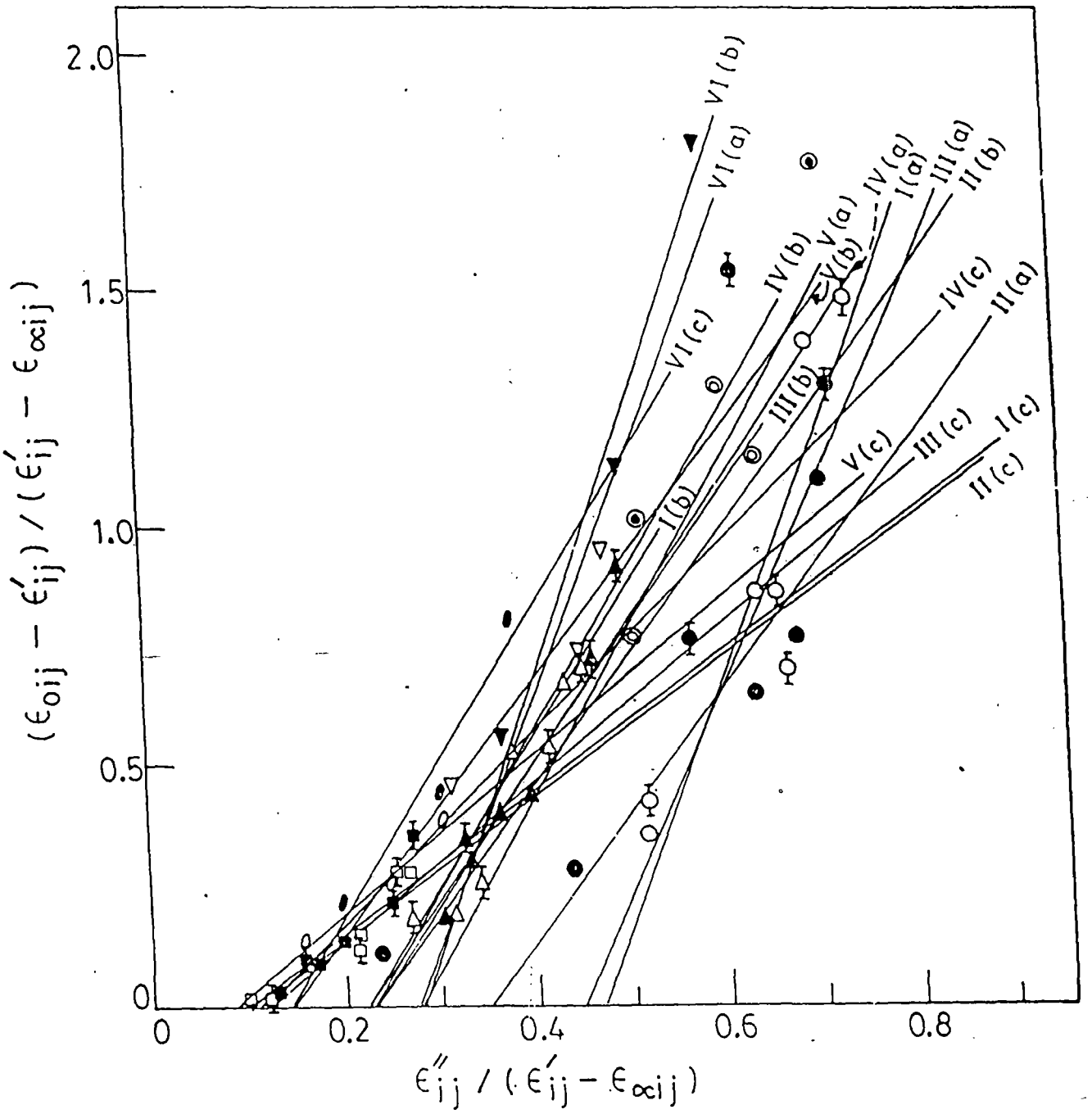

Figure 7.1 Plot of $(\varepsilon_{0ij} - \varepsilon'_{ij}) / (\varepsilon'_{ij} - \varepsilon_{\infty ij})$ against $\varepsilon''_{ij} / (\varepsilon'_{ij} - \varepsilon_{\infty ij})$ of some isomeric octyl alcohols

System-I(a) (-O-), I(b) (-Δ-), I(c) (-□-) for 2-methyl-3-heptanol

System-II(a) (-●-), II(b) (-▲-), II(c) (-■-) for 3-methyl-3-heptanol

System-III(a) (-Ǫ-), III(b) (-Ą-), III(c) (-ǫ-) for 4-methyl-3-heptanol

System-IV(a) (-◖-), IV(b) (-▲-), IV(c) (-■-) for 5-methyl-3-heptanol

System-V(a) (-Ⓞ-), V(b) (-▽-), V(c) (-○-) for 4-octanol

System-VI(a) (-◑-), VI(b) (-▼-), VI(c) (-●-) for 2-octanol

under 24.33, 9.25 and 3.00 GHz respectively

weight fractions ω_js' of a polar solute (j) in a nonpolar solvent (i) at a given temperature. The technique had already been applied on disubstituted benzenes and anilines [6] at 9.945 GHz electric field as well as monosubstituted anilines at 22.06, 3.86, 2.02 GHz [7]electric fields respectively. All these investigations reveal that they often showed the double relaxation behaviours at certain frequency of the electric field.

The aliphatic alcohols, on the other hand, are long straight chain, hydrogen bonded polymer type molecules having possibility of their bending, twisting and rotation under hf electric field each with a characteristic τ , besides the average macroscopic distribution of τ. These alcohols have high dipole moments owing to their strong intermolecular forces exerted by them like polymers in solution. Onsager's equation may be a better choice for such associative liquids, but it is not so simple like Debye's equation because of the presence of quadratic term ε^*_{ij}. The relaxation behaviour of aliphatic alcohols are very interesting because they show more than two τ s' in pure state, but for a polar-nonpolar liquid mixture hf process becomes increasingly important on dilution [8,9]. An extensive study to detect the frequency dependence of double relaxation behaviours of four long chain normal aliphatic alcohols like 1-butanol, 1-hexanol, 1-heptanol, 1-decanol in solvent n-heptane [10] including methanol and ethanol at 9.84 GHz in benzene [11,12] at 25°C was already made [13]. All the alcohols showed τ_1 and τ_2 at all frequencies of the electric field except methanol which is a simple molecule to posses expected τ_2 only.

We, therefore, thought to apply the method as developed earlier [6] on six isomeric octyl alcohols like 2-methyl-3-heptanol, 3-methyl-3-heptanol, 4-methyl-3-heptanol, 5-methyl-3-heptanol, 4-octanol and 2-octanol at 24.33, 9.25 and 3.00 GHz electric fields, as reported in Tables 7.1- 7.4 respectively, because of the availability of ε'_{ij}, ε''_{ij}, ε_{0ij} and $\varepsilon_{\infty ij}$ measured by Crossley et al [14] in n-heptane at 25°C. The straight line equations between $(\varepsilon_{0ij}-\varepsilon'_{ij})/(\varepsilon'_{ij}-\varepsilon_{\infty ij})$ and $\varepsilon''_{ij}/(\varepsilon'_{ij}-\varepsilon_{\infty ij})$ for all the octyl alcohols at different ω_js' are linear as illustrated graphically in Fig. 7.1 only to establish the applicability of Debye model in such isomeric alcohols like normal alcohols once again [13]. Moreover, all the long chain octyl alcohols are structural isomers with the molecular formula $C_8H_{18}O$ having greater number of C-atoms in their structures. They are, therefore,

expected to possess two relaxation processes at audio and radio frequencies of electric field at low temperature in pure state [14].

The purpose of the present paper is to observe the frequency dependence of τ_1 and τ_2 at all frequencies of 24.33, 9.25 and 3.00 GHz electric field for all the octyl alcohols like normal alcohols from the measured relaxation data as shown in Table 7.1. The measured τ_s from the slope of the linear equation of imaginary K''_{ij} and real K'_{ij} parts of the total complex hf conductivity K^*_{ij} and the most probable relaxation time τ_0 from $\tau_0 = \sqrt{\tau_1 \tau_2}$ are placed in Table 7.2 together with the estimated τ_1 and τ_2 in order to see their trends with frequency of the applied electric field.

The relative contributions c_1 and c_2 towards dielectric relaxations in terms of τ_1 and τ_2, are estimated from Fröhlich's equations [15] as well as the graphical method of Figs. 7.2 and 7.3 adopted here. The estimated c_1 and c_2 are, however, placed in Table 7.3

The dipole moments μ_1 and μ_2 due to flexible parts as well as the whole molecules in terms of the estimated τ_1 and τ_2 (Table 7.2) and the slopes β of the linear variation of hf conductivity K_{ij} with ωj are shown in Table 7.4. The slopes β and the intercepts α of the linear variation of K_{ij} with ω_j, as placed in Table 7.4 at each frequency for all the isomers in n-heptane are almost the same probably due to their same polarity [16]. This fact is also supported by their conformations as sketched in Fig. 7.4. It was, therefore, very difficult to plot K_{ij} against ω_j. The computed μ_2 for most of the isomeric alcohols show larger values at 24.33 GHz and gradually decrease with lower frequencies unlike μ_1. In order to compare μ_2 and μ_1 with theoretical dipole moments μ_{theo} a special attention is to be paid on the conformational structure of each isomer from the available bond angles and bond moments point of view and they are shown in Fig. 7.4. Using the usual C-C bond moment of 0.09 D from methanol and ethanol [13] μ_{theo} for four methyl substituted octanols are found to show slightly larger values (see Fig 7.4 and Table 7.4) than 1-heptanol [13] except the desired values for 2-octanol and 4-octanol perhaps due to bond moments of C $\leftarrow$ H_3 and O $\rightarrow$ H groups in their structures. The calculated μ_1 from $\mu_1 = \mu_2 (c_1/c_2)^{1/2}$ assuming two relaxation processes are equally probable are also placed in the last column of Table 7.4 with all the estimated μ's for comparison.

Table 7.1 Dielectric relaxation parameters like ε'_{ij}, ε''_{ij}, ε_{0ij}, $\varepsilon_{\infty ij}$ and of some isomeric octyl alcohols in n-heptane at 25°C from high frequency abroption measurements.

Weight fraction (ω_j) of solute	frequency f in GHz	ε'_{ij}	ε''_{ij}	ε_{0ij}	$\varepsilon_{\infty ij}$
		System I :- 2-methyl -3-heptanol in n-heptane			
	24.33	1.960	0.0156		
0.04337	9.25	1.967	0.0088	1.971	1.930
	3.00	1.970	0.0040		
	24.33	2.022	0.0361	2.059	1.966
0.1299	9.25	2.044	0.0244		
	3.00	2.052	0.0137		
0.2522	24.33	2.095	0.0565		
	9.25	2.115	0.0412	2.172	2.007
	3.00	2.150	0.0309		
0.4081	24.33	2.169	0.0809		
	9.25	2.218	0.0710	2.330	2.054
	3.00	2.269	0.0583		
		System II : - 3-methyl-3-heptanol in n-heptane			
	24.33	1.965	0.0137		
0.0450	9.25	1.968	0.0103	1.9740	1.934
	3.00	1.974	0.0043		
	24.33	2.028	0.0393		
0.1334	9.25	2.045	0.0263	2.069	1.966
	3.00	2.065	0.0131		
	24.33	2.103	0.0674		
0.2538	9.25	2.130	0.0458	2.180	2.004
	3.00	2.166	0.0272		
	24.33	2.188	0.0928		
0.4084	9.25	2.249	0.0766	2.334	2.057
	3.00	2.299	0.0489		
		System III : - 4 methyl-3-heptanol in n-heptane			
	24.33	1.964	0.0146		
0.0466	9.25	1.970	0.0091	1.976	1.936
	3.00	1.975	0.0046		
	24.33	2.025	0.0375		
0.1326	9.25	2.045	0.0262	2.065	1.969
	3.00	2.059	0.0147		

	24.33	2.104	0.0616		
0.2590	9.25	2.123	0.0472	2.185	2.011
	3.00	2.167	0.0333		
	24.33	2.180	0.0849		
0.4124	9.25	2.233	0.0766	2.352	2.065
	3.00	2.289	0.0572		
		System IV : - 5-methyl-3-heptanol in n-heptane			
	24.33	2.008	0.0296		
0.1228	9.25	2.024	0.0225	2.048	1.956
	3.00	2.040	0.0133		
	24.33	2.075	0.0511		
0.2489	9.25	2.099	0.0441	2.168	2.004
	3.00	2.138	0.0337		
	24.33	2.148	0.0676		
0.3898	9.25	2.183	0.0706	2.315	2.040
	3.00	2.242	0.0554		
		System V : - 4-octanol in n-heptane			
	24.33	2.000	0.0265		
0.1201	9.25	2.011	0.0198	2.040	1.948
	3.00	2.029	0.0129		
	24.33	2.067	0.0449		
0.2444	9.25	2.084	0.0397	2.148	1.997
	3.00	2.117	0.0302		
	24.33	2.140	0.0659		
0.3838	9.25	2.159	0.0616	2.282	2.031
	3.00	2.212	0.0549		
		System VI : - 2-octanol in n-heptane			
	24.33	2.001	0.0245		
0.1236	9.25	2.015	0.0227	2.049	1.954
	3.00	2.032	0.0156		
	24.33	2.068	0.0513		
0.2479	9.25	2.089	0.0467	2.195	1.996
	3.00	2.133	0.0419		
	24.33	2.141	0.0680		
0.3844	9.25	2.169	0.0786	2.410	2.036
	3.00	2.243	0.0791		

7.2 Theoretical Formulations to Estimate Relaxation Parameters

The complex dielectric constant ε^*_{ij} of a polar-nonpolar liquid mixture can be represented as the sum of a number of non-interacting Debye type dispersions in accordance with Budo's [3] relation.

$$\frac{\varepsilon^*_{ij} - \varepsilon_{\infty ij}}{\varepsilon_{0ij} - \varepsilon_{\infty ij}} = \sum_k \frac{c_k}{1 + j\,\omega\tau_k}, \qquad \text{.....(7.1)}$$

where $j = \sqrt{-1}$ is a complex number and $\sum c_k = 1$. The term c_k is the relative contribution for the k th type of relaxation process. When the complex dielectric constant ε^*_{ij} consists of two Debye type dispersions, Budo's relation reduces to Bergmann's equations [4]:

$$\frac{\varepsilon'_{ij} - \varepsilon_{\infty ij}}{\varepsilon_{0ij} - \varepsilon_{\infty ij}} = \frac{c_1}{1 + \omega^2\tau_1^2} + \frac{c_2}{1 + \omega^2\tau_2^2}, \qquad \text{.....(7.2)}$$

$$\frac{\varepsilon''_{ij}}{\varepsilon_{0ij} - \varepsilon_{\infty ij}} = c_1 \frac{\omega\tau_1}{1 + \omega^2\tau_1^2} + c_2 \frac{\omega\tau_2}{1 + \omega^2\tau_2^2}, \qquad \text{.....(7.3)}$$

such that $c_1 + c_2 = 1$, where c_1 and c_2 are the relative contributions towards dielectric relaxations due to intramolecular relaxation time τ_1 and molecular relaxation time τ_2. Now with

$$\frac{\varepsilon'_{ij} - \varepsilon_{\infty ij}}{\varepsilon_{0ij} - \varepsilon_{\infty ij}} = x, \quad \frac{\varepsilon''_{ij}}{\varepsilon_{0ij} - \varepsilon_{\infty ij}} = y,$$

$\omega\tau = \alpha$ and using $a = \dfrac{1}{1 + \alpha^2}$ and $b = \dfrac{\alpha}{1 + \alpha^2}$

the above Eqs (7.2) and (7.3) can be written as,

$$x = c_1 a_1 + c_2 a_2 \qquad \text{.....(7.4)}$$

$$y = c_1 b_1 + c_2 b_2 \qquad \text{.....(7.5)}$$

where suffices 1 and 2 with a and b are related to τ_1 and τ_2 respectively. From Eqs (7.4) and (7.5). since $\alpha_2 - \alpha_1 \neq 0$ and $\alpha_2 > \alpha_1$ we have

$$c_1 = \frac{(x\alpha_2 - y)(1 + \alpha_1^2)}{\alpha_2 - \alpha_1} \qquad \text{..... (7.6)}$$

$$c_2 = \frac{(y - x\alpha_1)(1 + \alpha_2^2)}{\alpha_2 - \alpha_1} \qquad \text{.....(7.7)}$$

Since $c_1 + c_2 = 1$. we get the following equation with the help of Eqs (7.6) and (7.7) :

$\frac{1 - x}{y} = (\alpha_1 + \alpha_2) - \frac{x}{y}\alpha_1\alpha_2$ which on substitution of the values x, y and α yields

$$\frac{\varepsilon_{0ij} - \varepsilon'_{ij}}{\varepsilon'_{ij} - \varepsilon_{\infty ij}} = \omega(\tau_1 + \tau_2)\frac{\varepsilon''_{ij}}{\varepsilon'_{ij} - \varepsilon_{\infty ij}} - \omega^2\tau_1\tau_2, \qquad \text{.....(7.8)}$$

Equation (7.8) is thus a straight line equation between $\frac{\varepsilon_{0ij} - \varepsilon'_{ij}}{\varepsilon'_{ij} - \varepsilon_{\infty ij}}$ and $\frac{\varepsilon''_{ij}}{\varepsilon'_{ij} - \varepsilon_{\infty ij}}$ with slope $\omega(\tau_1 + \tau_2)$ and intercept $-\omega^2\tau_1\tau_2$ respectively. Here, ω = angular frequency of the applied electric field of frequency f in GHz. With the measured dielectric relaxation data of ε'_{ij}, ε''_{ij}, ε_{0ij} and $\varepsilon_{\infty ij}$ and for different weight fractions ω_js' of each octyl alcohol in n-heptane at 25°C under 24.33, 9.25 and 3.00 GHz electric fields [14] we get slope and intercept of Eq. (7.8) to yield τ_1 and τ_2 as shown in Table 7.2

The relative contributions c_1 and c_2 towards the dielectric relaxations in terms of x, y and τ_1, τ_2 for each octyl alcohol are found out and placed in Table 7.3. The theoretical values of x and y are, however, calculated from Fröhlich's equations [15] :

$$x = \frac{\varepsilon'_{ij} - \varepsilon_{\infty ij}}{\varepsilon_{0ij} - \varepsilon_{\infty ij}} = 1 - \frac{1}{2A}\ln\left(\frac{1 + e^{2A}\omega^2\tau_s^2}{1 + \omega^2\tau_s^2}\right) \qquad \text{.....(7.9)}$$

$$y = \frac{\varepsilon''_{ij}}{\varepsilon_{0ij} - \varepsilon_{\infty ij}} = \frac{1}{A}\left[\tan^{-1}(e^A\,\omega\tau_s) - \tan^{-1}(\omega\tau_s)\right] \qquad \text{.....(7.10)}$$

where A = Fröhlich parameter = $\ln(\tau_2/\tau_1)$ and τ_s is called the small limiting relaxation time as obtained from the double relaxation method. A simple graphical extrapolation technique, on the other hand, was considered to get the values of x and y at $\omega_j \to 0$ from the graphical plots of Figs.7.2 and 7.3 respectively. This is really in accord with

Table 7.2 The estimated relaxation times τ_2 and τ_1 from the slopes and the intercept of straight line Eq (7.8) with errors and correlation coefficients r together with measured τ_s from $K''_{ij} - K'_{ij}$ curve and most probable relaxation time $\tau_0 = \sqrt{\tau_1 \tau_2}$ for six isomeric octyl alcohols at 25°C under different frequencies of electric fields.

System with Sl. No. & Mole wt. M_j	Frequency in GHz	Intercept & slope of Eq. (7.8)		Correlation coefficient (r)	% error in regression technique	Estimated values of τ_2 & τ_1 in pSec.		Measured τ_s in pSec.	Most probable relaxation time $\tau_0 = \sqrt{\tau_1 \tau_2}$
I. 2-methyl-3-heptanol in n-heptane M_j =130 gm.	a) 24.33	2.3718	5.0952	0.9011	6.34	29.96	3.39	1.84	10.08
	b) 9.25	0.6871	3.1205	0.9700	1.99	49.61	4.10	3.58	14.26
	c) 3.00	0.1408	1.4830	0.9771	1.50	73.31	5.41	6.74	19.91
II 3-methyl-3-heptanol in n-heptane M_j = 130gm	a) 24.33	0.9087	2.6282	0.9294	4.59	14.52	2.68	2.19	6.24
	b) 9.25	0.6389	2.7714	0.9709	1.93	43.34	4.37	3.70	13.76
	c) 3.00	0.1611	1.5018	0.9985	0.10	73.55	6.17	5.58	21.30
III. 4-methyl-3-heptanol in n-heptane M_j = 130gm	a) 24.33	1.9653	4.3873	0.8851	7.30	25.40	3.31	1.90	9.17
	b) 9.25	0.6411	2.8636	0.9682	2.11	45.08	4.21	4.13	13.78
	c) 3.00	0.2008	1.7153	0.9206	5.14	84.34	6.71	11.98	23.79
IV. 5-methyl-3-heptanol in n-heptane M_j - 130gm	a) 24.33	0.6929	2.9788	0.5684	26.36	17.83	1.66	1.71	5.44
	b) 9.25	0.7445	3.2866	0.9846	1.19	52.36	4.21	5.39	14.85
	c) 3.00	0.2362	2.0308	0.9371	4.74	101.22	6.58	13.11	25.81
V. 4-octanol in n-heptane M_j = 130gm	a) 24.33	0.9572	3.4750	0.8569	10.34	20.77	1.97	1.83	6.40
	b) 9.25	0.3810	2.6361	0.9470	4.02	42.74	2.64	5.46	10.62
	c) 3.00	0.1428	1.6929	0.9846	1.18	85.13	4.72	12.76	20.05
VI. 2-octanol in n-heptane M_j = 130gm	a) 24.33	1.3664	5.0208	0.6336	23.30	30.97	1.89	1.83	7.65
	b) 9.25	1.5853	5.6407	0.9888	0.86	92.00	5.11	6.26	21.68
	c) 3.00	0.4458	3.1697	0.9780	1.69	160.41	7.83	18.70	35.44

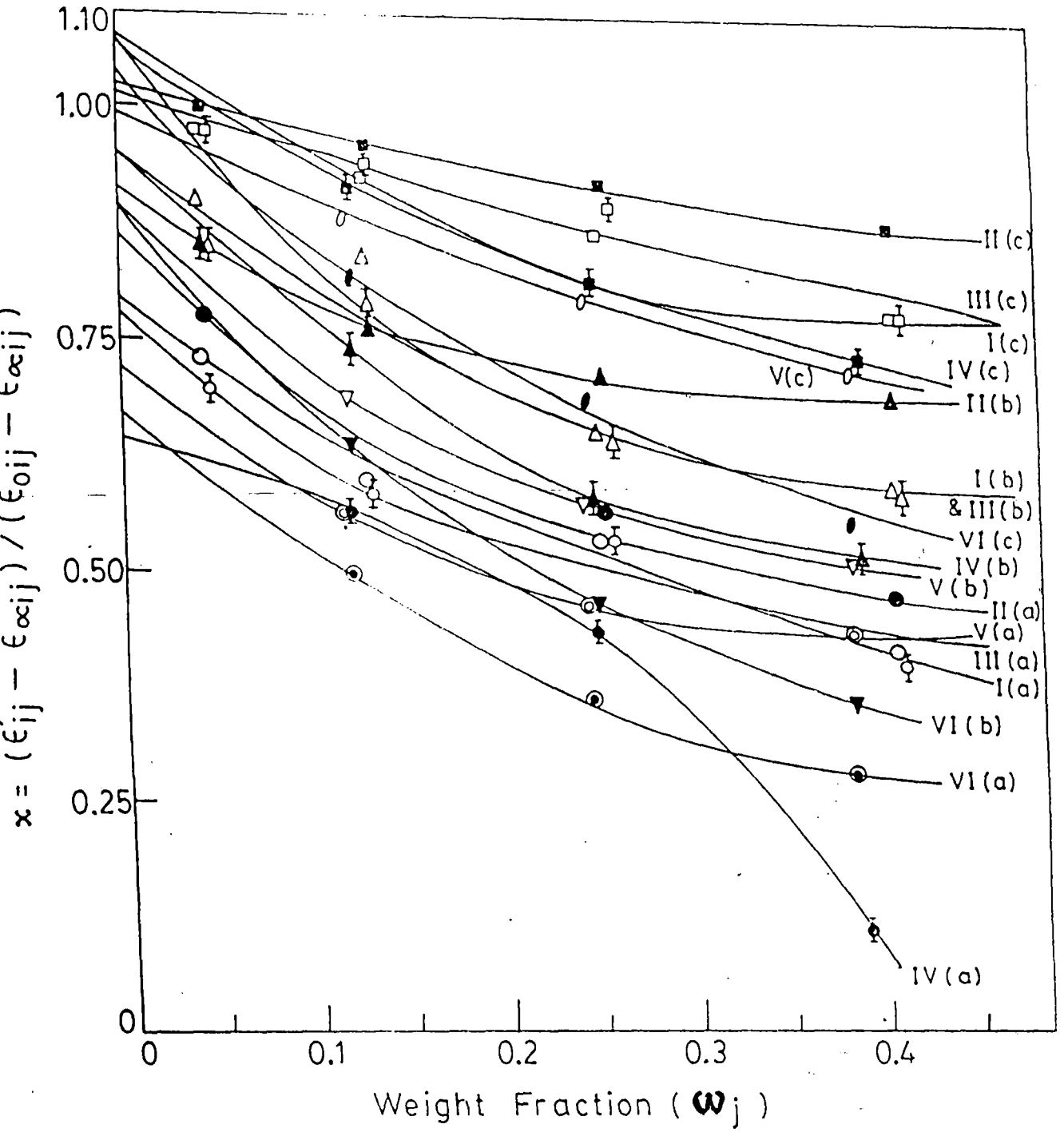

Figure 7.2 **Plot of $(\varepsilon'_{ij} - \varepsilon_{\infty ij}) / (\varepsilon_{0ij} - \varepsilon_{\infty ij})$ against weight fraction ω_j of some isomeric octyl alcohols in n-heptane at 25°C**

System-I(a) (-O-), I(b) (-Δ-), I(c) (-□-) for 2-methyl-3-heptanol

System-II(a) (-●-), II(b) (-▲-), II(c) (-■-) for 3-methyl-3-heptanol

System-III(a) (-Ǫ-), III(b) (-Δ̣-), III(c) (-□̣-) for 4-methyl-3-heptanol

System-IV(a) (-Ǫ-), IV(b) (-▲̣-), IV(c) (-■̣-) for 5-methyl-3-heptanol

System-V(a) (-Ⓞ-), V(b) (-▽-), V(c) (-◌̇-) for 4-octanol

System-VI(a) (-Θ), VI(b) (-▼-), VI(c) (-⬬-) for 2-octanol

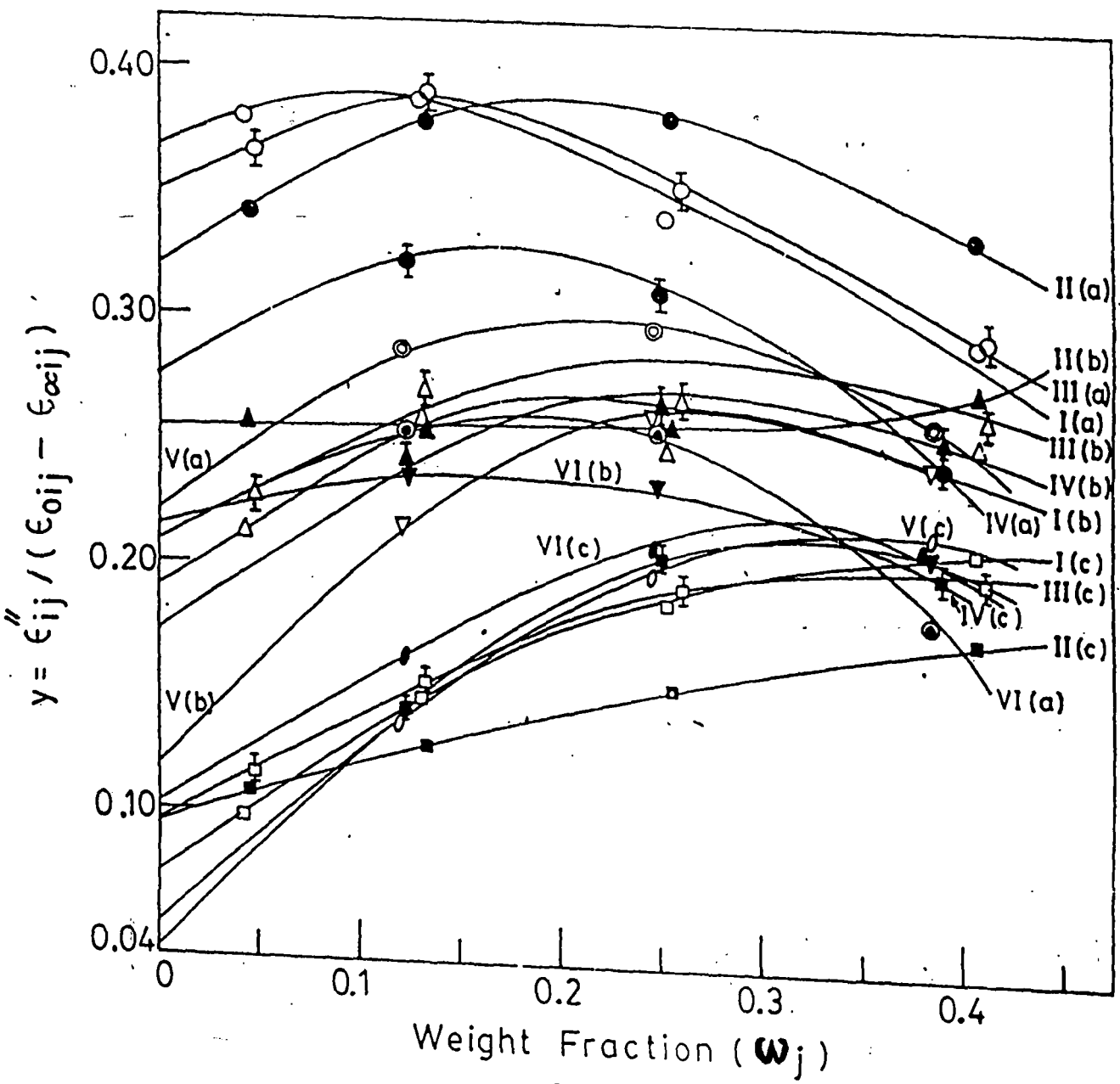

Figure 7.3 Plot of $\varepsilon''_{ij} / (\varepsilon'_{ij} - \varepsilon_{\infty ij})$ against weight fraction ω_j of some isomeric octyl alcohols in n-heptane at 25°C

System-I(a) (-O-), I(b) (-Δ-), I(c) (-□-) for 2-methyl-3-heptanol

System-II(a) (-●-), II(b) (-▲-), II(c) (-■-) for 3-methyl-3-heptanol

System-III(a) (-Ọ-), III(b) (-Δ̣-), III(c) (-□̣-) for 4-methyl-3-heptanol

System-IV(a) (-◖-), IV(b) (-▲̣-), IV(c) (-■̣-) for 5-methyl-3-heptanol

System-V(a) (-Ⓞ-), V(b) (-∇-), V(c) (-◯-) for 4-octanol

System-VI(a) (-Θ-), VI(b) (-▼-), VI(c) (-◖-) for 2-octanol

Bergmann's Eqs. (7.2) and (7.3) when the once estimated τ_1 and τ_2 from Eq. (7.8) are substituted in the right hand sides of the above Eqs (7.2) and (7.3)

The dipole moments μ_1 and μ_2 of octyl alcohols in terms of τ_1 and τ_2 and slope β of the concentration variation of the experimental hf conductivity K_{ij} were then estimated. The hf conductivity K_{ij} is, however, given by Murphy and Morgan [17]:

$$K_{ij} = \frac{\omega}{4\pi}(\varepsilon''^2_{ij} + \varepsilon'^2_{ij})^{\frac{1}{2}} \qquad \text{.....(7.11)}$$

as a function of ω_j of polar solute. Since $\varepsilon''_{ij} << \varepsilon'_{ij}$ in the hf electric field, the term ε''_{ij} offers resistance to polarisation. Thus the real part K'_{ij} of the hf K^*_{ij} of a polar-nonpolar liquid mixture at T K can be written according to Smyth [18] as :

$$K'_{ij} = \frac{\mu_j^2 N \rho_{ij} F_{ij}}{3 M_j k T}\left(\frac{\omega^2\tau}{1+\omega^2\tau^2}\right)\omega_j \qquad \text{.....(7.12)}$$

which on differentiation with respect to ω_j and for $\omega_j \rightarrow 0$ yields that

$$\left(\frac{d K'_{ij}}{d \omega_j}\right)_{\omega_j \rightarrow 0} = \frac{\mu_j^2 N \rho_i F_i}{3 M_j k T}\left(\frac{\omega^2\tau}{1+\omega^2\tau^2}\right) \qquad \text{.....(7.13)}$$

where M_j is the molecular weight of a polar solute, N is the Avogadro's number, k is the Boltzman's constant, the local field $F_{ij} = \frac{1}{9}(\varepsilon_{ij} + 2)^2$ becomes $F_i = \frac{1}{9}(\varepsilon_i + 2)^2$ and the density $\rho_{ij} \rightarrow \rho_i$ the density of solvent at $\omega_j \rightarrow 0$

Again, the total hf conductivity $K_{ij} = \frac{\omega}{4\pi}\varepsilon'_{ij}$ can be written as

$$K_{ij} = K_{ij\infty} + \frac{1}{\omega\tau}K'_{ij}$$

$$\text{or, } \left(\frac{d K'_{ij}}{d \omega_j}\right)_{\omega_j \rightarrow 0} = \omega\tau\left(\frac{d K_{ij}}{d \omega_j}\right)_{\omega_j \rightarrow 0} = \omega\tau\beta \qquad \text{.....(7.14)}$$

where β is the slope of K_{ij} - ω_j curve at infinite dilution. From Eqs (7.13) and (7.14) we get

$$\mu_j = \left(\frac{27\, M_j k T}{N \rho_i (\varepsilon_i + 2)^2 \omega} \frac{\beta}{b} \right)^{1/2} \qquad \text{.....(7.15)}$$

as the dipole moment of each octyl alcohol in terms of b, where b is a dimensionless parameter given by

$$b = \frac{1}{1 + \omega^2 \tau^2} \qquad \text{.....(7.16)}$$

The computed μ_1 and μ_2 together with b_1, b_2 and β of K_{ij} - ω_j equations for all the octyl alcohols are placed in Table 7.4

7.3 Results and Discussion

The least square fitted straight line equations of $(\varepsilon_{0ij} - \varepsilon'_{ij})/(\varepsilon'_{ij} - \varepsilon_{\infty_{ij}})$ against $\varepsilon''_{ij}/(\varepsilon'_{ij} - \varepsilon_{\infty ij})$ for six isomeric octyl alcohols like 2-methyl-3-heptanol, 3-methyl-3-heptanol, 4-methyl-3-heptanol, 5-methyl-3-heptanol, 4-octanol and 2-octanol in solvent n-heptane at 25°C under 24.33, 9.25 and 3.00 GHz electric field at different ω_js' of polar solutes in terms of measured data (Table 7.1) are shown in Fig 7.1 together with the experimental points on them. ω_js' are however, calculated from the mole fractions x_i and x_j of solvent and solute with molecular weights M_i and M_j respectively according to the relation [19]:

$$\omega_j = \frac{x_j M_j}{x_i M_i + x_j M_j}$$

All the straight line equations are almost perfectly linear as evident from the correlation coefficients r lying in the range 0.9985 to 0.5684. The corresponding % of errors in terms of r in getting the slopes and intercepts of all the straight lines are placed in the 6th and 5th columns of Table 7.2. The errors are, however, large at 24.33 GHz indicating departure from the linear behaviour by low values of r perhaps due to inherent uncertainty in measured data for such higher frequency [13].

The estimated τ_2 and τ_1 for all the isomeric octyl alcohols from the slope and the intercept of straight line equations are of smaller magnitude at 24.33 GHz and increase gradually to attain maximum value at 3.00 GHz under the present investigation. This may be due to the fact that at higher frequency the rate of hydrogen bond rupture in long chain alcohols is maximum thereby reducing τ for each rotating unit [13]. τ_2 and τ_1 are then compared with the measured τ_s from the relation:

$$K''_{ij} = K_{\infty ij} + \frac{1}{\omega \tau_s} K'_{ij}$$

and τ_0 where $\tau_0 = \sqrt{\tau_1 \tau_2}$. As evident from Table 7.2 although $\tau_0 > \tau_i$; τ_s agrees well with τ_1 for most of the solutes except slight disagreement at 3.00 GHz for 4-methyl-3-heptanol, 5-methyl-3-heptanol, 4-octanol and 2-octanol. This is explained on the basis of the fact that conductivity measurement may be applicable in higher frequency in yielding microscopic τ only whereas the double relaxation method offers a better understanding of molecular relaxation phenomena showing microscopic as well as macroscopic τ as observed earlier [13]. Unlike normal aliphatic alcohols, — OH groups are screened by the substituted — CH_3 group, broad dispersion characterised by relatively short relaxation times were thus observed. The respective positions of — CH_3 and — OH groups also greatly influence the static dielectric constant, correlation factor, their temperature dependence and type of hydrogen bonding in them.

The relative contributions c_1 and c_2 toward dielectric relaxations are also estimated in terms of $\frac{\varepsilon'_{ij} - \varepsilon_{\infty ij}}{\varepsilon_{0ij} - \varepsilon_{\infty ij}}$, $\frac{\varepsilon''_{ij}}{\varepsilon_{0ij} - \varepsilon_{\infty ij}}$ with the estimated τ_1, τ_2 as shown in Table 7.3 by Fröhlich and graphical methods. $x = (\varepsilon'_{ij} - \varepsilon_{\infty ij})/(\varepsilon_{0ij} - \varepsilon_{\infty ij})$ and $y = \varepsilon''_{ij}/(\varepsilon_{0ij} - \varepsilon_{\infty ij})$ were, however, evaluated from Fröhlich's Eqs. (7.9) and (7.10) in the first case. The usual variations of $(\varepsilon'_{ij} - \varepsilon_{\infty ij})/(\varepsilon_{0ij} - \varepsilon_{\infty ij})$ and $\varepsilon''_{ij}/(\varepsilon_{0ij} - \varepsilon_{\infty ij})$ with ω_j are concave and convex as found in Figs 7.2, and 7.3 in accordance with Bergmann equations (7.2) and (7.3) except 5-methyl-3-heptanol at 24.33 GHz whose $[(\varepsilon'_{ij} - \varepsilon_{\infty ij})/(\varepsilon_{0ij} - \varepsilon_{\infty ij})]$ - ω_j curve is convex in nature perhaps due to its nonaccurate ε_{0ij} and $\varepsilon_{\infty ij}$ values like ethanol

as observed earlier [13]. x and y were also obtained graphically from Figs 7.2, and (7.3' in the limit $\omega_j = 0$.

In Fröhlich-method c_1 and c_2 are all + ve as evident from 6th and 7th columns of Table 7.3 with $c_2 > c_1$. In graphical method $c_1 > c_2$ with - ve c_2 for most of the systems probably due to inertia of the flexible parts under hf electric field, as shown in 10th and 11th columns of same Table 7.3. c_2 are, however, + ve for the systems 5-methyl-3-heptanol. 4-octanol and 2-octanol at 24.33 GHz as well as 3-methyl-3-heptanol at 9.25 GHz. Both the methods in most cases yield $|c_1 + c_2| \geq 1$; signifying thus the possibility of occurrence of more than two relaxation processes in them [13].

The dipole moments μ_1 and μ_2 of all the isomeric alcohols due to their flexible parts and the whole molecules are estimated in terms of dimensionless parameters b_1, b_2 and slope β of K_{ij}-ω_j curves by using Eq. (7.15). The variation of K_{ij} with ω_j are all linear having almost same intercepts α and slopes β at each frequency of electric field. It was, therefore, difficult to plot them as they almost coincide. The values of α and β of K_{ij}'s are little different and comparatively large at 24.33 GHz (Table 7.4). This sort of behaviour is perhaps due to same dipole moments [16] possessed by the polar molecules under investigation as evident from μ_2 and μ_1 placed in 7th and 8th columns of Table 7.4. μ_2 for most of the polar molecules shows high values at 24.33 GHz and decrease gradually with lower frequencies except 3-methyl-3-heptanol, 5-methyl-3-heptanol and 2-octanol whose μ_2s' are found greater at 9.25 GHz electric field. This type of behaviour may be explained on the basis of the fact that such alcohols behaving almost like polymer molecules have long chain of C-atoms and tend to break up in a nonpolar solvent in order to reduce or even eliminate the absorption under hf electric field. The proportion of smaller molecular species having comparatively small number of C-atoms and their corresponding absorption will increase thereby [10]. The values of μ_1s', on the other hand, are almost constant exhibiting a trend to increase a little towards low frequency. They are finally compared with bond moments of 1.5 D of —O—H group making an angle 105° with the C—O bond axis according to the preferred conformations of all the isomers as sketched in Fig 7.4. This confirms that μ_1 arises due to the rotation of —OH group around C-O bond in the

Table 7.3 Fröhlich parameter A, relative contributions c_1 and c_2 due to τ_1 and τ_2, theoretical values of x and y from Fröhlich's equations (7.9) and (7.10) and from graphical extrapolation technique at $\omega_j \rightarrow 0$

System with Sl. No.	Frequency in GHz	Fröhlich parameter A = ln (τ_2/τ_1)	Theoretical values of x & y from eqs (7.9) and (7.10)		Theoretical values of c_1 and c_2		Estimated values of x and y at $\omega_j \rightarrow 0$		Estimated values of c_1 and c_2	
I. 2-methyl-3-heptanol in n-heptane	a) 24.33	2.1790	0.3457	0.4028	0.3686	1.2101	0.795	0.366	1.0226	-0.2476
	b) 9.25	2.4932	0.5637	0.4023	0.4886	0.9434	1.075	0.19	1.1624	-0.2324
	c) 3.00	2.6063	0.7973	0.3232	0.6144	0.5500	1.075	0.074	1.1143	-0.0808
II. 3-methyl-3-heptanol in n-heptane	a) 24.33	1.6897	0.5195	0.4490	0.4542	0.7733	0.865	0.32	1.0321	-0.1120
	b) 9.25	2.2943	0.5792	0.4115	0.4922	0.8573	0.91	0.256	0.9569	0.0810
	c) 3.00	2.4781	0.7865	0.3349	0.6028	0.5600	1.025	0.094	1.0589	-0.0579
III. 4-methyl -3- heptanol in n-heptane	a) 24.33	2.0378	0.3747	0.4173	0.3857	1.0842	0.78	0.35	0.9961	-0.2117
	b) 9.25	2.3710	0.5775	0.4075	0.4932	0.8812	0.95	0.208	1.0177	-0.0805
	c) 3.00	2.5313	0.7543	0.3490	0.5902	0.6112	1.015	0.094	1.0551	-0.0827
IV. 5-methyl - 3-heptanol in n-heptane	a) 24.33	2.3741	0.5644	0.4088	0.4862	0.9057	0.645	0.274	0.6389	0.3763
	b) 9.25	2.5207	0.5499	0.4020	0.4814	0.9805	0.95	0.172	1.0297	-0.2211
	c) 3.00	2.7332	0.7222	0.3529	0.5833	0.6848	1.065	0.042	1.1326	-0.2341
V. 4-octanol in n-heptane	a) 24.33	2.3555	0.5080	0.4131	0.4553	1.0030	0.72	0.22	0.7840	0.0126
	b) 9.25	2.7844	0.6506	0.3720	0.5463	0.8372	0.895	0.116	0.9254	-0.0654
	c) 3.00	2.8924	0.7813	0.3197	0.6210	0.5900	0.99	0.052	1.0218	-0.0850
VI. 2-octanol in n-heptane	a) 24.33	2.7964	0.4507	0.3867	0.4257	1.3507	0.67	0.208	0.7223	0.0764
	b) 9.25	2.8925	0.4292	0.3795	0.4124	1.4780	0.895	0.214	0.9850	-0.3026
	c) 3.00	3.0198	0.6201	0.3658	0.5361	0.9672	1.04	0.102	1.0810	-0.1813

Table 7.4 Estimated intercept and slope of $K_{ij} - \omega_j$ equation, dimensionless parameters b_2, b_1 (Eq. (7.16)), estimated dipole moments μ_2, μ_1 (eq. (7.15)), μ_{theo} from bond angles and bond moments together with μ_1 from $\mu_1 = \mu_2 \ (c_1 / c_2)^{1/2}$ in Debye.

System with Sl. No. & Mol. wt.	Frequency in GHz	Intercept & slope of K_{ij}-ω_j equation $\alpha \times 10^{-10}$	$\beta \times 10^{-10}$	Dimensionless parameters b_2	b_1	Estimated dipole moments (in Debye) μ_2	μ_1	μ_{theo} in D	Estimated μ_1 in D from $\mu_1 = \mu_2 \left(\frac{c_1}{c_2}\right)^{\frac{1}{2}}$
I. 2-methyl-3-heptanol in n-heptane M_j = 130gm	a) 24.33	2.3632	0.6974	0.0455	0.7885	4.80	1.15		2.65
	b) 9.25	0.8998	0.3126	0.1075	0.9463	3.39	1.14	1.76	2.44
	c) 3.00	0.2911	0.1224	0.3439	0.9897	2.08	1.23		2.20
II. 3-methyl-3-heptanol in n-heptane M_j = 130gm	a) 24.33	2.3630	0.7490	0.1689	0.8564	2.58	1.15		1.98
	b) 9.25	0.8959	0.3554	0.1363	0.9395	3.21	1.22	1.76	2.43
	c) 3.00	0.2910	0.1330	0.3425	0.9867	2.18	1.28		2.26
III. 4-methyl -3- heptanol in n-heptane M_j = 130gm	a) 24.33	2.3635	0.7213	0.0623	0.7963	4.17	1.17		2.49
	b) 9.25	0.8984	0.3278	0.1273	0.9436	3.19	1.17	1.76	2.39
	c) 3.00	0.2911	0.1283	0.2837	0.9843	2.35	1.26		2.31
IV. 5-methyl -3-heptanol in n-heptane M_j = 130gm	a) 24.33	2.3646	0.6415	0.1187	0.9396	2.85	1.01		2.09
	b) 9.25	0.9021	0.2771	0.0975	0.9436	3.35	1.08	1.76	2.35
	c) 3.00	0.2922	0.1138	0.2157	0.9849	2.54	1.19		2.34
V. 4-octanol in n-heptane M_j = 130gm	a) 24.33	2.3561	0.6492	0.0903	0.9169	3.29	1.03		2.22
	b) 9.25	0.8965	0.2618	0.1396	0.9770	2.72	1.03	1.08	2.20
	c) 3.00	0.2919	0.1044	0.2799	0.9922	2.13	1.13		2.19
VI. 2-octanol in n-heptane M_j = 130gm	a) 24.33	2.3533	0.6572	0.0428	0.9230	4.80	1.03		2.69
	b) 9.25	0.8980	0.2753	0.0338	0.9190	5.67	1.09	1.08	3.00
	c) 3.00	0.2897	0.1221	0.0987	0.9787	3.88	1.23		2.89

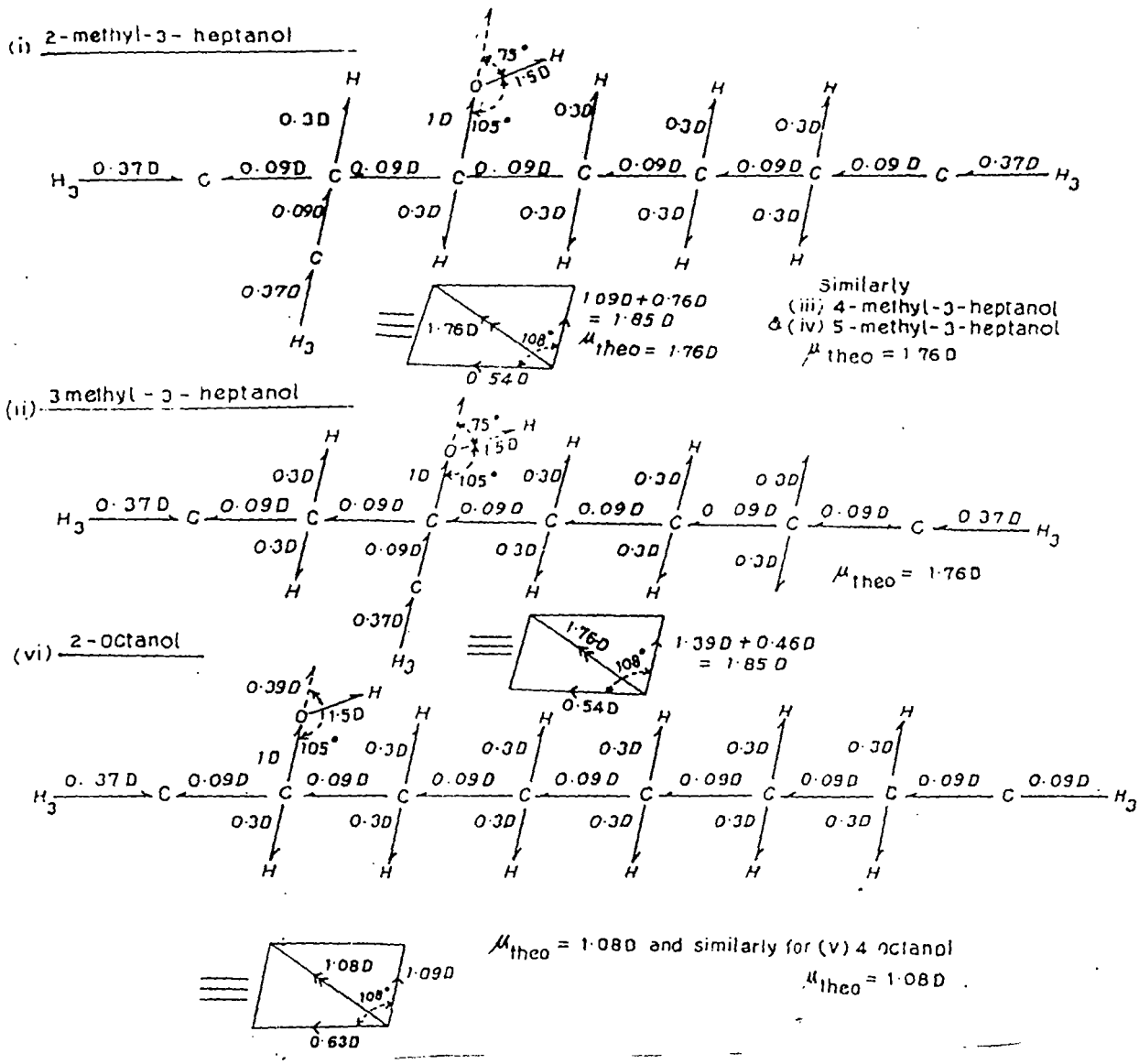

Figure 7.4 Conformations of some isomeric octyl alcohols

long chain alcohols studied so far [13]. The slight difference is due to difference in steric hindrances as a result of structural configurations at different frequencies. μ_1s' also estimated from $\mu_1 = \mu_2 (c_1/c_2)^{1/2}$ assuming two relaxation processes are equally probable as shown in the last column of Table 7.4. The other bond moments 0.37, 0.3, 1 and 0.09 D for C $\leftarrow$ H_3 C $\rightarrow$ H, C$\rightarrow$ O and C $\leftarrow$ C bonds are also involved to justify their conformations. The resultant of all these bonds by vector addition method yields μ_{theo} of 1.76 D and 1.08 D for four methyl substituted heptanols and two octanols respectively. The derived result should decrease with increase in the number of C-atoms and μ_{theo} for them should be less than that for 1-heptanol [13]. But μ_{theo} in Fig 7.4 for three isomers are only displayed due to typical positions of their — CH_3 and — OH groups. This may probably be the reason of having slightly larger values of μ_{theo} from 1-heptanol as observd earlier [13].

4. Conclusion

The methodology so far advanced for the double broad dispersions of the polar-nonpolar liquid mixtures based on Debye's model seems to be much simpler, straight forward and significant one to detect the very existence of double relaxation times τ_1 and τ_2 of polar liquid in a nonpolar solvent. The correlation coefficients between the desired dielectric relaxation parameters involved in the desired equation (7.8) could, however, be estimated to find out % of errors entered in the estimated τ_1 and τ_2 of a polar liquid, because τ is claimed to be accurate within $\pm$ 10%. The isomeric octyl alcohols like normal aliphatic alcohols are found to yield both τ_1 and τ_2 at all frequencies of the electric field of GHz range. The corresponding dipole moments μ_1 and μ_2 can then be estimated from Eq. (7.15) in terms of b_1 and b_2 which are, however, involved with τ_1 and τ_2 as estimated, to arrive at their preferred conformations sketched in Fig 7.4

Acknowledgement

The authors are thankful to Mr. A.R.Sit, B.E. (Electrical) for his interest in this work.

References :

1. Saha U and Acharyya S 1994 Ind. J. Pure Appl. Phys. **32** 346.
2. Gopalakrishna K V 1957 Trans. Faraday Soc. **53** 767
3. Budo A 1938 Phys. Z **39** 706.
4. Bergmann K, Roberti D M and Smyth C P 1960 J. Phys. Chem. 64 665.
5. Bhattacharyya J, Hasan A, Roy S B and Kastha G S 1970 J. Phys. Soc. Japan **28** 204.
6. Saha U, Sit S K, Basak R C and Acharyya S 1994 J. Phys. D : Appl. Phys. **27** 596.
7. Sit S K, Basak R C, Saha U and Acharyya S 1994 J. Phys. D:Appl. Phys. **27** 2194.
8. Denny D J and Ring J W 1963 J. Chem. Phys. **39** 1268.
9. Moriamez M and Lebrun A 1960 Arch. Sci. (Geneva) **13** 40.
10. Glasser L, Crossley J and Smyth C P 1972. J. Chem. Phys. **57** 3977.
11. Purohit H D and Sharma H S 1970 Ind J. Pure Appl. Phys. **8** 107.
12. Ghosh A K 1981 Ph. D. Dissertation (N.B.U.)
13. Sit S K and Acharyya S 1996 Ind. J. Phys. **70B** 19
14. Crossley J, Glasser L and Smyth C P 1971 J. Chem. Phys. **55** 2197.
15. Fröhlich H 1949 Theory of Dielectrics (Oxford : Oxford University Press) p 94.
16. Chatterjee A K, Saha U, Nandi N, Basak R C and Acharyya S 1992 Ind. J. Phys. **66B** 291.
17. Murphy F J and Morgan S O 1939 Bull. Syst. Techn. J. **18** 502.
18. Smyth C P 1955 Dielectric Behaviour and Structure (New York : Mc Graw - Hill)
19. Ghosh A K and Acharyya S 1978 Ind. J. Phys. **52B** 129.

CHAPTER 8

STRUCTURAL AND ASSOCIATIONAL ASPECTS OF BINARY AND SINGLE POLAR LIQUIDS IN NONPOLAR SOLVENT UNDER HIGH FREQUENCY ELECTRIC FIELD

The dielectric relaxation mechanism of a polar nonpolar liquid mixture under the microwave electric field is of special interest [1,2] for its inherent ability to predict the associational aspects of polar solutes in nonpolar solvents. An investigation was, however, made on ternary solution of binary polar liquids in which both or even one of them are aprotic [2,3] in order to throw much light on various types of weak molecular associations formed by polar liquids in nonpolar solvents. We are, therefore, tempted further to study more mixture of binary aprotic polar liquids like N, N-dimethyl formamide (DMF) and dimethyl sulphoxide (DMSO) together with a single aprotic polar liquid like N, N diethyl formatmide (DEF) and DMSO in C_6H_6 and CCl_4 [4-6] respectively. DMSO, DMF and DEF are very interesting aprotic liquids for their wide application in medicine and industry. They also act as building blocks of proteins and enzymes.

The concentration variation of the measured real ε'_{ijk}, ε'_{ij}, or ε'_{ik} and imaginary ε''_{ijk}, ε''_{ij} or ε''_{ik} parts of hf complex dielectric constants ε^*_{ijk}, ε^*_{ij} or ε^*_{ik} of jk, j or k polar solutes of such liquids in nonpolar solvents are used to detect the weak molecular interactions among the molecules [7] at a single or different temperatures under nearly 3 cm. wagelength electric field.

The relaxation times τ_{jk}'s of jk polar mixtures as well as τ_j's or τ_k's of j or k polar solutes in a nonpolar solvent were estimated from :

$$K''_{ijk} = K_{\infty ijk} + \frac{1}{\omega \tau_{jk}} K'_{ijk} \qquad \ldots\ldots (8.1)$$

where $K''_{ijk} = \frac{\omega}{4\pi} \varepsilon'_{ijk}$ and $K'_{ijk} = \frac{\omega}{4\pi} \varepsilon''_{ijk}$ are the imaginary and real parts of complex hf conductivity K^*_{ijk} [8]. The other terms carry usual significance as presented elsewhere [2]. The τ_{jk}'s are estimated from the slopes of the linear variations of K''_{ijk} against K'_{ijk} as placed in Table 8.1 together with the corresponding intercepts of eq (8.1). The linearity of eq. (8.1) is also supported in almost all cases, by the correlation coefficients r and the % of errors (Table 8.1) involved in the measurement. τ_{jk} (Table 8.1) are then plotted with different mole fractions x_k's of DMSO at various experimental temperatures as shown in Figures 8.1. The formation of dimer is responsible for the

gradual rise of τ_{lk} (Figure 8.1) from τ_l of DMF at $x_k = 0$ to $x_k = 0.5$ and then its rapid fall to τ_k due to the rupture of dimerisation and self association [4]. The estimated τ's are slightly larger than those of Gopalakrishna's method [9] as placed in the last column of Table 8.1. But τ's from conductivity measurement are much more reliable as they provide one with microscopic relaxation times already observed [10].

The energy parameters due to dielectric relaxation process were then obtained in terms of measured τ from the rate process equation of Eyring *et al* [11], which is given by:

$$\tau_S = \frac{A}{T} e^{\Delta F_\tau / RT}$$

$$\text{or, } \ln(\tau_s T) = \ln A' + \frac{\Delta H_\tau}{RT} \qquad \text{.....(8.2)}$$

$$\text{where } A' = A\, e^{-\Delta S_\tau / R}$$

Equation (8.2) is a straight line of $\ln(\tau_s T)$ against $\frac{1}{T}$ (Figure 8.2) having certain intercepts and slopes placed in Table 8.2 to yield the entropy of activation ΔS_τ, enthalpy of activation ΔH_τ and free energy of activation ΔF_τ due to dielectric relaxation. They are placed in the 6th, 5th and 7th columns of Table 8.2. The values of γ for all the liquids except DMSO in CCl_4 are greater than 0.55 as obtained from the slope of the linear relation of $\ln(\tau_s T)$ with $\ln\eta$ indicating them as solid phase rotators in solvent environment. η is the coefficient of viscosity of solvent. ΔH_η due to viscous flow of the solvent is, however, obtained from the linear slope of $\ln(\tau_s T)$ against $\frac{1}{T}$ and known γ. Table 8.2 also shows that $\Delta H_\eta > \Delta H_\tau$ for all the mixtures except 0,50 and 60 mole % DMSO in DMF and C_6H_6. The difference in ΔH_τ and ΔH_η is due to involvement of various types of bondings which are either formed or broken to some extent, depending on the temperature and concentration of the system. The negative values of ΔS_τ's for all the systems except 0 and 60 mole % DMSO in DMF and C_6H_6 indicate the existence of cooperative orientation of the molecules arising out of steric forces to yield more ordered state while

Table 8.1 The intercepts and slopes of the linear relations of the imaginary K''_{ijk}, K''_{ij} or K''_{ik} with the real K'_{ijk}, K'_{ijk} or K'_{ijk} parts of complex hf conductivity, correlation coefficient r and % of error in regression technique, estimated and reported τ of binary and single polar solutes in nonpolar solvents at different temperatures.

System with Serial No.	Temp in °C	Intercept & Slope of $K''_{ijk} - K'_{ijk}$ curve		Correlation Coefficient (r)	% of Error.	Estimated τ in p. Sec.	Reported τ in p. Sec.
		c x 10^{-10}	m				
i) DMF	25	1.0270	2.2815	0.6536	19.32	7.60	7.50
+	30	1.0329	2.2924	0.9399	3.93	7.57	6.90
0 mole %	35	1.0201	2.8166	0.9867	0.89	6.16	6.10
DMSO in C_6H_6	40	1.0207	2.8856	0.9930	0.47	6.01	5.50
ii) DMF	25	1.0407	1.3405	0.9586	2.73	12.94	16.40
+	30	1.0372	1.3818	0.9809	1.28	12.55	14.10
17 mole %	35	0.9992	1.4029	0.9905	0.64	12.37	12.60
DMSO in C_6H_6	40	1.0244	1.6536	0.9983	0.12	10.49	11.10
iii) DMF	25	1.0612	1.0817	0.9955	0.30	16.04	15.70
+	30	1.0523	1.1954	0.9988	0.08	14.51	13.50
50 mole %	35	1.0431	1.3389	0.9994	0.04	12.96	11.20
DMSO in C_6H_6	40	1.0370	1.4018	0.9940	0.40	12.38	9.90

Table 8.1 The intercepts and slopes of the linear relations of the imaginary K''_{ijk}, K''_{ij} or K''_{ik} with the real K'_{ijk}, K'_{ij} or K'_{ik} parts of complex hf conductivity, correlation coefficient r and % of error in regression technique, estimated and reported τ of binary and single polar solutes in nonpolar solvents at different temperatures.

System with Serial No.	Temp in °C	Intercept & Slope of $K''_{ijk} - K'_{ijk}$ curve		Correlation Coefficient (r)	% of Error.	Estimated τ in p. Sec.	Reported τ in p. Sec.
		$c \times 10^{-10}$	m				
iv) DMF	25	1.0332	1.5302	0.9807	1.29	11.34	11.20
+	30	1.0326	1.5914	0.9838	1.08	10.90	10.90
60 mole %	35	1.0252	1.7063	0.9872	0.86	10.17	10.00
DMSO in	40	1.0255	2.5944	0.9920	0.54	6.69	9.30
C_6H_6							
v) DMF	25	1.0392	2.2158	0.9829	1.14	7.83	7.80
+	30	1.0264	2.4256	0.9924	0.51	7.15	7.70
80 mole %	35	1.0266	2.4994	0.9747	1.68	6.94	7.40
DMSO in	40	1.0228	2.6178	0.9987	0.09	6.63	6.20
C_6H_6							
vi) DMF	25	1.0347	2.4653	0.9364	4.15	7.04	5.40
+	30	1.0319	2.4835	0.9487	3.37	6.99	5.00
100 mole %	35	1.0278	2.4849	0.9822	1.19	6.98	4.70
DMSO in	40	1.0203	2.8905	0.9966	0.23	6.00	4.30
C_6H_6							
vii) DMSO	25	1.0347	2.4652	0.9381	4.04	7.04	5.37
in	30	1.0319	2.4835	0.9485	3.38	6.99	4.96
C_6H_6	35	1.0278	2.4848	0.9821	1.20	6.98	4.70
	40	1.0303	2.8903	0.9966	0.23	6.01	4.33
viii) DMSO	25	0.9851	2.9469	0.9994	0.04	5.89	5.08
in	30	0.9854	2.9839	0.9975	0.17	5.82	4.51
CCl_4	35	0.9843	3.0828	0.9981	0.13	5.63	4.16
	40	0.9827	3.2424	0.9982	0.12	5.35	3.99
ix) DEF	30	1.0853	3.0231	0.9645	2.35	5.43	2.42
in							
C_6H_6							

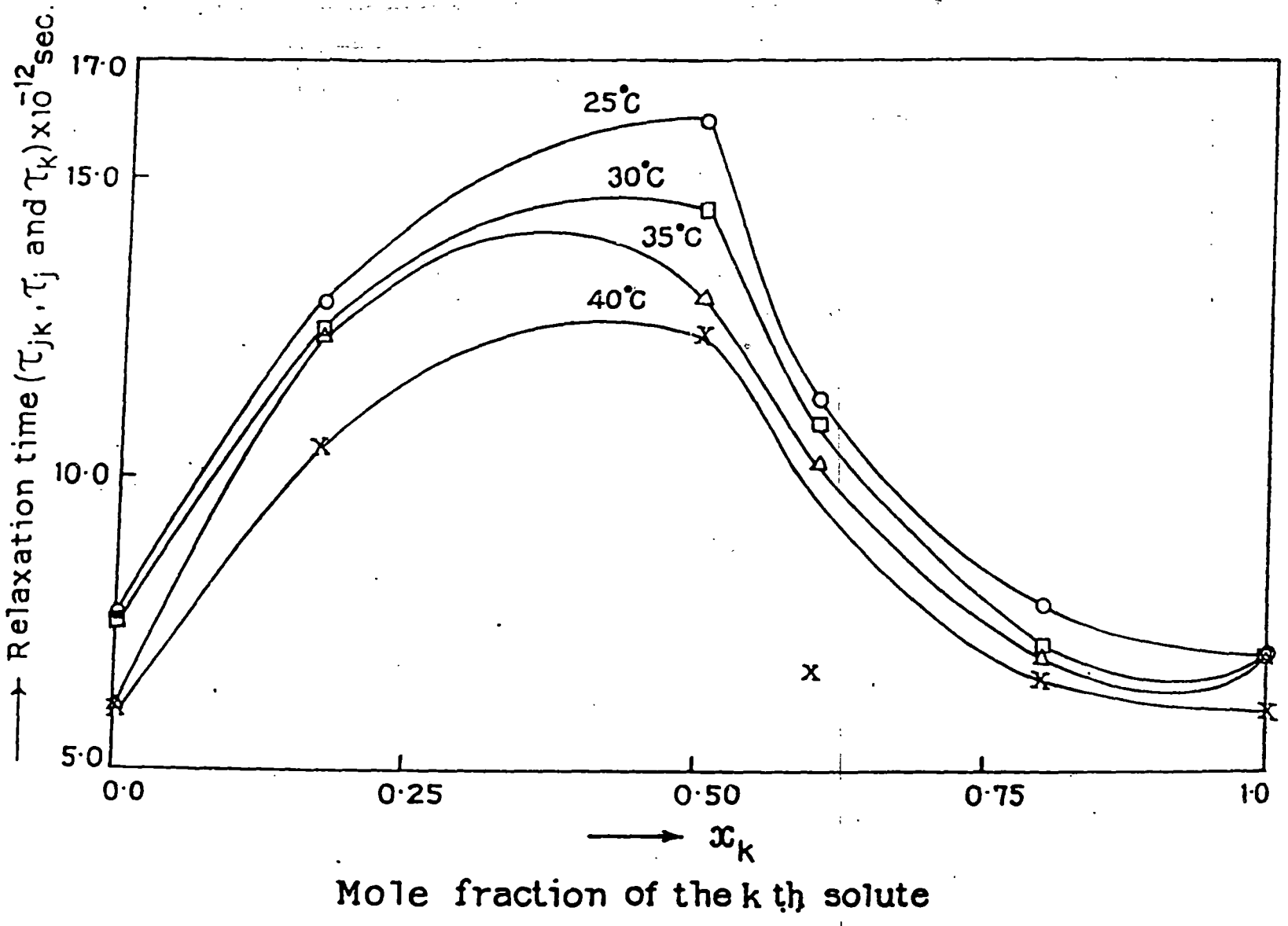

Figure 8.1 Variation of τ_{jk} of DMF-DMSO mixtures in C_6H_6 with mole fraction x_k of DMSO at different temperatures (-O-) at 25°C, (-□-) at 30°C, (-Δ-) at 35°C and (-X-) at 40°C

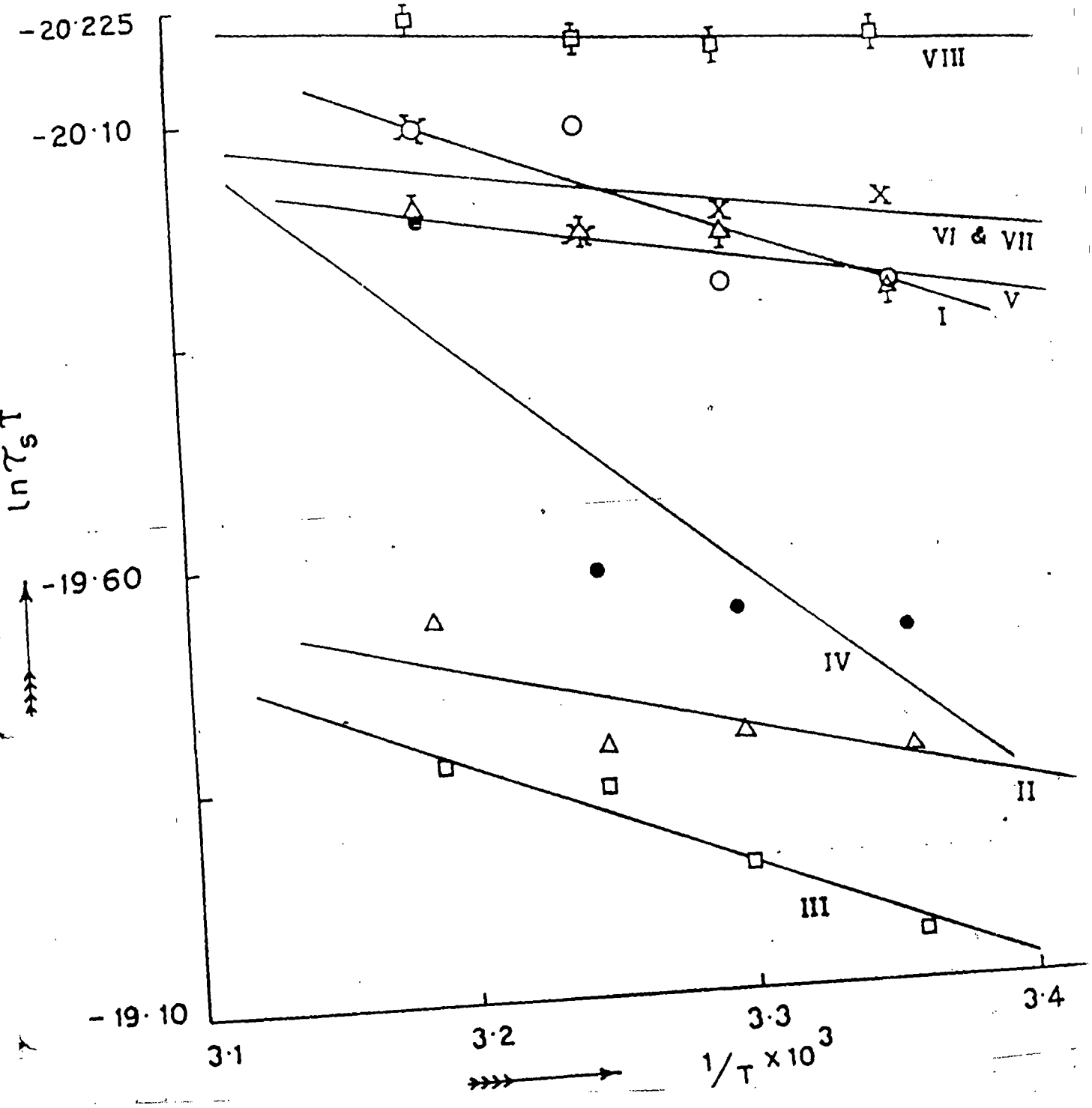

Figure 8.2 Variation of ln (τ_sT) against $\frac{1}{T}$ of binary and single polar solutes in nonpolar solvent.

System-I: -DMF + 0 mole % DMSO in C_6H_6, (-O-),
System-II: -DMF +17 mole % DMSO in C_6H_6, (-Δ-)
System-III: -DMF+ 50 mole % DMSO in C_6H_6, (-□-)
System-IV: -DMF+ 60 mole % DMSO in C_6H_6, (-●-)
System-V: -DMF+ 80 mole % DMSO in C_6H_6, (-▲-)
System-VI: -DMF+ 100 mole % DMSO in C_6H_6(-X-)
System-VII: -DMSO in C_6H_6, (-X-)
System-VIII: -DMSO in CCl_4 (-▽-)

the reverse is true for positive ΔS_τ's. Although, ΔF_τ's in all cases are almost constant at all temperatures, they increase with x_k of DMSO from $x_k = 0.0$ to $x_k = 0.5$ and then decrease gradually to $x_k = 1.0$ signifying the maximum dimerisation of DMF-DMSO mixture around $x_k = 0.5$. The formation of dimer causes larger molecular size and hence the energy needed for rotation in the relaxation process is higher.

The total hf conductivity K_{ijk} as a function weight fraction ω_{jk} given by :

$$K_{ijk} = \frac{\omega}{4\pi} (\varepsilon'^{2}_{ijk} + \varepsilon''^{2}_{ijk})^{\frac{1}{2}} \qquad \text{.....(8.3)}$$

since $\varepsilon'_{ijk} >> \varepsilon''_{ijk}$, eq (8.1) can be written as

$$K_{ijk} = K_{\infty ijk} + \frac{1}{\omega \tau_{jk}} K'_{ijk}$$

$$\text{or,} \left(\frac{d K'_{ijk}}{d \omega_{jk}} \right)_{\omega_{jk} \to 0} = \omega \tau_{jk} \beta \qquad \text{..... (8.4)}$$

where β's are the slopes of K_{ijk} - ω_{jk}, K_{ij} - ω_j or K_{ik} -ω_k curves respectively, which are linear with almost identical intercepts α's and slopes β's placed in Table 8.3 probably due to same polarity of the molecules [2]. The corresponding r and % of errors are also placed in Table 8.3

The real part of hf conductivity, K'_{ijk} is again related to ω_{jk} of jk polar solute dissolved in a nonpolar solvent (i) at temperature T K [12] as :

$$K'_{ijk} = \frac{\mu^2_{jk} N \rho_{ijk} F_{ijk}}{3 M_{jk} k T} \left(\frac{\omega^2 \tau_{jk}}{1 + \omega^2 \tau^2_{jk}} \right) \omega_{jk} \qquad \text{.....(8.5)}$$

Differentiating eq (8.5) with respect to ω_{jk} and comparing the result at $\omega_{jk} \to 0$ to eq. (8.4), one obtains the following relation:

$$\mu_{jk} = \left[\frac{27 M_{jk} k T}{N \rho_i (\varepsilon_i + 2)^2} \cdot \frac{\beta}{\omega b} \right]^{\frac{1}{2}} \qquad \text{.....(8.6)}$$

Table 8.2 Thermodynamic parameters like enthalpy ΔH_τ, entropy ΔS_τ and free energy ΔF_τ ($=\Delta H_\tau - T\Delta S_\tau$) of activation due to dielectric relaxation and the enthalpy of activation $\Delta H\eta$ due to viscous flow, γ where $\gamma = \Delta H_\tau / \Delta H\eta$ together with the coefficients a, b, c in the temperature dependence of μ_{jk} where $\mu_{jk} = a + bt + ct^2$

System with serial No.	Temp in °C	Intercept & slope of $\ln(\tau_s T)$ Vs 1/T Curve Intercept Slope		ΔH_τ Kcal/Mole	ΔS_τ Cal/Mole deg.	ΔF_τ Kcal/Mole	$\gamma = \frac{\Delta H_\tau}{\Delta H_\eta}$	$\Delta H\eta$ Kcal/Mole	Coefficients of μ_{jk} - t curve a	b	c
i) DMF + 0 mole % DMSO in C_6H_6	25	-24.06	1240.87	2.47	0.62	2.28	1.62	1.52	3.2305	2.21×10^{-2}	-3×10^{-4}
	30				0.45	2.33					
	35				0.70	2.25					
	40				0.59	2.29					
ii) DMF + 17 mole% DMSO in C_6H_6	25	-21.90	758.36	1.51	-3.66	2.60	0.97	1.56	9.1435	-30.93×10^{-2}	4.7×10^{-3}
	30				-3.71	2.63					
	35				-3.80	2.68					
	40				-3.58	2.63					
iii) DMF + 50 Mole % DMSO in C_6H_6	25	-23.26	12.15.74	2.42	-1.03	2.73	1.66	1.46	6.7995	-11.91×10^{-2}	1.7×10^{-3}
	30				-1.00	2.72					
	35				-0.94	2.71					
	40				-1.01	2.74					
iv) DMF + 60 mole % DMSO in C_6H_6	25	-28.04	2560.96	5.09	8.62	2.52	3.02	1.68	7.1285	-19.23×10^{-2}	3.3×10^{-3}
	30				8.39	2.55					
	35				8.22	2.56					
	40				8.76	2.35					

Contd

Table 8.2 Thermodynamic parameters like enthalpy ΔH_τ, entropy ΔS_τ and free energy ΔF_τ ($=\Delta H_\tau - T\Delta S_\tau$) of activation due to dielectric relaxation and the enthalpy of activation $\Delta H\eta$ due to viscous flow, γ where $\gamma = \Delta H_\tau / \Delta H\eta$ together with the coefficients a, b, c in the temperature dependence of μ_{jk} where $\mu_{jk} = a + bt + ct^2$

System with serial No.	Temp in °C	Intercept & slope of $\ln(\tau_s T)$ Vs 1/T Curve Intercept	Slope	ΔH_τ Kcal/Mole	ΔS_τ Cal/Mole deg.	ΔF_τ Kcal/Mole	$\gamma = \frac{\Delta H_\tau}{\Delta H\eta}$	$\Delta H\eta$ Kcal/Mole	Coefficients of μ_{jk} - t curve a	b	c
v) DMF + 80 mole % DMSO in C_6H_6	25	-21.78	559.61	1.11	-3.98	2.30	0.85	1.30	5.0470	-2.36×10^{-2}	4×10^{-1}
	30				-3.90	2.29					
	35				-3.93	2.32					
	40				-3.93	2.34					
vi) DMF + 100 mole% DMSO C_6H_6	25	-21.51	461.28	0.92	-4.42	2.24	0.60	1.53	4.3580	-2.4×10^{-3}	0
	30				-4.49	2.28					
	35				-4.58	2.33					
	40				-4.36	2.28					
vii) DMSO in C_6H_6	25	-21.48	452.74	0.90	-4.49	2.23	0.59	1.52	3.7610	3.62×10^{-2}	-6×10^{-1}
	30				-4.56	2.28					
	35				-4.63	2.33					
	40				-4.41	2.28					
viii) DMSO in CCl_4	25	-20.76	179.17	0.36	-5.96	2.14	0.23	1.56	4.9470	-2.86×10^{-2}	2×10^{-1}
	30				-5.98	2.17					
	35				-5.97	2.20					
	40				-5.92	2.21					

Table 8.3 The intercepts and slopes of the linear equations of K_{ijk}, K_{ij} or K_{ik} with ω_{jk} ω_j or ω_k, Correlation coefficient r, % of error in fitting technique, dimensionless parameter b, reported and estimated μ in D together with μ_{theo} from bond angles and bond moments of DMSO and DMF in C_6H_6 as well as DMSO and DEF in either C_6H_6 or in CCl_4 or both at different temperatures.

System with Serial No.	Temp in °C	Intercept & Slope of K_{ijk} - ω_{jk} Curve $\alpha \times 10^{-10}$ $\beta \times 10^{-10}$ in e.s.u		Correlation Coefficient (r)	% of Error.	Dimension less parameter $b = \frac{1}{1+\omega^2\tau^2}$	Estimated Dipole moment	Average & reported Dipole moment.	μ from bond angle & bond moment
i) DMF	25	1.0609	7.4251	0.9905	0.64	0.8390	3.60	3.60*	
+	30	1.0538	7.2791	0.9500	3.29	0.8401	3.61	3.61*	3.82
0 mole %	35	1.0464	7.6682	0.9732	1.78	0.8880	3.65	3.65*	
DMSO in C_6H_6	40	1.0445	7.4392	0.9753	1.64	0.8928	3.63	3.63*	
ii) DMF	25	1.0591	8.2560	0.9930	0.47	0.6425	4.36	4.36*	
+	30	1.0580	7.1363	0.9876	0.83	0.6565	4.06	4.06*	4.77
17 mole %	35	1.0540	7.1868	0.9638	2.40	0.6629	4.11	4.11*	
DMSO in C_6H_6	40	1.0384	8.3820	0.9515	3.19	0.7323	4.28	4.28*	
iii) DMF	25	1.0580	8.4951	0.9859	0.94	0.5391	4.88	4.88*	
+	30	1.0491	8.6211	0.9689	2.06	0.5884	4.77	4.77*	4.77
50 mole %	35	1.0404	8.8880	0.9826	1.16	0.6418	4.70	4.70*	
DMSO in C_6H_6	40	1.0317	9.1736	0.9865	0.90	0.6626	4.76	4.74*	
iv) DMF	25	1.0536	8.8642	0.9906	0.63	0.7006	4.39	4.39*	
+	30	1.0442	8.5023	0.9958	0.28	0.7170	4.31	4.30*	4.77
60 mole %	35	1.0301	9.2115	0.9872	0.86	0.7442	4.46	4.45*	
DMSO in C_6H_6	40	1.0324	11.7088	0.9661	2.25	0.8705	4.71	4.71*	
v) DMF	25	1.0380	11.9482	0.9919	0.54	0.8308	4.71	4.71*	
+	30	1.0280	11.8948	0.9998	0.01	0.8548	4.69	4.69*	4.77
80 mole %	35	1.0228	11.8176	0.9971	0.19	0.8620	4.72	4.72*	
DMSO in C_6H_6	40	1.0165	11.7301	0.9976	0.16	0.8726	4.74	4.73*	

Table 8.3 The intercepts and slopes of the linear equations of K_{ijk}, K_{ij} or K_{ik} with ω_{jk} ω_j or ω_k, Correlation coefficient r, % of error in fitting technique, dimensionless parameter b, reported and estimated μ in D together with μ_{theo} from bond angles and bond moments of DMSO and DMF in C_6H_6 as well as DMSO and DEF in either C_6H_6 or in CCl_4 or both at different temperatures.

System with Serial No.	Temp in °C	Intercpt & Slope of K_{ijk} - ω_{jk} Curve $\alpha \times 10^{-10}$ $\beta \times 10^{-10}$ in e.s.u		Correlation Coefficient (r)	% of Error.	Dimension less parameter $b = \frac{1}{1+\omega^2\tau^2}$	Estimated Dipole moment	Average & reported Dipole moment.	μ from bond angle & bond moment
vi) DMF	25	1.0352	10.1219	0.9954	0.31	0.8586	4.29	4.29*	
+	30	1.0310	9.8652	0.9926	0.50	0.8603	4.29	4.29*	4.55
100 mole %	35	1.0223	9.6089	0.9860	0.94	0.8607	4.29	4.29*	
DMSO in C_6H_6	40	1.0158	9.5319	0.9714	1.90	0.8932	4.25	4.25*	
vii) DMSO	25	1.0352	10.1208	0.9952	0.32	0.8586	4.29	3.79**	
in C_6H_6	30	1.0310	9.8652	0.9926	0.50	0.8603	4.31	3.83**	4.55
	35	1.0223	9.6039	0.9860	0.94	0.8606	4.29	4.04**	
	40	1.0158	9.5319	0.9714	1.90	0.8928	4.25	4.11	
viii) DMSO	25	1.0082	19.1986	0.9825	1.17	0.8966	4.35	3.47**	
in CCl_4	30	1.0052	18.1914	0.9905	0.64	0.8988	4.29	3.57**	4.55
	35	1.0058	16.8151	0.9948	0.35	0.9047	4.17	3.69**	
	40	1.0031	16.1261	0.9964	0.24	0.9132	4.13	3.86**	
ix) DEF									
in C_6H_6	30	1.0761	7.8626	0.9489	3.36	0.9014	4.14	3.88$^{\phi}$	3.99

* Average dipole moment $\mu_{jk} = \mu_j x_j + \mu_k x_k$

** Reported dipole moment Sharma & Sharma (1992) &

$^{\phi}$ Saksena (1978)

to estimate μ_{jk}, μ_j, μ_k of the respective solutes. b is a dimensionless parameter (Table 8.3) in terms of estimated τ_{jk}, τ_j or τ_k given by :

$$b = \frac{1}{1 + \omega^2 \tau_{jk}^2} \qquad \text{.....(8.7)}$$

The other terms in eq (8.6) carry usual significance [2]. All the μ's are placed in Table 8.3 The μ's are then plotted against different x_k's of DMSO at each temperature as shown in Figure 8.3. It shown the gradual rise of μ_{jk} in the range $0 < x_k \leq 0.5$. It then decreases slowly in order to exhibit the convex nature of each curve with an abnormally low value of μ_{jk} around $x_k = 0.6$. This sort of behaviours of μ_{jk} - x_k curves is explained by the fact that dimers are being formed from $x_k \geq 0$ to $x_k = 0.6$ causing increase of μ. The rupture of dimerisation i.e. self association occurs in higher concentrations in the range $0.6 \leq x_k < 1.0$ to yield lower values of μ's. But around $x_k = 0.6$, all μ_{jk}'s are minimum (Table 8.3 and Figure 8.3) indicating the possible occurrence of double relaxation phenomena in such mixtures to be studied later on. μ_{jk} together with μ_j and μ_k for each mixture of a fixed concentration are shown graphically in Figure 8.4 as a function of temperatures in t°C. The purpose is to observe their temperature dependence like $\mu_{jk} = a + bt + ct^2$ with coefficients a,b and c as seen in Table 8.2. The variation is concave with maximum depression at 17 mole% DMSO in DMF mixture. The depression gradually decreases upto $x_k = 0.6$ of DMSO in DMF and C_6H_6 probably due to solute - solute molecular association in the range $0 < x_k < 0.6$. The maximum dimerisation is, however, inferred from the larger molecular size having low dipole moment in the depressed region. As temperature increases the dipole-dipole interaction is weakened and the absorption of hf electric energy increases resulting in the rupture of dimer to yield high μ values for smaller molecular species [10]. The slight convex nature of curves for 0 mole% DMSO in DMF and C_6H_6 and DMSO in C_6H_6, along with almost straight line variation of 100 mole % DMSO in DMF and C_6H_6 and DMSO in CCl_4 is probably due to solute-solvent molecular interaction of either DMF with C_6H_6 or DMSO with C_6H_6 and CCl_4 respectively as illustrated in Figures 8.4

Table 8.4 Reports factor $\frac{\tau_s T}{\eta^\gamma}$ of the rotating units, factor of $\frac{\mu_{cal}}{\mu_{theo}}$, reduced bond moments of substituent groups in DMF, DMSO and DEF under hf electric field at different temperature.

Systems with Sl. No.	Temp t	Factor $\frac{\tau_s T}{\eta^\gamma} \times 10^8$ proportional to volume of rotating unit)	Ratio of $\frac{\mu_{cal}}{\mu_{theo}}$	Reduced bond moments of DMF				Reduced bond moments of DMSO		Corrected μ in D
				C ← H	C ← N	C ⇐ O	N ← CH_3	O ⇐ S	S ← CH_3	
i) DMF +	25°C	908	0.9424	0.2827	0.4241	2.9214	0.6031	—	—	3.60
0 mole %	30°C	1017	0.9450	0.2835	0.4253	2.9295	0.6048	—	—	3.61
DMSO in	35°C	897	0.9555	0.2867	0.4300	2.9621	0.6115	—	—	3.65
C_6H_6	40°C	934	0.9503	0.2851	0.4276	2.9459	0.6082	—	—	3.63
ii) DMF +	25°C	55.39	0.9140	0.2584	0.3876	2.6700	0.5512	1.3387	2.0997	4.38
17 mole %	30°C	58.02	0.8512	0.2407	0.3610	2.4868	0.5134	1.2468	1.8903	4.08
DMSO in	35°C	60.43	0.8616	0.2436	0.3654	2.5172	0.5197	1.2622	1.9136	4.13
C_6H_6	40°C	53.62	0.8973	0.2537	0.3805	2.6214	0.5412	1.3144	1.9928	4.30
iii) DMF +	25°C	2351	1.0231	0.2893	0.4339	2.9890	0.6171	1.4987	2.2722	4.90
50 mole%	30°C	2398	1.0000	0.2827	0.4241	2.9214	0.6031	1.4649	2.2209	4.79
DMSO in	35°C	2326	0.9853	0.2786	0.4179	2.8787	0.5943	1.4434	2.1883	4.72
C_6H_6	40°C	2374	0.9979	0.2821	0.4232	2.9152	0.6019	1.4618	2.2163	4.78
iv) DMF +	25°C		0.9203	0.2602	0.3903	2.6886	0.5551	1.3480	2.0438	4.41
60 mole%	30°C	very	0.9036	0.2555	0.3832	2.6400	0.5450	1.3237	2.0069	4.33
DMSO in	35°C	high	0.9350	0.2644	0.3965	2.7317	0.5640	1.3696	2.0765	4.48
C_6H_6	40°C	value	0.9874	0.2792	0.4187	2.8846	0.5955	1.4463	2.1928	4.73
v) DMF +	25°C	18.13	0.9874	0.2792	0.4187	2.8846	0.5955	1.4463	2.1928	4.73
80 mole %	30°C	17.75	0.9832	0.2780	0.4170	2.8725	0.5930	1.4403	2.1836	4.71
DMSO in	35°C	18.11	0.9895	0.2798	0.4196	2.8908	0.5968	1.4494	2.1975	4.74
C_6H_6	40°C	18.04	0.9937	0.2810	0.4214	2.9032	0.5994	1.4556	2.2069	4.76

Table 8.4 Reports factor $\frac{\tau_S T}{\eta^{\gamma}}$ of the rotating units, factor of $\frac{\mu_{cal}}{\mu_{theo}}$, reduced bond moments of substituent groups in DMF, DMSO and DEF under hf electric field at different temperature.

Systems with Sl. No.	Temp t	Factor $\frac{\tau_S T}{\eta^{\gamma}} \times 10^8$ (proportional to volume of rotating unit)	Ratio of $\frac{\mu_{cal}}{\mu_{theo}}$	Reduced bond moments of DMF				Reduced bond moments of DMSO		Corrected μ in D
				C ← H	C ← N	C ⇆ O	N ←CH_3	O ⇐ S	S ← CH_3	
vi) DMF + 100 mole% DMSO in C_6H_6	25°C	4.53	0.9429	—	—	—	—	1.4615	2.2158	4.29
	30°C	4.75	0.9429	—	—	—	—	1.4615	2.2158	4.29
	35°C	4.93	0.9429	—	—	—	—	1.4615	2.2158	4.29
	40°C	4.39	0.9341	—	—	—	—	1.4479	2.1951	4.25
vii) DMSO in C_6H_6	25°C	4.30	0.9429	—	—	—	—	1.4615	2.2158	4.29
	30°C	4.51	0.9473	—	—	—	—	1.4683	2.2262	4.31
	35°C	4.68	0.9429	—	—	—	—	1.4615	2.2158	4.29
	40°C	4.17	0.9341	—	—	—	—	1.4479	2.1951	4.25
viii) DMSO in CCl_4	25°C	0.5174	0.9560	—	—	—	—	1.4818	2.2466	4.35
	30°C	0.5301	0.9429	—	—	—	—	1.4615	2.2158	4.29
	35°C	0.5278	0.9165	—	—	—	—	1.4206	2.1538	4.17
	40°C	0.5168	0.9077	—	—	—	—	1.4069	2.1331	4.13
ix) DEF in C_6H_6	30°C	—	1.0376	0.3113	0.4669	3.2166	0.8093 (N←C_2H_5)	—	—	4.14

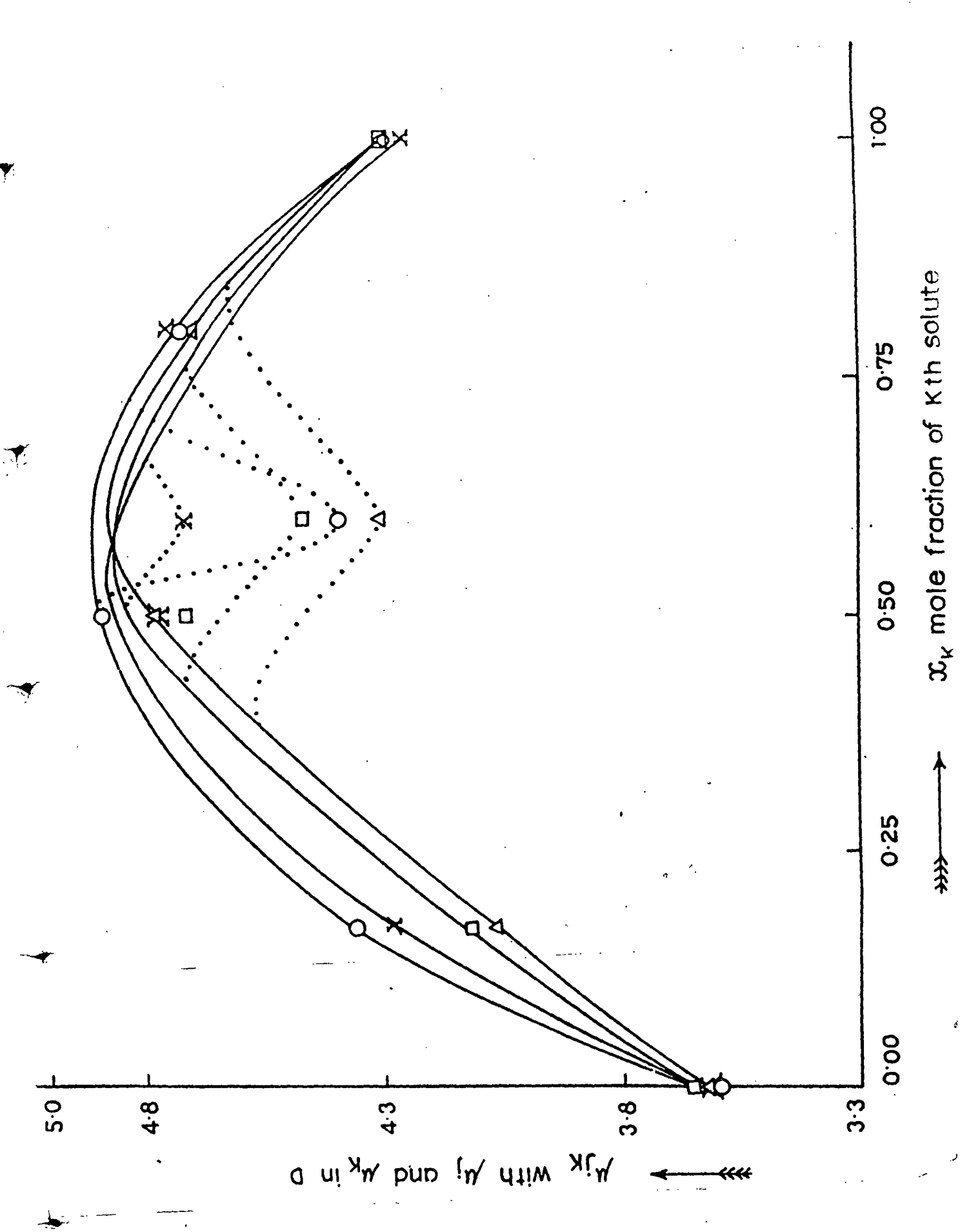

Figure 8.3 Variation of μ_{jk} with μ_j and μ_k of DMF-DMSO mixtures in C_6H_6 with x_k of DMSO at different temperatures

(-O-) at 25°C, (-Δ-) at 30°C, (-□-) at 35°C and (-X-) at 40°C

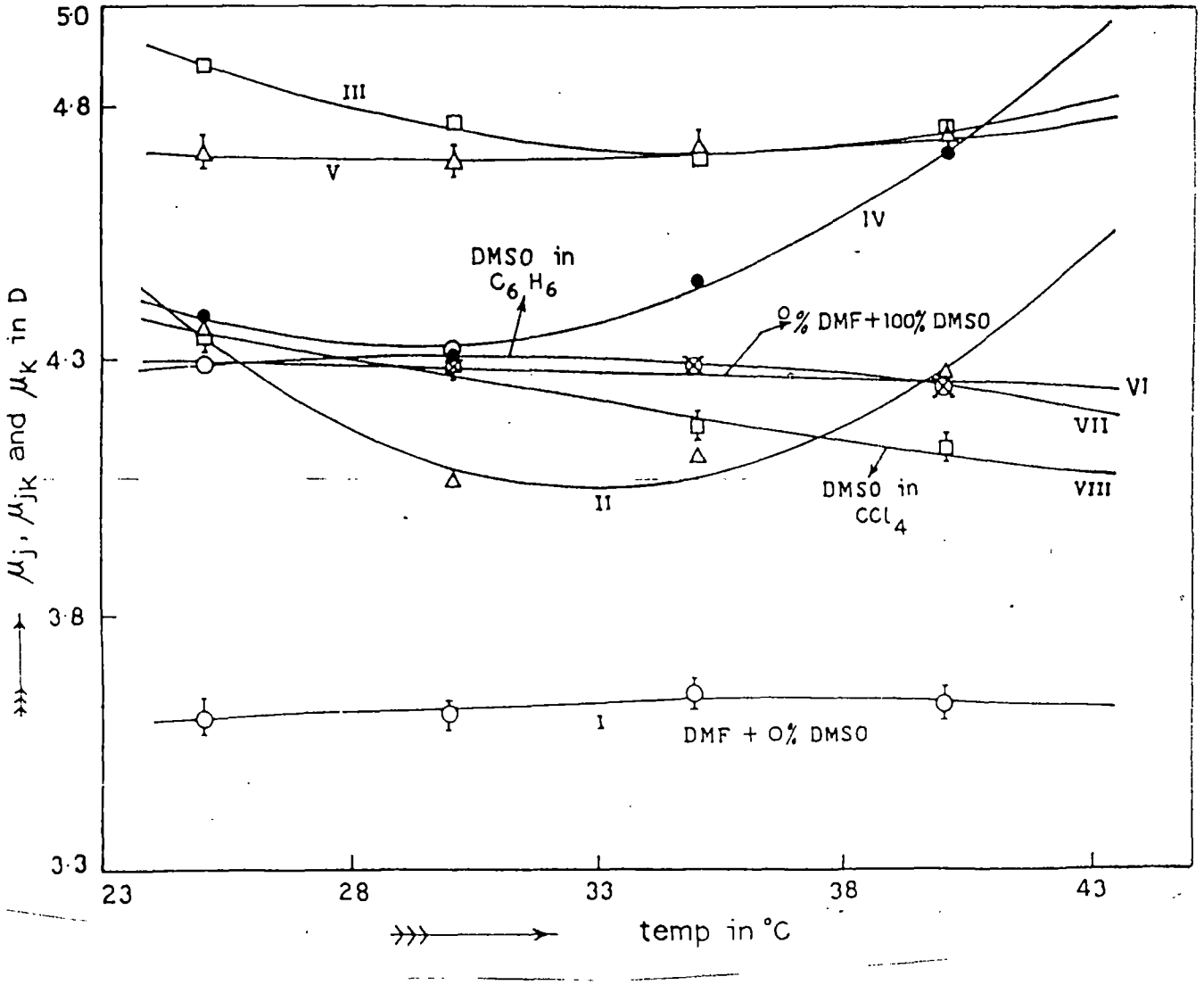

Figure 8.4 **Variation of μ_j μ_{jk} and μ_k of binary and single polar solutes in nonpolar solvent with temperature t in °C.**

System-I:-DMF + 0 mole % DMSO in C_6H_6 (-Φ-)
System-II:- DMF +17 mole % DMSO in C_6H_6 (-Δ-)
System-III:-DMF+ 50 mole % DMSO in C_6H_6 (-□-)
System-IV: -DMF+ 60 mole % DMSO in C_6H_6 (-●-)
System- V: -DMF+ 80 mole % DMSO in C_6H_6 (-Δ-)
System-VI: -DMF+ 100 mole % DMSO in C_6H_6(X-)
System-VII: -DMSO in C_6H_6 (-O-) and
System-VIII:-DMSO in CCl_4 (-□-)

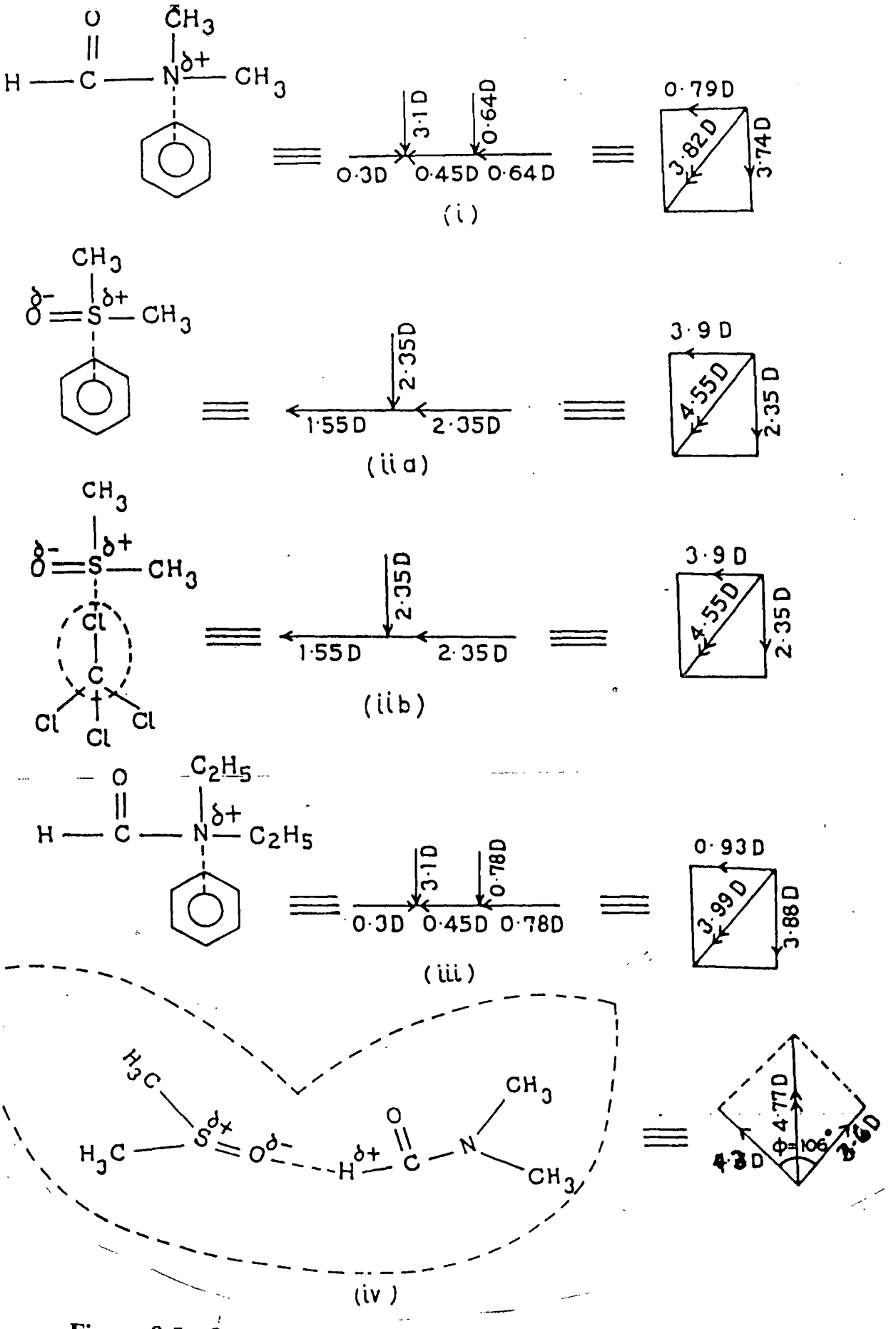

Figure 8.5 **Conformational structures along with solute-solvent and solute-solute interaction of molecules.**

(i) DMF in C_6H_6 (iia) DMSO in C_6H_6 (iib) DMSO in CCl_4
(iii) DEF in C_6H_6 (iV) DMSO-DMF dimer

The solute-solvent molecular associations of DMF, DEF, and DMSO in C_6H_6 can arise due to interactions of fractional positive charges of N and S atoms of the molecules with the π-delocalised electron cloud of C_6H_6 ring in Figure 8.5 (i), (iii) and (iia) respectively. Again, one of C—C1 dipoles of CCl_4, owing to the more - ve charge on C1 atom, interacts with the fractional + ve charge of S-atom of DMSO (Figure 8.5 (iib)). The μ_{theo} = 4.55D of DMSO is, however, computed from the vector addition of available bond moments of 2.35D and 1.55D for S $\leftarrow$ CH_3 and 0 $\Leftarrow$ S respectively assuming the molecule to be planar one. The major contributions to μ_{theo} for DMF and DEF are due to 0.64 D and 0.78 D for N $\leftarrow$ CH_3 and N $\leftarrow$ C_2H_5 since the other common bond moments in them are the same with values of 0.3D, 0.45 D and 3.10 D for C $\leftarrow$H, C $\leftarrow$ N and C $\Leftarrow$ 0 respectively. Figure 8.5 (iv) however, shows a certain angle ϕ ($\cong$ 106°) between monomeric μ's of DMF and DMSO to have μ_{theo} = 4.77 D of the solute-solute molecular association i.e. dimer below x_k = 0.6.

Table 8.3, however, shows slight deviations of estimated μ's or average μ calculated from $\mu_{jk} = \mu_j x_j + \mu_k x_k$, with the μ_{theo} (Table 8.3) probably due to the presence of inductive or mesomeric moments of the substituent groups of the molecules under GHz electric field at different experimental temperatures. They are also observed elsewhere [13]. and placed in Table 8.4 together with the factor $\tau\, T/\eta^{\gamma}$ proportional to volume of the rotating unit. Table 8.4 also shows the reduced bond moments due to possible existence of mesomeric and inductive moments at each temperature in order to arrive at the estimated μ of Table 8.3. This fact at once reveals that the mesomeric and inductive moments are temperature dependent quantities under hf electric field. Thus the relaxation parameters as obtained by hf conductivity offers a convenient and interesting tool to arrive at the structural and associational aspects as well as temperature dependence of mesomeric and inductive moments of the substituent groups of nonspherical binary or single polar liquids under investigation.

Acknowledgment

The authors are thankful to Sri R.C. Basak, M.Sc. for his interest in this work.

References

1. C.R. Acharyya, A.K. Chatterjee, P.K. Sanyal and S. Acharyyya Indian J. Pure & Appl. Phys. **24** 234 (1986)

2. A K Chatterjee, U saha, N Nandi, R C Basak and S Acharyya Indian J. Phys. **66B** 291 (1992)

3. U Saha and S Acharyya Indian J. Pure & Appl. Phys. **31** 181 (1993)

4. A Sharma, D R Sharma and M S Chauhan Indian J. Pure & Appl. Phys. **31** 841 (1993)

5. A Sharma and D R Sharma J Phys. Soc Jpn. **61** 1049 (1992)

6. A R Saksena Indian J. Pure & Appl. Phys. **16** 1079 (1978)

7. U Saha and S Acharyya Indian J. Pure & Appl. Phys. **32** 346 (1994)

8. F J Murphy and S O Morgan Bull Syst. Tech. J. **18** 502 (1939)

9. K V Gopalakrishna Trans. Faraday Soc. **53** 767 (1957)

10. S K Sit and S Acharyya Indian J. Phys. **70B** 19 (1996)

11. H Eyring, S Glasstone and K J Laidler The Theory of Rate Process (McGraw Hill, New York) (1941)

12. C P Smyth Dielectric Behaviour and Structure (McGraw Hill : New York) (1955)

13. R C Basak, S K Sit, N Nandi and S Acharyya Indian J. Phys. **70B** 37 (1996)

CHAPTER 9

DOUBLE RELAXATION TIMES, DIPOLE MOMENTS AND MOLECULAR STRUCTURES OF SOME NON-SPHERICAL APROTIC POLAR LIQUIDS IN BENZENE FROM HIGH FREQUENCY ABSORPTION MEASUREMENT

9.1 Introduction

The dielectric relaxation mechanism of dipolar aprotic polar liquids in nonpolar solvent from high frequency absorption studies have attracted the attention of a large number of workers [1,2]. Such type of liquids are of great importance for their wide biological applications. They possess high values of dielectric constant and act as building blocks of proteins and enzymes. Moreover, they are good constituent of binary mixture of polar liquids. Under the application of high frequency (hf) X-band electric field of nearly 10 GHz they are expected to throw much light on weak molecular associations like monomer (solute-solvent) and dimer (solute-solute) formations. Many workers [3,4] have already studied the structural and associational aspects of aprotic liquids from the X-band microwave electric field by applying the single frequency concentration variation method of Gopalakrishna [5]. However,, no attempt has yet been made so far whether such type of liquids may possess the double relaxation times τ_2 due to end over end rotation for the whole molecule and τ_1 due to the flexible part attached to the parent ring of the molecule under hf electric field of 10 GHz. The X-band electric field (~ 10 GHz) is supposed to be the most effective dispersive region of such molecules like mono or disubstituted benzenes and anilines [6] to reveal interesting facts for these molecules.

We, therefore, thought to undertake a thorough measurement of static dielectric constant ε_{0ij}, real part of the dielectric constant ε'_{ij}, dielectric loss ε''_{ij} of complex dielectric constant ε^*_{ij} and infinite frequency dielectric constant $\varepsilon_{\infty ij}$ of some available aprotic liquids (j) like dimethyl sulphoxide (DMSO), N, N - diethyl formamide (DEF), N, N-dimethyl formamide (DMF) and N, N-dimethyl acetamide (DMA) in solvent C_6H_6 (i) under nearly 10 GHz electric fields. The data thus obtained are, however, used to see how far they exhibit double relaxation phenomena under 10 GHz electric field by the recently developed method of single frequency measurement [7,8] within the framework of Debye and Smyth model.

The data of ε_{0ij}, ε'_{ij}, ε''_{ij} and $\varepsilon_{\infty ij}$ ($= n^2_{Dij}$ by Abbe's refractometer) of the polar nonpolar liquid mixtures as a function of weight fractions ω_j's of DMSO were measured by a Hewlett Packard (HP) analyser at 25°, 30°, 35° and 40°C together with DEF at

30°C and DMF and DMA at 25°C respectively. The purpose of such experimental observations as referred to table 9.1 is to show that all of them exhibit double relaxation phenomena except DMA at nearly 10 GHz. The data were, however, selected from the peaks of the respective graphical plots of ε''_{ij} against frequency as well as ε'_{ij} for a polar nonpolar liquid mixture at a given temperature and concentration.

The static dipole moments μ_s (table 9.2) are then estimated from the slope of the static experimental parameters X_{ij} involved with the measured ε_{0ij} and $\varepsilon_{\infty ij}$ of table 9.1 with ω_j's of polar liquids as shown in figure 9.1.

τ_2 and τ_1 are, however, obtained from the slope and intercept of $(\varepsilon_{0ij} - \varepsilon'_{ij})/ (\varepsilon'_{ij} - \varepsilon_{\infty ij})$ with $\varepsilon''_{ij} / (\varepsilon'_{ij} - \varepsilon_{\infty ij})$ as illustrated graphically in figure 9.2 for different ω_j's of solutes. The intercepts and slopes are also placed in table 9.3. As evident from table 9.3, τ_1 is very close to τ due to Gopalakrishna's method [5]. The relative contributions c_1 and c_2 due to τ_1 and τ_2 are, however, calculated from the values of $x=\left[\frac{\varepsilon'_{ij} - \varepsilon_{\infty ij}}{\varepsilon_{0ij} - \varepsilon_{\infty ij}}\right]$ and y [= $\varepsilon''_{ij} / (\varepsilon_{0ij} - \varepsilon_{\infty ij})$] at $\omega_{j\to 0}$ from the plots of them with ω_j's as displayed in figures 9.3 and 9.4 respectively. The estimated values of c_1 and c_2 together with those due to Fröhlich's equations are presented in table 9.4 for comparison. Moreover, the comparison of μ_2 and μ_1 (table 9.5) due to τ_2 and τ_1 in terms of slope β of the hf conductivity K_{ij} against ω_j (figure 9.5) with the estimated μ_s from the measured static relaxation data seems to evolve an interesting fact for the polar molecules under investigation. The conformational structures of the polar molecules are estimated as shown in figure 9.6 by considering the reduced bond moments due to mesomeric and inductive moments of the substituent groups of polar molecules. They are compared with the μ_s under static electric field as placed in table 9.2.

9.2 Experimental set up

The Block diagram for the measurement of dielectric relaxation solution (ij) data and experimental details has been given elsewhere [9]. It consists of sample holder,

Table 9.1 Concentration variation of dielectric relaxation parameters like dielectric constant, (ε'_{ij}) dielectric loss (ε''_{ij}) static dielectrc constant (ε_{0ij}) optical dielectric constant ($\varepsilon_{\infty ij}$) of some aprotic polar liquids in benzene at different temperature measured under high frequency electric field of nearly 10 GHz.

DMSO in C_6H_6 at 9.174 GHz.

Temperature in °C.	Weight fraction (ω_j) of solute	ε'_{ij}	ε''_{ij}	ε_{0ij} at 1 KH_z	$\varepsilon_{\infty ij} = n^2_{D\,ij}$,
	0.0022	2.311	0.0280	2.3230	2.2499
	0.0043	2.342	0.0420	2.3624	2.2530
25	0.0047	2.350	0.0460	2.3731	2.2550
	0.0069	2.381	0.0616	2.4173	2.2579
	0.0086	2.414	0.0798	2.4602	2.2620
	0.0022	2.310	0.0274	2.3210	2.2470
	0.0043	2.341	0.0400	2.3610	2.2515
30	0.0047	2.348	0.0440	2.3720	2.2500
	0.0069	2.370	0.0526	2.4045	2.2545
	0.0086	2.390	0.0648	2.4362	2.2560
	0.0022	2.290	0.0234	2.2993	2.2300
	0.0043	2.312	0.0330	2.3400	2.2320
35	0.0047	2.316	0.0360	2.3470	2.2335
	0.0069	2.350	0.0496	2.3960	2.2396
	0.0086	2.370	0.0580	2.4270	2.2440
	0.0022	2.270	0.0170	2.2849	2.2201
	0.0043	2.302	0.0282	2.3300	2.2246
40	0.0047	2.304	0.0286	2.3350	2.2256
	0.0069	2.338	0.0420	2.3838	2.2297
	0.0086	2.350	0.0500	2.4120	2.2345

DEF in C_6H_6 at 9.695 GHz

Temperature in °C.	Weight fraction (ω_j) of solute	ε'_{ij}	ε''_{ij}	ε_{0ij} at 1 KH,	$\varepsilon_{\infty ij}=n^2_{D\,ij}$,
30	0.0023	2.2780	0.0256	2.3067	2.0939
	0.00415	2.2900	0.0288	2.3336	2.1141
	0.00786	2.3140	0.0384	2.3965	2.1543
	0.00952	2.3260	0.0448	2.4208	2.1727

DMF in C_6H_6 at 9.987 GHz

25	0.0027	2.324	0.0256	2.3446	2.2498
	0.0036	2.339	0.0302	2.3680	2.2518
	0.0048	2.359	0.0386	2.3968	2.2545
	0.0063	2.387	0.0484	2.4434	2.2579

DMA in C_6H_6 at 9.987 GHz

25	0.0026	2.3250	0.0186	2.3663	2.2432
	0.0045	2.3475	0.0278	2.3988	2.2429
	0.0056	2.3625	0.0330	2.4278	2.2427
	0.0066	2.3795	0.0393	2.4508	2.2425

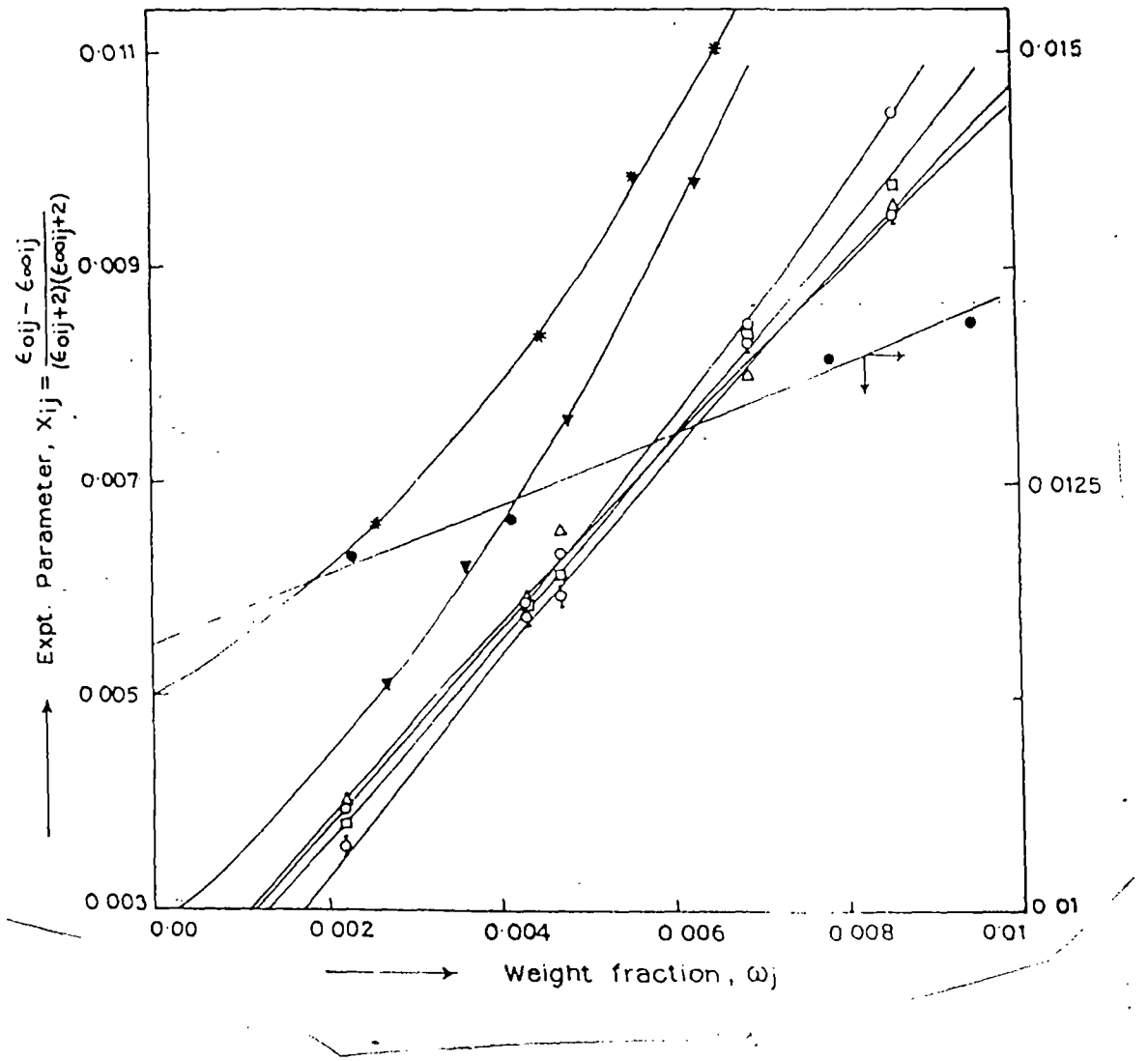

Figure 9.1 **Variation of the measured values of the experimental parameter, X_{ij} with weight fraction ω_j of some aportic polar liquids in benzene:**

(i) DMSO at 25°C (-O-), (ii) DMSO at 30°C (-Δ-)
(iii) DMSO at 35°C (-□-), (iv) DMSO at 40°C (-◊-),
(v) DEF at 30°C (-●-), (vi) DMF at 25°C (-▼-),
(vii) DMA at 25°C (-✱-).

temperature chamber, temperature controller and a Hewlett Packard Bridge 4192 A. A cell with sample holder consists of two glass plates coated with conducting Indium Tin Oxide (ITO) in their inner surfaces. They are separated by myler spacer of 40μm thickness and kept on temperature chamber Mettler Hot Stage FP 52. The Hewlett Packard Impedence Analyser (HP 4192 A) measures the complex impedence of the cell to evaluate capacitance and conductance values. Air capacitance C_o of the cell can be written as

$$C_o = C_L + C_S \qquad \text{.....(9.1)}$$

where C_L is the capacitance of the empty cell excluding stray capacitance C_S.

When the cell is filled with the sample of known dielectric constant ε, the measured capacitance will be :

$$C = \varepsilon C_L + C_S \qquad \text{.....(9.2)}$$

The real part of the dielectric permittivity of the sample is given by:

$$\varepsilon'_{ij} = \frac{C - C_S}{C_o - C_S} \qquad \text{.....(9.3)}$$

The dielectric loss due to absorption is

$$\varepsilon''_{ij} = \frac{G_{ij}}{2\pi f C_o} \qquad \text{.....(9.4)}$$

where "G_{ij}" and "f" are conductance and frequency of the electric field.

The values of ε'_{ij} and ε''_{ij} are plotted against frequency for a temperature and concentration to get the desired values, as reported in table 9.1, for which maximum peak of ε''_{ij} occured. ε_{0ij} was, measured at 1 KHz. $\varepsilon_{\infty ij}$ is, however, estimated from n^2_{Dij} of polar nonpolar liquid mixture measured by a Abbe's refractometer.

The solvent C_6H_6 (Spec. pure) and aprotic liquids like DMSO, DMF, DEF and DMA (E Merck, Bombay) were used after distillation for 8 hours. The solutions of different concentrations were made by mixing a certain weight of solute in a solvent of known weight. They were kept in dried and clean capsules for the measurement.

9.3 Theoretical Formulations:

(i) Static dipole moment μ_s : -

The Debye equation [10] for a polar nonpolar liquid mixture of molar concentration C_j of a polar liquid at a given temperature T°K is :

$$\frac{\varepsilon_{0ij} - 1}{\varepsilon_{0ij} + 2} - \frac{n^2_{Dij} - 1}{n^2_{Dij} + 2} = \frac{\varepsilon_{0i} - 1}{\varepsilon_{0i} + 2} - \frac{n^2_{Di} - 1}{n^2_{Di} + 2} + \frac{4\pi N \mu_s^2}{9kT} C_j \qquad \text{.....(9.5)}$$

which is, however, based on the assumption that atomic polarisation is equal to the electronic polarisation. The symbols used in equation (9.5) are of usual significance. The molar concentration C_j is related to weight fraction ω_j of a polar liquid by:

$$C_j = \frac{\rho_{ij}\,\omega_j}{M_j} \qquad \text{.....(9.6)}$$

where M_j is the molecular weight of a polar liquid and ρ_{ij}, the density of solution.

If a given weight w_j of a solute of volume v_j is made to mix with the weight w_i of a solvent of volume v_i, the solution density ρ_{ij} is written as :

$$\rho_{ij} = \frac{w_i + w_j}{v_i + v_j} = \frac{w_i + w_j}{\frac{w_i}{\rho_i} + \frac{w_j}{\rho_j}}$$

where ρ_i and ρ_j are the densities of the solvent and solute respectively.

$$\text{Again, } \rho_{ij} = \frac{\rho_i \rho_j}{\rho_j\left(\frac{w_i}{w_i + w_j}\right) + \rho_i\left(\frac{w_j}{w_i + w_j}\right)}$$

$$= \frac{\rho_i\rho_j}{\rho_j\omega_i + \rho_i\,\omega_j} = \frac{\rho_i\rho_j}{\rho_j(1 - \omega_j) + \rho_i\omega_j}$$

$$= \frac{\rho_i}{1 - \left(1 - \frac{\rho_i}{\rho_j}\right)\omega_j} = \frac{\rho_i}{1 - \gamma\omega_j} \qquad \text{..... (9.7)}$$

where $\gamma = \left(1 - \frac{\rho_i}{\rho_j}\right)$, $\omega_i = \left(\frac{w_i}{w_i + w_j}\right)$ and $\omega_j \left(= \frac{w_j}{w_i + w_j}\right)$ are the weight fractions of the solvent and solute respectively so that $\omega_i + \omega_j = 1$.

Hence, equation (9.5) is finally written as :

$$\frac{\varepsilon_{0ij} - n^2_{Dij}}{(\varepsilon_{0ij} + 2)(n^2_{Dij} + 2)} = \frac{\varepsilon_{0i} - n^2_{Di}}{(\varepsilon_{0i} + 2)(n^2_{Di} + 2)} + \frac{4\pi N \mu_s^2}{27 k T} \frac{\rho_i}{M_j} \omega_j (1 - \gamma \omega_j)^{-1}$$

$$\text{or, } X_{ij} = X_i + \frac{4\pi N \mu_s^2 \rho_i}{27 M_j kT} \omega_j + \frac{4\pi N \mu_s^2 \rho_i}{27 M_j kT} \gamma \omega_j^2 +$$

$$= X_i + R\omega_j + R\gamma\omega_j^2 + \quad \text{.....(9.8)}$$

where X_{ij} and X_i are the static experimental parameters of solution and solvent and

$R = \frac{4\pi N \mu_s^2 \rho_i}{27 M_j k T}$ respectively.

The usual variation of X_{ij} with ω_j is expected to be almost linear but often found to be nonlinear in nature as evident from the curves of figure 9.1. The curves are found to obey the relation.

$$X_{ij} = a_o + a_1\omega_j + a_2\omega_j^2 \quad \text{.....(9.9)}$$

The coefficients a_o, a_1 and a_2 are placed in table 9.2

Equating the first power of ω_j of equations (9.8) and (9.9) and neglecting higher powers of ω_j for their involvement of various types of interactions such as solvent effect, relative density effect, orientational effect and dipole-dipole interaction etc, one gets.

$$\mu_s = \left(\frac{27 M_j kT}{4\pi N \rho_i} a_1 \right)^{\frac{1}{2}} \quad \text{.....(9.10)}$$

The estimated static dipole moment μ_s are presented in table 9.2 in order to compare with μ_1 and μ_2 from the hf absorption method (table 9.5)

(ii) Dipole moments μ_2 and μ_1 due to τ_2 and τ_1 : -

The complex dielectric constant ε^*_{ij} of a polar - nonpolar liquid mixture under hf electric field of nearly 10 GHz can be represented as two Debye type dispersions [11] as:

$$\frac{\varepsilon'_{ij} - \varepsilon_{\infty ij}}{\varepsilon_{0ij} - \varepsilon_{\infty ij}} = \frac{c_1}{1 + \omega^2\tau_1^2} + \frac{c_2}{1 + \omega^2\tau_2^2} \quad \text{.....(9.11)}$$

Table 9.2 Coefficients a_0, a_1 and a_2 in equation $X_{ij} = a_0 + a_1 \omega_j + a_2 \omega_j^2$, static dipole moment μ_s in D, theoretical dipole moment μ_{theo} by considering inductive and mesomeric moments of substituent groups of some aprotic polar liquids in benzene.

System with serial no and Mol. wt.	Temperature in °C	Coefficients in eq a_0.	a_0, a_1, a_2, $X_{ij}=a_0+a_1\omega j + a_2 \omega_j^2$ a_1. a_2.	μ_s in Debye	μ_{theo} in Debye	μ_{cal} in Debye	Ratio $\frac{\mu_s}{\mu_{theo}}$
I) DMSO in C_6H_6 M_j = 78 gm.	25	0.00218	0.77564 20.93539	3.19	4.55	3.20	0.7011
II) DMSO in C_6H_6 M_j = 78 gm.	30	0.00187	1.03149 -17.18275	3.72	4.55	3.72	0.8176
III) DMSO in C_6H_6 M_j = 78 gm.	35	0.00181	0.93459 0	3.58	4.55	3.58	0.7868
IV) DMSO in C_6H_6 M_j = 78 gm.	40	0.00104	1.19130 -23.28196	4.08	4.55	4.08	0.8967
V) DEF in C_6H_6 M_j = 101.15 gm.	30	0.01155	0.20471 0	1.89	3.99	1.89	0.4737
VI) DMF in C_6H_6 M_j = 73 gm.	25	0.00275	0.73007 61.43789	2.99	3.82	2.99	0.7827
VII) DMA in C_6H_6 M_j = 87 gm.	25	0.00503	0.41784 75.47872	2.47	4.02	2.46	0.6144

$$\frac{\varepsilon''_{ij}}{\varepsilon_{0ij} - \varepsilon_{\infty ij}} = c_1 \frac{\omega \tau_1}{1 + \omega^2 \tau_1^2} + c_2 \frac{\omega \tau_2}{1 + \omega^2 \tau_2^2} \qquad \text{.....(9.12)}$$

so that $c_1 + c_2 = 1$. c_1 and c_2 are the relative contributions towards dielectric relaxations due to τ_1 and τ_2 respectively.

Substituting $\frac{\varepsilon'_{ij} - \varepsilon_{\infty ij}}{\varepsilon_{0ij} - \varepsilon_{\infty ij}} = x$ and $\frac{\varepsilon''_{ij}}{\varepsilon_{0ij} - \varepsilon_{\infty ij}} = y$

equations (9.11) and (9.12) become :

$$x = c_1 a_1 + c_2 a_2 \qquad \text{..... (9.13)}$$

$$y = c_1 b_1 + c_2 b_2 \qquad \text{.....(9.14)}$$

where $a = \frac{1}{1 + \alpha^2}$, $b = \frac{\alpha}{1 + \alpha^2}$ and $\omega\tau = \alpha$

The suffices 1 and 2 with a and b are, however, related to τ_1 and τ_2 respectively. Solving equations (9.13) and (9.14) for c_1 and c_2 one gets :

$$c_1 = \frac{(x \alpha_2 - y)(1 + \alpha_1^2)}{\alpha_2 - \alpha_1} \qquad \text{.....(9.15)}$$

$$c_2 = \frac{(y - x \alpha_1)(1 + \alpha_2^2)}{\alpha_2 - \alpha_1} \qquad \text{.....(9.16)}$$

provided $\alpha_2 - \alpha_1 \neq 0$ and $\alpha_2 > \alpha_1$

Now, using $c_1 + c_2 = 1$: one gets the following equations from (9.15) and (9.16)

$$\frac{1 - x}{y} = (\alpha_1 + \alpha_2) - \frac{x}{y} \alpha_1 \alpha_2$$

$$\text{or, } \frac{\varepsilon_{0ij} - \varepsilon'_{ij}}{\varepsilon'_{ij} - \varepsilon_{\infty ij}} = \omega (\tau_2 + \tau_1) \frac{\varepsilon''_{ij}}{\varepsilon'_{ij} - \varepsilon_{\infty ij}} - \omega^2 \tau_1 \tau_2 \qquad \text{.....(9.17)}$$

This is a straight line equation of $\frac{\varepsilon_{0ij} - \varepsilon'_{ij}}{\varepsilon'_{ij} - \varepsilon_{\infty ij}}$ against $\frac{\varepsilon''_{ij}}{\varepsilon'_{ij} - \varepsilon_{\infty ij}}$ with intercept $-\omega^2\tau_1\tau_2$

and slope $\omega (\tau_1 + \tau_2)$. The slopes and intercepts are, however, obtained with the measured dielectric relaxation data like ε_{0ij}, ε'_{ij}, ε''_{ij} and $\varepsilon_{\infty ij}$ of table 9.1 at different weight fractions ω_j's of a polar liquid at a fixed temperature and electric field frequency. The slopes and

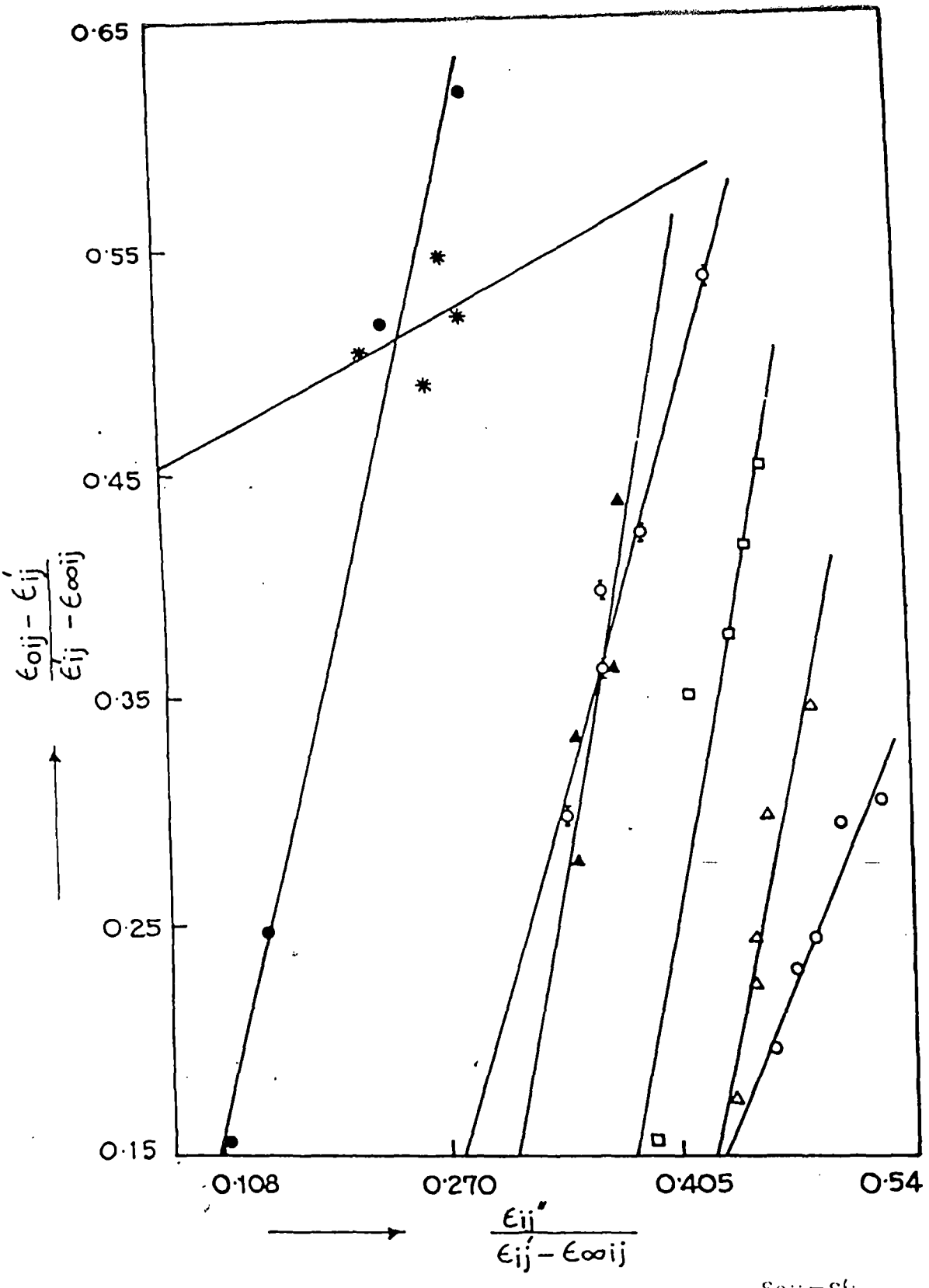

Figure 9.2 The plot of the measured values of $\frac{\varepsilon_{0ij}-\varepsilon'_{ij}}{\varepsilon'_{ij}-\varepsilon_{\infty ij}}$ against $\frac{\varepsilon''_{ij}}{\varepsilon'_{ij}-\varepsilon_{\infty ij}}$ as a function of weight ω_j of some aprotic polar liquids in benzene:

(i) DMSO at 25° C (-O-), (ii) DMSO at 30°C (-Δ-)
(iii) DMSO at 35°C (-□-), (iv) DMSO at 40°C (-◊-)
(v) DEF at 30°C (-●-), (vi) DMF at 25°C (-▲-)
(vii) DMA at 25°C (-✱-).

Table - 9.3 The estimated intercepts and slopes of straight line equation of $\frac{\varepsilon_{0ij}-\varepsilon_{ij}}{\varepsilon'_{ij}-\varepsilon_{\infty ij}}$ against $\frac{\varepsilon_{ij}}{\varepsilon'_{ij}-\varepsilon_{\infty ij}}$ correlation coefficient r, % of error involved in fitting technique, the most probable relaxation time $\tau_o = \sqrt{\tau_1\tau_2}$ and reported τ of some nonspherical aprotic polar liquids under hf electric field of nearly 10 GHz.

System with serial No. and Mol. wt.	temperature t in °C	Intercept and slope of eq. (9.17)	Correlation coefficient (r)	% of error in fitting technique.	Estimated values of τ_2 and τ_1 in pSec		Most probable relaxation time $\tau_o = \sqrt{\tau_1\tau_2}$ in pSec	Reported τ in pSec. (G. K. Method)
I) DMSO in C_6H_6 M_j = 78 gm.	25	0.56708	1.68169	0.9605	2.34	21.08	8.10	13.07	5.37
II) DMSO in C_6H_6 M_j = 78 gm.	30	1.30241	3.43579	0.9429	3.35	52.11	7.53	19.81	4.96
III) DMSO in C_6H_6 M_j = 78 gm.	35	1.28988	3.81623	0.9377	3.64	59.73	6.51	19.72	4.70
IV) DMSO in C_6H_6 M_j = 78 gm.	40	0.53759	2.48795	0.9862	0.83	39.04	4.15	12.73	4.33
V) DEF in C_6H_6 M_j =101.1 gm.	30	0.2592	3.08290	0.9933	0.45	49.21	1.42	8.36	2.42
VI) DMF in C_6H_6 M_j = 73 gm.	25	1.0183	3.81856	0.8896	7.03	56.28	4.60	16.09	5.09
VII) DMA in C_6H_6 M_j = 87 gm.	25	-0.41023	0.39775	0.4389	27.23	13.86	--	--	6.53

intercepts and the corresponding τ_1 and τ_2 are shown in table 9.3 with the reported τ due to Gopalakrishna method [5].

The relative contributions c_1 and c_2 towards dielectric relaxations are calculated from the theoretical formulations of x and y due to Fröhlich [12].

$$x = \frac{\varepsilon'_{ij} - \varepsilon_{\infty ij}}{\varepsilon_{0ij} - \varepsilon_{\infty ij}} = 1 - \frac{1}{2A} \ln \left(\frac{1 + e^{2A} \omega^2 \tau_s^2}{1 + \omega^2 \tau_s^2} \right) \qquad \text{.....(9.18)}$$

$$\text{and } y = \frac{\varepsilon''_{ij}}{\varepsilon_{0ij} - \varepsilon_{\infty ij}} = \frac{1}{A} \left[\tan^{-1} (e^A \omega \tau_s) - \tan^{-1} (\omega \tau_s) \right] \qquad \text{.....(9.19)}$$

and are shown in table 9.4. Here τ_s = small limiting relaxation time = τ_1 and A = Fröhlich parameter = $\ln \left(\frac{\tau_2}{\tau_1} \right)$. 'A' is a constant which can be expressed in terms of the difference in activation energies E_2 and E_1 of a rotating unit at a given temperature because $\tau_2/\tau_1 = \exp (E_2 - E_1)/RT$. The values of x and y at $\omega_j \rightarrow 0$ from the graphical plots of figures 9.3 and 9.4 respectively can also be had to yield c_1 and c_2, because the L.H.S. of Bergmann's equation are fixed for τ_1 and τ_2 once estimated from the intercept and slope of equation (9.17) when substituted on the R.H.S. of equation (9.11) and (9.12).

The hf conductivity K^*_{ij} of a polar - nonpolar liquid mixture is expressed by the measured ε'_{ij} and ε''_{ij} of table 9.1 in the forms:

$$K_{ij} = \frac{\omega}{4\pi} \sqrt{\varepsilon'^2_{ij} + \varepsilon''^2_{ij}} \qquad \text{.....(9.20)}$$

as a function of ω_j. Although, ε''_{ij} offers resistance to polarisation still in the hf region $\varepsilon'_{ij} >> \varepsilon''_{ij}$.

Thus the real part of conductivity K'_{ij} at T K is written as [13].

$$K'_{ij} = \frac{\mu_j^2 N \rho_{ij} F_{ij}}{3 M_j k T} \left(\frac{\omega^2 \tau}{1 + \omega^2 \tau^2} \right) \omega_j \qquad \text{.....(9.21)}$$

which on differentiation w.r. to ω_j and at $\omega_j \rightarrow 0$ yields

Table - 9.4 Fröhlich parameter A, relative contributions c_1 and c_2 due to τ_1 and τ_2, theoretical values of x and y due to Fröhlich eqs.(9.18) and (9.19) and those by graphical method at infinite dilution for some aprotic polar liquids at different and single temperature under hf electric field.

System with serial no. and Mol. ωt.	temperature in °C	Fröhlich parameter A	Theoretical x and eq. (9.18)	values of y from and (9.19)	Theoretical c_1 and c_2 eqs. (9.15)	values of from and 9.16	Estimated values of x and y at $\omega_j \to 0$ from figures 9.3 and 9.4		Estimated c_1 and c_2 from technique.	values of graphical
I) DMSO in C_6H_6 M_j = 78 gm.	25	2.6025	0.8637	0.1710	1.4296	-0.7679	0.892	0.3625	1.1738	-0.1779
II) DMSO in C_6H_6 M_j = 78 gm.	30	1.9344	0.4491	0.4340	0.4230	0.9324	0.900	0.3375	1.0939	-0.2064
III) DMSO in C_6H_6 M_j = 78 gm.	35	9.1751	0.8681	0.1012	1.0737	-0.9398	0.834	0.295	0.9579	-0.0745
IV) DMSO in C_6H_6 M_j = 78 gm.	40	2.2415	0.6105	0.4092	0.5070	0.7935	0.848	0.225	0.8848	0.0671
V) DEF in C_6H_6 M_j = 101.15 gm.	30	3.5454	0.6767	0.3277	0.5885	0.9230	0.988	0.055	1.0059	-0.1043
VI) DMF in C_6H_6 M_j = 73 gm.	25	2.5043	0.4969	0.4046	0.4510	1.0850	0.872	0.210	0.9585	-0.1726

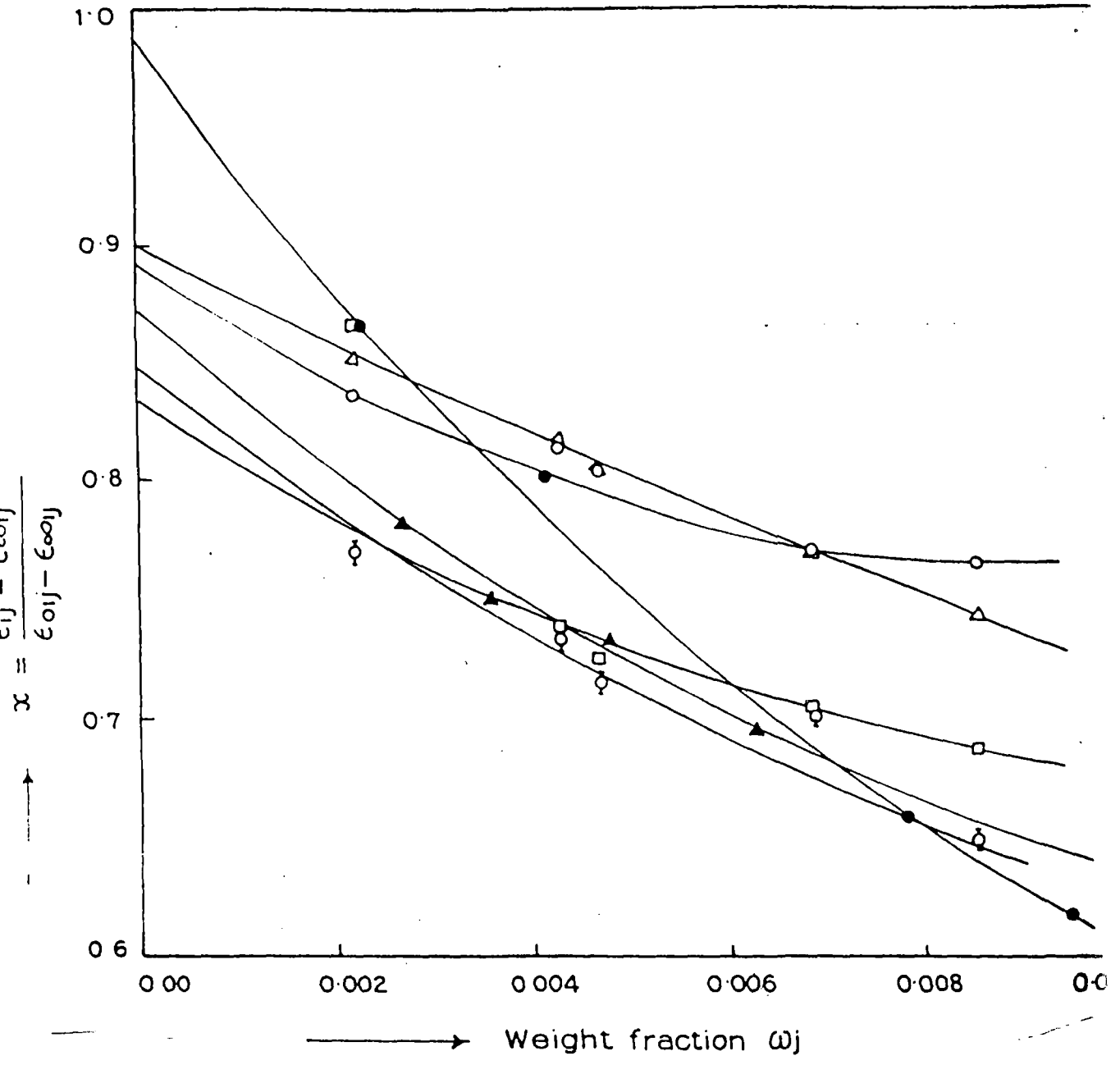

Figure 9.3 Variation of measured $x = \frac{\varepsilon'_{ij} - \varepsilon_{\infty ij}}{\varepsilon_{0ij} - \varepsilon_{\infty ij}}$ with weight fraction ω_j of some aprotic polar liquids :

(i) DMSO at 25° C (-O-), (ii) DMSO at 30°C (-Δ-)
(ii) DMSO at 35°C (-□-), (iv) DMSO at 40°C (-◊-)
(iii) DEF at 30°C (-●-), (vi) DMF at 25°C (-▲-)

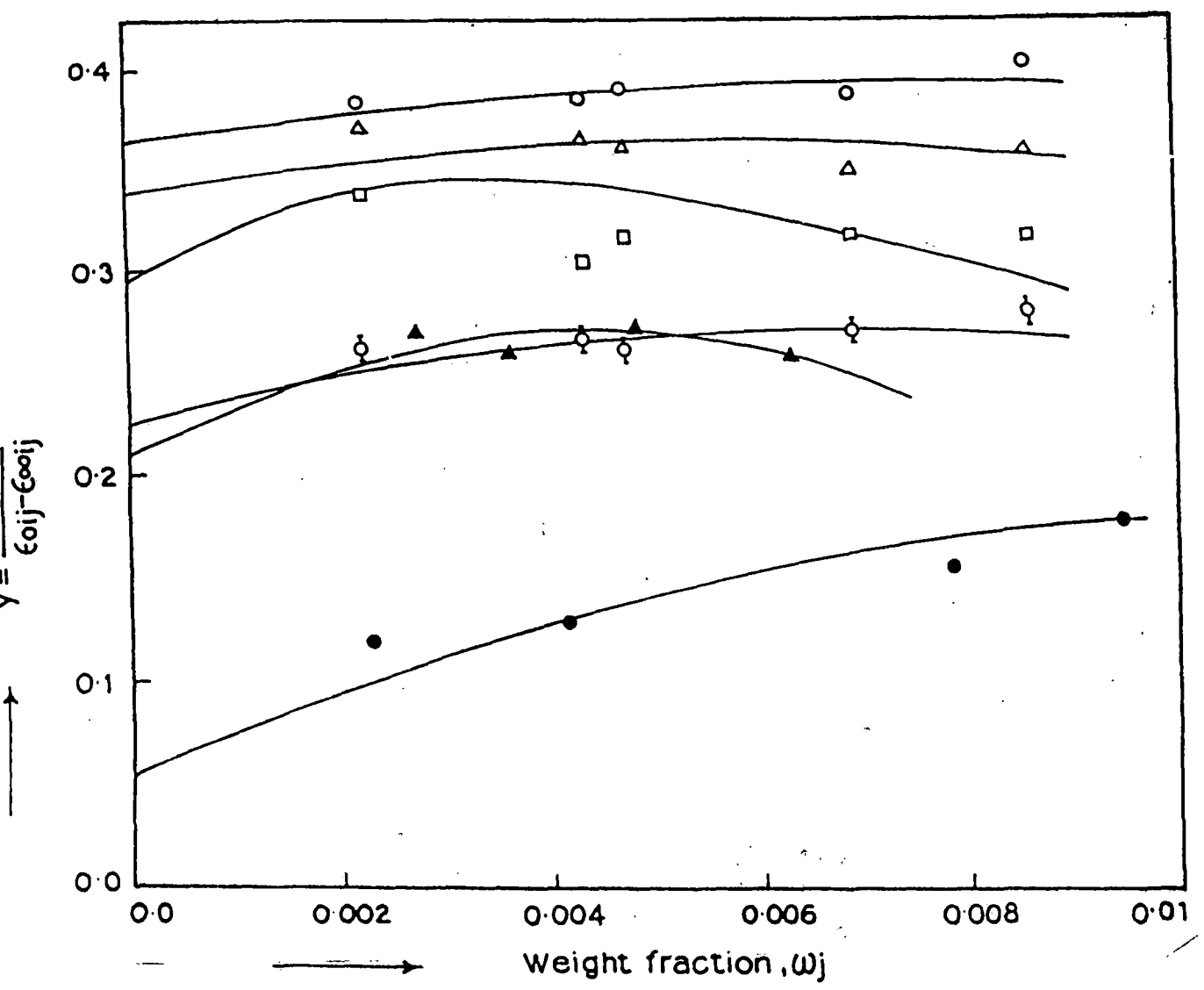

Figure 9.4 Variation of measured $y = \frac{\varepsilon''_{ij}}{\varepsilon_{0ij} - \varepsilon_{\infty ij}}$ with weight fraction ω_j of some aprotic polar liquids :

(i) DMSO at 25° C (-O-), (ii) DMSO at 30°C (-Δ-)
(ii) DMSO at 35°C (-□-), (iv) DMSO at 40°C (-◊-)
(iii) DEF at 30°C (-●-), (vi) DMF at 25°C (-▲-)

$$\left(\frac{d K'_{ij}}{d \omega_j}\right)_{\omega_j \to 0} = \frac{\mu_j^2 N \rho_i F_i}{3 M_j k T}\left(\frac{\omega^2 \tau}{1+\omega^2 \tau^2}\right) \qquad \text{.....(9.22)}$$

where all the symbols carry usual significance [7,8].

Again, the total hf conductivity K_{ij} ($= \frac{\omega}{4\pi} \varepsilon''_{ij}$)is again given by :

$$K_{ij} = K_{\infty ij} + \frac{1}{\omega \tau} K'_{ij}$$

$$\text{or, } \left(\frac{d K'_{ij}}{d \omega_j}\right)_{\omega_j \to 0} = \omega \tau \left(\frac{d K_{ij}}{d \omega_j}\right)_{\omega_j \to 0} = \omega \tau \beta \qquad \text{.....(9.23)}$$

where β is the slope of K_{ij} - ω_j curve at $\omega_j \to 0$

From equations (9.22) and (9.23) one gets

$$\mu_j = \left(\frac{3 M_j k T \beta}{N \rho_i F_i \omega b}\right)^{\frac{1}{2}} \qquad \text{.....(9.24)}$$

in order to obtain the hf dipole moments μ_1 or μ_2 in terms of b_1 and b_2 where b_1 and b_2 are the dimensionless parameters in terms of τ_1 and τ_2 i.e.

$$b_1 = \frac{1}{1+\omega^2 \tau_1^2} \text{ and } b_2 = \frac{1}{1+\omega^2 \tau_2^2} \qquad \text{.....(9.25)}$$

Both b_1 and b_2 as well as the coefficients α, β, γ of K_{ij} - ω_j equations as displayed in figure 9.5 are shown in table 9.5 together with μ_1 and μ_2 as dipole moments of the flexible part and the whole molecule of a polar liquid.

9. 4. Result and Discussion

The static dipole moments μ_s's of the aprotic polar liquids are calculated from the measured data, reported in table 9.1 in terms of linear coefficients of the static experimental parameter X_{ij} against ω_j curves as displayed in figure 9.1. The coefficients a_0,

Table - 9.5 The estimated coefficients α, β and γ of $K_{ij} - \omega_{ij}$ equations, dimensionless parameters b's, dipole moments μ_j's in D of some nonspherical aprotic polar liquids in benzene under hf electric field of nearly 10 GHz at single and different temperatures.

System with Serial No and Mol. wt.	Temperature in °C	Coeffi ients of α, of $K_{ij} = \alpha + \beta\omega_j + \gamma\omega_j^2$ $\alpha \times 10^{-10}$ in e. s. u.	$\beta \times 10^{-10}$ in e. s. u.	β and γ eq. $\gamma \times 10^{-10}$ in e. s. u.	Dimensionless $b_2 = \frac{1}{1+\omega^2\tau_2^2}$	parameters $b_1 = \frac{1}{1+\omega^2\tau_1^2}$	Estimated. dipole moments μ_2	in Debye μ_1	Reported dipole moment μ_j in D
I) DMSO in C_6H_6 $M_j = 78$ gm.	25	1.04721	5.64874	157.35206	0.4040	0.8212	4.67	3.28	3.79
II) DMSO in C_6H_6 $M_j = 78$ gm.	30	1.04305	8.18	-231.74466	0.0999	0.8416	11.47	3.95	3.83
III) DMSO in C_6H_6 $M_j = 78$ gm.	35	1.04013	4.15828	164.83118	0.0779	0.8767	9.38	2.80	4.04
IV) DMSO in C_6H_6 $M_j = 78$ gm.	40	1.02267	8.89703	-274.82628	0.1650	0.9459	9.55	3.99	4.11
V) DEF in C_6H_6 $M_j = 101.15$ gm.	30	1.09770	2.83901	32.44643	0.1002	0.9926	7.47	2.38	3.88
VI) DMF in C_6H_6 $M_j = 73$ gm.	25	1.14117	6.54378	245.94935	0.0743	0.9232	10.88	3.09	3.62
VII) DMA in C_6H_6 $M_j = 87$ gm.	25	1.15138	2.50904	466.67233	0.5696	—	2.66	—	3.37

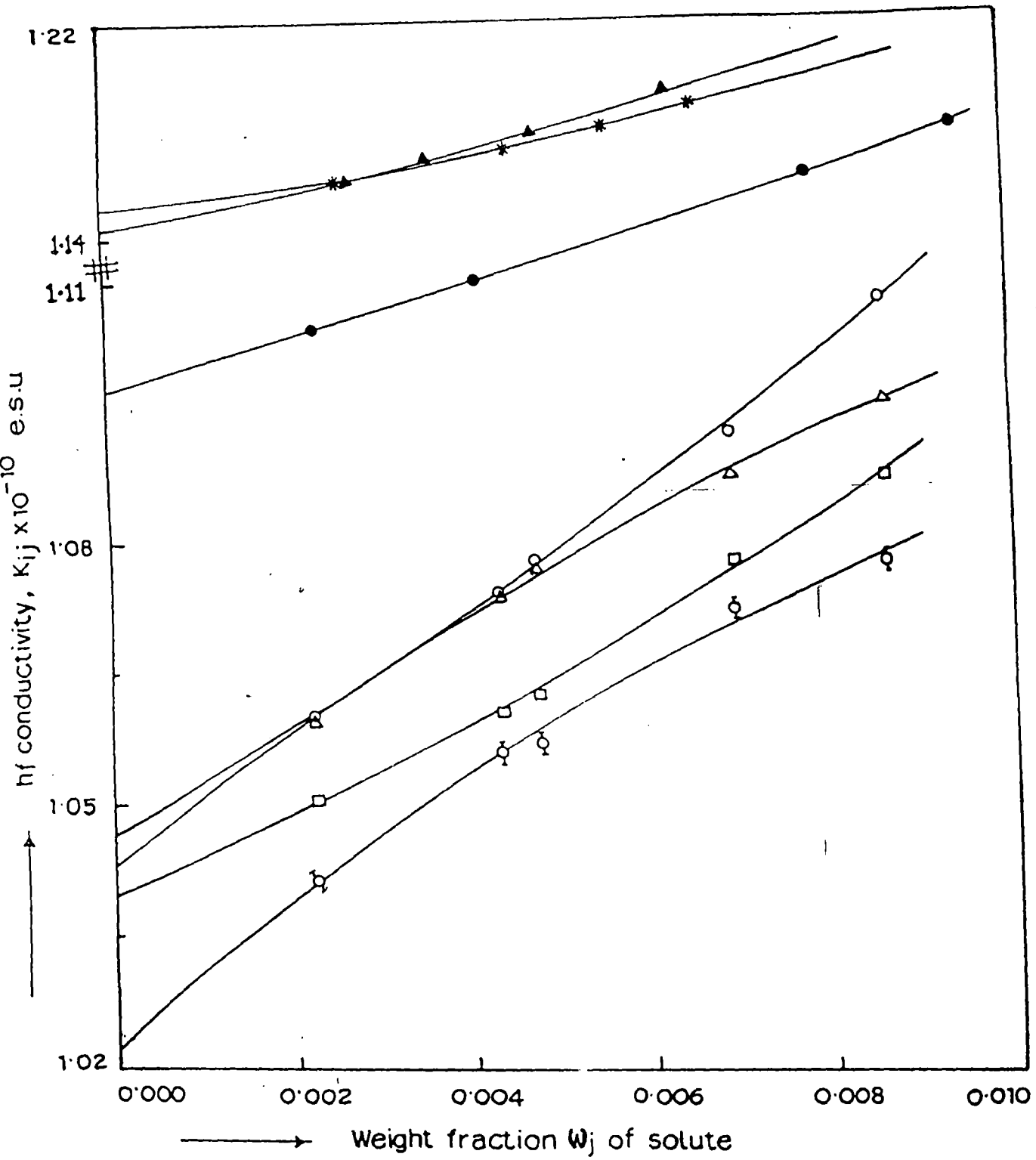

Figure 9.5 Variation of hf conductivity K_{ij} as a function of weight fraction ω_j of polar liquids :

(i) DMSO at 25° C (-O-), (ii) DMSO at 30°C (-Δ-)
(ii) DMSO at 35°C (-□-), (iv) DMSO at 40°C (-◫-)
(iii) DEF at 30°C (-●-), (vi) DMF at 25°C (-▲-)
(vii) DMA at 25°C (-✱-).

a_1 and a_2 of the X_{ij}-ω_j curves with the estimated μ_s are presented in table 9.2. As evident from figure 9.1 and table 9.2 all the curves are found to be of almost same intercepts and slopes for DMSO in C_6H_6 under 9.174 GHz at 25°, 30°, 35° and 40° C respectively. The curves of X_{ij}-ω_j in case of DMF and DMA at 25°C under 9.987 GHz electric field are, however, non-linear in nature probably due to the presence of the substituent group -CH_3 attached to the parent rings under identical environment. But X_{ij} varies with ω_j linearly in case of DEF (figure 9.1) at 30°C under 9.695 GHz electric field. All these curves in figures 9.1 at once suggest that the measured data of table 9.1 are more than accurate.

The variation of $(\varepsilon_{0ij} - \varepsilon'_{ij}) / (\varepsilon'_{ij} - \varepsilon_{\infty ij})$ with $\varepsilon''_{ij} / (\varepsilon'_{ij} - \varepsilon_{\infty ij})$ are found to be linear in figure 9.2 with measured experimental data of table 9.1. The slopes and intercepts of the fitted linear equations for all these aprotic liquids are presented in table 9.3 alongwith their estimated τ_2 and τ_1. The variation of the parameters (figure 9.2) are almost strictly linear for all cases as supported by the correlation coefficient r and % of errors introduced in getting the straight lines of figure 9.2. This indicates the applicability of Debye and Smyth model for such aprotic polar molecules under investigation. The error in fitting technique, is, however, large for DMA indicating the probable uncertainty in the measurements of the dielectric relaxation data of DMA in table 9.1. It is evident from table 9.3 that τ_1's of all the molecules agree well with the reported τ due to Gopalakrishna's method [2-3, 14-15]. It signifies the fact that the hf electric field of GHz frequency is the most dispersive region [6] for these molecules. This also indicates that the probability of rotations of the flexible parts of the molecule is possible as observed earlier[10]. Unlike τ_1's of DMSO; τ_2's are found to increase with temperature. This may be explained on the basis of the fact that τ_1's obey Eyring's rate process of Debye type relaxation. The increase of τ_2 with the rise of temperature is due to elongation in sizes of the entire rotating units under hf electric field. DMA is an exception. It only showed τ_2 because the flexible groups are more rigid in DMA. It is, therefore, expected that N, methyl acetamide (NMA) may show the same effect like DMA. Due to nonavailability of the sample of NMA it was not possible to measure ε_{0ij} and $\varepsilon_{\infty ij}$.

The theoretical values of relative contributions c_1 and c_2 towards dielectric relaxation due to Fröhlich were calculated from x and y of equations (9.18) and (9.19) and presented in table 9.4 together with those found from the graphical plots of $x = (\varepsilon'_{ij} - \varepsilon_{\infty ij}) / (\varepsilon_{0ij} - \varepsilon_{\infty ij})$ and $y = \varepsilon''_{ij} / (\varepsilon_{0ij} - \varepsilon_{\infty ij})$ at $\omega_j \rightarrow 0$ in figures 9.3 and 9.4. The variations of x and y with ω_j's strictly obey the Bergmann's equations (9.11) and (9.12) respectively. As seen from table 9.4 : c_1 and c_2 for Fröhlich's method is + ve almost in all cases. However, c_2 is, - ve for graphical method probably due to the inertia of the flexible parts of the substituent groups of polar molecules[7].

The values of μ_2 and μ_1 in terms of the dimensionless parameters b's involved with τ_2's and τ_1's and slopes β's of $K_{ij} - \omega_j$ curves of figure 9.5 were estimated and placed in table 9.5. The variation of K_{ij} with ω_j are not linear as they are governed by α, β and γ coefficients as seen in table 9.5. It is interesting to note that μ_1 due to flexible part of the molecule agree well with the reported μ_j's of Gopalakrishna's method [2-3, 14-15]. This indicates that a part of the molecule is rotating under hf electric field of nearly 10 GHz as observed earlier [10]. μ_2, on the other hand, are found to be of higher magnitudes for the low values of b_2 in terms of high values of τ_2's according to equations (9.25) and (9.24), respectively. Both μ_2 and μ_1 vary with temperature t in °C for DMSO in C_6H_6 like :

$$\mu_2 = -67.35 + 4.56t - 0.066\ t^2 \qquad \text{.....(9.26)}$$

$$\mu_1 = 8.20 - 0.32\ t + 0.005\ t^2 \qquad \text{.....(9.27)}$$

This may be due to either change in bond moments and bond angles or rupture of solute - solvent (monomer) association with the increase of temperature [16]. The conformational structures of the nonspherical aprotic type polar molecules as mentioned above, are calculated from the reduced bond moment consideration of substituent groups assuming the molecules to be planar as shown in figure 9.6. The theoretical dipole moments μ_{theo}'s were also calculated from the available bond angles and bond moments 2.35 D, 1.55D for $S \leftarrow CH_3$, $O \Leftarrow S$ of DMSO; 0.64 D, 0.78 D, 0.37D of $N \leftarrow CH_3$, $N \leftarrow C_2H_5$, $CH_3 \leftarrow C$ for DMF, DEF and DMA and other common bond moments 0.3 D, 0.45 D, 3.10 D of $C \leftarrow H$, $C \leftarrow N$ and $C \Leftarrow O$ respectively. The μ_{theo}'s are placed in table 9.2 to compare with

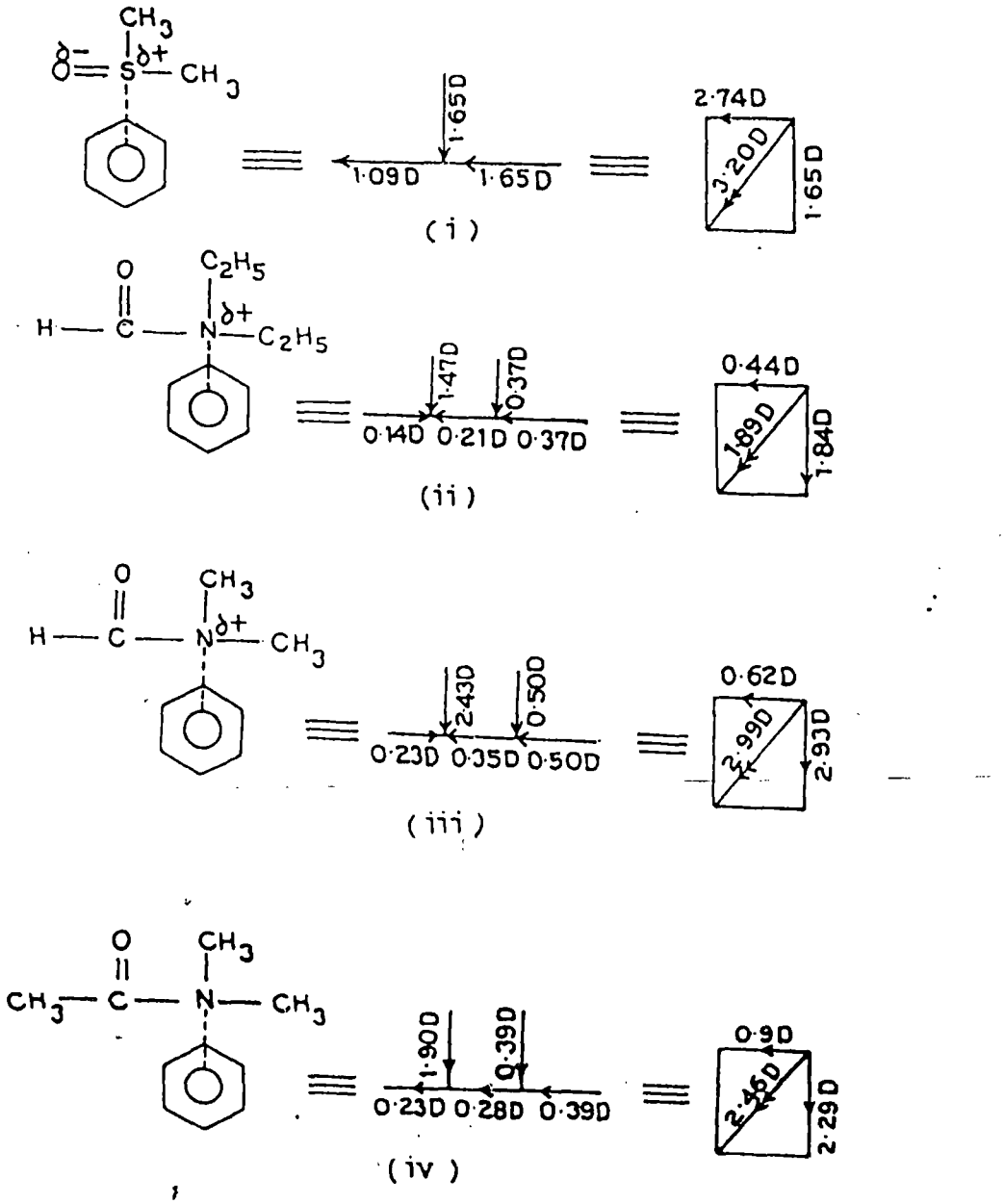

Figure 9.6 Conformational structures of aprotic polar liquids in terms of reduced bond lengths due to mesomeric and inductive moments of the substituent groups consideration:

(i) DMSO in C_6H_6 (ii) DEF in C_6H_6 (iii) DMF in C_6H_6 (iv) DMA in C_6H_6.

μ_s and μ_{cal} from the reduced bond lengths of the substituent groups by the ratio of μ_s/μ_{theo} due to mesomeric and inductive moments.

The energy parameters like enthalpy of activation (ΔH_τ). entropy of activation (ΔS_τ) and free energy of activation (ΔF_τ) are also estimated from Eyring's rate process equations [17] from the measured τ's at four different temperatures of DMSO. They are calculated from the intercepts and slopes of the linear curve ln ($\tau_2 T$) and ln ($\tau_1 T$) with $\frac{1}{T}$.

The equations for DMSO are :

$$\ln(\tau_2 T) = -4.8261 - 4.0905 \times 10^3 \frac{1}{T} \qquad \text{.....(9.28)}$$

$$\ln(\tau_1 T) = -32.1273 + 3.6861 \times 10^3 \frac{1}{T} \qquad \text{.....(9.29)}$$

From the above two equations it seems that unlike rotation of flexible part of the molecule, the rotation of whole molecule does not obey Eyring's rate theory [17]. The values of ΔH_{τ_2}, ΔH_{τ_1} and ΔS_{τ_2}, ΔS_{τ_1} are - 8.13, 7.32 K cal/mole and - 37.62, 16.63 cal/mole/degree respectively. ΔF_{τ_2}'s and ΔF_{τ_1}'s at 25°, 30°, 35° and 40°C are, however, 11.20, 11.39, 11.58, 11.77 and – 4.95, – 5.03,– 5.11, –5.20 Kcal/mole respectively. The data thus obtained indicate that whole molecular rotations under hf electric field is a cooperative process while reverse is true for rotation of the flexible groups.

Thus the present study seems to establish the fact that non-spherical aprotic type polar liquids obey Debye and Smyth model of dielectric relaxation. Moreover, they usually show the double relaxation behaviour under X-band microwave electric field of nearly 10 GHz frequency as predicted elsewhere [6].

References

1. Sharma A K and Sharma D R 1984 J. Phys. Soc. Japan **53** 4771.
2. Dhull J S and Sharma D R 1983 Indian J. Pure Appl. Phys. **21** 694.
3. Sharma A and Sharma D R 1992 J. Phys. Soc. Japan **61** 1049.

4. Sharma A R. Sharma D R and Chauhan M S 1993 Indian J. Pure Appl. Phys. **31** 841.
5. Gopalakrishna K V 1957 Trans. Faraday Soc. **53** 767.
6. Sit S K and Acharyya S 1996 Indian J. Pure Appl. Phys. **34** 255.
7. Saha U, Sit S K, Basak R C and Acharyya S 1994 J. Phys. D : Appl. Phys. **27** 596.
8. Sit S K, Basak R C, Saha U and Acharyya S 1994 J. Phys. D : Appl. Phys. **27** 2194.
9. Palmajumder T 1996 Ph.D Dissertation, Jadavpur University, Calcutta.
10. Basak R C, Sit S K, Nandi N and Acharyya S 1996 Indian J. Phys. **70B** 37.
11. Bergmann K, Roberti D M and Smyth C P 1960 J. Phys. Chem : **64** 665.
12. Fröhlich H 1949 Theory of Dielectrics (Oxford : Oxford University Press) P 94.
13. Smyth C P 1955 Dielectric Behaviour and Structure (New-York : McGraw - Hill).
14. Dhull J S and Sharma D R 1982 J. Phys. D : Appl Phys. **15** 2307.
15. Saksena A R 1978 Indian J. Pure Appl. Phys. **16** 1079.
16. Saha U and Acharyya S 1994 Indian J. Pure Appl. Phys **32** 346.
17. Eyring H, Glasstone S and Laidler K J 1941. The Theory of Rate Process (Mc Graw Hill, New-York).

PART B

CHAPTER 10

DIPOLE MOMENT OF ISOTOPOMER MOLECULE

10.1 Introduction

The estimation of dipole moments of polar molecules either in pure state or for a polar-nonpolar mixture are usually made in terms of measured relaxation data through the standard methods [1,2]. However, there are very few theoretical works and no experimental methods hitherto known for the determination of dipole moment of isotopomer molecular ions like HD^+, HT^+ etc. The accurate values of dipole moments of such ions, on the other hand, are of great importance in the photoinduced dissociation process. Photodissociation is a significant mechanism for destruction of interstellar molecules and the process enables one to make a spectral predictions of ions for astrophysical interest [3]. The simplest heteronuclear molecular ion like HD^+ was studied by Saha [4] and Bunker [5] to obtain dipole moment of such molecule in course of their study of the collision induced dissociation of HD^+ ion by electron impact.

We in this paper developed a method to calculate the dipole moments of molecular ions like HD^+ in the ground state for vibrational level v = 0 using Morse-wave function within the framework of Born-Oppenheimer approximation. The potential for nuclear vibration is assumed to be of Morse-type [6] because of its very simple nature and the isotopomer molecular ions are expected to obey Morse-potential.

10.2 Theoretical Formulation

The electrical dipole moment operator of isotopomer molecular ions like HD^+ can be written as :

$$\begin{aligned}\vec{\rho} &= \sum e_i \vec{r}_i \\ &= -e\vec{r} + e\vec{R}_H + e\vec{R}_D \\ &= -e\vec{r} + e\frac{M_H - M_D}{M_H + M_D}\vec{R}\end{aligned} \qquad \text{.....(10.1)}$$

where $\vec{r}$, $\vec{R}_H$ and $\vec{R}_D$ are the vector distances of the electron, the nuclei H and D respectively from the centre of mass of the ions as shown in the figure (10.1), e., being the magnitude of the charge of a proton or an electron. M_H and M_D are the masses of H and D

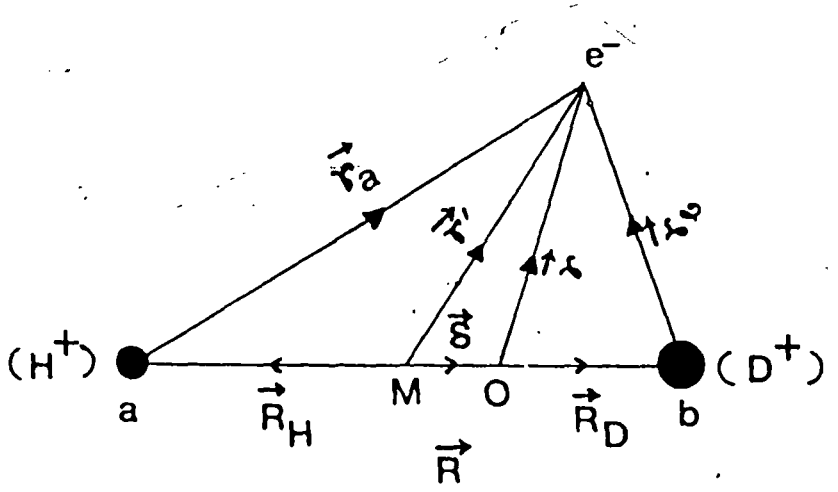

Figure 10.1 Coordinate system describing the position vectors of the electron and the neuclei of HD^+ ion.

respectively. $\vec{R}$ is the intermolecular distance directed from H to D. The dipole moment in the ground state is :

$$\vec{D} = \int \Psi_0^*(\vec{r},\vec{R})\ \vec{\rho}\ \Psi_0(\vec{r},\vec{R})\ d\vec{r}\ d\vec{R} \qquad \text{..... (10.2)}$$

The ground state wave function of molecular ion $\Psi_0(\vec{r},\vec{R})$ can be written according to Born-Oppenheimer approximation as :

$$\psi_0(\vec{r},\vec{R}) = \psi_0(\vec{r},R)\,\xi^{V}_{JM_J}(\vec{R})$$

$$= \Psi_0(\vec{r},R)\,Y_{JM_J}(\theta,\phi)\,\chi_{v}(\vec{R})$$

.....(10.3)

Where ψ and ξ represent the electronic and nuclear parts of the wave function. Y and χ describe the rotation and vibration of the ions respectively.

The equation (10.2) in a.u can now be written as :

$$\vec{D} = -\int \psi_0^*(\vec{r},R)\ \vec{r}\ \psi_0(\vec{r},R)\,\xi^{v*}_{JM_J}(\vec{R})\,\xi^{v}_{JM_J}(R)\,d\vec{r}\,d\vec{R}$$

$$+\frac{M_H - M_D}{M_H + M_D}\int \psi_0^*(\vec{r},R)\,\psi_0(\vec{r},R)\,\xi^{v*}_{JM_J}(\vec{R})\,\vec{R}\,\xi^{v}_{JM_J}(R)\,d\vec{r}\,d\vec{R}$$

.....(10.4)

Now using the definition of electronic centroid we have :

$$\int \psi_0^*(\vec{r'},R)\ \vec{r'}\ \psi_0(\vec{r'},R)\,d\vec{r'} = 0 \qquad \text{.....(10.5)}$$

where $\vec{r} = \vec{r'} - \vec{\delta}$ and $\vec{\delta} = \frac{1}{2}\frac{M_D - M_H}{M_D + M_H}\vec{R}$ .....(10.6)

Thus by using equations (10.4), (10.5) and (10.6) one gets :

$$D = -\frac{1}{2}\frac{M_D - M_H}{M_D + M_H}\int \xi^{v*}_{JM_J}(\vec{R})\ \vec{R}\ \xi^{v}_{JM_J}(\vec{R})\,d\vec{R}$$

$$D = -\frac{1}{2}\frac{MD - M_H}{M_D + M_H}\int \chi^{*}_{V}(R)\,R\,\chi_{V}(R)\,R^2 dR \qquad \text{.....(10.7)}$$

where $\psi_0(\vec{r}', R)$ or $\psi_0(\vec{r}, R)$ and $Y_{JM_J}(\theta,\phi)$ are normalised wave functions.

As the dipole moment is directed opposite to $\vec{R}$ equation (10.7) yields :

$$D = \frac{1}{2}\frac{M_D - M_H}{M_D - M_H}\int_0^\infty \chi_v^*(R)\, R\, \chi_v(R)\, R^2 dR \qquad \text{..... (10.8)}$$

Now, the potential of nuclear vibration for a given electronic state is represented by Morse function [6] as :

$$U(R) = D_e\left[1 - \exp\{-\alpha(R - R_e)\}\right]^2 \qquad \text{.....(10.9)}$$

where R_e = equilibrium distance between the nuclei and α is a constant for a given molecule. The ground state nuclear vibrational wave function $\chi_v(R)$ for level v is given by Fraser and Jarmain as [7], neglecting a phase factor :

$$\chi_v(R) = \left[\frac{\alpha(K - 2v - 1)}{v!\Gamma K - v}\right]^{\frac{1}{2}} \exp\left(\frac{-z}{2}\right) z^{(K-2v-1)/2}$$

$$(-1)^v \sum_{k=0}^{v}(-1)^k \binom{v}{k} \frac{\Gamma K - v}{\Gamma K - v - k} z^{v-k}$$

$$= N_v \exp\left(\frac{-z}{2}\right) z^{(K-2v-1)/2} L_{K-v-1}^{K-2v-1}(z) \qquad \text{.....(10.10)}$$

where $L_{K-v-1}^{K-2v-1}(z)$ is the associated Laguerre polynomial of degree v in Z.

$$Z = K \exp[-\alpha(R - Re)] = \lambda \exp(-\alpha R) \qquad \text{.....(10.11)}$$

The terms K and λ carry usual meanings as mentioned elsewhere [7]. For vibrational level $v = 0$, $\chi_0(R)$ is given by :

$$\chi_0(R) = N_0 \exp\left(\frac{-z}{2}\right) z^{(K-1)/2} \qquad \text{.....(10.12)}$$

Substituting the value of $\chi_0(R)$ in the equation (10.8) yields

$$D = \frac{1}{2}\frac{N_0^2}{\alpha 4}\frac{M_D - M_H}{M_D + M_H}\int_0^\lambda \exp(-z)\, z^{(K-2)}\left(\ln\frac{\lambda}{z}\right)^3 dz \qquad \text{.....(10.13)}$$

According to Ter Haar [8], the upper limit of integration λ [= K exp (αR_e)] is replaced by ∞, since the error introduced is negligible [9]. The equation (10.13) becomes :

$$D = \frac{1}{2}\frac{N_0^2}{\alpha^4}\frac{M_D - M_H}{M_D + M_H}\int_0^\infty \exp(-z)\, z^{(K-2)}\left(\ln\frac{\lambda}{z}\right)^3 dz \qquad .....(10.14)$$

10.3 Results and Discussions

The integral appearing in the equation (10.14) is evaluated using standard integrals [10.] The final expression for the dipole moment of HD^+ molecular ion is given by :

$$D = \frac{1}{2}\frac{M_D - M_H}{M_D + M_H}\frac{1}{\alpha^3}[(\ln\lambda)^3 - 3(\ln\lambda)^2\,\psi(K-1) + 3\ln\lambda\{[\psi(K-1)]^2 + \zeta(2, K-1)\} - \{[\psi(K-1)]^3 + 2\psi(K-1)\zeta(2, K-2) - 2\zeta(3, K-1)\}]$$

..... (10.15)

The functions ψ and ζ are presented elsewhere [10], The values of constants in a.u are given by :

$R_e = 2$, $\alpha = 3.2752$, $K = 277.86$, $\lambda = 194369.72$, $\frac{M_D - M_H}{M_D + M_H} = \frac{1}{3}$ and

$D_e = 2.67$ eV respectively

Hence the value of the dipole moment came out to be D = 1.354 a.u which is found to be slightly larger than 0.34 a.u as calculated by Saha [4]. The result is still reliable and useful in view of the approximate nature of Morse-potential. Moreover, Morse-potential yields accurate values of dissociation energy D_e and vibrational frequency ν_0 of the ions while the Fues vibrator type potential as was used by Saha [4] gives ν_0 only [11]. The Morse-potential and the Fues vibrator type potential differ in the sense that the former supports a few number of bound states while the latter has infinite numbers. But, in practice, there exist only finite number of bound vibrational levels [12]. An attempt is, however, made to calculate D by using Morse-Kratzer potential [13], but the value does not conform to the reported one. Thus it seems to be an established fact that Morse-potential is readily applicable to isotopomer molecular ions like HD^+, HT^+, HeH^+ etc. to get dipole moments from equation(10.15) provided values of constants are known.

References

1. Gopalakrishna K V 1957 Trans. Faraday Soc. **53** 767.
2. Acharyya S and Chatterjee A K 1985 Indian J. Pure Appl. Phys. **23** 484.
3. Saha S, Datta K K and Barua A K 1978 J. Phys. B : Atom. Molec. Phys. **11** 3349
4. Saha S 1974 Indian J. Phys. **48** 849
5. Bunker P R 1974 Chemical Phys. Letter **27** 322
6. Morse P M 1929 Phys. Rev. **34** 57.
7. Fraser P A and Jarmain W R 1953 Proc. Phys. Soc. **A66** 1145
8. Ter Haar D 1946 Phys. Rev. **70** 222
9. Gallas A C 1980 Phys. Rev. **A21** 1829
10. Gradshteyn I S and Ryzhik I M 1965 Tables of Integrals, Series and Product (Academic Press : N.Y.).
11. Kerner E H 1953 Phys. Rev. **91** 1174
12. Moss R E and Sadler I A 1989 Molec. Phys. **68** 1015
13. Singh H N and Singh V B 1993 Indian J. Pure & Appl. Phys. **31** 341

CHAPTER 11

SUMMARY AND CONCLUSION

The subject matter of the thesis works entitled **"High frequency absorptions, double relaxation times, dipole moments and molecular structures of some nonspherical polar and isotopomer molecules"** has been finally summarised chapterwise as presented earlier for convenience.

The **Chapter I** of this thesis entitled **"The general introduction and brief review of the previous works"** deals with the dielectric investigation of pure polar liquids and polar nonpolar liquid mixtures under static as well as high frequency electirc field. This study enables one to realise the shapes, sizes and conformational structures of the nonspherical polar liquids under investigation. A brief survey work has also been added in the latter part of this chapter to observe the usual trend of the investigations in this line.

"The scope and the objective of the present works" in Chapter II contains the beautiful mathematical developments and elaborate discussions on the works. They have been widely used in the latter parts of the thesis. This includes the distribution of relaxation times between two limiting values as was done by Fröhlich (1949). Bergmann et al (1960) and Bhattacharyya *et al* (1970), however, devised different mathematical procedures to get molecular and intramolecular relaxation times τ_2 and τ_1 of pure polar liquids under high frequency electric field of Giga hertz range. The methods proposed by them involved with experimental measurements of dielectric relaxation parameters at different frequencies of the hf electric field. In order to eliminate experimental hazards of measurements at different hf electric field, we (1994) within the framework of Debye and Smyth model, however, developed a technique to get τ_2 and τ_1 of polar liquids in nonpolar solvents from the dielectric relaxation data measured under a single frequency electirc field at a given temperature. The procedure is concerned with a derived straight line equation having certain intercept and slope to get τ_2 and τ_1 respectively. The dipole moments μ_1 and μ_2 could however, be estimated in terms of τ_1 of the flexible part attached to the parent molecule and τ_2 of the whole molecule itself together with slope β of the hf conductivity K_{ij} against ω_j curve of polar liquids at infinite dilution. The procedure is really very simple because the microwave conductivity is applicable to polar - nonpolar liquid mixture. Due to existence of distribution of relaxation times, polar molecules may possess either

symmetric or asymmetric distributions. They have been found out by using graphical technique for a polar - nonpolar liquid mixture. An experiment is performed to show whether aprotc polar liquids exhibit either double or monorelaxation behaviour using the theory mentioned above. In the last part of **Chapter II (Part B)** an approximate formulation is suggested to obtain dipole moment of isotopomer molecular ion like HD^+ using Morse - wave function because of the applicability of Morse - potential for nuclear vibration of such molecule.

The double relaxation times τ_2 and τ_1 of some highly nonspherical disubstituted benzene and aniline molecules in solvent benzene and carbon tetrachloride have been obtained from the single frequency measurements of the dielectric relaxation solution data under hf electric field at a given temperature. The weighted contributions c_1 and c_2 due to τ_1 and τ_2 are calculated from Fröhlich's equation as well as by new technique adopted here. The dipole moments μ_1 and μ_2 are computed from the slope β of ultra high frequency conductivity K_{ij} against the weight fraction ω_j of the respective solutes, in terms of estimated τ_1 and τ_2. The conformational structures of polar molecules are obtained from the available bond moments and bond angles of molecules assuming the molecules to be planar. Again, the close agreement of μ_2 values from single frequency measurement technique with the existing methods immediately indicates that the approach suggested is a correct one. This has been presented in **Chapter III** under the heading **"Double relaxation times of nonspherical polar liquids in nonpolar solvent : A new approach based on single frequency measurement".**

The **Chapter IV**, entitled **"Single frequency measurement of double relaxation times of monosubstituted anilines in benzene"**, however, reports the double relaxation times τ_2 (larger) and τ_1 (smaller) of some monosubstituted anilines in benzene at 35°C for 2.02, 3.86 and 22.06 GHz electric fields respectively from the single frequency measurement of dielectric relaxation parameters at different concentrations. The o- and m-anisidines like p-toluidines exhibit double relaxation phenomena at 3.86 and 22.06 GHz whereas o-and m-toluidines show the same effect at 2.02 and 3.86 GHz respectively. Only p-anisidine, however, shows the monorelaxation behaviour at all frequencies. The relative

contributions c_1 and c_2 towards dielectric relaxation for τ_1 and τ_2 are computed from Fröhlich's equations only for comparison with those of the graphical techniques. The dipole moments μ_1 and μ_2 in terms of τ_1 and τ_2 are then determined from the slope β of K_{ij} - ω_j curve for these compounds to establish their conformations.

"Double relaxations of monosubstituted anilines in benzene under effective dispersive region" in the **Chapter V** deals with the mono or disubstituted anilines in benzene at 35°C under 9.945 GHz electric field to show some interesting property by those liquids from single frequency measurement technique. The mono or disubstituted benzenes and anilines are thought to absorb energy much more strongly in the effective dispersive region of nearly 10 GHz electric field. The dielectric relaxation data of the monosubstituted anilines measured at different frequencies (Sit et al 1994) showed either double or monorelaxation behaviour. When the same data are extended to 9.945 GHz ($\cong$ 3 cm. wavelength) electric field, each of them, on the other hand ; exhibits the double relaxation phenomenon by showing the reasonable relaxation times τ_1 (smaller) and τ_2 (larger) for the flexible part as well as the whole molecule itself for their rotations in hf electric field. τ_1 and τ_2 are, however, obtained from the slopes and intercepts of a derived equation involved with dielectric relaxation data for different weight fractions ω_j's measured under a single frequency electric field. The relative contributions c_1 and c_2 in terms of τ_1 and τ_2 towards relaxation are calculated from Fröhlich equations and the graphical technique. The values of symmetric and asymmetric distribution parameter γ and δ are also calculated to test the rigidity of the molecules under investigation. The dipole moments μ_1 and μ_2 in terms of τ_1 and τ_2 are finally estimated from the slope β of hf conductivity K_{ij} as a function of ω_j's in order to support their conformations.

The **Chapter VI** of **"Double relaxation of straight chain alcohols under high frequency electric field"** is concerned with some interesting property of a few normal alcohols under different hf electric fields at a given temperature. Alcohols like 1-butanol, 1-hexanol, 1-heptanol and 1-decanol are long straight chain polar molecules almost like polymers. In these alcohols as well as in methanol and ethanol there exist many possibilities of having internal rotations, bending and twisting each with a characteristic

relaxation time under high frequency electric field. An attempt is, therefore, made to detect the double relaxation phenomena by the new approach suggested earlier. It involves single frequency measurements of the dielectric relaxation data of those compounds in solvent n-heptane at 25°C under three different frequencies of 24.33, 9.25 and 3.00 GHz electric field as well as those of methanol and ethanol in benzene at 9.84 GHz, respectively to get τ_1 and τ_2 of their flexible part and the whole molecules. The alcohols under investigation, always exhibit the double relaxation behaviours at all frequencies except methanol at 9.84 GHz, indicating separate broad dispersions in them. The relative contributions c_1 and c_2 towards dielectric relaxations due to τ_1 and τ_2 are calculated from Fröhlich's equations to compare with those as obtained by graphical method. The dipole moments μ's are also estimated in terms of the relaxation times τ_1 and τ_2, obtained from the slopes and intercepts of straight line equation and in terms of slopes β's of the hf conductivities K_{ij}'s of the solutions against the weight fraction ω_j's of the solutes in order to support their usual conformations.

Some isomeric octyl alcohols in n-heptane at 25°C under the electric field frequencies of 24.33, 9.25 and 3.00 GHz as straight chain alcohols are also studied to detect the double relaxation times τ_1 and τ_2 for their flexible parts and whole molecules by the single frequency measurement of dielectric relaxation parameters. This has been given in **Chapter VII** of **"Double relaxations of some isomeric octyl alcohols by high frequency absorption in nonpolar solvent"** of this thesis. The isomers of alcohols are long chain, hydrogen bonded, polymer type molecules having methyl and hydroxyl groups attached to their C-atoms which may bend, twist or rotate internally under hf electric field each with a characteristic relaxation time. The relative contributions c_1 and c_2 towards dielectric relaxations due to τ_1 and τ_2 are also estimated by using Fröhlich's equations and the graphical technique. The dipole moments μ_1 and μ_2 in terms of τ_1 and τ_2 are again found out from the slope β of the total hf conductivity K_{ij} as a function of weight fractions ω_j's of the solutes indicating μ_1 for the rotation of -OH groups about - C - O bonds only. μ_1 and μ_2 are finally compared with the theoretical dipole moments μ_{theo}'s arising out of

their structures with bond angles and bond moments of their substituent groups to establish their conformations which are justified like normal alcohols as observed earlier.

The **Chapter VIII** under the title of "**Structural and associational aspects of binary and single polar liquids in nonpolar solvents under high frequency electric field**" deals with the structural and associational aspects of binary (jk) polar mixtures of N, N - dimethyl formamide (DMF) and dimethyl sulphoxide (DMSO) together with a single (j or k) N, N-diethyl formamide (DEF) and DMSO in nonpolar solvents (i). They, however, studied in terms of their high frequency (hf) conductivities. The relaxation times τ's and dipole moments μ's of respective solutes under hf electric field of Giga hertz range at various temperatures are estimated from the measured real and imaginary parts of hf complex dielectric constants at different weight fractions of polar solutes. The variation of τ_{jk}'s with mole fractions x_k's of DMSO in DMF and C_6H_6 reveals the probable solute - solute molecular associations around $x_k = 0.5$ of DMSO in DMF. The solute - solvent molecular association i.e the rupture of dimers begins at and around 50 mole % of DMSO in DMF and continues up to 100 mole % DMSO. The concentration and temperature variation of τ_{jk} of these aprotic liquids are in accord with the information of variation of τ_{jk} of jk polar mixtures with x_k's of DMSO. Thermodynamic energy parameters are also obtained from Eyring's rate process equation with the estimated τ's to support the molecular associations. The slight disagreement between the theoretical dipole moment μ_{theo} from the bond angles and bond moments is noticed with the measured τ's in terms of slopes of concentration variation of hf conductivity curves at infinite dilutions and τ's. This indicates the temperature dependence of mesomeric and inductive moments of different substituent groups in such polar molecules.

An experiment is, therefore, made to measure the dielectric relaxation parameters like real ε'_{ij} ., imaginary ε''_{ij} parts of complex dielectric constant ε^*_{ij}, static dielectric constant ε_{0ij} and dielectric constant at infinite frequency $\varepsilon_{\infty ij}$ ($= n^2_{Dij}$) of some aprotic polar liquids (j) dissolved in benzene (i) at different temperatures under nearly 10 GHz electric field as a function of weight fraction ω_j of polar solutes. The aprotic liquids like dimethyl sulphoxide (DMSO), N,N-diethyl formamide (DEF), N, N-dimethyl formamide (DMF)

and N. N-dimethyl acetamide (DMA) are chosen because of their wide biological applications and importance in medicine and industry. The measured data at nearly 10 GHz are seen to predict the double relaxation times τ_1 and τ_2, except DMA, due to rotations of their flexible parts and the whole molecules by the method of single frequency measurement. τ_1 agrees well with the reported τ signifying the fact that under hf electric field of 10 GHz a part of the molecule is rotating. The relative weighted contributions c_1 and c_2 towards dielectric relaxations due to τ_1 and τ_2 are also ascertained from Fröhlich's equations and graphical technique. The corresponding dipole moments μ_2 and μ_1 in terms of τ_2 and τ_1 and slope β of hf conductivity K_{ij} against ω_j at $\omega_j \to 0$ are compared with reported μ_j. μ_1's, however, agree well with μ_j's and static μ_s. The molecular conformational structures are obtained by μ_{cal} from μ_s and μ_{theo} from available bond angles and bond moments by considering mesomeric and inductive moments of the substituent groups. The comparison of μ_1, μ_2 and μ_j with μ_s shows that μ's are very little affected by hf electric field. The energy parameters like enthalpy of activation ΔH_τ, entropy of activation ΔS_τ and activation energy ΔF_τ from ln (τT) against $\frac{1}{T}$ equations of DMSO seem to establish that unlike the rotation of the whole molecule, the flexible part satisfies the Eyring rate theory. These observations have been included in the **IXth Chapter** of the thesis. entitled **"Double relaxation times, dipole moments and molecular structures of some nonspherical aprotic polar liquids in benzene from high frequency absorption measurement "**.

Part B of the thesis containing the single **Chapter** X under the heading **"Dipole moment of isotopomer molecule"** deals with an approximate formulation to calculate the dipole moments of isotopomer molecular ions like HD^+, HT^+ etc. in the ground state for the vibrational quantum number v = 0 using Morse wave function because of the applicability of Morse potential for nuclear vibration of such molecular ions. It also provides one with the finite number of bound vibrational level as seen in practice. The computed value is a little larger than the literature one probably due to the approximate nature of the potential used, although it gives accurate dissociation energy D_e and

vibrational frequency ν_0 of ionic moleculess unlike Fues vibrator type potential yielding ν_0 only.

The summary and a concluding remark at the end of all the chapters of this thesis is presented in the **Chapter XI**.

Thus, the first part of the thesis (i.e Part A) contains beautiful, systematically developed theoretical formulations to estimate the double relaxation times τ_1 and τ_2 of polar solutes dissolved in nonpolar solvents from the measured dielectric relaxation parameters at a given temperature under a high frequency (microwave) electric field as a function of weight fractions of polar solutes. The theories are tested for a large number of nonspherical or chain like polar molecules of different shapes and sizes presented in Chapters III to IX. They reveal interesting information on their structures in terms of estimated τ's and μ's from hf absorption studies of solution data. So, it can be concluded that the study of nonspherical type polar liquids in nonpolar solvents has opened a new and vast scope for the future works. The different models of Onsager, Kirkwood, Fröhlich etc may be expected to be the better choice for the polymer type long chain polar liquids or liquid crystals in nonpolar solvents like benzene, dioxane, carbon tetrachloride, n-heptane, paraxylene etc. in addition to Debye - Smyth model which is supposed to be successful in predicting dielectric relaxations of nearly spherical type of polar liquids of simpler configurations.

The Part B of the thesis presents a quantum mechanical approach to suggest an approximate formulation of dipole moment of isotopomer molecular ions like HD^+, HT^+ etc. for $v = 0$ vibrational level assuming Morse - potential for nuclear vibration of such molecules. The technique is very simple and staightforward. This may be extended to $v = 1$ and $v = 2$ vibration levels too. Further, dipole moment calculation may be made assuming rotation - vibration wave function of molecular ions.

LIST OF PUBLISHED AND COMMUNICATED PAPERS

The subject matter of this thesis has been published in different Indian and foreign journals of international repute

1) **"Double relaxation times of nonspherical polar liquids in nonpolar solvent: A new approach based on single frequency measurement"** U Saha, **S K Sit**, R C Basak and S Acharyya; J. Phys D: Appl. Phys. (London) **27** (1994) 596-603.

2) **"Single frequency measurement of double relaxation times of monosubstituted anilines in benzene" S K Sit**, R C Basak, U Saha and S Acharyya; J. Phys D: Appl. Phys. (London) **27** (1994) 2194-2202.

3) **"Double relaxations of monosubstituted anilines in benzene under effective dispersive region" S K Sit** and S Acharyya; Indian J. Pure & Appl. Phys **34** (1996) 255-262.

4) **"Double relaxation of straight chain alcohols under high frequency electric field"** **S K Sit** and S Acharyya; Indian J. Phys **70B** (1996) 19-36.

5) **"Double relaxation of some isomeric octyl alcohols by high frequency absorption in nonpolar solvent" S K Sit,** N Ghosh and S Acharyya; Indian J. Pure & Appl. Phys. **35** (1997) press.

6) **"Structural and associational aspects of binary and single polar liquids in nonpolar solvent under high frequency electric field" S K Sit**, N Ghosh, U Saha and S Acharyya; Indian J. Phys **71B** (1997) to be published in August issue of the Journal.

7) **"Double relaxation times, dipole moments and molecular structures of some non-spherical aprotic polar liquids in benzene from high frequency absorption measurement" S K Sit**, S Acharyya, T Palmajumder and S Roy; J Phys. D: Appl. Phys (London) 1997 Communicated.

8) **"Dipole moment of isotopomer molecule" S K Sit** and S Acharyya; J Phys B: Atom. Mole. Phys (London) 1997 communicated.

J. Phys. D: Appl. Phys. 27 (1994) 596–603. Printed in the UK

Double relaxation times of non-spherical polar liquids in non-polar solvent: a new approach based on single frequency measurement

U Saha, S K Sit, R C Basak and S Acharyya

Department of Physics, University College, PO Raiganj, Uttar Dinajpur (WB), 733 134 India

Received 7 April 1993, in final form 16 August 1993

Abstract. A new approach based on single frequency measurement is suggested to estimate the double relaxation times, τ_1 and τ_2 of some highly non-spherical polar liquids in solvents benzene and carbon tetrachloride. The smaller relaxation time τ_1 refers to the smallest flexible part attached to the parent molecule while the larger one τ_2 is due to end-over-end rotation of the polar molecule. The weighted contributions c_1 and c_2 towards relaxations are calculated from Fröhlich's equations as well as by a new technique adopted here. The dipole moments μ_1 and μ_2 are also computed from the slope β of the ultra-high-frequency conductivity K_{ij} against the weight fraction ω_j for the compounds in terms of τ_1 and τ_2. The close agreement of μ_2 values thus computed with those of existing methods immediately indicates that the approach suggested is correct.

1. Introduction

The dielectric relaxation of polar liquids in non-polar solvents is much simpler in comparison to the case in pure polar liquids because, in dilute polar liquid solutions, the effects of the macroscopic viscosity, dipole–dipole interaction, internal field etc. are minimized. The dielectric relaxation parameters, namely the relaxation times τ_1 and τ_2, the dipole moments μ_1 and μ_2 etc. are the effective tools to investigate the molecular and intramolecular rotations, sizes, shapes and structures of polar molecules. Careful investigation of the phenomenon of dielectric relaxation in binary (Acharyya and Chatterjee 1985) and ternary (Chatterjee *et al* 1992, Saha and Acharyya 1993) solute–solvent mixtures is therefore necessary to throw much light on the structures of the polar liquids.

Khameshara and Sisodia (1980), Gupta *et al* (1978) and Arrawatia *et al* (1977) measured the static dielectric constant ε_{0ij}, the square of the refractive indices n^2_{Dij}, the real ε'_{ij} and imaginary ε''_{ij} parts of the complex dielectric constant ε^*_{ij} of five and seven disubstituted anilines and benzenes respectively in solvents benzene and carbon tetrachloride at 35 °C under a single high-frequency 9.945 GHz electric field. Aniline as well as benzene derivatives are expected to absorb very strongly in the microwave electric field due to the presence of their flexible parts such as methyl or other groups. They are, therefore, expected to have more than one relaxation time because of the existence of internal rotation of these groups. Although one should not make strong conclusions based on single frequency measurements, provided that the experimental values of ε_{0ij} and $\varepsilon_{\infty ij}$ are not accurately known. Non-spherical molecular liquids on the other hand, are known to have non-Debye relaxation behaviour.

The existing method of Bergmann *et al* (1960) was involved in measurements of ε'_{ij}, ε''_{ij}, $\varepsilon_{\infty ij}$ and ε_{0ij} of a non-spherical polar liquid (j) in solvent (i) for various frequencies at a given experimental temperature in degrees Celsius to yield τ_1 and τ_2. They actually used the Cole–Cole plot to make τ_1 and τ_2 represent the relaxation times of the smallest flexible unit attached to the parent ring and the molecule itself. Kastha *et al* (1969) subsequently simplified the procedure of Bergmann *et al* (1960) by measuring the experimental parameters at two given frequencies of the electric field in the microwave region.

We, in this context, therefore thought to suggest an alternative method in which single frequency measurements of dielectric relaxation parameters like ε'_{ij}, ε''_{ij}, ε_{0ij} and $\varepsilon_{\infty ij}$ (Khameshara and Sisodia 1980, Gupta *et al* 1978 and Arrawatia *et al* 1977) for some highly non-spherical polar liquids like anilines and

0022-3727/94/030596+08$19.50

Table 1. The double relaxation times τ_1 (smaller) and τ_2 (larger) estimated from intercepts and slopes of equation (7) with errors and correlation coefficients together with reported τ of polar liquids.

System with slope number and molecular weight M_j (g)	Intercept and slope of equation (7)		Correlation coefficient	Percentage error in regression technique	Estimated values of τ_1 and τ_2 (ps)		Reported τ (ps)
(i) 4-chloro-2-methyl aniline in benzene $M_j = 141.52$	−1.4276	3.2169	0.9964	1.33	8.51	42.97	18.5
(ii) 3-chloro-4-methyl aniline in benzene $M_j = 141.52$	−0.5605	1.8913	0.9982	0.76	5.89	24.38	13.6
(iii) 5-chloro-2-methyl aniline in benzene $M_j = 141.52$	−0.8107	2.0749	0.9727	3.67	8.36	24.85	16.6
(iv) 3-chloro-2-methyl aniline in benzene $M_j = 141.52$	−0.3862	1.5960	0.9918	1.09	4.76	20.78	9.9
(v) 2-chloro-6-methyl aniline in benzene $M_j = 141.52$	−0.3132	1.3711	0.9250	2.77	4.63	17.31	7.8
(vi) *o*-chloronitrobenzene in benzene $M_j = 157.5$	−0.3033	1.3129	0.8170	3.77	4.79	16.22	13.5
(vii) 4-chloro-3-nitrotoluene in benzene $M_j = 171.5$	−0.3863	1.8623	0.8776	11.90	3.81	25.99	20.9
(viii) *m*-nitrobenzo-trifluoride in benzene $M_j = 191.0$	−0.6003	1.9038	0.9929	2.44	6.38	24.09	19.7
(ix) 4-chloro-3-nitro-benzotrifluoride in carbon tetrachloride $M_j = 225.5$	−0.0587	1.6634	0.9524	5.33	0.58	26.04	21.1
(x) *o*-nitrobenzotrifluoride in benzene $M_j = 191.039$	−0.0620	1.0560	0.6992	4.17	0.99	15.90	13.7
(xi) 4-chloro-3-nitrotoluene in carbon tetrachloride $M_j = 171.5$	−0.1335	2.2819	0.9771	7.51	0.96	35.56	35.0
(xii) 4-chloro-3-nitro-benzotrifluoride in benzene $M_j = 225.5$	2.5194	−3.0302	−0.8599	13.07	—	10.87	10.2
(xiii) m-aminobenzo-trifluoride in benzene $M_j = 161.05$	0.8445	0.0452	0.0088	11.38	—	15.07	14.5
(xiv) *o*-chloronitro-benzene in carbon tetrachloride $M_j = 157.5$	0.0194	1.2973	0.9277	5.57	—	21.00	15.8
(xv) o-chlorobenzo-trifluoride in benzene $M_j = 180.5$	0.2856	0.5696	0.1405	19.10	—	14.25	12.3

benzene derivatives in solvents benzene and carbon tetrachloride respectively are enough to estimate τ_1 and τ_2 within the framework of the Debye model (Bergmann *et al* 1960). The systems of polar–non-polar liquid mixtures under investigation are placed in the first columns of tables 1–3. Moreover, such rigorous studies on various types of di- or even mono-substituted polar compounds in non-polar solvents could be made in order to detect the existence of double relaxation phenomena from available data measured under a single-frequency electric field in the gigahertz region. Finally, τ_1 and τ_2 thus estimated (table 1) from our method on the basis of single frequency measurement, which appears to be much simpler, can be used to obtain μ_1 and μ_2 (see table 3 later) of the polar molecules from the slope β of the concentration variation of ultra-high-frequency conductivity K_{ij} of the solution (see figure 4 and table 3 later) in order to explore their conformations (see figure 5 later).

2. Theoretical formulations to estimate τ_1, τ_2 and c_1 and c_2

The relative contributions c_1 and c_2 towards the dielectric relaxation by the two extreme values τ_1 and τ_2 (Higasi *et al* 1960) can be given by (Bergmann *et al* 1960)

$$\frac{\varepsilon'_{ij}-\varepsilon_{\infty ij}}{\varepsilon_{0ij}-\varepsilon_{\infty ij}} = c_1\frac{1}{1+\omega^2\tau_1^2} + c_2\frac{1}{1+\omega^2\tau_2^2} \qquad (1)$$

$$\frac{\varepsilon''_{ij}}{\varepsilon_{0ij}-\varepsilon_{\infty ij}} = c_1\frac{\omega\tau_1}{1+\omega^2\tau_1^2} + c_2\frac{\omega\tau_2}{1+\omega^2\tau_2^2} \qquad (2)$$

provided that $c_1 + c_2 = 1$. The symbols used in equations (1) and (2) have their usual meanings. Let

$$x = \frac{\varepsilon'_{ij}-\varepsilon_{\infty ij}}{\varepsilon_{0ij}-\varepsilon_{\infty ij}} \qquad y = \frac{\varepsilon''_{ij}}{\varepsilon_{0ij}-\varepsilon_{\infty ij}}$$

and $\omega\tau = \alpha$. Equations (1) and (2) can be written as

$$x = c_1a_1 + c_2a_2 \qquad (3)$$

$$y = c_1b_1 + c_2b_2 \qquad (4)$$

where $a = 1/(1+\alpha^2)$ and $b = \alpha/(1+\alpha^2)$. The suffixes 1 and 2 are related to τ_1 and τ_2 respectively. Solving equations (3) and (4) for c_1 and c_2, one gets

$$c_1 = \frac{(x\alpha_2 - y)(1+\alpha_1^2)}{\alpha_2-\alpha_1} \qquad (5)$$

$$c_2 = \frac{(y - x\alpha_1)(1+\alpha_2^2)}{\alpha_2-\alpha_1} \qquad (6)$$

provided that $\alpha_2 > \alpha_1$. Now adding equations (5) and (6) we get, since $c_1 + c_2 = 1$,

$$\frac{1-x}{y} = (\alpha_1+\alpha_2) - \frac{x}{y}\alpha_1\alpha_2$$

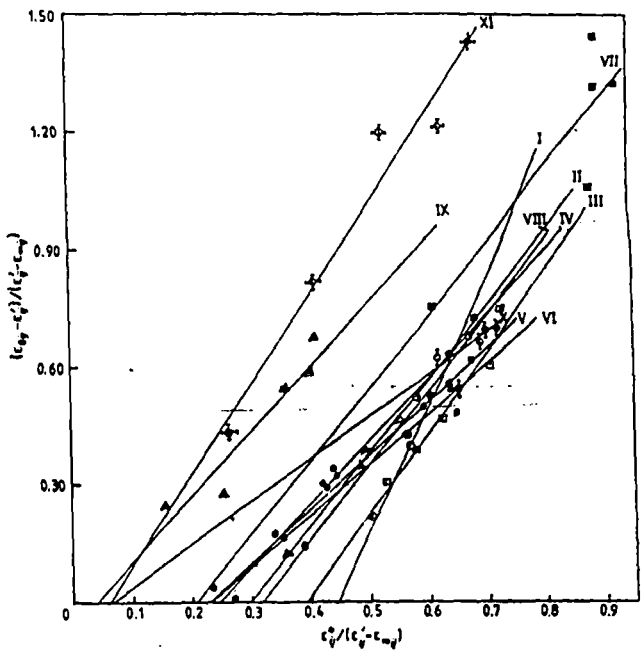

Figure 1. Straight line plots of $(\varepsilon_{0ij}-\varepsilon'_{ij})/(\varepsilon'_{ij}-\varepsilon_{\infty ij})$ against $\varepsilon''_{ij}/(\varepsilon'_{ij}-\varepsilon_{\infty ij})$ for the polar–non-polar liquid mixtures: (I), (II), (III), (IV), (V), of disubstituted anilines, (VI), (VII), (VIII), (IX), (X) and (XI) of disubstituted benzenes respectively at 35 °C (table 1).

or

$$\frac{\varepsilon_{0ij}-\varepsilon'_{ij}}{\varepsilon'_{ij}-\varepsilon_{\infty ij}} = \omega(\tau_1+\tau_2)\frac{\varepsilon''_{ij}}{\varepsilon'_{ij}-\varepsilon_{\infty ij}} - \omega^2\tau_1\tau_2 \qquad (7)$$

which is simply a straight line between $(\varepsilon_{0ij}-\varepsilon'_{ij})/(\varepsilon'_{ij}-\varepsilon_{\infty ij})$ and $\varepsilon''_{ij}/(\varepsilon'_{ij}-\varepsilon_{\infty ij})$ having intercept $-\omega^2\tau_1\tau_2$ and slope $\omega(\tau_1+\tau_2)$ where $\omega = 2\pi f$, f being the frequency of the applied electric field in the gigahertz region. When equation (7) is fitted to the experimental data ε'_{ij}, ε''_{ij}, ε_{0ij} and $\varepsilon_{\infty ij}$ for different concentrations ω_j of each of the polar molecules at 35 °C, we get the intercept and slope and the corresponding values of τ_1 and τ_2 found as shown in table 1 together with the reported τ. The error as well as correlation coefficient were also found for each curve of equation (7) and placed in table 1, only to see how far they are linear as shown in figure 1.

The Fröhlich parameters A, where $A = \ln(\tau_2/\tau_1)$ shown in table 2 for all the polar compounds, are used to evaluate both x and y of equations (3) and (4) in terms of ω and small limiting relaxation time τ_s, where $\tau_s = \tau_1$ by the following equations (Fröhlich 1949):

$$\frac{\varepsilon'_{ij}-\varepsilon_{\infty ij}}{\varepsilon_{0ij}-\varepsilon_{\infty ij}} = 1 - \frac{1}{2A}\ln\left(\frac{1+e^{2A}\omega^2\tau_s^2}{1+\omega^2\tau_s^2}\right) \qquad (8)$$

$$\frac{\varepsilon''_{ij}}{\varepsilon_{0ij}-\varepsilon_{\infty ij}} = \frac{1}{A}[\tan^{-1}(e^A\omega\tau_s) - \tan^{-1}(\omega\tau_s)]. \qquad (9)$$

The computed values of x and y from the above equations and the corresponding c_1 and c_2 from equations (1) and (2) are presented in table 2. Again the left-hand sides of equations (1) and (2) are obviously

Table 2. Reported Fröhlich parameter A, relative contributions c_1 and c_2 towards dielectric relaxations with estimated values x and y due to Fröhlich equations (8) and (9) and those by our method.

System with slope number and molecular weight M_j (g)	Fröhlich parameter $A = \ln(\tau_2/\tau_1)$	Theoretical values of x and y using equations (8) and (9)		Theoretical values of c_1 and c_2		Estimated values of $x = \left(\frac{\varepsilon'-\varepsilon_\infty}{\varepsilon_0-\varepsilon_\infty}\right)_{\omega j\to 0}$ $y = \left(\frac{\varepsilon''}{\varepsilon_0-\varepsilon_\infty}\right)_{\omega j\to 0}$		Estimated values of c_1 and c_2	
(i) 4-chloro-2-methyl aniline in benzene $M_j = 141.52$	1.6193	0.4269	0.4478	0.4159	0.8418	1.14	0.4455	1.5577	−0.6112
(ii) 3-chloro-4-methyl aniline in benzene $M_j = 141.52$	1.4205	0.8448	0.4483	0.8239	0.3953	1.32	0.2745	1.7061	−0.6065
(iii) 5-chloro-2-methyl aniline in benzene $M_j = 141.52$	1.0894	0.5478	0.4745	0.4642	0.6239	1.08	0.3758	1.6069	−0.6227
(iv) 3-chloro-2-methyl aniline in benzene $M_j = 141.52$	1.4737	0.6937	0.4241	0.5180	0.5845	0.99	0.2385	1.1382	−0.1497
(v) 2-chloro-6-methyl aniline in benzene $M_j = 141.52$	1.3187	0.7369	0.4114	0.5272	0.5430	1.17	0.1440	1.5339	−0.5334
(vi) *o*-chloro nitrobenzene in benzene $M_j = 157.5$	1.2197	0.7456	0.4107	0.5259	0.5326	0.82	0.3803	0.6874	0.3832
(vii) 4-chloro-3-nitrotoluene in benzene $M_j = 171.5$	1.9201	0.6783	0.4086	0.5282	0.6486	0.64	0.3173	0.5504	0.4328
(viii) *m*-nitrobenzotrifluoride in benzene $M_j = 191.0$	1.3286	0.6103	0.4551	0.4852	0.6252	0.97	0.3128	1.2013	−0.2176
(ix) 4-chloro-3-nitrobenzo-trifluoride in carbon tetrachloride $M_j = 225.5$	3.8044	0.8302	0.2583	0.6876	0.5231	0.91	0.1012	0.8682	0.1565
(x) *o*-nitrobenzotrifluoride in benzene $M_j = 191.039$	2.7764	0.8771	0.2592	0.6595	0.4371	0.67	0.3487	0.3413	0.6554
(xi) 4-chloro-3-nitrotoluene in carbontetrachloride $M_j = 171.5$	3.6120	0.7540	0.3010	0.6379	0.7022	0.88	0.1642	0.8314	0.3061

the functions of ω_j of the solute in a given solvent, as is evident from the plots of x and y against ω_j in figures 2 and 3 respectively. This at once prompted us to get the fixed values of x and y when $\omega_j \to 0$ from figures 2 and 3 to estimate c_1 and c_2, which are shown in table 2 for comparison with those of Fröhlich (1949). This is really in conformity with the fixed estimated values of τ_1 and τ_2 from the slope and intercept of equation (7) for each compound when substituted on the right-hand sides of equations (1) and (2).

3. Mathematical formulations to estimate μ_1 and μ_2

According to Murphy and Morgan (1939) the ultra-high-frequency (UHF) conductivity K_{ij} as given by

$$K_{ij} = \frac{\omega}{4\pi}(\varepsilon_{ij}''^2 + \varepsilon_{ij}'^2)^{1/2} \tag{10}$$

is a function of ω_j of a polar solute. Even in the high-frequency (HF) electric field $\varepsilon_{ij}'' \ll \varepsilon_{ij}'$, ε_{ij}'' is responsible for offering resistance to polarization. Hence the real part K_{ij}' of the HF conductivity of a polar–non-polar liquid mixture at a given temperature T K is given by (Smyth 1955)

$$K_{ij}' = \frac{\mu_j^2 N \rho_{ij} F_{ij}}{3M_j kT}\left(\frac{\omega^2\tau}{1+\omega^2\tau^2}\right)\omega_j \tag{11}$$

where M_j is the molecular weight of a polar solute, N is Avogadro's number, k is the Boltzmann constant and $F_{ij}(= [(\varepsilon_{ij}+2)/3]^2)$ is the local field. The total HF

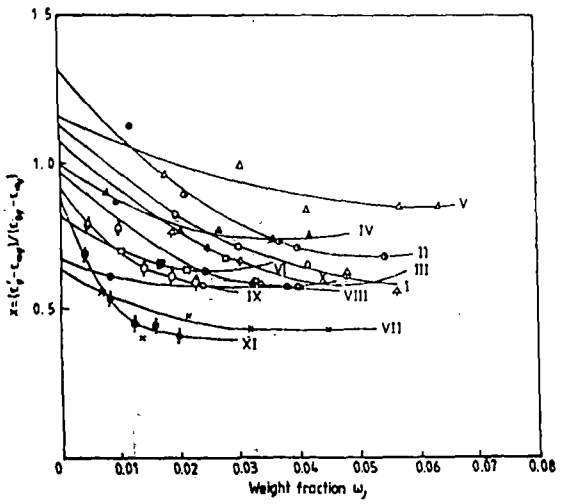

Figure 2. Variation of $(\varepsilon'_{ij} - \varepsilon_{\infty ij})/(\varepsilon_{0ij} - \varepsilon_{\infty ij})$ against weight fraction ω_j of polar solutes in dilute solutions at 35 °C (table 2): (I), (II), (III), (IV), (V) of disubstituted anilines, (VI), (VII), (VIII), (IX), (X) and (XI) of disubstituted benzenes respectively.

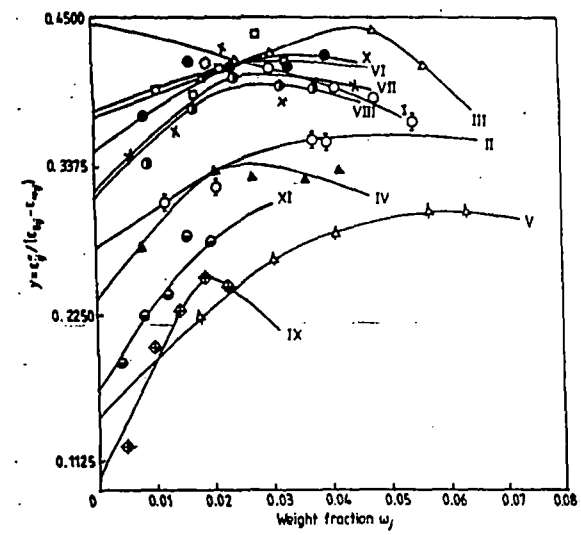

Figure 3. Variation of $\varepsilon''_{ij}/(\varepsilon_{0ij} - \varepsilon_{\infty ij})$ against weight fraction ω_j of polar solutes in dilute solutions at 35 °C (table 2): (I), (II), (III), (IV), (V) of disubstituted anilines, (VI), (VII), (VIII), (IX), (X) and (XI) of disubstituted benzenes respectively.

conductivity $K_{ij} = \omega\varepsilon'_{ij}/4\pi$ can be represented by

$$K_{ij} = K_{ij\infty} + K'_{ij}/\omega\tau$$

$$\left(\frac{dK'_{ij}}{d\omega_j}\right)_{\omega_j \to 0} = \omega\tau \left(\frac{dK_{ij}}{d\omega_j}\right)_{\omega_j \to 0} = \omega\tau\beta \qquad (12)$$

where β is the slope of the K_{ij}–ω_j curve at $\omega_j \to 0$.

Equation (11), on being differentiated with respect to ω_j for $\omega_j \to 0$, becomes

$$\left(\frac{dK'_{ij}}{d\omega_j}\right)_{\omega_j \to 0} = \frac{\mu_j^2 N\rho_i F_i}{3M_j kT}\left(\frac{\omega^2\tau}{1+\omega^2\tau^2}\right) \qquad (13)$$

because $\rho_{ij} \to \rho_i$, the density of the solvent $F_{ij} \to F_i$ the local field of the solvent, in the limit $\omega_j = 0$. Using

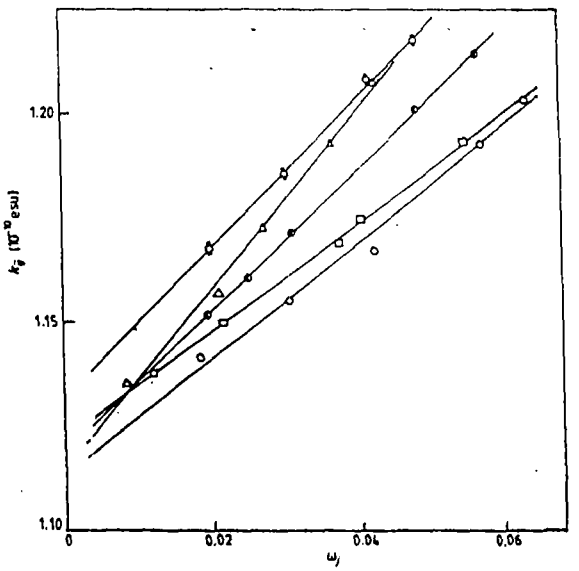

Figure 4. Concentration variation of microwave conductivity K_{ij} of five disubstituted anilines at 35 °C.

equations (12) and (13) we finally get

$$\mu_j = \left(\frac{3M_j kT\beta}{N\rho_i F_i \omega b}\right)^{1/2} \qquad (14)$$

to evaluate μ_1 and μ_2 in terms of b, where b is a dimensionless parameter given by

$$b = \frac{1}{1+\omega^2\tau^2} \qquad (15)$$

for τ_1 and τ_2 respectively. The values of b as well as μ_1 and μ_2 thus computed from equations (14) and (15) are placed in table 3.

4. Results and discussion

Figure 1 represents the linear relationship of $(\varepsilon_{0ij} - \varepsilon'_{ij})/(\varepsilon'_{ij} - \varepsilon_{\infty ij})$ to $\varepsilon''_{ij}/(\varepsilon'_{ij} - \varepsilon_{\infty ij})$, satisfying equation (7) having intercepts and slopes presented in table 1 with the experimental points placed on each curve for 11 systems possessing double relaxation phenomena. The error involved in such regressions as well as the correlation coefficients for all the curves were also calculated and placed in table 1 in order to test their linearity and to assess the errors introduced in τ values, which may normally be claimed to be accurate up to ±10%. Attempts were made to measure the double relaxation times of the molecules as mentioned in tables 1–3 in order to calculate μ_1 and μ_2 of the flexible parts as well as the whole molecules. They are shown in tables 1 and 3 respectively. In 11 systems out of 15, nevertheless, double relaxation phenomena were found by showing the lower as well as higher values of τ_1 and τ_2 respectively. As shown in table 1, eight molecules, namely all the disubstituted anilines and three benzene derivatives namely *o*-chloronitrobenzene,

Table 3. Reports of the estimated intercepts and slopes of the concentration variation of UHF conductivity, dimensionless parameter b, dipole moments μ_1 and μ_2 in Debye (D) for the flexible part and the end-over-end rotation of a polar molecule, reported μ_1 and μ_2 in D due to existing methods, the theoretical μ values from the bond length and bond moments.

	Intercepts and slopes of K_{ij} against ω_j		Dimensionless parameters b		Estimated dipole moment		Reported μ (D)		Theoretical μ (D)	Experimental μ_1 (D)
Slope number and systems	α (10^{-10} esu)	β (10^{-10} esu)	$b_1 = \frac{1}{1+\omega^2\tau_1^2}$	$b_2 = \frac{1}{1+\omega^2\tau_2^2}$	μ_1 (D)	μ_2 (D)	Guggenheim	Higasi *et al*	μ_2 from bond length and bond moments	Using $\mu_1 = \mu_2 (c_1/c_2)^{1/2}$
(i) 4-chloro-2-methyl aniline in C_6H_6	1.1323	1.7863	0.7797	0.1219	2.51	6.36	3.28	3.12	3.06	4.47
(ii) 3-chloro-4-methyl aniline in C_6H_6	1.1220	1.2865	0.8808	0.3014	2.01	3.43	2.61	2.43	2.20	4.95
(iii) 5-chloro-2-methyl aniline in C_6H_6	1.1189	1.6848	0.7858	0.2934	2.43	3.98	3.10	2.92	2.83	3.43
(iv) 3-chloro-2-methyl aniline in C_6H_6	1.1144	2.1490	0.9188	0.3725	2.54	3.99	3.02	2.86	2.48	3.75
(v) 2-chloro-6-methyl aniline in C_6H_6	1.1135	1.3766	0.9228	0.4611	2.03	2.87	2.32	2.20	1.85	2.83
(vi) *o*-chloronitrobenzene in C_6H_6	1.1265	4.0539	0.9178	0.4935	3.68	5.02	4.35	4.43	5.28	4.99
(vii) 4-chloro-3-nitrotoluene in C_6H_6	1.1250	2.8594	0.9464	0.2751	3.18	5.89	4.49	4.59	5.58	5.31
(viii) *m*-nitrobenzotrifluoride in C_6H_6	1.1262	1.7747	0.8630	0.3064	2.77	4.64	3.67	3.80	3.74	4.08
(ix) 4-chloro-3-nitrobenzotrifluoride in CCl_4	1.0999	1.5781	0.9987	0.2744	1.99	3.79	3.17	3.15	3.78	4.34
(x) *o*-nitrobenzotrifluoride in C_6H_6	1.1169	4.1557	0.9962	0.5035	3.94	5.54	4.96	5.07	6.18	6.80
(xi) 4-chloro-3-nitrotoluene in CCl_4	1.1044	3.2769	0.9964	0.1686	2.50	6.07	4.68	4.63	5.58	5.78
(xii) 4-chloro-3-nitrobenzotrifluoride in C_6H_6	1.1286	1.1894	—	0.6845	—	2.76	2.97	2.98	3.78	—
(xiii) *m*-aminobenzotrifluoride in C_6H_6	1.1106	2.3536	—	0.5303	—	3.73	3.51	3.60	2.48	—
(xiv) *o*-chloronitrobenzene in CCl_4	1.0973	5.4508	—	0.3676	—	5.08	4.19	4.13	5.28	—
(xv) *o*-chlorobenzotrifluoride in C_6H_6	1.1199	2.0159	—	0.5580	—	3.57	3.38	3.49	3.98	—

4-chloro-3-nitrotoluene and *m*-nitrobenzotrifluoride, all in C_6H_6, show considerably larger values of τ_1 in their relaxation behaviours. This is perhaps due to the fact that the flexible $-CH_3$ group in aniline, and those attached to the benzene rings mentioned above, absorb energy much more strongly in the microwave electric field and thereby yield large values of τ_1. 4-chloro-3-nitrobenzotrifluoride in CCl_4, *o*-nitrobenzotrifluoride in C_6H_6 and 4-chloro-3-nitrotoluene in CCl_4 have their τ_1 much smaller, presumably due to the fact that their flexible parts are comparatively rigidly fixed to the parent ones (table 1). It is, however, interesting to note that the last four systems of table 1 show single relaxation processes, probably owing to their rigid attachment to the flexible parts. The slopes and intercepts of equation (7) yield τ_1 with negative sign for the aforesaid molecules.

Again, *o*-chloronitrobenzene shows a double relaxation phenomenon in C_6H_6 but a single relaxation process in CCl_4. The reverse case, however, occurs in 4-chloro-3-nitrobenzotrifluoride, which shows a low value of τ_1 in CCl_4 and a single relaxation process in C_6H_6. This may perhaps be attributed to solvent effects upon the polar molecules. So a firm conclusion on solvent effects seems to be of utmost importance if measure-

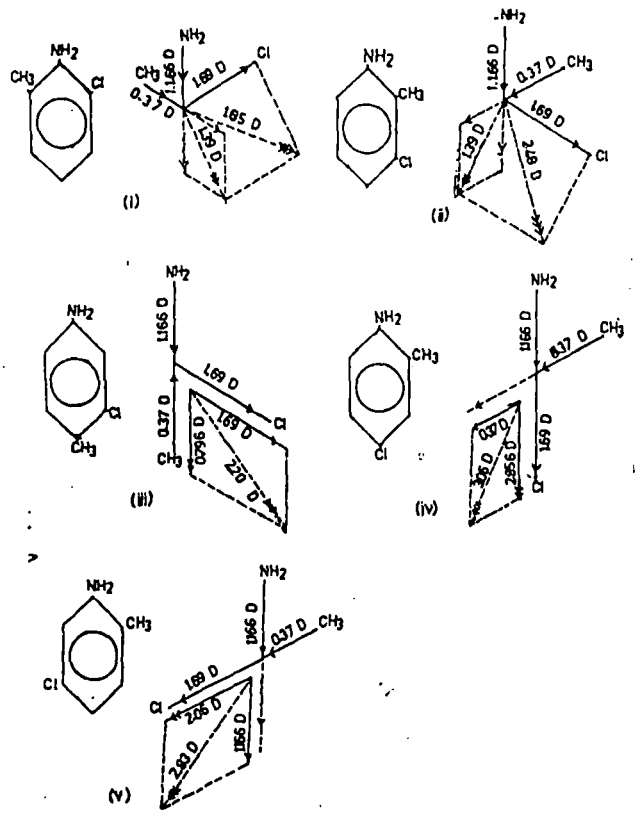

Figure 5. Conformations of five disubstituted anilines showing the orientation of the bond axes and bond moments and dipole moments.

ments are to be performed on a single polar molecule in different non-polar solvents.

Table 2 reports the relative contributions c_1 and c_2 due to τ_1 and τ_2 (table 1) towards relaxation as computed from Fröhlich's equations (8) and (9) for x and y as well as by our graphical technique (figures 2 and 3). In total, c_2 values calculated for six polar molecules are negative although they fulfil the condition $c_1 + c_2 \simeq 1$. The disagreements in c_1 and c_2 with those of Fröhlich (1949) indicate that their flexible parts are loosely bound. In HF electric field the contribution by the rest of the molecule towards relaxation could not be in accord with the flexible one, due to inertia.

The variation of HF conductivities K_{ij} of five disubstituted anilines with respect to ω_j of polar solutes is shown in figure 4. The intercept α and slope β are placed in table 3 to compute μ_1 and μ_2 using relaxation times τ_1 and τ_2 of table 1 from equations (14) and (15). The values of b_1 and b_2 are also placed in the fourth and fifth columns of table 3. The corresponding μ_1 and μ_2 from equation (14) are shown in table 3. They are compared with μ values of Guggenheim (1949) and Higasi *et al* (1952). The disubstituted benzenes had already been studied by Acharyya and Chatterjee (1985) by the conductivity method. The theoretical μ_j from bond lengths and bond angles had also previously been studied. The same data, with those of disubstituted anilines, are shown again in table 3 for comparison only.

In figure 5 the bond moments of $CH_3 \rightarrow C$ and $C \rightarrow Cl$ are 0.37 D and 1.69 D respectively. The bond moment 1.48 D of $C \rightarrow NH_2$ makes an angle 142° with the bond axis. The component along the bond axis in these molecules becomes 1.166 D. With these preferred conformational structures of the disubstituted anilines, the theoretical μ_j were computed by the vector addition method and are placed in table 3. The close agreement of these μ_j with our experimental μ_2 values suggests their correct conformational structures as shown in figure 5.

The values of μ_1 may also be obtained from $\mu_1 = \mu_2(c_1/c_2)^{1/2}$ when the two relaxation phenomena are equally probable (Fröhlich 1949). However, the present investigation finds that μ_1 values as calculated from the above relation are larger for c_1 and c_2 due to Fröhlich's equations. The τ values gradually decrease due to various conformations of the disubstituted anilines (figure 5 and table 1), probably due to decrease in the effective radii of the rotating units under HF electric field. Although the molecules are in the same environment and their molecular weights are the same, the most probable relaxation time due to Higasi (1966) and Guggenheim (1957) also show a trend similar to ours as shown in table 1.

5. Conclusions

The close agreement of μ_2 values with literature values at once suggests that our new approach can justifiably be claimed to be a simple, straightforward and useful one. The method of single frequency measurements of dielectric relaxation data at a given temperature is comparatively easy to perform. It requires only easy and time-saving calculations, unlike other existing methods, to detect the very existence of double relaxation phenomena in polar–non-polar liquid mixtures. Thus the present procedure offers a significant improvement for derivation of τ_1 and τ_2 and μ_1 and μ_2 because it allows one to find not only an estimate of the errors, but also the correlation coefficients between the desired values generated from the dielectric relaxation.

Acknowledgments

The authors are grateful to Mr S N Roy MA, Principal and Mr Amal Bhattacharya MSc of Raiganj University College for their kind interest in this work.

References

Acharyya S and Chatterjee A K 1985 *Indian J. Pure Appl. Phys.* **23** 484

Arrawatia M L, Gupta P C and Sisodia M L 1977 *Indian J. Pure Appl. Phys.* **15** 770

Bergmann K, Roberti D M and Smyth C P 1960 *J. Phys. Chem.* **64** 665

Battacharyya J, Sinha B, Roy S B and Kastha G S 1964 *Indian J. Phys.* **38** 413

Chatterjee A K, Saha U, Nandi N, Basak R C and Acharyya S 1992 *Indian J. Phys.* **66** 291

Fröhlich H 1949 *Theory of Dielectrics* (Oxford: Oxford University Press) p 94
Guggenheim E A 1949 *Trans. Faraday Soc.* **45** 714
Gupta P C, Arrawatia M L and Sisodia M L 1978 *Indian J. Pure Appl. Phys.* **16** 934
Higasi K 1952 *Denaki Kenkyusho Iho* **4** 231
—— 1966 *Bull. Chem. Soc. Japan* **39** 2157
Higasi K, Bergmann K and Smyth C P 1960 *J. Phys. Chem.* **64** 880
Kastha G S, Dutta B, Bhattacharyya J and Roy S B 1969 *Indian J. Phys.* **43** 14
Khameshara S M and Sisodia M L 1980 *Indian J. Pure Appl. Phys.* **18** 110
Murphy F J and Morgan S O 1939 *Bell. Syst. Tech. J.* **18** 502
Saha U and Acharyya S 1993 *Indian J. Pure Appl. Phys.* **31** 181
Smyth C P 1955 *Dielectric Behaviour and Structure* (New York: McGraw-Hill)

J. Phys. D: Appl. Phys. 27 (1994) 2194–2202. Printed in the UK

Single-frequency measurement of double-relaxation times of mono-substituted anilines in benzene

S K Sit, R C Basak, U Saha and S Acharyya

Raiganj College (University College), Department of Physics, PO Raiganj, Dt Uttar Dinajpur (WB) 733134, India

Received 26 January 1994, in final form 15 June 1994

Abstract. Single-frequency measurements of dielectric relaxation parameters at different concentrations are used to estimate the double-relaxation times τ_1 (smaller) and τ_2 (larger) of some mono-substituted anilines in benzene at 35 °C for 2.02, 3.86 and 22.06 GHz electric fields respectively. The *o*- and *m*-anisidines like *p*-toluidines exhibit double-relaxation phenomena at 3.86 and 22.06 GHz whereas *o*- and *m*-toluidines show the same effect at 2.02 and 3.86 GHz respectively. Only *p*-anisidine, however, shows the mono-relaxation behaviour at all frequencies. The relative contributions c_1 and c_2 towards dielectric relaxation for τ_1 and τ_2 are computed from Fröhlich's equations only for comparison with those of the graphical techniques adopted here. The dipole moments μ_1 and μ_2 in terms of τ_1 and τ_2 are then determined from the slope β of concentration variation of the ultra-high-frequency conductivity K_{ij} for those compounds to establish their conformations.

List of symbols used

ϵ'_{ij}, ϵ''_{ij}	real and imaginary parts of the dielectric constant of a solution
$\epsilon^*_{ij}=\epsilon'_{ij}-j\epsilon''_{ij}$	where $j=\sqrt{-1}$ is a complex number
ϵ_{0ij}, $\epsilon_{\infty ij}$	static and optical dielectric constants of the solution
$\omega=2\pi f$	angular frequency of the applied electric field, f being the frequency in hertz
K'_{ij}, K''_{ij}	real and imaginary parts of the complex electrical conductivity K^*_{ij} of a solution
$K^*_{ij}=K'_{ij}+jK''_{ij}$	where $j=\sqrt{-1}$ is a complex number
$K_{\infty ij}$	constant conductivity of the solution at $w_j \to 0$
μ_j	dipole moment of the jth type of solute
μ_1, μ_2	dipole moments of the flexible part and the parent molecule
τ_s	relaxation time of the solute
τ_1, τ_2	relaxation times of the flexible part and the parent molecule
τ_0	most probable relaxation time of the solute
$A=\ln(\tau_2/\tau_1)$	the Fröhlich parameter
w_j	weight fraction of the solute
c_1, c_2	relative contributions due to τ_1 and τ_2 respectively
M_j	molecular weight of the jth type of solute
β	slope of $K_{ij}-w_j$ curve.

1. Introduction

In recent years the dielectric relaxation phenomena of polar–non-polar liquid mixtures under ultra-high-frequency (UHF) electric fields have gradually gained the attention of a large number of workers [1–3] as they reveal significant information on various types of molecular associations. There exist several methods [4–6] of estimating the relaxation time τ_s as well as the dipole moment μ_j of a polar liquid within the framework of the Debye and Smyth model. We [7], however, observe that the imaginary K''_{ij} and real K'_{ij} of the complex UHF conductivity K^*_{ij} of a polar–non-polar liquid mixture vary linearly and independently in the low-concentration region. The relaxation time, which is the lag in response to the alternation of the electric field, could, however, be estimated from their slopes.

Bergmann *et al* [8] devised a graphical technique in order to obtain τ_1 and τ_2 to represent relaxation times of the flexible part attached to the parent molecule and the molecule itself respectively. The corresponding contributions c_1 and c_2 towards dielectric relaxations in terms of τ_1 and τ_2 were also found for some complex molecules. The method is based on plotting the normalized experimental points involved with the measured data of the real ϵ', the imaginary ϵ'' of the complex dielectric constant ϵ^*, the static dielectric constant ϵ_0 and the optical dielectric constant ϵ_∞ at various frequencies ω on a semicircle in a complex plane. A point was then selected on the chord through

0022-3727/94/102194+09$19.50

the two fixed points on the semicircle in consistency with all the experimental points. Bhattacharyya *et al* [9] subsequently modified the above procedure to get τ_1, τ_2, c_1 and c_2 with the experimental values measured at two different frequencies.

Under such conditions, an alternative procedure [10] has recently been suggested to determine τ_1 and τ_2 based on a single-frequency measurement of dielectric relaxation parameters like ϵ'_{ij}, ϵ''_{ij}, ϵ_{0ij} and $\epsilon_{\infty ij}$ of a polar molecule (j) for different weight fractions w_j in a non-polar solvent (i) at a given temperature in degrees Celsius. They are, however, estimated from the slope and intercept of the straight line equation between $(\epsilon_{0ij}-\epsilon'_{ij})/(\epsilon'_{ij}-\epsilon_{\infty ij})$ and $\epsilon''_{ij}/(\epsilon'_{ij}-\epsilon_{\infty ij})$. This is derived from the dielectric relaxation data for different w_j of a polar solute measured under a single-frequency electric field in the GHz region. The correlation coefficient, r, could also be calculated because of the linear behaviour of the derived parameters. This helps one find out the percentage error introduced in the obtained results, too.

The corresponding contributions c_1 and c_2 towards dielectric relaxation in terms of the estimated τ_1 and τ_2 can, however, be calculated from x and y where

$$x = \frac{\epsilon'_{ij} - \epsilon_{\infty ij}}{\epsilon_{0ij} - \epsilon_{\infty ij}}$$

$$y = \frac{\epsilon''_{ij}}{\epsilon_{0ij} - \epsilon_{\infty ij}}$$

in Fröhlich's equations [11]. The variations of x and y with w_j of a polar solute in a system of a polar–non-polar liquid mixture are found to obey the equations of Bergmann *et al* [8] almost exactly. c_1 and c_2 can also be calculated by the graphical technique suggested by Saha *et al* [10], which consists of plotting those experimental values at different w_j with a view to getting x and y at infinite dilution. The UHF electrical conductivity K_{ij} of a polar–non-polar liquid mixture, on the other hand, is thought to be a sensitive tool in ascertaining the dipole moment μ_j of a polar liquid in terms of τ_s.

Some of the disubstituted aniline and benzene derivatives had already been studied in detail by the new approach suggested by Saha *et al* [10]. Ten out of 12 highly non-spherical disubstituted anilines and benzenes were found to exhibit the double-relaxation phenomena as their flexible parts are not rigidly fixed in relation to the parent ones.

We, therefore, thought to study the available solution data of ϵ'_{ij}, ϵ''_{ij}, ϵ_{0ij} and $\epsilon_{\infty ij}$ of mono-substituted anilines like anisidines and toluidines in their *ortho*, *meta* and *para* forms for their various concentrations as measured by Srivastava and Suresh Chandra [12] at different frequencies of 2.02, 3.86 and 22.06 GHz electric fields at 35 °C to obtain τ_1 and τ_2 based on the new approach of Saha *et al* [10]. Highly non-spherical molecules like mono-substituted anilines are also expected to possess the double-relaxation phenomena by showing τ_1 and τ_2. Although they are strongly of non-Debye type in their relaxation behaviour, it is found, in the present investigation, that they do not exhibit the effect of double-relaxation phenomena at all frequencies of the electric field. When the available data [12] were extended to 9.945 GHz (about 3 cm wavelength), which is supposed to be the most effective dispersive region for such polar molecules, all of them, on the other hand, showed the double-relaxation phenomena of reasonable τ_1 and τ_2 [13]. However, out of 18 systems, as shown in tables and figures, eight systems like *o*- and *m*-anisidine and *p*-toluidine at 3.86 and 22.06 GHz together with *o*- and *m*-toluidine at 2.02 and 3.86 GHz are found to show τ_1 and τ_2. Only *p*-anisidine is an exception. It shows mono-relaxation behaviour at all frequencies. This sort of mono-relaxation behaviour may equally well be explained by considering a distribution of relaxation times, namely a single broad dispersion. Only τ_2 values of the compounds showing mono-relaxation are, however, obtained from the slopes of the straight line equations (such as (15), see later) of $(\epsilon_{0ij} - \epsilon'_{ij})/(\epsilon'_{ij} - \epsilon_{\infty ij})$ with $\epsilon''_{ij}/(\epsilon'_{ij} - \epsilon_{\infty ij})$ having zero intercepts.

The relaxation times τ, since accurate values for mono-substituted anilines are not available, are also estimated from the slopes of K''_{ij} versus K'_{ij}. They may be called the most probable relaxation time τ_0 of the three isomers of anisidine and toluidine. τ_0 is often given by $\tau_0 = (\tau_1\tau_2)^{1/2}$ where τ_1 and τ_2 convey their usual meanings. c_1 and c_2 in terms of τ_1 and τ_2 are also calculated from Fröhlich's equations [11] as well as by our graphical technique. The dipole moments μ_1 and μ_2 of these three isomers of anisidine and toluidine are finally estimated from the slope β of their concentration variation of UHF conductivities K_{ij} at $w_j \to 0$ and in terms of the estimated τ_1 and τ_2 in order to establish the conformational structures of those compounds under investigation.

2. Theoretical formulations of c_1 and c_2 in terms of τ_1 and τ_2 based on the single-frequency method

When the complex dielectric constants ϵ^*_{ij} is represented as the sum of two non-interacting Debye-type dispersions; the dielectric relaxation by the two extreme values of τ, τ_1 and τ_2; their relative contributions c_1 and c_2 can, however, be expressed for a polar–non-polar liquid mixture [8] by

$$\frac{\epsilon'_{ij} - \epsilon_{\infty ij}}{\epsilon_{0ij} - \epsilon_{\infty ij}} = c_1 \frac{1}{1 + \omega^2\tau_1^2} + c_2 \frac{1}{1 + \omega^2\tau_2^2} \qquad (1)$$

$$\frac{\epsilon''_{ij}}{\epsilon_{0ij} - \epsilon_{\infty ij}} = c_1 \frac{\omega\tau_1}{1 + \omega^2\tau_1^2} + c_2 \frac{\omega\tau_2}{1 + \omega^2\tau_2^2} \qquad (2)$$

such that $c_1 + c_2 = 1$. All the symbols used are of their usual significance. Putting

$$\frac{\epsilon'_{ij} - \epsilon_{\infty ij}}{\epsilon_{0ij} - \epsilon_{\infty ij}} = x \qquad \frac{\epsilon''_{ij}}{\epsilon_{0ij} - \epsilon_{\infty ij}} = y$$

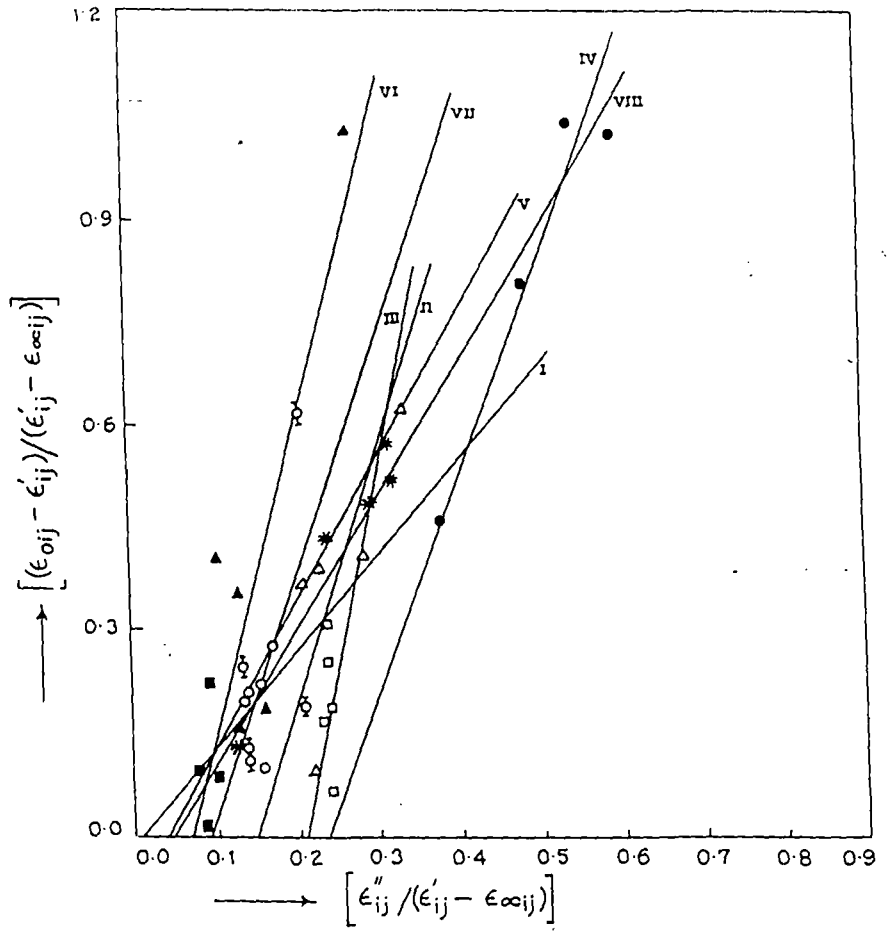

Figure 1. Variation of $(\epsilon_{0ij}-\epsilon'_{ij})/(\epsilon'_{ij}-\epsilon_{\infty ij})$ against $\epsilon''_{ij}/(\epsilon'_{ij}-\epsilon_{\infty ij})$ at 35 °C for different weight fraction w_j (table 1): (I) *o*-anisidine at 3.86 GHz (○); (II) *o*-anisidine at 22.06 GHz (△); (III) *m*-anisidine at 3.86 GHz (□); (IV) *m*-anisidine at 22.06 GHz (●); (V) *o*-toluidine at 2.02 GHz (■); (VI) *m*-toluidine at 3.86 GHz (▲); (VII) *p*-toluidine at 3.86 GHz (◇); and (VIII) *p*-toluidine at 22.06 GHz (*).

with $\omega\tau = \alpha$ and using the abbreviations $a = 1/(1+\alpha^2)$ and $b = \alpha/(1+\alpha^2)$, the above equations (1) and (2) can be written as

$$x = c_1 a_1 + c_2 a_2 \tag{3}$$

$$y = c_1 b_1 + c_2 b_2 \tag{4}$$

where suffices 1 and 2 with a and b are related to τ_1 and τ_2 respectively.

From equations (3) and (4), since $\alpha_2 - \alpha_1 \neq 0$ and $\alpha_2 > \alpha_1$ we have

$$c_1 = \frac{(x\alpha_2 - y)(1+\alpha_1^2)}{\alpha_2 - \alpha_1} \tag{5}$$

$$c_2 = \frac{(y - x\alpha_1)(1+\alpha_2^2)}{\alpha_2 - \alpha_1} \tag{6}$$

Now, using the relation $c_1 + c_2 = 1$; one can easily get the following equation with the help of equations (5) and (6):

$$\frac{1-x}{y} = (\alpha_1 + \alpha_2) - \frac{x}{y}\alpha_1\alpha_2$$

which, on substitution of the values of x, y and α, becomes

$$\frac{\epsilon_{0ij} - \epsilon'_{ij}}{\epsilon'_{ij} - \epsilon_{\infty ij}} = \omega(\tau_1 + \tau_2)\frac{\epsilon''_{ij}}{\epsilon'_{ij} - \epsilon_{\infty ij}} - \omega^2\tau_1\tau_2. \tag{7}$$

Equation (7) is simply a straight line relation between $(\epsilon_{0ij} - \epsilon'_{ij})/(\epsilon'_{ij} - \epsilon_{\infty ij})$ and $\epsilon''_{ij}/(\epsilon'_{ij} - \epsilon_{\infty ij})$ having slope $\omega(\tau_1 + \tau_2)$ and intercept $-\omega^2\tau_1\tau_2$ respectively. Here $\omega = 2\pi f$, f being the frequency of the alternating electric field in gigahertz. When equation (7) is fitted with the measured data of ϵ'_{ij}, ϵ''_{ij}, ϵ_{0ij} and $\epsilon_{\infty ij}$ for different weight fractions w_j of *ortho*, *meta* and *para* anisidines and toluidines in benzene at 35 °C [12] we get slopes and intercepts as shown in table 1 to determine τ_1 and τ_2 for each single frequency of 2.02, 3.86 and 22.06 GHz electric fields respectively. The error as well as the correlation coefficient were also found out for each curve of equation (7) and placed in table 1, only to verify their linearity as illustrated graphically in figure 1 together with the experimental points upon them.

The Fröhlich parameter A as shown in table 2 for polar solutes exhibiting the double-relaxation

Table 1. The intercepts and the slopes of the straight line curves of $(\epsilon_{0ij} - \epsilon'_{ij})/(\epsilon'_{ij} - \epsilon_{\infty ij})$ against $\epsilon''_{ij}/(\epsilon'_{ij} - \epsilon_{\infty ij})$ of anisidines and toluidines at 35 °C to estimate the relaxation times τ_1 (smaller) and τ_2 (larger) with respective errors and correlation coefficients involved in the calculations as well as their estimated τs'.

System with molecular wt M_j in gm.	Frequency f in GHz	Intercept and slope of $(\epsilon_{0ij} - \epsilon'_{ij})/(\epsilon'_{ij} - \epsilon_{\infty ij})$ versus $\epsilon''_{ij}/(\epsilon'_{ij} - \epsilon_{\infty ij})$ curve		Estimated relaxation times $\tau_1 \times 10^{12}$ s	$\tau_2 \times 10^{12}$ s	Correlation coefficient r	% error involved in calculation	Estimated relaxation time $\tau_0 \times 10^{12}$ s	$\tau_2 \times 10^{12}$ due to single broad dispersion
o-anisidine	2.02	−0.0596	0.3759	—	39.10	0.1082	29.81	6.02	96.83
$M_j = 123$	3.86	0.0179	1.4360	0.52	58.72	0.3021	27.41	5.89	—
	22.06	0.5406	3.6741	1.11	25.41	0.8274	9.52	1.61	—
m-anisidine	2.02	−0.2109	−0.4703	—	22.13	−0.2588	28.14	11.87	120.9
$M_j = 123$	3.86	−1.1404	5.5485	8.82	220.07	−0.9999	0	8.46	—
	22.06	0.7318	3.1447	1.83	20.87	0.9805	1.16	3.88	—
p-anisidine	2.02	−0.2406	−2.1899	—	8.27	−0.7375	13.75	6.64	61.63
$M_j = 123$	3.86	−0.4927	−2.2136	—	8.41	−0.4782	23.27	6.53	34.31
	22.06	−1.2868	−1.2818	—	4.77	−0.3395	26.69	3.15	9.91
o-toluidine	2.02	0.0773	2.0910	2.97	161.86	0.0743	33.54	5.01	—
$M_j = 107$	3.86	−0.5925	−2.3787	—	9.38	−0.6779	16.30	6.84	35.94
	22.06	−0.4603	0.6684	—	7.87	0.3732	25.96	4.06	8.76
m-toluidine	2.02	−0.4062	−3.0101	—	10.20	−0.5757	20.17	8.70	258.61
$M_j = 107$	3.86	0.2938	4.5092	2.73	183.29	0.8469	8.53	6.78	—
	22.06	−1.2064	−0.6295	—	5.98	−0.3213	27.05	3.42	13.31
p-toluidine	2.02	−0.6655	−3.5127	—	14.21	−0.5101	22.31	4.08	167.73
$M_j = 107$	3.86	0.3149	3.4446	3.88	138.22	0.6477	17.51	5.15	—
	22.06	0.0821	1.9151	0.32	13.51	0.9408	3.47	2.91	—

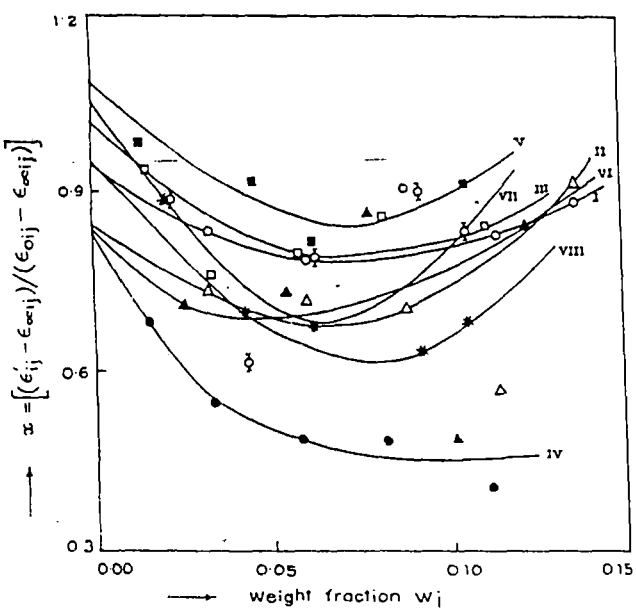

Figure 2. Plot of $(\epsilon'_{ij} - \epsilon_{\infty ij})/(\epsilon_{0ij} - \epsilon_{\infty ij})$ against weight fraction w_j for the polar–non-polar liquid mixture at 35 °C (table 2): (I) *o*-anisidine at 3.86 GHz (○); (II) *o*-anisidine at 22.06 GHz (△); (III) *m*-anisidine at 3.86 GHz (□); (IV) *m*-anisidine at 22.06 GHz (●); (V) *o*-toluidine at 2.02 GHz (■); (VI) *m*-toluidine at 3.86 GHz (▲); (VII) *p*-toluidine at 3.86 GHz (◇); and (VIII) *p*-toluidine at 22.06 GHz (*).

phenomena are used to evaluate both x and y of equations (3) and (4) in terms of ω and the small limiting relaxation time $\tau_s = \tau_1$ by the following equations [11]:

$$\frac{\epsilon'_{ij} - \epsilon_{\infty ij}}{\epsilon_{0ij} - \epsilon_{\infty ij}} = 1 - \frac{1}{2A} \ln\left(\frac{1 + e^{2A}\omega^2\tau_s^2}{1 + \omega^2\tau_s^2}\right) \qquad (8)$$

$$\frac{\epsilon''_{ij}}{\epsilon_{0ij} - \epsilon_{\infty ij}} = \frac{1}{A}[\tan^{-1}(e^A\omega\tau_s) - \tan^{-1}(\omega\tau_s)] \qquad (9)$$

where $A = \ln(\tau_2/\tau_1)$. The computed values of x and y are placed in table 2 to obtain c_1 and c_2 from equations (5) and (6). The latter are also shown in table 2. The left-hand sides of equations (1) and (2) are really the function of w_j of the solutes in a given solvent as shown from the plots of x and y against w_j in figures 2 and 3 respectively. The fixed values of x and y when $w_j \to 0$ for each system, as shown in table 2, can then be used to estimate c_1 and c_2 from equations (5) and (6) in order to compare them with those of Fröhlich [11]. The τ_1 and τ_2 values estimated from the slope and intercept of equation (7) for each solute, when substituted on the right-hand sides of equations (1) and (2), suggest the limiting values of x and y as obtained from figures 2 and 3 at infinite dilution.

3. Estimated μ_1 and μ_2 from UHF conductivity K_{ij} in terms of τ_1 and τ_2

The UHF conductivity K_{ij} is given by Murphy and Morgan [14] as

$$K_{ij} = \frac{\omega}{4\pi}(\epsilon''^2_{ij} + \epsilon'^2_{ij})^{1/2} \qquad (10)$$

Table 2. The relative contributions c_1 and c_2 towards dielectric relaxations, Fröhlich parameters $A(= \ln(\tau_2/\tau_1))$ together with the estimated values of x and y due to Fröhlich equations (equations (8) and (9)) and those by our graphical techniques (figures 2 and 3).

System with Sl No.	Frequency in GHz	Fröhlich parameter A $(= \ln(\tau_2/\tau_1))$	Theoretical values of x and y using equations (8) and (9)		Theoretical values c_1 and c_2		Estimated values of $x = \left(\frac{\epsilon' - \epsilon_\infty}{\epsilon_0 - \epsilon_\infty}\right)_{w_j \to 0}$ and $y = (\epsilon''/(\epsilon_0 - \epsilon_\infty))_{w_j \to 0}$		Estimated values of c_1 and c_2 from figures 2 and 3	
									c_1	c_2
1 *o*-anisidine	3.86	4.7267	0.8829	0.1999	0.7491	0.4051	0.942	0.072	0.8995	0.1278
2 *o*-anisidine	22.06	3.1308	0.5894	0.3645	0.5200	1.0893	0.840	0.117	0.8636	−0.0484
3 *m*-anisidine	3.86	3.2169	0.4811	0.3650	0.4496	1.5081	1.017	0.132	1.081	−0.4915
4 *m*-anisidine	22.06	2.4340	0.5534	0.4063	0.4816	0.9439	0.828	0.221	0.8767	0.0393
5 *o*-toluidine	2.02	3.9982	0.7936	0.2699	0.6755	0.6212	1.086	0.066	1.0751	0.0649
6 *m*-toluidine	3.86	4.2067	0.6401	0.3049	0.5827	1.2441	0.834	0.014	0.8471	−0.1952
7 *p*-toluidine	3.86	3.5730	0.6509	0.3320	0.5727	1.0167	1.050	0.048	1.0750	−0.1905
8 *p*-toluidine	22.06	3.7428	0.7992	0.2766	0.6685	0.5943	0.948	0.036	0.9532	−0.0149

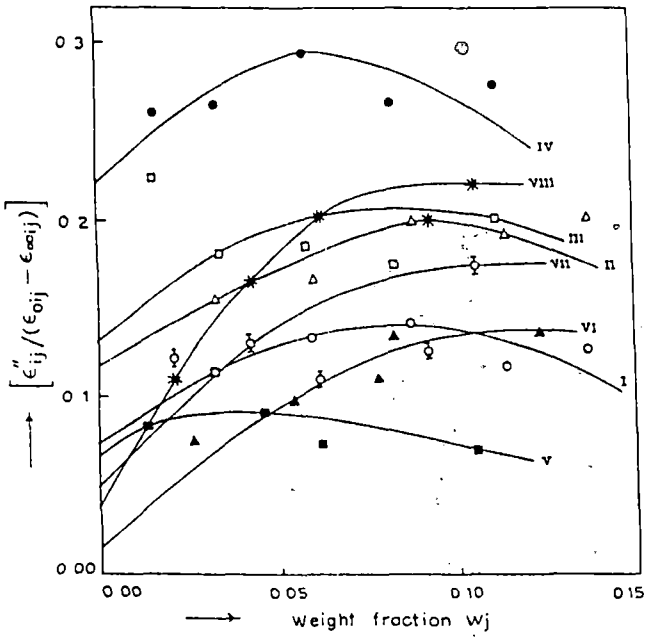

Figure 3. Plot of $\epsilon''_{ij}/(\epsilon_{0ij} - \epsilon_{\infty ij})$ against weight fraction w_j of polar solutes in dilute solutions at 35 °C (table 2): (I) *o*-anisidine at 3.86 GHz (○); (II) *o*-anisidine at 22.06 GHz (△); (III) *m*-anisidine at 3.86 GHz (□); (IV) *m*-anisidine at 22.06 GHz (●); (V) *o*-toluidine at 2.02 GHz (■); (VI) *m*-toluidine at 3.86 GHz (▲); (VII) *p*-toluidine at 3.86 GHz (◇); and (VIII) *p*-toluidine at 22.06 GHz (*).

namely as a function of w_j of a polar solute. In the UHF electric field, although $\epsilon''_{ij} \ll \epsilon'_{ij}$, the ϵ''_{ij} term still offers resistance to polarization. Thus the real part K'_{ij} of the UHF conductivity of a polar–non-polar liquid mixture at T K is [15]

$$K'_{ij} = \frac{\mu_j^2 N \rho_{ij} F_{ij}}{3 M_j k T} \left(\frac{\omega^2 \tau}{1 + \omega^2 \tau^2}\right) w_j$$

which on differentiation with respect to w_j and for $w_j \to 0$ yields that

$$\left(\frac{dK'_{ij}}{dw_j}\right)_{w_j \to 0} = \frac{\mu_j^2 N \rho_i F_i}{3 M_j k T} \left(\frac{\omega^2 \tau}{1 + \omega^2 \tau^2}\right) \qquad (11)$$

where M_j is the molecular weight of a polar solute, N is Avogadro's number, k is the Boltzmann constant, the local field $F_{ij} = \frac{1}{9}(\epsilon_{ij} + 2)^2$, becomes $F_i = \frac{1}{9}(\epsilon_i + 2)^2$ and the density $\rho_{ij} \to \rho_i$ the density of the solvent at $w_j \to 0$.

Again the total UHF conductivity $K_{ij} = \omega \epsilon'_{ij}/(4\pi)$ can be written as

$$K_{ij} = K_{ij\infty} + \frac{1}{\omega \tau} K'_{ij}$$

or

$$\left(\frac{dK'_{ij}}{dw_j}\right)_{w_j \to 0} = \omega \tau \left(\frac{dK_{ij}}{dw_j}\right)_{w_j \to 0} = \omega \tau \beta \qquad (12)$$

where β is the slope of the K_{ij}–w_j curve at $w_j \to 0$. From equations (11) and (12) we thus get

$$\mu_j = \left(\frac{3 M_j k T \beta}{N \rho_i F_i \omega b}\right)^{1/2} \qquad (13)$$

as the dipole moments μ_1 and μ_2 in terms of b, where b is a dimensionless parameter given by

$$b = 1/(1 + \omega^2 \tau^2) \qquad (14)$$

for τ_0, τ_1 and τ_2. The computed values of μ_0, μ_1 and μ_2 with b are given in table 3.

Table 3. Estimated slope β of $K_{ij} - w_j$ equations with % of error involved, the dimensionless parameters b_0, b_1, b_2 in terms of most probable relaxation time τ_0, relaxation time due to flexible part τ_1 and the same due to end-over-end rotation of the molecule τ_2; corresponding estimated dipole moments μ_0, μ_1 and μ_2 together with the theoretical values of μ_j from bond angles and bond moments and estimated values of μ_1 from $\mu_1 = \mu_2(c_1/c_2)^{1/2}$ respectively.

System	Frequency in GHz	Slope $\beta \times 10^{10}$ of $K_{ij} - w_j$ equations	% error involved in calculation	Dimensionless parameters $b_0=\frac{1}{1+\omega^2\tau_0^2}$	$b_1=\frac{1}{1+\omega^2\tau_1^2}$	$b_2=\frac{1}{1+\omega^2\tau_2^2}$	Estimated dipole moments (in Debye) μ_0	μ_1	μ_2	Theoretical μ_j in D from bond angle and bond moment	Estimated μ_1 in D from $\mu_1=\mu_2(c_1/c_2)^{1/2}$
o-anisidine	2.02	0.1620	0.40	0.9942		0.8026	1.39		1.54		
	3.86	0.1786	0.41	0.9800	0.9998	0.3119	1.06	1.05	1.88	1.02	2.56
	22.06	0.3870	1.01	0.9526	0.9769	0.0747	0.66	0.65	2.37		1.64
m-anisidine	2.02	0.3347	0.18	0.9778		0.9269	2.01		2.07		
	3.86	0.2311	2.06	0.9596	0.9563	0.0339	1.22	1.22	6.49	1.65	3.54
	22.06	2.2841	0.08	0.7758	0.9396	0.1068	1.78	1.62	4.81		3.44
p-anisidine	2.02	0.3380	0.35	0.9930		0.9891	2.01		2.01		
	3.86	0.6473	0.09	0.9756		0.9601	2.03		2.04	1.89	
	22.06	2.8513	0.31	0.8400		0.6960	1.91		2.10		
o-toluidine	2.02	0.2097	0.26	0.9960	0.9986	0.1917	1.47	1.47	3.35		3.49
	3.86	0.5507	0.37	0.9732		0.9508	1.74		1.76	1.39	
	22.06	1.3618	0.09	0.7597		0.4569	1.29		1.67		
m-toluidine	2.02	0.2359	0.39	0.9879		0.9835	1.56		1.57		
	3.86	0.4889	1.82	0.9737	0.9956	0.0482	1.64	1.63	7.38	1.03	5.05
	22.06	0.9826	1.30	0.8167		0.5930	1.06		1.24		
p-toluidine	2.02	0.0906	0.21	0.9973		0.9685	0.97		0.98		
	3.86	0.1583	0.44	0.1873	0.9912	0.0818	2.13	0.93	3.23	1.54	2.42
	22.06	1.2927	0.34	0.8602	0.9980	0.2221	1.19	1.10	2.34		2.48

4. Results and discussion

Figure 1 represents the fitted straight line curves between $(\epsilon_{0ij} - \epsilon'_{ij})/(\epsilon'_{ij} - \epsilon_{\infty ij})$ and $\epsilon''_{ij}/(\epsilon'_{ij} - \epsilon_{\infty ij})$ for different weight fractions w_j of *o*-anisidine, *m*-anisidine and *p*-toluidine for 3.86 and 22.06 GHz, and for *o*-toluidine and *m*-toluidine at 2.02 and 3.86 GHz respectively, together with their experimental points. The w_j for the compounds in benzene were, however, calculated from the experimental mole fractions x_i and x_j of solvent and solutes of molecular weights M_i and M_j respectively by using the relation [16]

$$w_j = \frac{x_j M_j}{x_i M_i + x_j M_j}.$$

The correlation coefficients r for each curve were also calculated to confirm their linearity. Some of the coefficients were found to be negative only due to their negative slopes, as is evidenced from table 1. The percentage of error involved in the calculation was found for each curve. The slope and intercept of equation (7) for each straight line were, however, used to determine τ_1 and τ_2 for each compound as shown in table 1. Although equation (7) is based on assumption of the existence of τ_1 and τ_2, the mono-relaxation behaviour showing only τ_2 for some compounds at different frequencies of the electric field may be equally explained by taking into account a single braod dispersion. The resulting equation (7) becomes, when $\tau_1 = 0$,

$$\frac{\epsilon_{0ij} - \epsilon'_{ij}}{\epsilon'_{ij} - \epsilon_{\infty ij}} = \omega\tau_2 \frac{\epsilon''_{ij}}{\epsilon'_{ij} - \epsilon_{\infty ij}} \qquad (15)$$

which may also be derived by using $c_1 = 0$ in equations (1) and (2) of section 2. Equation (15) for ten different frequencies of the electric field was then used to obtain τ_2 values, which are shown in the last column of table 1 for comparison. It is, however, interesting to note that the agreement is closer with τ_2 values obtained from the method of double-relaxation phenomena, as the frequency of the electric field increases from 2.02 to 22.06 GHz. The most probable relaxation time τ_0, as accurate values for these mono-substituted anilines are not available, was also calculated from the slope m of the linear plot of the imaginary K''_{ij} versus the real K'_{ij} parts [7] of the complex conductivity K^*_{ij} under UHF electric field in the relation:

$$K''_{ij} = K_{ij\infty} + \frac{1}{\omega\tau_s} K'_{ij} \qquad (16)$$

where $\tau_0 = 1/(2\pi f m)$. They are seen to correspond to the relation $\tau_0 = (\tau_1\tau_2)^{1/2}$ approximately, which gives 5.53, 5.31, 44.06, 6.18, 21.93, 22.37, 23.16 and 4.32 ps respectively for the mono-substituted anilines showing the double-relaxation phenomena at different frequencies

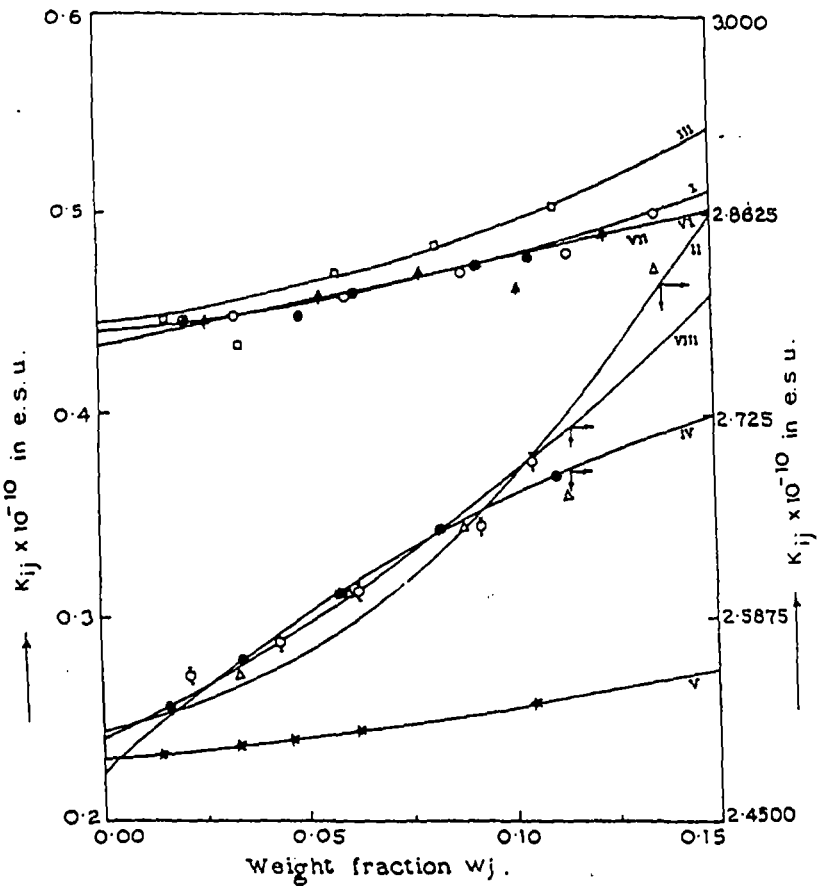

Figure 4. Concentration variation of ultra-high-frequency conductivity K_{ij} of mono-substituted anilines at 35 °C: (I) *o*-anisidine at 3.86 GHz (○); (II) *o*-anisidine at 22.06 GHz (△); (III) *m*-anisidine at 3.86 GHz (□); (IV) *m*-anisidine at 22.06 GHz (●); (V) *o*-toluidine at 2.02 GHz (*); (VI) *m*-toluidine at 3.86 GHz (▲); (VII) *p*-toluidine at 3.86 GHz (⊕); and (VIII) *p*-toluidine at 22.06 GHz (◇).

of the applied electric field. Some of these relaxation times are reasonably good. The estimated values of τ_1, τ_2 and τ_0 are all given in table 1.

It is found in table 1 that *m*-anisidine, *m*- and *p*-toluidines at 3.86 GHz and *o*-toluidine at 2.02 GHz show considerably high values of τ_1 in the range 9–3 ps; while their τ_2 values are comparatively much larger in the range 220–138 ps. This fact confirms that, under such frequencies of alternating electric field, the flexible parts are loosely bound to the parent molecules. They, therefore, require longer times to accommodate their flexible parts towards dielectric relaxation as shown by c_2 values in table 2 being greater than unity. The other molecules like *o*-anisidine at 3.86 and 22.06 GHz and *m*-anisidine and *p*-toluidine at 22.06 GHz show very small values of τ_1, often less than or equal to unity, while their τ_2 values are more or less consistent with the expected values that are often observed in the literature. However, *p*-anisidine shows the mono-relaxation behaviour at all frequencies by showing only τ_2 in agreement with τ_0. Hence *p*-anisidine unlike *p*-toluidine appears to be highly rigid at all the experimental frequencies. The *o*- and *m*-anisidines at 2.02 GHz, *o*-toluidine at 3.86 and 22.06 GHz, *m*-toluidine at 2.02 and 22.06 GHz and *p*-toluidine at 2.02 GHz exhibit the mono-relaxation behaviour in yielding τ_2 values in agreement with our τ_0 values. They indicate their rigidity at those frequencies. When the dielectric relaxation data are extended to 9.945 GHz [13] it is really interesting to note that all these mono-substituted anilines show τ_1 and τ_2 in close agreement with the expected literature values. This fact establishes that an X-band microwave electric field is actually the most effective dispersive region for highly non-spherical polar molecules like mono- or disubstituted aniline and benzene respectively [10].

The c_1 and c_2 values were also calculated from the values of x and y in Fröhlich's equations (8) and (9) with $\tau_1 = \tau_s$ (table 1) and Fröhlich's parameter A, where $A = \ln(\tau_2/\tau_1)$. They are given in table 2 together with those values obtained from the graphical technique of determination of x and y from figures 2 and 3 at infinite dilution. The experimental x and y values on the left-hand sides of equations (1) and (2) as plotted with different w_j in figures 2 and 3 show the usual decrease in x while the latter increases with w_j in concave and convex ways respectively indicating the values of τ_1 and

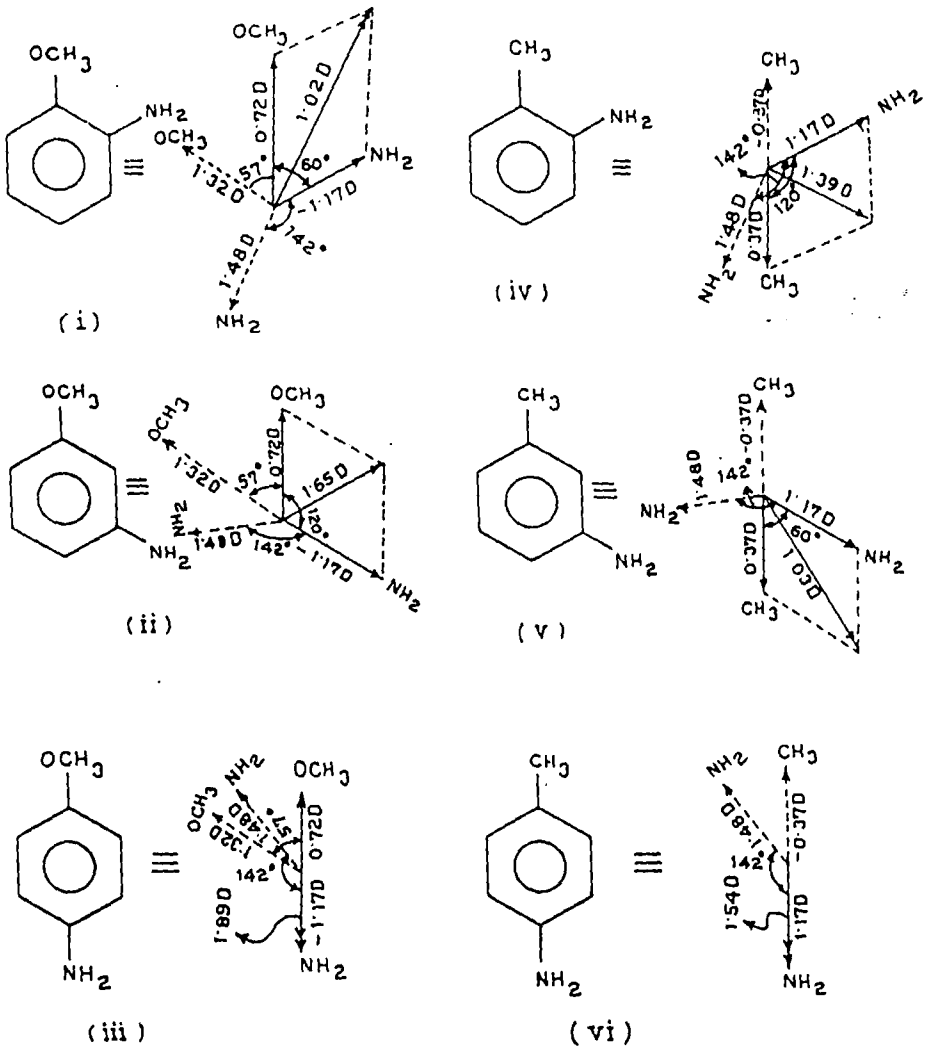

Figure 5. Conformational structures of anisidines and toluidines in *ortho*, *meta* and *para* forms: (i) *o*-anisidine, (ii) *m*-anisidine, (iii) *p*-anisidine, (iv) *o*-toluidine, (v) *m*-toluidine and (vi) *p*-toluidine.

τ_2 as a function of concentration [5]. τ_1 and τ_2, as obtained from the slope and intercept of equation (7) for a polar–non-polar liquid mixture are, therefore, fixed for a polar compound in consistency with the right-hand sides of equations (1) and (2). The values of c_1 by Fröhlich's method are found to be less than unity while c_2 values are greater than and nearly equal to unity. The graphical technique adopted here yields the opposite results by showing $c_1 \geqslant 1.0$ and c_2 very small, often becoming negative (table 2), probably due to inertia [10]. The values of c_1 and c_2 in table 2 suggest that the two double-relaxation phenomena are not equally probable.

The UHF K_{ij} as a function of w_j for the following mono-substituted anilines showing τ_1 and τ_2 were, however, arrived at:

(i) *o*-anisidine at 3.86 GHz: $K_{ij} \times 10^{-10} = 0.4398 + 0.1786w_j + 1.9381w_j^2$

(ii) *o*-anisidine at 22.06 GHz: $K_{ij} \times 10^{-10} = 2.5112 + 0.3870w_j + 13.011w_j^2$

(iii) *m*-anisidine at 3.86 GHz: $K_{ij} \times 10^{-10} = 0.4438 + 0.2311w_j + 2.9354w_j^2$

(iv) *m*-anisidine at 22.06 GHz: $K_{ij} \times 10^{-10} = 2.4896 + 2.2841w_j - 4.7796w_j^2$

(v) *o*-toluidine at 2.02 GHz: $K_{ij} \times 10^{-10} = 0.2294 + 0.2097w_j + 0.5641w_j^2$

(vi) *m*-toluidine at 3.86 GHz: $K_{ij} \times 10^{-10} = 0.4326 + 0.4889w_j - 0.1380w_j^2$

(vii) *p*-toluidine at 3.86 GHz: $K_{ij} \times 10^{-10} = 0.4402 + 0.1583w_j + 2.1467w_j^2$ and

(viii) *p*-toluidine at 22.06 GHz: $K_{ij} \times 10^{-10} = 2.5063 + 1.2927w_j + 4.5909w_j^2$

which are shown graphically in figure 4 together with the experimental points upon the curves. The slopes of K_{ij}–w_j curves are, however, listed in table 3 together with those of the other ten K_{ij}–w_j equations showing the monorelaxation behaviour. The percentage of error in computation of K_{ij}–w_j equations are also shown in table 3. The slopes β are finally used to estimate μ_1 and μ_2 from equations (13) and (14) in terms of τ_1 and τ_2 as presented in table 1. The dimensionless parameters b_0, b_1 and b_2 in terms of τ_0, τ_1 and τ_2 are also given in

table 3.

An attempt was made to estimate from the available bond moments and bond angles the theoretical μ values of the polar liquids, assuming the molecules to be planar. The bond moments and bond angles of C → OCH_3 in anisidine and C ← CH_3 in toluidine are 1.32 D, 0.37 D and 57°, 180° with respect to the benzene ring while those of C → NH_2 are 1.48 D and 142° respectively [17]. The conformational structures thus obtained by the vector addition method for anisidine and toluidine in their *ortho*, *meta* and *para* forms are displayed in figure 5. The estimated μ_j are given in table 3, with those of μ_1, where $\mu_1 = \mu_2(c_1/c_2)^{1/2}$ assuming that the two relaxation phenomena are equally probable. The close agreement of μ values as shown in table 3 at once indicates that the method as suggested is a simple, straightforward and unique one.

5. Conclusion

The determination of slope and intercept of the derived linear equation (equation (7)) involved with a single UHF dielectric relaxation recording of a polar–non-polar liquid mixture at different w_j and at a given temperature in degrees Celsius is an analytical and reliable method by which to calculate τ_1 and τ_2 of the flexible part as well as of the whole molecule itself. The relative contributions c_1 and c_2 towards dielectric relaxations in terms of τ_1 and τ_2 can be calculated by using Fröhlich's equations. The graphical techniques used are also convenient tools to estimate c_1 and c_2. The dipole moments μ_1 and μ_2 in terms of τ_1 and τ_2, and from the slope β of the concentration variation of K_{ij} of polar–non-polar liquid mixtures, throw much light on the structural conformation of a complex polar liquid under investigation. The methodology so far advanced seems to be a significant improvement over the existing ones in that it allows estimation of correlation coefficients between the data used and the percentage of error introduced in the obtained results. The procedure is thus simple, straightforward and requires less computational work than the existing methods, in which experimental data of a pure polar liquid at two or more electric field frequencies are usually needed.

References

[1] Kastha G S, Dutta J, Bhattacharyya J and Roy S B 1969 *Ind. J. Phys.* **43** 14

[2] Acharyya C R, Chatterjee A K, Sanyal P K and Acharyya S 1986 *Ind. J. Pure Appl. Phys.* **24** 234

[3] Saha U and Acharyya S 1993 *Ind. J. Pure Appl. Phys.* **31** 181

[4] Gopalakrishna K V 1957 *Trans. Faraday Soc.* **53** 767

[5] Sen S N and Ghosh R 1972 *Ind. J. Pure Appl. Phys.* **10** 701

[6] Acharyya S and Chatterjee A K 1985 *Ind. J. Pure Appl. Phys.* **23** 484

[7] Saha U and Acharyya S 1994 *Ind. J. Pure Appl. Phys.* **32** 346

[8] Bergmann K, Roberti D M and Smyth C P 1960 *J. Phys. Chem.* **64** 665

[9] Bhattacharyya J, Hasan A, Roy S B and Kastha G S 1970 *J. Phys. Soc. Japan* **28** 204

[10] Saha U, Sit S K, Basak R C and Acharyya S 1994 *J. Phys. D: Appl. Phys.* **27** 596

[11] Fröhlich H 1949 *Theory of Dielectrics* (Oxford: Oxford University Press) p 94

[12] Srivastava S C and Suresch Chandra 1975 *Ind. J. Pure Appl. Phys.* **13** 101

[13] Sit S K and Acharyya S 1994 *J. Phys. Soc. Japan* submitted

[14] Murphy F J and Morgan S O 1939 *Bull. Syst. Techn. J.* **18** 502

[15] Smyth C P 1955 *Dielectric Behaviour and Structure* (New York: McGraw-Hill)

[16] Ghosh A K and Acharyya S 1978 *Ind. J. Phys.* B **52** 129

[17] Weast R C (ed) 1976–77 *Handbook of Chemistry and Physics* 5th edn

Indian Journal of Pure & Applied Physics
Vol. 34, April 1996, pp. 255-262

Double relaxations of monosubstituted anilines in benzene under effective dispersive region

S K Sit* & S Acharyya
Department of Physics, University College, P O Raiganj Dt Uttar Dinajpur (WB) 733 134

Received 5 June 1995; revised received 20 November 1995

Mono- or di-substituted aniline and benzene derivatives are thought to absorb energy much more strongly in the effective dispersive region of nearly 10 GHz electric field. The dielectric relaxation data of the monosubstituted anilines measured at different frequencies (Sit *et al* 1994) showed either double or monorelaxation behaviour. When the same data are extended to 9.945 GHz ($\simeq$ 3 cm wavelength) electric field, each of them, on the other hand; exhibits the double relaxation phenomenon by showing the reasonable relaxation times τ_1 (smaller) and τ_2 (larger) for the flexible part as well as the whole molecule itself for their rotations in *hf* electric field. τ_1 and τ_2 are, however, obtained from the slope and intercept of a derived equation involved with dielectric relaxation data for different weight fractions ω_js' measured under a single frequency electric field. The relative contributions c_1 and c_2 in terms of τ_1 and τ_2 towards relaxation are calculated from Fröhlich's equations and our graphical technique. The values of symmetric and asymmetric distribution parameters γ and δ are also calculated to test the regidity of the molecules under investigation. The dipole moments μ_1 and μ_2 in terms of τ_1 and τ_2 are finally estimated from the slope β of *hf* conductivity K_{ij} as a function of ω_js' in order to support their conformations.

1 Introduction

The highly nonspherical molecules like mono- or di-substituted benzenes and anilines have more than one relaxation times τs' due to presence of their flexible parts attached to the parent molecule[1,2]. The study of dielectric relaxation phenomena of such polar molecules in nonpolar solvent provides one with the valuable information of various types of interactions such as monomer and dimer formations[3-5] in liquids. The polar nonpolar liquid mixtures instead of pure polar liquids deserve much more advantages as the polar-polar interactions, viscosity effect and the other factors become minimized. Moreover, much disputed ambiguity concerning the internal field correction can also be avoided.

Bergmann *et al*.[6] however, devised a graphical method to obtain τ_1 and τ_2 to represent the relaxation times of the smallest flexible part as well as the whole molecule for their end-over-end rotations under an electric field of Giga hertz frequency. The respective contributions c_1 and c_2 towards dielectric relaxations were also estimated in terms of τ_1 and τ_2. The method consists of plotting the normalised experimental points involved with the measured data of the real ε', the imaginary ε'' parts of the complex dielectric constant ε^*, the static dielectric constant ε_0 and the optical dielectric constant ε_∞ at different frequencies ω on a semicircle in a complex plane. A point was, however, then selected on the chord through the two fixed points lying on the said semicircle which contained all the experimental points in consistency with the measured data for various frequencies. Bhattacharyya *et al*.[7] subsequently simplified the above procedure to get τ_1, τ_2 and the weighted contributions c_1 and c_2 towards dielectric relaxations with the experimental values of ε', ε'', ε_0 and ε_∞ of a pure polar liquid measured at two different frequencies in GHz regions.

The highly nonspherical polar liquid molecules like mono- or di-substituted anilines and benzenes are usually thought to absorb energy much more strongly in a high frequency electric field of nearly 10 GHz. Moreover, such type of polar liquids are supposed to be non-Debye in their relaxation behaviours. From this point of view, the study of dielectric relaxation of polar-nonpolar liquid mixtures under the electric field of nearly 3 cm wavelength is preferable. Saha *et al*.[1] and Sit *et al*.[2] recently presented an alternative approach to estimate τ_1 and τ_2 from the intercept and the slope of a derived straight line equation involved with dielectric relaxation solution data like ε'_{ij}, ε''_{ij}, ε_{0ij} and $\varepsilon_{\infty ij}$

*Department of Physics, Raiganj Polytechnic, Raiganj 733 134

measured under a single frequency electric field of GHz range. One could not make a strong conclusion if ε_{0ij} and $\varepsilon_{\infty ij}$ of a polar solute (j) dissolved in a nonpolar solvent (i) were not accurately known.

Disubstituted anilines and benzenes were found to possess the double relaxation phenomena[1] by showing considerable values of τ_1 and τ_2 in solvent benzene under the electric field of 9.945 GHz. Monosubstituted anilines, however, showed mono as well as often the double relaxation phenomena[2] in solvent benzene under the electric field of different frequencies of 2.02 to 22.06 GHz. We, therefore, thought to use ε'_{ij}, ε''_{ij}, ε_{0ij} and $\varepsilon_{\infty ij}$ of such monosubstituted anilines for different weight fractions ω_js' under 9.945 GHz electric field which is supposed to be the most effective dispersive region for such isomers of anisidine and toluidine. The dielectric relaxation parameters were, however, obtained at 35°C from the careful graphical interpolation made by the available data measured by Srivastava and Suresh Chandra[8] at different frequencies.

The monosubstituted anilines are really found to exhibit the expected double relaxation phenomenon under 9.945 GHz electric field at 35°C by showing reasonable values of τ_1 and τ_2 as presented in Table 1, from the slopes and the intercepts of curves of Fig. 1 as derived from Bergmann's equations. The relative contributions c_1 and c_2 (Table 2) towards dielectric relaxations in terms of estimated τ_1 and τ_2 (Table 1) were evaluated by the graphical method[1,2] using Figs 2 and 3 as well as by Fröhlich's equations[9] respectively. The symmetric and the asymmetric distribution parameters of such compounds under the effective dispersive region of 9.945 GHz electric field can also be judged to throw much light on their distribution behaviour (Table 2). In absence of the reliable τ of such isomers of anisidine and toluidine, the slope of the linear variations of the imaginary

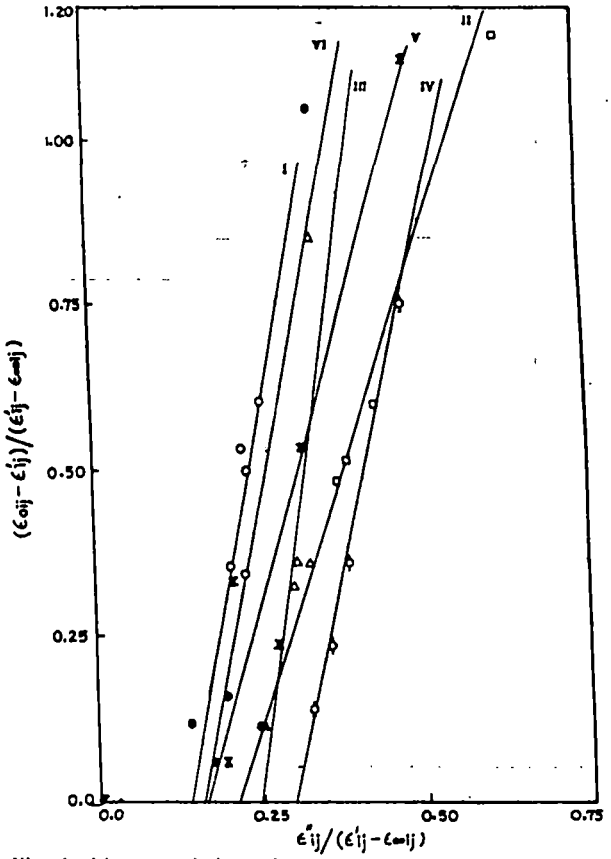

Fig. 1—Linear variation of $(\varepsilon_{0ij}-\varepsilon'_{ij})/(\varepsilon'_{ij}-\varepsilon_{\infty ij})$ against $\varepsilon''_{ij}/(\varepsilon'_{ij}-\varepsilon_{\infty ij})$ of mono-substituted anilines under 9·945 GHz electric field at 35°C. (System-I: *o*-anisidine, (−○−) System-II: *m*-anisidine, (−□−) System-III: *p*-anisidine, (−△−) System-IV: *o*-toluidine, (−⧖−) System-V: *m*-toluidine, (−⧗−) System-VI: *p*-toluidine, (−●−).

Table 1—The slope and intercept of the straight lines of $[(\varepsilon_{0ij}-\varepsilon'_{ij})/(\varepsilon'_{ij}-\varepsilon_{\infty ij})]$ against $[\varepsilon''_{ij}/(\varepsilon'_{ij}-\varepsilon_{\infty ij})]$, correlation co-efficients (r), % of error involved, relaxation times τ_1 and τ_2 of the flexible parts as well as the whole molecules, measured τ from $K''_{ij}-K'_{ij}$ equations and the most probable relaxation times τ_0 together with τ_s and τ_{as} from symmetric and asymmetric distribution parameters γ and δ of monosubstituted anilines at 35°C under 9.945 GHz electric field

System with Sl. No.	Slope and intercept of straight line Eq. (7) $[(\varepsilon_{0ij}-\varepsilon'_{ij})/(\varepsilon'_{ij}-\varepsilon_{\infty ij})]$ versus $[\varepsilon''_{ij}/(\varepsilon'_{ij}-\varepsilon_{\infty ij})]$		Correlation Co-efficient (r)	% of error involved in Eq. (7)	Estimated relaxation times τ_1 & τ_2 in p sec		Most probable relaxation time $\tau_0=\sqrt{\tau_1\tau_2}$ in p sec	Measured τ from $K''_{ij}-K'_{ij}$ Eq. (20) in p sec	τ_s from symmetric distribution parameter γ of Eq. (13)	τ_{as} from asymmetric distribution parameter δ of Eq. (15)
I *o*-anisidine	4.9294	0.6583	0.7789	11.86	2.20	76.73	12.99	3.54	0.55	61.91
II *m*-anisidine	2.9043	0.6073	0.9888	0.67	3.63	42.87	12.47	4.77	14.78	86.39
III *p*-anisidine	6.2098	1.4923	0.8308	9.34	4.01	95.42	19.56	4.20	1.41	75.33
IV *o*-toluidine	4.2660	1.2707	0.9994	0.04	5.16	63.15	18.05	4.56	4.62	41.71
V *m*-toluidine	3.3514	0.5415	0.9622	2.24	2.73	50.94	11.79	5.52	0.64	66.69
VI *p*-toluidine	4.7133	0.7348	0.8684	7.41	2.58	72.88	13.71	3.57	0.66	20.13

Table 2—The estimated values of $x[=(\varepsilon'_{ij}-\varepsilon_{\infty ij})/(\varepsilon_{0ij}-\varepsilon_{\infty ij})]$ and $y[=\varepsilon''_{ij}/(\varepsilon_{0ij}-\varepsilon_{\infty ij})]$ from Fröhlich's equations and by the graphical techniques at $\omega_j \to 0$, Fröhlich's parameter A, symmetric and asymmetric distribution parameters γ and δ from x and y at $\omega_j \to 0$ along with the relative contributions c_1 and c_2 due to Fröhlich and the graphical technique under 9.945 GHz electric field

System with Sl. No	Fröhlich's parameter $A=\ln(\tau_2/\tau_1)$	Estimated values of x and y from Fröhlich's Eqs (8) and (9)		Weighted contributions c_1 & c_2 from Eqs (5) & (6)		Estimated values of x & y from Figs (2) & (3) at $\omega_j \to 0$		Weighted contributions c_1 & c_2 from the graphical technique		Symmetric & asymmetric distribution parameters γ & δ	
I *o*-anisidine	3.5518	0.5555	0.3457	0.5069	1.3869	0.0875	0.106	0.8946	−0.0732	0.47	0.09
II *m*-anisidine	2.4689	0.5848	0.4009	0.4997	0.8945	0.515	0.254	0.4825	0.4574	0.40	0.33
III *p*-anisdine	3.1695	0.4420	0.3655	0.4223	1.6298	0.810	0.140	0.8725	−0.4020	0.49	0.13
IV *p*-toluidine	2.5046	0.4594	0.4033	0.4293	1.1669	0.740	0.228	1.1326	−0.0478	0.35	0.25
V *m*-toluidine	2.9263	0.5933	0.3748	0.5170	1.0107	0.870	0.106	0.9097	−0.1564	0.49	0.09
VI *p*-toluidine	3.3410	0.5432	0.3574	0.4942	1.3351	0.950	0.084	0.9908	−0.3417	0.29	0.09

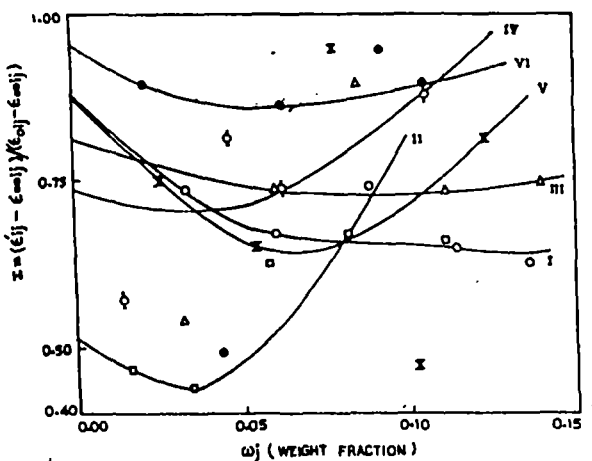

Fig. 2—Variation of $(\varepsilon'_{ij}-\varepsilon_{\infty ij})/(\varepsilon_{0ij}-\varepsilon_{\infty ij})$ against weight fraction ω_js' of solutes under 9.945 GHz electric field at 35°C. (System-I: *o*-anisidine, (−○−) System-II: *m*-anisidine, (−□−) System-III: *p*-anisidine, (−△−) System-IV: *o*-toluidine, (−⧩−) System-V: *m*-toluidine, (−⧗−) System-VI: *p*-toluidine, (−●−).

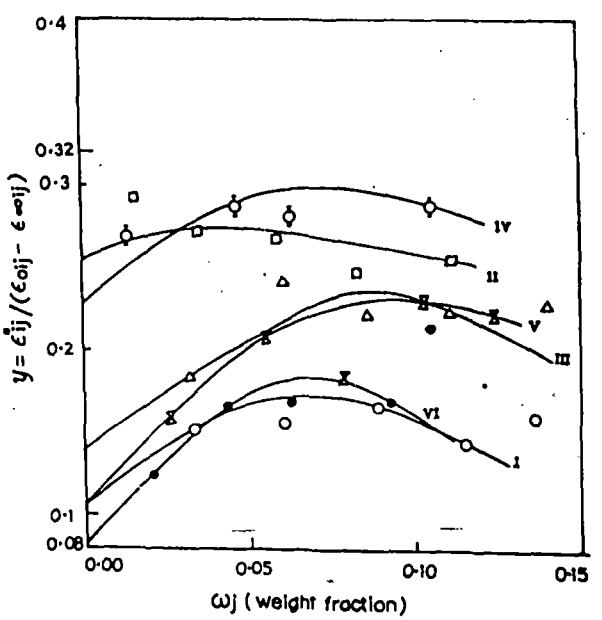

Fig. 3—Variation of $\varepsilon''_{ij}/(\varepsilon_{0ij}-\varepsilon_{\infty ij})$ against ω_js' of isomers of anisidines and toluidines under 9.945 GHz electric field at 35°C. (System-I: *o*-anisidine, (−○−) System-II: *m*-anisidine, (−□−) System-III: *p*-anisidine, (−△−) System-IV: *o*-toluidine, (−⧩−) System-V: *m*-toluidine, (−⧗−) System-VI: *p*-toluidine, (−●−).

parts K''_{ij} against the real parts K'_{ij} of the complex *hf* conductivities K^*_{ij} of the solutions were used to τ as shown in Table 1, together with τ_1, get τ_s and τ_{cs} where τ_0 is the most probable relaxation time given by $\tau_0=\sqrt{\tau_1\tau_2}$, τ_s and τ_{cs} are called symmetric and characteristic relaxation times associated with symmetric and asymmetric distribution parameters γ and δ respectively. The respective dipole moments μ_1, μ_2 and μ_0 in terms of τ_1, τ_2 and τ_0 of these compounds as obtained from the slope β of the linear variations of total *hf* conductivities K_{ij}s' of the solutions against ω_js' of monosubstituted anilines in benzene (Fig. 4) are in close agreement with the theoretical dipole moments μ_{theo}s', (Table 3) as computed from bond angles and bond moments of several groups in anisidines and toluidines with respect to benzene ring.

2 Theory and Formulation

When the polar molecule is provided with more than one relaxation times i.e., τ_1 and τ_2 Debye's equations of polar-nonpolar liquid mixture lead to Bergmann's equatons:

$$\frac{\varepsilon'_{ij}-\varepsilon_{\infty ij}}{\varepsilon_{0ij}-\varepsilon_{\infty ij}}=\frac{c_1}{1+\omega^2\tau_1^2}+\frac{c_2}{1+\omega^2\tau_2^2} \quad \ldots(1)$$

$$\frac{\varepsilon''_{ij}}{\varepsilon_{0ij}-\varepsilon_{\infty ij}}=c_1\frac{\omega\tau_1}{1+\omega^2\tau_1^2}+c_2\frac{\omega\tau_2}{1+\omega^2\tau_2^2} \quad \ldots(2)$$

such that $c_1+c_2=1$.

The co-efficients c_1 and c_2 are the weight factors of the two Debye processes governed by τ_1 and

Table 3—Intercept and slope of $K_{ij}-\omega_j$ curve, dimensionless parameters bs' dipole moments μ_is' in Debye (D) together with estimated μ_1 from $\mu_1=\mu_2(c_1/c_2)^{1/2}$ and theoretical μ from bond angles and bond moments of isomers of anisidine and toluidine at 9.945 GHz electric field and at 35°C

System with Sl. No. & mol wt	Intercept & slope of $K_{ij}-\omega_j$ equation		Dimensionless parameters			Estimated dipole moments in Debye			Theoretical μ_{theo} in D from bond angles and bond moments	Estimated $\mu_{theo}\mu_1$ from $\mu_2(c_1/c_2)^{1/2}$ D
	$\alpha\times10^{-10}$ esu	$\beta\times10^{-10}$ esu	$b_0=\frac{1}{1+\omega^2\tau_0^2}$	$b_1=\frac{1}{1+\omega^2\tau_1^2}$	$b_2=\frac{1}{1+\omega^2\tau_2^2}$	μ_0 D	μ_1 D	μ_2 D		
I *o*-anisidine $M_1=123$ gm	1.1244	0.7757	0.6030	0.9815	0.0417	2.45	1.92	9.33	1.02	5.64
II *m*-anisidine	1.1039	1.4215	0.6224	0.9511	0.1224	3.27	2.264	7.37	1.65	5.51
III *m*-anisidine $M_1=123$ gm	1.1060	1.4663	0.4012	0.9410	0.0274	4.13	2.70	15.82	1.89	8.05
IV *o*-toluidine $M_1=107$ gm	1.1151	1.1932	0.4404	0.9059	0.0604	3.32	2.31	8.96	1.39	5.43
V *m*-toluidine $M_1=107$ gm	1.1359	0.5788	0.6484	0.9718	0.0899	1.91	1.56	5.12	1.03	3.66
VI *p*-toluidine $M_1=107$ gm	1.1323	0.3501	0.5770	0.9747	0.0460	1.57	1.21	5.56	1.54	3.38

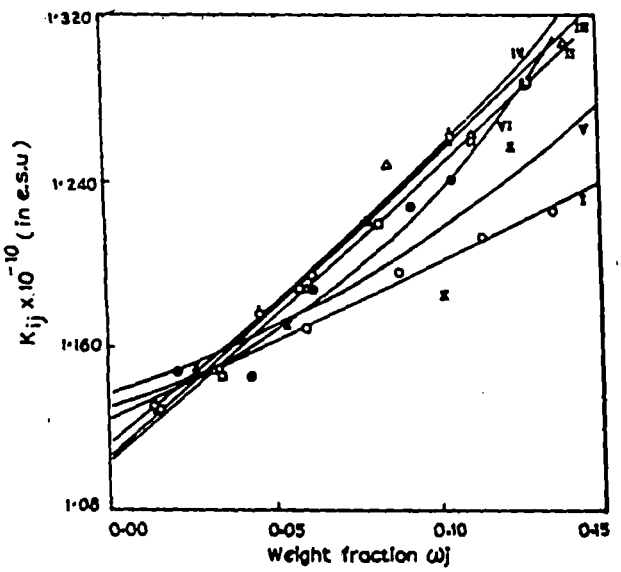

Fig. 4—Variation of hf conductivity K_{ij} with different weight fractions ω_js' of solutes at 35°C and 9.945 GHz electric field. (System-I: *o*-anisidine, (−○−) System-II' *m*-anisidine, (−□−) System-III: *p*-anisidine, (−△−) System-IV: *o*-toluidine, (−⧖−) System-V: *m*-toluidine, (−⧗−) System-VI: *p*-toluidine, (−●−).

τ_2 respectively. The symbols used in Eqs (1) and (2) convey the usual meanings:

$$\text{Let } x=\frac{\varepsilon'_{ij}-\varepsilon_{\infty ij}}{\varepsilon_{0ij}-\varepsilon_{\infty ij}}, \qquad y=\frac{\varepsilon''_{ij}}{\varepsilon_{0ij}-\varepsilon_{\infty ij}}$$

and $\omega\tau=\alpha$. Using the notations $a=1/(1+\alpha^2)$ and $b=\alpha/(1+\alpha^2)$ the above Eqs (1) and (2) can be written as:

$$x=c_1a_1+c_2a_2 \qquad \ldots(3)$$

$$y=c_1b_1+c_2b_2 \qquad \ldots(4)$$

The suffices 1 and 2 with a and b are related to τ_1 and τ_2 respectively.

Evaluating c_1 and c_2 from Eqs (3) and (4) one gets:

$$c_1=\frac{(x\alpha_2-y)(1+\alpha_1^2)}{\alpha_2-\alpha_1} \qquad \ldots(5)$$

and

$$c_2=\frac{(y-x\alpha_1)(1+\alpha_2^2)}{\alpha_2-\alpha_1} \qquad \ldots(6)$$

provided $\alpha_2>\alpha_1$. Now adding Eqs (5) and (6) and since $c_1+c_2=1$ we get:

$$\frac{1-x}{y}=(\alpha_1+\alpha_2)-\frac{x}{y}\alpha_1\alpha_2$$

which on substitution of the values of x, y and α yields:

$$\frac{\varepsilon_{0ij}-\varepsilon'_{ij}}{\varepsilon'_{ij}-\varepsilon_{\infty ij}}=\omega(\tau_1+\tau_2)\frac{\varepsilon''_{ij}}{\varepsilon'_{ij}-\varepsilon_{\infty ij}}-\omega^2\tau_1\tau_2 \qquad \ldots(7)$$

representing a straight line of $[(\varepsilon_{0ij}-\varepsilon'_{ij})/(\varepsilon'_{ij}-\varepsilon_{\infty ij})]$ against $[\varepsilon''_{ij}/(\varepsilon'_{ij}-\varepsilon_{\infty ij})]$ with slope $\omega(\tau_1+\tau_2)$

and intercept $-\omega^2\tau_1\tau_2$. The slopes and intercepts of Eq.(7) were, however, evaluated by fitting ε'_{ij}, ε''_{ij}, ε_{0ij} and $\varepsilon_{\infty ij}$ for different ω_is' of the mono-substituted anilines, referred to Tables (1-3) and Figs (1-4) at 35°C under 9.945 GHz electric field. They are finally placed in Table 1, to yield τ_1 and τ_2 respectively for them.

The weighted contributions c_1 and c_2 towards dielectric relaxation may be computed from Eqs (5) and (6) by using x and y in Fröhlich's equations (Ref. 9)

$$x=\frac{\varepsilon'_{ij}-\varepsilon_{\infty ij}}{\varepsilon_{0ij}-\varepsilon_{\infty ij}}=1-\frac{1}{2A}\ln\left(\frac{1+e^{2A}\omega^2\tau_s^2}{1+\omega^2\tau_s^2}\right) \quad \ldots(8)$$

and

$$y=\frac{\varepsilon''_{ij}}{\varepsilon_{0ij}-\varepsilon_{\infty ij}}=\frac{1}{A}[\tan^{-1}(e^A\omega\tau_s)-\tan^{-1}(\omega\tau_s)] \quad \ldots(9)$$

where A = Fröhlich parameter $=\ln(\tau_2/\tau_1)$ and τ_s = small limiting relaxation time $=\tau_1$. Both c_1 and c_2 may also be calculated from Eqs (5) and (6) with the graphically extrapolated fixed values of x and y when $\omega_i\to 0$ as shown in Figs (2) and (3). They are shown in Table 2.

The molecules appear to behave like nonrigid ones having either symmetric or asymmetric distribution parameters γ and δ which may be calculated from Eqs (10-11)

$$\varepsilon^*_{ij}=\varepsilon_{\infty ij}+\frac{\varepsilon_{0ij}-\varepsilon_{\infty ij}}{1+(j\omega\tau_s)^{1-\gamma}} \quad \ldots(10)$$

or

$$\varepsilon^*_{ij}=\varepsilon_{\infty ij}+\frac{\varepsilon_{0ij}-\varepsilon_{\infty ij}}{(1+j\omega\tau_{cs})^{\delta}} \quad \ldots(11)$$

the former and the latter ones are associated with τ_s and τ_{cs} where τ_s and τ_{cs} are called the symmetric as well as the characteristic relaxation times. Separating the real and the imaginary parts of Eqs (10) and (11) and rearranging them in terms of x and y as shown in Figs (2) and (3) at $\omega_i\to 0$ we have the symmetric parameter γ from:

$$\gamma=\frac{2}{\pi}\tan^{-1}\left[(1-x)\frac{x}{y}-y\right] \quad \ldots(12)$$

and the symmetric relaxation time τ_s from:

$$\tau_s=\frac{1}{\omega}\left\{\frac{1}{\left[\frac{x}{y}\cos\left(\frac{\gamma\pi}{2}\right)-\sin\left(\frac{\gamma\pi}{2}\right)\right]}\right\}^{1/(1-\gamma)} \quad \ldots(13)$$

similarly, δ and τ_{cs} can be had from Eqs (11) as:

$$\tan(\delta\phi)=\frac{y}{x} \quad \ldots(14)$$

and

$$\tan\phi=\omega\tau_{cs} \quad \ldots(15)$$

As the values of ϕ cannot be estimated directly we draw a theoretical curve for $\log(\cos\phi)^{1/\phi}$ against ϕ as shown in Fig. 5 from which

$$\log(\cos\phi)^{1/\phi}=\frac{\log\dfrac{x}{\cos(\delta\phi)}}{\delta\phi} \quad \ldots(16)$$

can be known. With the known ϕ from Fig. 5; τ_{cs} and δ can be estimated from Eqs (14) and (15) respectively. The τ_s and τ_{cs} thus estimated are placed in Table 1 to compare with τ_1 and τ_2 from double relaxation method, but γ and δ are placed in Table 2.

The complex high frequency conductivity K^*_{ij} of a dilute polar-nonpolar liquid mixture[12] is given by:

$$K^*_{ij}=K'_{ij}+jK''_{ij} \quad \ldots(17)$$

where

$$K'_{ij}=\frac{\omega}{4\pi}\varepsilon''_{ij} \text{ and } K''_{ij}=\frac{\omega}{4\pi}\varepsilon'_{ij}$$

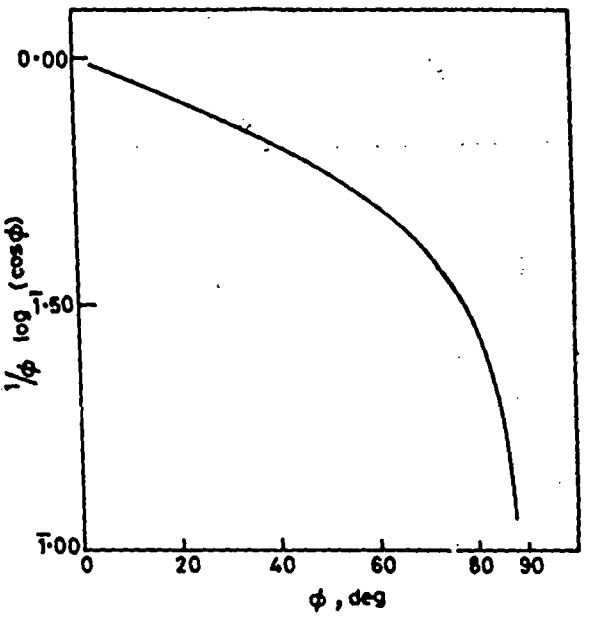

Fig. 5—Variation of $\log(\cos\phi)^{1/\phi}$ against ϕ.

The magnitude of the total *hf* conductivity is:

$$K_{ij} = \frac{\omega}{4\pi} (\varepsilon''^2_{ij} + \varepsilon'^2_{ij})^{1/2} \quad \ldots (18)$$

The dielectric permittivity ε'_{ij} of solution in *hf* region is very small and eventually equals the optical dielectric constant. The dielectric loss ε''_{ij} is responsible for the absorption of electrical energy and, therefore, offers resistance to polarisation. The K_{ij} may thus be approximated as:

$$K_{ij} = \frac{\omega}{4\pi} \varepsilon'_{ij} \text{ since } \varepsilon'_{ij} \gg \varepsilon''_{ij}$$

The real part of the complex conductivity of a solution of weight-fraction ω_j of polar solute at TK is:

$$K'_{ij} = \frac{\mu_j^2 N \rho_{ij} F_{ij}}{3 M_j k T} \left(\frac{\omega^2 \tau}{1 + \omega^2 \tau^2} \right) \omega_j \quad \ldots (19)$$

where the symbols have their usual significance. But for *hf* region it can be shown that

$$K''_{ij} = K_{\infty ij} + \frac{K'_{ij}}{\omega \tau}$$

or

$$K_{ij} = K_{\infty ij} + \frac{K'_{ij}}{\omega \tau} \quad \ldots (20)$$

Since K_{ij} is a function of ω_j it can be shown at infinite dilution:

$$\left(\frac{d K'_{ij}}{d \omega_j} \right)_{\omega_j \to 0} = \omega \tau \beta \quad \ldots (21)$$

where β is the slope of $K_{ij} - \omega_j$ curve at $\omega_j \to 0$. Eq. (19) on being differentiated with respect to ω_j and at $\omega_j \to 0$ becomes:

$$\left(\frac{d K'_{ij}}{d \omega_j} \right)_{\omega_j \to 0} = \frac{\mu_j^2 N \rho_i F_i}{3 M_j k T} \left(\frac{\omega^2 \tau}{1 + \omega^2 \tau^2} \right) \quad \ldots (22)$$

because at $\omega_j \to 0$, ρ_{ij} the density of the solution becomes ρ_i, the density of the solvent and F_{ij} the local field in the solution becomes F_i, where $F_i = [(\varepsilon_i + 2)/3]^2$, ε_i, is the dielectric constant of the solvent. From Eqs (21) and (22) we finally get:

$$\mu_j = \left(\frac{3 M_j k T \beta}{N \rho_i F_i \omega b} \right)^{1/2} \quad \ldots (23)$$

as the dipole moment of the polar liquid in terms of b where

$$b = \frac{1}{1 + \omega^2 \tau^2} \quad \ldots (24)$$

which is a dimensionless parameter. The μ_1, μ_2 and μ_0 in terms of b_1, b_2 and b_0 involved with τ_1, τ_2 and τ_0 respectively were then computed with the knowledge of β. They are finally placed in Table 3 together with μ_{theo} obtained from bond angles and bond moments for comparison.

3 Results and Discussion

The values of x and y in terms of dielectric relaxation data at 9.945 GHz are first estimated for different ω_js' with the available data[8] measured under 2.02, 3.86 and 22.06 GHz electric field. They are then plotted against ω_js' as shown in Figs (2) and (3) which are found to agree well with the Bergmann Eqs (1) and (2) almost exactly. The close agreement of the curves in Figs (2) and (3) with Eqs (1) and (2) suggests that the data selected by graphical interpolations at 3 cm wavelength electric field are almost accurate. The dielectric relaxation parameters ε'_{ij}, ε''_{ij}, ε_{0ij} and $\varepsilon_{\infty ij}$ thus obtained, are used to calculate the slopes and the intercepts of the fitted straight lines of Eq. (7) with the experimental points placed upon them as shown in Fig. 1. The correlation coefficient r for each straight line is, however, estimated and found to lie within the range of 0.9994 to 0.7789 together with % error involved in each case. They are shown in 4th and 5th columns of Table 1. Table 1 also shows that *o*- and *p*-anisidine like *p*-toluidine exhibit errors of larger magnitudes than the other systems. This may, perhaps, be due to the uncertainty in the estimation of dielectric relaxation data for such systems. Monosubstituted anilines often showed double as well as mono relaxation behaviour as observed earlier[2]. *p*-anisidine, however, is an exception[2]. It showed the mono relaxation behaviour at 2.02, 3.86 and 22.06 GHz respectively. It is again very much interesting to note that all the anisidines and toluidines as referred to Table 1, nevertheless exhibit the double relaxation behaviour by showing reasonably considerable values of τ_1 (smaller) and τ_2 (larger) to represent the relaxation times for their flexible parts attached to the parent ring and the whole molecules respectively. It signifies that 9.945 GHz (≈ 3 cm, wavelength) electric field seems to be the most effective dispersive region for such molecule to yield τ_1 and τ_2.

The τ_2s' as observed from the slopes and the

intercepts of Eq. (7) gradually increase from *meta*- to *ortho*- and to *para*-forms of all the anisidines and toluidines probably due to $C \rightarrow NH_2$ groups which is highly influenced by 9.945 GHz ($\simeq$ 3 cm wavelength) electric field for its different positions in them. The τ_1s', on the other hand, increase from ortho to para for anisidines while reverse is true for toluidines. The increase in the values of τ_1s' indicates the flexible parts of the molecules are more loosley bound to parent molecules[1,2].

The most probable relaxation time τ_0 as shown in the 8th column of Table 1, can be compared with the measured τs' from the slopes[5] of $K''_{ij} - K'_{ij}$ along with symmetric τ_s and characteristic τ_{cs} from γ and δ. The τs' as shown in the 9th column of Table 1 agree excellently well with τ_1. This fact indicates that the *hf* conductivity measurement of polar-nonpolar liquid mixture yields the microscopic relaxation time while the double relaxation method gives macroscopic as well as microscopic relaxation times as observed earlier[13]. τ_ss' in Table 1 are slightly smaller than τs; as obtained from *hf* conductivity for almost all systems besides *m*-anisidine and *o*-toluidine whose τ_ss' agree well with τ_0 and τ respectively. The slight difference is due to different steric hindrances as a result of structural conformations. All these discussions made above, confirms τ_s to represent microscopic relaxation time. τ_{cs}s, on the other hand, are larger in magnitude and agree with τ_2 as obtained by double relaxation method. Thus τ_{cs} under the electric field of 9.945 GHz gives τ_2.

The relative contributions c_1 and c_2 towards dielectric relaxations were found out in the graphical method by using Figs 2 and 3 as well as Fröhlich's equations of $x\left[=\frac{\varepsilon'_{ij}-\varepsilon_{\infty ij}}{\varepsilon_{0ij}-\varepsilon_{\infty ij}}\right]$ and $y\left[=\frac{\varepsilon''_{ij}}{\varepsilon_{0ij}-\varepsilon_{\infty ij}}\right]$ both from Bergmann's Eqs (1) and (2) in terms of τ_1 and τ_2. The x and y in Fröhlich's Eqs (8) and (9) are related to Fröhlich parameter A which depends on the difference of the activation energies E_2 and E_1 of the rotating units and is expressed in terms of τ_2/τ_1 by $\tau_2/\tau_1 = \exp(E_2 - E_1)/RT$. The constancy of the factor $(E_2 - E_1)/RT$ at a fixed temperature may be put equal to A where $A = \ln(\tau_2/\tau_1)$. The positive values of c_1 and c_2 such that $c_2 > c_1$ and $c_1 + c_2 > 1$ in Fröhlich's method for all the systems are shown in the 5th and 6th columns of Table 2 together with the Fröhlich parameters A in the 2nd column respectively. But the graphical extrapolation technique suggested by Saha *et al.*[1] and Sit *et al.*[2], however, yields c_2 always negative except m-anisidine satisfying the condition that $c_1 + c_2 \simeq 1$ as shown in the 9th and 10th columns of same Table 2. The negative sign before c_2 in the latter method signifies the lag in inertia of the whole molecules with respect to their flexible parts[1,2] under *hf* electric field.

The double relaxation times showed by all the monosubstituted anilines under 9.945 GHz electric field at 35°C indicate the nonrigidity of the molecules. This fact at once inspired us to test the symmetric as well as asymmetric distribution parameters γ and δ for such compounds. They are calculated from Eqs (12) and (16) with the values of x and y at $\omega_j \rightarrow 0$ from Figs 2 and 3. The values of γ and δ thus obtained with the aid of the direct measurements of relaxation data seem to be accurate enough to specify the distribution parameters as placed in the last two columns of Table 2. It is observed from Table 2 that the values of γ lie in the range of $0.29 \leqslant \gamma \leqslant 0.49$ indicating thereby symmetric relaxation behaviour for such molecules under 9.945 GHz electric field. The low values of δ in the range of $0.09 \leqslant \delta \leqslant 0.33$ invariably rules out the possibility of occurrence of asymmetric dielectric distributions[14].

The dipole moments μ_1 and μ_2 of the flexible parts and the whole molecules of anisidines and toluidines are obtained from Eq. (23) in terms of dimensionless parameters b_1, b_2 from Eq. (24) involved with τ_1 and τ_2 respectively (Table 1) and the slope β of $K_{ij} - \omega_j$ curves in Fig. 4 which shows the variation of K_{ij}s' with ω_js'. The intercepts and slopes of $K_{ij} - \omega_j$ equations are shown in the 2nd and 3rd columns of Table 3. The intercepts are of almost equal in magnitudes in all them, but the slopes β increase slowly from *ortho*- to *para*- for anisidines and reverse in toluidines. The almost same intercepts and slopes of $K_{ij} - \omega_j$ curves in Fig. 4 arise probably due to the identical polarity[3] of the molecules. Some of the curves in Fig. 4 meet at a point near $\omega_j \rightarrow 0$ indicating thereby solute-solvent (monomer) or solute-solute (dimer) associations in the region $0.02 < \omega_j < 0.035$ of the concentration. Unlike toluidines the most probable dipole moments μ_0 and μ_1 gradually increase from *o*- to *p*- for anisidines as reported in 7th and 8th columns of Table 3. μ_2s, on the other hand, increase gradually from *m*- to *o*- with a high value in *p*-anisidine while in case of toluidines μ_2s' increase from *m*- to *p*- and *o*-configurations. The above facts, however, reveal that μ_0 as obtained from $\tau_0 = \sqrt{\tau_1 \tau_2}$ depends solely upon the group moments like μ_1 of their flexible parts. The gradual increase of μ_0 from *o*- to *p*-anisidine and from *p*- to *o*-toluidine like μ_1 is probably due to their almost same polarity as supported by the slopes βs' of K_{ij} as a function of ω_js' (Fig. 4).

The theoretical dipole moments μ_{theo}s' from the bond angles and bond moments of C→OCH_3 in anisidines and C→CH_3 in toluidines with C→NH_2 with respect to the benzene ring were already calculated elsewhere[2] and placed in the 10th column of Table 3. They are compared with all the μs' together with μ_1 from $\mu_1 = \mu_2(c_1/c_2)^{1/2}$ assuming the two relaxation processes are equally probable.

4 Conclusion

The correlation coefficients rs' and hence the % of errors introduced in Eq. (7) with the dielectric relaxation parameters like ε'_{ij}, ε''_{ij}, ε_{0ij} and $\varepsilon_{\infty ij}$ of the polar-nonpolar liquid mixtures under 9.945 GHz electric field at 35°C, as presented in Table 1, are within such range that τ_1 and τ_2 as obtained from the intercepts and slopes of Eq. (7) are of considerable accuracy because τs' are usually claimed to be accurate within ± 10%. The methodology of single frequency measurements of dielectric relaxation data at different ω_js' seems to be much simple in comparison to the existing methods where data of pure polar liquid at two or more electric field frequencies of GHz region are, usually required. The relative contributions c_1 and c_2 in terms of τ_1 and τ_2 are, however, obtained by using Fröhlich's equations as well as graphical technique which also offers a convenient method to decide either symmetric or asymmetric distribution behaviour under the electric field of given frequency. The dipole moments μ_1, μ_2 in terms of τ_1 and τ_2 and slop β of concentration variation of K_{ij} of polar-nonpolar liquid mixture provide the valuable information of the conformation of a complex polar liquid.

References

1 Saha U, Sit S K, Basak R C & Acharyya S, *J Phys D*, 27 (1994) 596.
2 Sit S K, Basak R C, Saha U & Acharyya S, *J Phys D*, 27 (1994) 2194.
3 Chatterjee A K, Saha U, Nandi N, Basak R C & Acharyya S, *Indian J Phys B*, 66 (1992) 291.
4 Saha U & Acharyya S, *Indian J Pure & Appl Phys*, 31 (1993) 181.
5 Saha U & Acharyya S, *Indian J Pure & Appl Phys*, 32 (1994) 346.
6 Bergmann K, Roberti D M & Smyth C P, *J Phys Chem*, 64 (1960) 665.
7 Bhattacharyya J, Hasan A, Roy S B & Kastha G S, *J Phys Soc Japan*, 28 (1970) 204.
8 Srivastava S C & Suresh Chandra, *Indian J Pure & Appl Phys*, 13 (1975) 101.
9 Fröhlich H, *Theory of dielectrics* (Oxford University Press, Oxford), 1949, p 94.
10 Cole K S & Cole R H, *J Chem Phys*, 9 (1941) 341.
11 Davidson D W & Cole R H, *J Chem Phys*, 19 (1951) 1484.
12 Murphy F J & Morgan S O, *Bull syst Techn J*, 18 (1939) 502.
13 Sit S K & Acharyya S, *Indian J Phys B*, 70 (1996) 14.
14 Suresh Chandra & Jai Prakash, J Phys Soc Japan, 35 (1975) 876.

Indian J. Phys. **70B** (1), 19–36 (1996)

I J P
an international journal

Double relaxation of straight chain alcohols under high frequency electric field

S K Sit* and S Acharyya

Department of Physics, Raiganj (University) College,
Raiganj, Uttar Dinajpur-733 134, West Bengal, India

Received 28 April 1995, accepted 30 August 1995

Abstract : Alcohols like 1-butanol, 1-hexanol, 1-heptanol and 1-decanol are long straight chain polar molecules almost like polymers. In these alcohols as well as in methanol and ethanol, there exist many possibilities of having internal rotation, bending and twisting, each with a characteristic relaxation time, under high frequency electric field of Giga hertz range. An attempt is, therefore, made to detect the double relaxation phenomena by the new approach suggested earlier. It involves single frequency measurements of the dielectric relaxation data of those compounds in solvent *n*-heptane at 25°C under three different frequencies of 24.33, 9.25 and 3.00 GHz electric field as well as those of methanol and ethanol in benzene at 9.84 GHz respectively to get τ_1 and τ_2 for their flexible parts and the whole molecules. The alcohols under investigation, always exhibit the double relaxation behaviours at all frequencies except methanol at 9.84 GHz, thus indicating separate broad dispersions in them. The relative contributions c_1 and c_2 towards dielectric relaxations due to τ_1 and τ_2, are calculated from Frohlich's equations to compare with those as obtained by graphical technique. The dipole moments μ's are also estimated in terms of the relaxation times τ_1 and τ_2, obtained from the slopes β's of the ht conductivities K_{ij}'s of the solutions against the weight fraction w_j's of the solutes in order to support their usual conformations.

Keywords : Double relaxation, dipole moments, straight chain alcohols

PACS Nos. : 33.15.Kr, 31.70.Dk, 31.70.Hq

1. Introduction

The dielectric relaxation phenomena of highly nonspherical polar liquids in nonpolar solvents under the ultra high frequency (uhf) electric fields have gained much attention [1,2] as they reveal various types of molecular interactions like solute-solute (dimer) and solute-solvent (monomer) formations in liquid mixtures. They also provide one with

The nomenclature of symbols used, are given in the Appendix.

* Department of Physics, Raiganj Polytechnic, Raiganj-733 134, West Bengal, India

valuable information regarding sizes, shapes, structures and different thermodynamic parameters due to relaxation of the polar liquids [3].

The relaxation phenomena of pure primary alcohols are very interesting as they were found to possess three distinct low frequency Debye type processes predicting inherently the single relaxation time [4,5]. The dilution of polar alcohols with nonpolar solvents, however, increases the relative contributions towards dielectric dispersions in the hf electric field [6]. The straight chain mono-alcohols, on the other hand, are almost like polymers having $-CH_3$ and $-OH$ groups in their structures. Obviously, there exist many possibilities of internal and molecular rotations, bending, twisting *etc* each with a characteristic relaxation time. In averaging to the macroscopic condition, a distribution of relaxation time may also be possible. Mishra *et al* [7] claimed that it is not possible to resolve dielectric dispersion in three relaxation processes from the measured relaxation data under a single frequency electric field.

Again, to detect the double relaxation phenomena of a polar solute, Bergmann *et al* [8] proposed a technique based on measured relaxation parameters of pure polar liquid like real ε', loss ε'' of the complex dielectric constant ε^* as well as static ε_0 and the high frequency dielectric constant ε_∞ at different frequencies of the electric field. The term $\frac{\varepsilon' - \varepsilon_\infty}{\varepsilon_0 - \varepsilon_\infty}$ was then plotted against $\frac{\varepsilon''}{\varepsilon_0 - \varepsilon_\infty}$ following Cole-Cole semi-circle equation. A suitable chord joining the two fixed points on the semi-circle consistent with all the experimental points is then chosen to yield the relaxation time τ_1 and τ_2 of the flexible part and the whole molecule itself. Bhattacharyya *et al* [9] had subsequently modified the procedure of Bergmann *et al* [8] to get τ_1 and τ_2 of a pure polar liquid in terms of the relaxation parameters measured at two different frequencies of the electric field in the GHz range.

In such a context, we have studied the double relaxation phenomena of some straight chain aliphatic alcohols, namely 1-butanol, 1-hexanol, 1-heptanol and 1-decanol dissolved in n-heptane at 24.33, 9.25 and 3.00 GHz electric field together with methanol and ethanol dissolved in benzene at 9.84 GHz electric field respectively at a temperature of 25°C by the recently developed method [10]. It is usually made with the single frequency measurements of the dielectric relaxation parameters like ε'_{ij}, ε''_{ij}, ε_{0ij} and $\varepsilon_{\infty ij}$ of a polar solute (j) in a nonpolar solvent (i) for different weight fractions w_j's of the polar solute. τ_1 and τ_2 are then obtained from the slope and the intercept of a straight line equation containing the dielectric relaxation data of which ε_{0ij} and $\varepsilon_{\infty ij}$ should be accurately known [11]. The approach as suggested earlier [10], seems to be an effective tool to detect the double relaxation phenomena of the polar liquid in a nonpolar solvent within the framework of Debye and Smyth model. For such straight chain alcohols behaving almost like polymers, Onsager's equation may be a better choice due to the strong intermolecular force exerted by alcohols in solution owing to their high dipole moments. But the resulting expressions can not be solved so easily as has been done in [10], because of the presence of the quadratic term ε^*_{ij}. The method [10] was already applied to mono-substituted anilines [12] in benzene in order

Table 1. The estimated intercept and slopes of straight line equation $\left[(\epsilon_{0ij} - \epsilon'_{ij})/(\epsilon'_{ij} - \epsilon_{\infty ij})\right]$ against $\left[\epsilon''_{ij}/(\epsilon'_{ij} - \epsilon_{\infty ij})\right]$ with errors and correlation coefficients together with measured τ's of some normal alcohols at 25°C under different ultra high frequency (~ gigahertz) electric field.

System with Sl. No. and molecular wt.	Frequency f in GHz	Intercept and slope of equation (8)		Correlation coefficient (r)	Percentage error in regression technique	Estimated values of τ_2 and τ_1 in p Sec		Measured τ_s in p Sec	Most probable relaxation time $\tau_0 = \sqrt{\tau_1 \tau_2}$ in p Sec
I) 1-Butanol in	(a) 24.33	2.6046	8.6557	0.9013	5.16	54.60	2.04	1.96	10.55
n-heptane	(b) 9.25	1.2809	6.1343	0.9347	3.47	101.87	3.73	4.30	19.49
$M_j = 74$ gm	(c) 3.00	0.6825	4.1544	0.9328	3.57	211.41	9.10	16.98	43.86
II) 1-Hexanol in	(a) 24.33	2.045	6.7079	0.6195	18.58	41.81	2.10	2.74	9.37
n-heptane	(b) 9.25	1.0803	5.1697	0.9163	4.42	85.24	3.76	5.86	17.90
$M_j = 102$ gm	(c) 3.00	0.6651	4.0210	0.9308	3.67	204.26	9.17	13.14	43.28
III) 1-Heptanol in	(a) 24.33	2.8273	7.9933	0.6752	14.98	49.89	2.43	2.11	11.01
n-heptane	(b) 9.25	0.9233	5.0147	0.9433	3.03	83.03	3.30	5.78	16.55
$M_j = 116$ gm	(c) 3.00	0.6823	4.1075	0.9638	1.95	208.81	9.20	13.49	43.83
IV) 1-Decanol in	(a) 24.33	2.4813	5.4316	0.8153	9.23	32.25	3.30	2.69	10.32
n-heptane	(b) 9.25	1.5735	5.1553	0.9463	2.87	83.14	5.61	5.71	21.60
$M_j = 158$ gm	(c) 3.00	0.3316	2.6855	0.9228	4.08	135.66	6.89	14.37	30.57
V) Ethanol in benzene									
$M_j = 46$ gm	9 84	4.5211	288.7386	0.9416	3.42	4672.26	0.25	3.9	34.18
VI) Methanol in benzene									
$M_j = 32$ gm	9.84	-5.4003	198.2809	0.8952	5.99	3209.12	—	4.3	—

Table 2. Fröhlich parameter A, relative contributions c_1 and c_2 due to τ_1 and τ_2, theoretical values of x and y due to Fröhlich eqs. (9) and (10) and those by our method at infinite dilution for monoalcohols under different uhf electric field at 25°C.

System with Sl. No. and molecular wt.		Frequency f in GHz	Fröhlich parameter $A = \ln(\tau_2/\tau_1)$	Theoretical values of x and y from eq. no. (9) and (10)		Theoretical values of c_1 and c_2 from eq. no. (4) and (5)		Estimated values of x and y at $w_j \to 0$ from Figs. (2) and (3)		Estimated values of c_1 and c_2 from graphical technique	
I) 1-Butanol in	(a)	24.33	3.2871	0.3666	0.3495	0.3701	2.0678	0.83	0.218	0.9162	–0.3579
n-heptane	(b)	9.25	3.3073	0.4651	0.3596	0.4394	1.6354	0.99	0.15	1.0483	–0.4076
M_j = 74 gm	(c)	3.00	3.1455	0.5556	0.3670	0.4985	1.2024	1.11	0.13	1.1589	–0.2668
II) 1-Hexanol in	(a)	24.33	2.9912	0.3924	0.3692	0.3885	1.6769	0.79	0.264	0.8694	0.0725
n-heptane	(b)	9.25	3.1211	0.4885	0.3704	0.4535	1.4215	0.70	0.130	0.7385	–0.1234
M_j = 102 gm	(c)	3.00	3.1035	0.5600	0.3689	0.5004	1.1707	1.005	0.078	1.0618	–0.4113
III) 1-Heptanol in	(a)	24.33	3.0219	0.3464	0.3588	0.3580	1.8763	0.655	0.236	0.7464	–0.0586
n-heptane	(b)	9.25	3.2253	0.5112	0.3647	0.4703	1.3973	0.835	0.130	0.8724	–0.1575
M_j = 116 gm	(c)	3.00	3.1222	0.5560	0.3682	0.4983	1.1910	1.045	0.116	1.0942	–0.2853
IV) 1-Decanol in	(a)	24.33	2.2796	0.3412	0.3962	0.3644	1.2809	1.11	0.29	1.4687	–1.5413
n-heptane	(b)	9.25	2.6960	0.4268	0.3899	0.4105	1.3544	0.955	0.17	1.0911	–0.7627
M_j = 158 gm	(c)	3.00	2.9801	0.6640	0.3585	0.5611	0.8453	1.005	0.012	1.0716	–0.3678
V) Ethanol in benzene											
M_j = 46 gm		9.84	9.8357	0.4240	0.1577	0.4236	43.6436	0.24	0.0099	0.2400	1.7937

to get the frequency dependence of τ_1 and τ_2 under three different electric fields of 22.06, 3.86 and 2.02 GHz respectively, showing either the double or the mono-relaxation behaviours. *p*-anisidine alone shows the mono-relaxation behaviour at all frequencies. When the data are extended to 9.945 GHz electric field, all of them, on the other hand, show the double relaxation phenomena [13]. No such rigorous study on monohydric alcohols has been made so far. So it seems worthwhile to make an extensive study on the available data of aliphatic alcohols [14] as well as ethanol and methanol [15,16] with special emphasis on possible occurrence of τ_1 and τ_2 in the hf electric field [6].

It is evident from Table 1 and Figure 1 that all the alcohols show the double relaxation phenomena in all the frequencies of GHz range except methanol at 9.84 GHz, indicating separate broad dispersions in them. Ethanol is a system with $\tau_2 \gg \tau_1$ while methanol shows very high value of τ_2 only. τ_1 and τ_2 are compared with most probable relaxation time τ_0 where $\tau_0 = \sqrt{\tau_1 \tau_2}$ as shown in the last column of Table 1. In absence of accurate τ for such alcohols, τ's are estimated from the slope of the imaginary part K''_{ij} and the real part K'_{ij} of the total uhf conductivity K^*_{ij} and placed in the 9th column of Table 1 for comparison with τ_1, τ_2 and τ_0 respectively.

The relative contributions towards the dielectric relaxation *i.e.* c_1 and c_2 due to τ_1 and τ_2 are estimated by using Fröhlich's equations [17] as well as graphical method (Figures 2 and 3). They are also shown in Table 2.

The dipole moments μ_1 and μ_2 of the flexible part as well as of the whole molecule are then estimated in terms of τ and slope β of the linear plot of K_{ij} against w_j (Figure 4). They are shown in Table 3 in order to compare with μ_0 due to τ_0 and μ_{theo} from bond angles and bond moments (Figure 5) respectively. The μ_1's in terms of c_1, c_2 and μ_2 are also calculated by assuming that the two relaxation processes are equally probable; and they are placed in the last column of Table 3 only to compare with μ_1 due to τ_1.

2. Theoretical formulations to estimate $\tau_1, \tau_2; c_1, c_2$ and μ_1, μ_2

The complex dielectric constant ε^*_{ij} of a polar non-polar liquid mixture can be represented as the sum of a number of non-interacting Debye type dispersions in accordance with the Budo's [18] relation as :

$$\frac{\varepsilon^*_{ij} - \varepsilon_{\infty ij}}{\varepsilon_{0ij} - \varepsilon_{\infty ij}} = \sum_k \frac{c_k}{1 + j\omega\tau_k}, \tag{1}$$

where $j = \sqrt{-1}$ and $\Sigma c_k = 1$. The term c_k is the weight factor for the k-th type of relaxation mechanism. When the complex dielectric constant ε^*_{ij} consists of two non-interacting Debye type dispersions, Budo's relation reduces to Bergmann's [8] equations :

$$\frac{\varepsilon'_{ij} - \varepsilon_{\infty ij}}{\varepsilon_{0ij} - \varepsilon_{\infty ij}} = \frac{c_1}{1 + \omega^2\tau_1^2} + \frac{c_2}{1 + \omega^2\tau_2^2} \tag{2}$$

and
$$\frac{\varepsilon''_{ij}}{\varepsilon_{0ij} - \varepsilon_{\infty ij}} = c_1 \frac{\omega\tau_1}{1 + \omega^2\tau_1^2} + c_2 \frac{\omega\tau_2}{1 + \omega^2\tau_2^2}, \quad (3)$$

such that $c_1 + c_2 = 1$, where c_1 and c_2 are the relative contributions towards dielectric relaxations due to intra-molecular relaxation time τ_1 and molecular relaxation time τ_2.

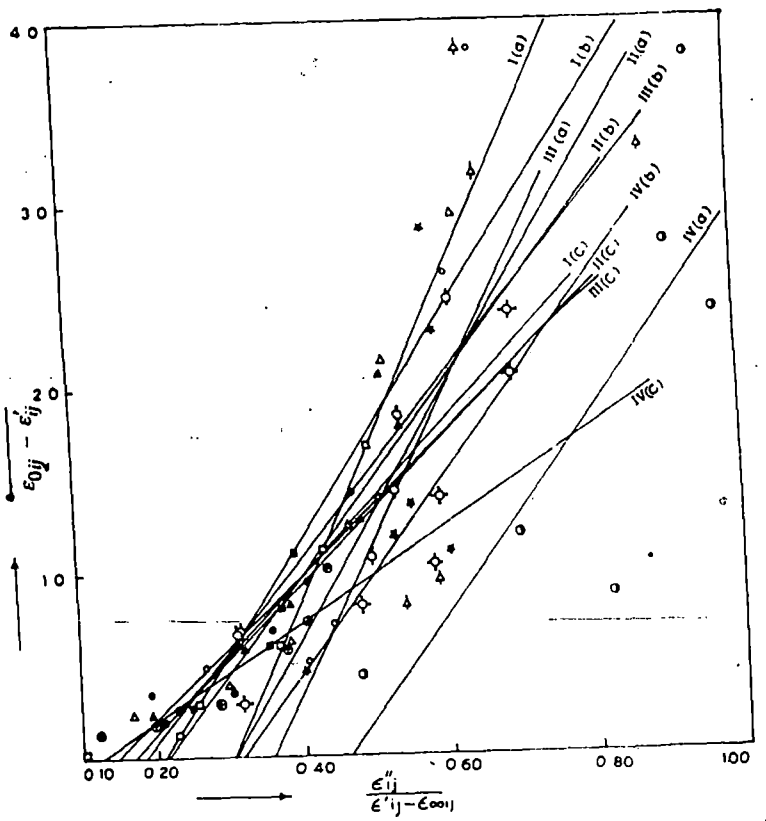

Figure 1. Straight line plots of $(\varepsilon_{0ij} - \varepsilon'_{ij})/(\varepsilon'_{ij} - \varepsilon_{\infty ij})$ against $\varepsilon''_{ij}/(\varepsilon'_{ij} - \varepsilon_{\infty ij})$ of monoalcohols at 25°C under different *uhf* electric field.

System I (a) —O—O— for 1-Butanol at 24.33 GHz.
I (b) —Δ—Δ— for 1-Butanol at 9.25 GHz.
I (c) —□—□— for 1-Butanol at 3.00 GHz.
System II (a) for 1-Hexanol at 24.33 GHz.
II (b) for 1-Hexanol at 9.25 GHz.
II (c) for 1-Hexanol at 3.00 GHz.
System III (a) for 1-Heptanol at 24.33 GHz.
III (b) for 1-Heptanol at 9.25 GHz.
III (c) for 1-Heptanol at 3.00 GHz.
System IV (a) for 1-Decanol at 24.33 GHz.
IV (b) for 1-Decanol at 9.25 GHz.
IV (c) for 1-Decanol at 3.00 GHz.

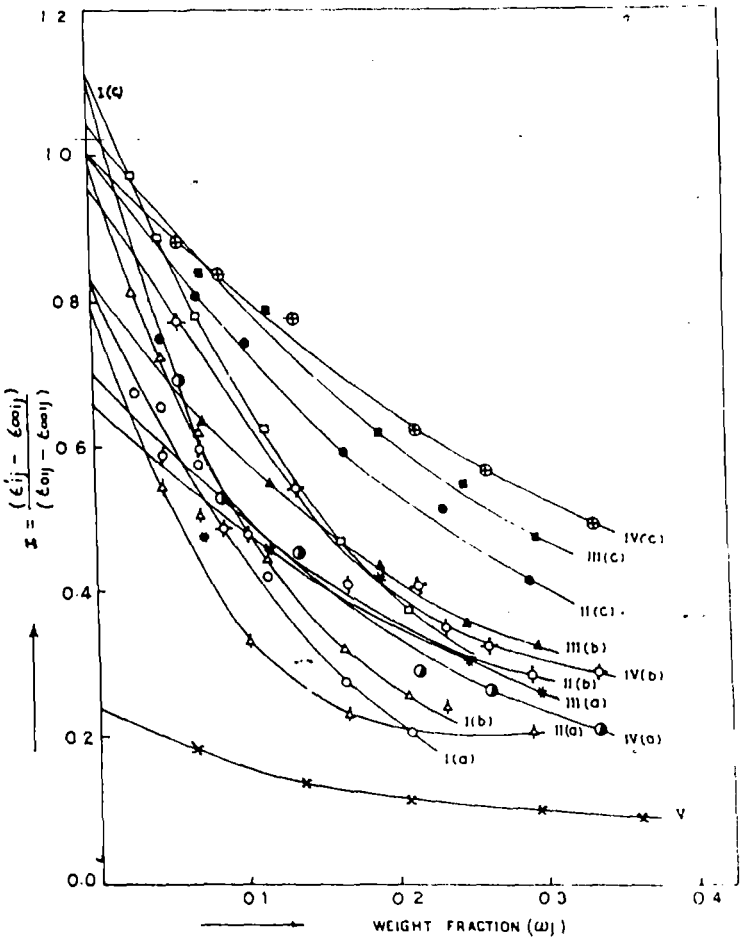

Figure 2. Variation of $(\varepsilon'_{ij} - \varepsilon_{\infty ij})/(\varepsilon_{0ij} - \varepsilon_{\infty ij})$ against weight fraction w_j for monoalcohols at different *uhf* electric field.

System I (a) —O—O— for 1-Butanol at 24.33 GHz.
I (b) —Δ—Δ— for 1-Butanol at 9.25 GHz.
I (c) —□—□— for 1-Butanol at 3.00 GHz.
System II (a) —Δ—Δ— for 1-Hexanol at 24.33 GHz.
II (b) —○—○— for 1-Hexanol at 9.25 GHz.
II (c) —●—●— for 1-Hexanol at 3.00 GHz.
System III (a) —*—*— for 1-Heptanol at 24.33 GHz.
III (b) —▲—▲— for 1-Heptanol at 9.25 GHz.
III (c) —■—■— for 1-Heptanol at 3.00 GHz.
System IV (a) —◑—◑— for 1-Decanol at 24.33 GHz.
IV (b) —✦—✦— for 1-Decanol at 9.25 GHz.
IV (c) —⊕—⊕— for 1-Decanol at 3.00 GHz.
System V —×—×— for 1-Ethanol at 9.84 GHz.

Putting $\frac{\varepsilon'_{ij} - \varepsilon_{\infty ij}}{\varepsilon_{0ij} - \varepsilon_{\infty ij}} = x$ and $\frac{\varepsilon''_{ij}}{\varepsilon_{0ij} - \varepsilon_{\infty ij}} = y$ with $\omega\tau = \alpha$ and using the abbreviations, $a = \frac{1}{1 + \alpha^2}$ and $b = \frac{\alpha}{1 + \alpha^2}$, the above eqs. (2) and (3) can be written as

$$x = c_1 a_1 + c_2 a_2, \tag{4}$$

$$y = c_1 b_1 + c_2 b_2, \tag{5}$$

where suffices 1 and 2 with a and b are related to τ_1 and τ_2 respectively. From eqs. (4) and (5), since $\alpha_2 - \alpha_1 \neq 0$ and $\alpha_2 > \alpha_1$ we have

$$c_1 = \frac{(x\alpha_2 - y)(1 + \alpha_1^2)}{\alpha_2 - \alpha_1} \tag{6}$$

$$c_2 = \frac{(y - x\alpha_1)(1 + \alpha_2^2)}{\alpha_2 - \alpha_1} \tag{7}$$

Now, using $c_1 + c_2 = 1$, one gets the following equation with the help of eqs. (6) and (7) :

$$\frac{1 - x}{y} = (\alpha_1 + \alpha_2) - \frac{x}{y}\alpha_1\alpha_2$$

which, on substitution of the values of x, y and α yields

$$\frac{\varepsilon_{0ij} - \varepsilon'_{ij}}{\varepsilon'_{ij} - \varepsilon_{\infty ij}} = \omega(\tau_1 + \tau_2)\frac{\varepsilon''_{ij}}{\varepsilon'_{ij} - \varepsilon_{\infty ij}} - \omega^2\tau_1\tau_2. \tag{8}$$

Equation (8) is a straight line between $\frac{\varepsilon_{0ij} - \varepsilon'_{ij}}{\varepsilon'_{ij} - \varepsilon_{\infty ij}}$ and $\frac{\varepsilon''_{ij}}{\varepsilon'_{ij} - \varepsilon_{\infty ij}}$ with slope $\omega(\tau_1 + \tau_2)$ and intercept $-\omega^2\tau_1\tau_2$ respectively. Here, ω = angular frequency of the applied electric field of frequency f in GHz. When the eq. (8) is fitted with the measured dielectric relaxation data ε'_{ij}, ε''_{ij}, ε_{0ij} and $\varepsilon_{\infty ij}$ for different weight fractions w_j's of each alcohol in n-heptane (at 25°C under 24.33, 9.25 and 3.00 GHz electric fields) as well as of methanol and ethanol in benzene (at 9.84 GHz), we get the slopes and intercepts as shown in Table 1, to yield τ_1 and τ_2.

The relative contributions c_1 and c_2 towards the dielectric relaxations in terms of x, y and τ_1, τ_2 for each alcohol are found out and shown in Table 2. The theoretical values of x and y are, however, calculated from Fröhlich's equations [17] as

$$x = \frac{\varepsilon'_{ij} - \varepsilon_{\infty ij}}{\varepsilon_{0ij} - \varepsilon_{\infty ij}} = 1 - \frac{1}{2A}\ln\left(\frac{e^{2A}\omega^2\tau_s^2 + 1}{1 + \omega^2\tau_s^2}\right), \tag{9}$$

and $$y = \frac{\varepsilon''_{ij}}{\quad} = \frac{1}{A}\left[\tan^{-1}(e^A\omega\tau_s) - \tan^{-1}(\omega\tau_s)\right]. \tag{10}$$

Table 3. The estimated intercept (α) and slope (β) of $K_{ij} - w_j$ equation with correlation coefficient (r) and percentage of error, dimensionless parameters b's and dipole moments μ_j's with theoretical μ's and μ calculated by using the relation $\mu_1 = \mu_2 (c_1/c_2)^{1/2}$ at 25°C of monoalcohols under different hf electric field

System with Sl no. and Mol. wt. of solute	Frequency f in GHz	Intercept and slope of $K_{ij} - w_j$ eqn.		Correlation coeff. (r)	% of error in regre. tech.	Dimensionless parameters			Estimated dipole moments in Debye				
		$\alpha \times 10^{-10}$ in e.s.u.	$\beta \times 10^{-10}$ in e.s.u.			$b_0 = \frac{1}{1+\omega^2\tau_0^2}$	$b_2 = \frac{1}{1+\omega^2\tau_2^2}$	$b_1 = \frac{1}{1+\omega^2\tau_1^2}$	μ_0	μ_2	μ_1	μ_{theo}	$\mu_1 = \mu_2\left(\frac{c_1}{c_2}\right)^{1/2}$
I) 1-Butanol in	(a) 24.33	2.3523	1.2679	0.9978	0.12	0.2777	0.0142	0.9115	1.97	8.75	1.09		3.70
n-heptane	(b) 9.25	0.8941	0.5400	0.9997	0.01	0.4382	0.0278	0.9552	1.66	6.62	1.13	1.49	3.43
$M_j = 74$ gm	(c) 3.00	0.2887	0.2338	0.9999	0.00	0.5942	0.0593	0.9715	1.65	5.23	1.29		3.37
II) 1-Hexanol	(a) 24.33	2.3522	0.8192	0.9961	0.21	0.3279	0.0239	0.9066	1.72	6.36	1.03		3.06
in n-heptane	(b) 9.25	0.8929	0.4005	0.9997	0.01	0.4804	0.0392	0.9545	1.61	5.63	1.14	1.31	3.18
$M_j = 102$ gm	(c) 3.00	0.2889	0.1695	0.9999	0.00	0.6006	0.0633	0.9710	1.64	5.06	1.29		3.31
III) 1-Heptanol	(a) 24.33	2.3169	0.8276	0.9927	0.40	0.2611	0.0169	0.8788	2.06	8.10	1.12		3.54
in n-heptane	(b) 9.25	0.8973	0.3555	0.9993	0.04	0.5196	0.0412	0.9646	1.55	5.52	1.14	1.22	3.20
$M_j = 116$ gm	(c) 3.00	0.2891	0.1519	0.9997	0.01	0.5946	0.0607	0.9708	1.67	5.22	1.30		3.38
IV) 1-Decanol	(a) 24.33	2.3575	0.5787	1.0002	0.01	0.2870	0.0396	0.7973	1.92	5.17	1.15		2.76
in n-heptane	(b) 9.25	0.8949	0.2609	0.9966	0.18	0.3885	0.0411	0.9040	1.79	5.52	1.18	[illegible]	3.04
$M_j = 158$ gm	(c) 3.00	0.2894	0.1151	0.9997	0.01	0.7509	0.1327	0.9834	1.51	3.58	1.32		2.92
V) Ethanol in benzene													
$M_j = 46$ gm	9.84	1.1925	0.1977	0.9927	0.44	0.1831	0.00001	0.9997	1.19	147.19	0.51	[illegible]	14.50
VI) Methanol in benzene													
$M_j = 32$ gm	9.84	1.2058	0.2161	0.9928	0.43	—	0.00002	—	—	88.17	—	[illegible]	—

where A = Fröhlich parameter = $\ln(\tau_2/\tau_1)$ and τ_s is called the small limiting relaxation time being given by $\tau_s = \tau_1$. A simple graphical extrapolation technique, on the other hand, has been adopted here to get the values of x and y at $w_j \to 0$, as illustrated graphically in Figures 2 and 3 respectively. This is really in accord with Bergmann's eqs. (2) and (3) when the once estimated τ_1 and τ_2 from eq. (8) are substituted in the right hand sides of the above eqs. (2) and (3).

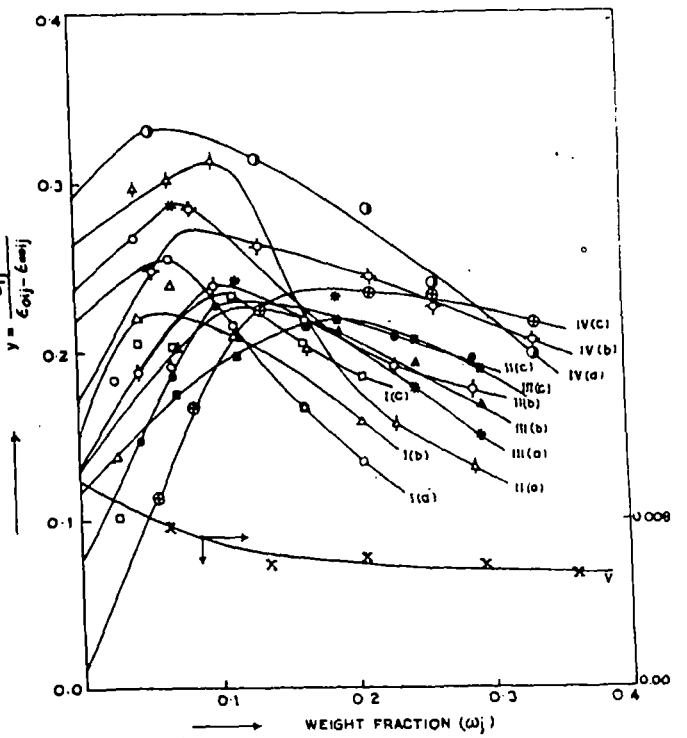

Figure 3. Variation of $\varepsilon''_{ij}/(\varepsilon_{0ij} - \varepsilon_{\infty ij})$ against weight fraction w_j for monoalcohols at different *uhf* electric field.

System I (a) —O—O— for 1-Butanol at 24.33 GHz.
I (b) - Δ - Δ - for 1-Butanol at 9.25 GHz
I (c) —( )—( )— for 1-Butanol at 3.00 GHz.
System II (a) —Δ—Δ— for 1-Hexanol at 24.33 GHz.
II (b) —○—○— for 1-Hexanol at 9.25 GHz.
II (c) —●—●— for 1-Hexanol at 3.00 GHz
System III (a) —✱—✱— for 1-Heptanol at 24.33 GHz.
III (b) —▲—▲— for 1-Heptanol at 9.25 GHz.
III (c) —■—■— for 1-Heptanol at 3.00 GHz.
System IV (a) —◑—◑— for 1-Decanol at 24.33 GHz.
IV (b) —✦—✦— for 1-Decanol at 9.25 GHz.
IV (c) —⊕—⊕— for 1-Decanol at 3.00 GHz.
System V —×—×— for 1-Ethanol at 9.84 GHz.

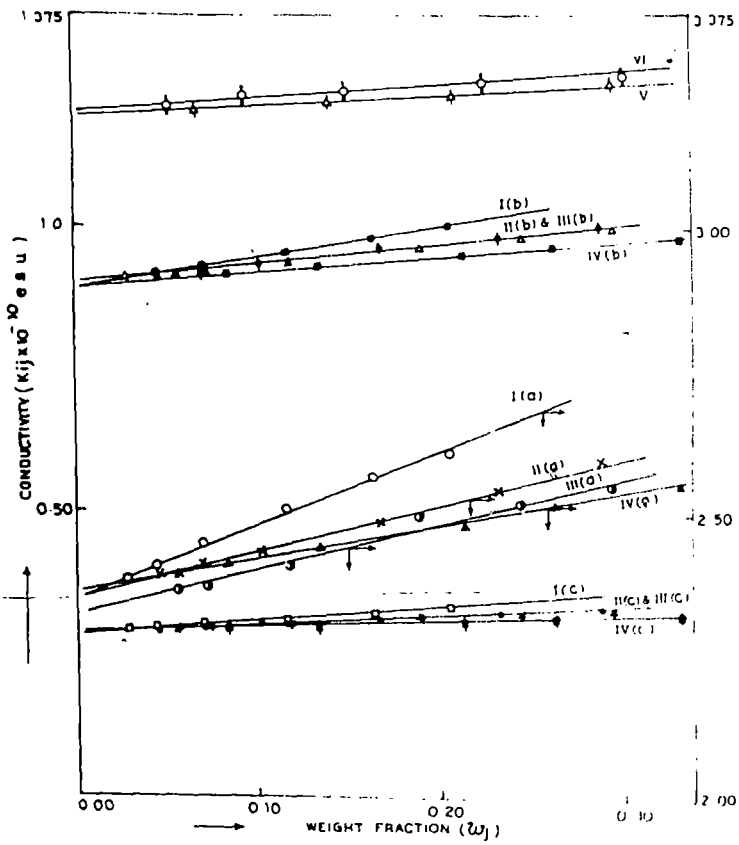

Figure 4. Straight line plots of K_{ij} against w_j under different *uhf* electric field at 25°C

System	I (a)	for 1-Butanol at 24.33 GHz
	I (b)	for 1-Butanol at 9.25 GHz
	I (c)	for 1-Butanol at 3.00 GHz
System	II (a)	for 1-Hexanol at 24.33 GHz
	II (b)	for 1-Hexanol at 9.25 GHz
	II (c)	for 1-Hexanol at 3.00 GHz
System	III (a)	for 1-Heptanol at 24.33 GHz
	III (b)	for 1-Heptanol at 9.25 GHz
	III (c)	for 1-Heptanol at 3.00 GHz
System	IV (a)	for 1-Decanol at 24.33 GHz
	IV (b)	for 1-Decanol at 9.25 GHz
	IV (c)	for 1-Decanol at 3.00 GHz
System	V	for Ethanol at 9.84 GHz
System	VI	for Methanol at 9.84 GHz

The dipole moments μ_1 and μ_2 of polar solutes in terms of τ_1 and τ_2 as obtained from the double relaxation method and slope β of the concentration variation of the experimental

uhf conductivity K_{ij} are then estimated. The uhf conductivity K_{ij} is, however, given by Murphy and Morgan [19] as

$$K_{ij} = \frac{\omega}{4\pi}\left(\varepsilon_{ij}''^2 + \varepsilon_{ij}'^2\right)^{1/2}, \tag{11}$$

which is a function of w_j of polar solute. Although $\varepsilon_{ij}'' < \varepsilon_{ij}'$ in the uhf electric field, still the term ε_{ij}'' offers resistance to polarisation. Thus, the real part K_{ij}' of the uhf conductivity of a polar-nonpolar liquid mixture at T°K can be written according to Smyth [20] as :

$$K_{ij}' = \frac{\mu_j^2 N \rho_{ij} F_{ij}}{3M_j kT}\left(\frac{\omega^2\tau}{1 + \omega^2\tau^2}\right)w_j. \tag{12}$$

Differentiating the above eq. (12) with respect to w_j and for $w_j \to 0$, the eq. (12) reduces to

$$\left(\frac{dK_{ij}'}{dw_j}\right)_{w_j\to 0} = \frac{\mu_j^2 N\rho_i F_i}{3M_j kT}\left(\frac{\omega^2\tau}{1 + \omega^2\tau^2}\right), \tag{13}$$

where, M_j is the molecular weight of a polar solute, N is the Åvogadro's number, k is the Boltzman's constant, the local field $F_{ij} = \frac{1}{9}(\varepsilon_{ij} + 2)^2$ becomes $F_i = \frac{1}{9}(\varepsilon_i + 2)^2$ and the density $\rho_{ij} \to \rho_i$ the density of solvent at $w_j \to 0$.

Again, the total uhf conductivity $K_{ij} = \frac{\omega}{4\pi}\varepsilon_{ij}'$ can now be written as :

$$K_{ij} = K_{\infty ij} + \frac{1}{\omega\tau}K_{ij}'$$

or,
$$\left(\frac{dK_{ij}'}{dw_j}\right)_{w_j\to 0} = \omega\tau\left(\frac{dK_{ij}}{dw_j}\right)_{w_j\to 0} = \omega\tau\beta, \tag{14}$$

where β is the slope of $K_{ij} - w_j$ curve at infinite dilution. From eqs. (13) and (14) we thus get

$$\mu_j = \left(\frac{3M_j kT\beta}{N\rho_i F_i \omega b}\right)^{1/2} \tag{15}$$

in order to obtain the dipole moment in terms of b, where b is a dimensionless parameter given by

$$b = \frac{1}{1 + \omega^2\tau^2}. \tag{16}$$

The computed μ_1, μ_2 and μ_0 together with b_1, b_2 and b_0 and β's of $K_{ij} - w_j$ equations for all the alcohols are given in Table 3.

3. Results and discussions

The least-square-fitted straight line equations of $(\varepsilon_{0ij} - \varepsilon'_{ij})/(\varepsilon'_{ij} - \varepsilon_{\infty ij})$ against $\varepsilon''_{ij}/(\varepsilon'_{ij} - \varepsilon_{\infty ij})$ for different weight fractions w_j's of 1-butanol, 1-hexanol, 1-heptanol and 1-decanol in n-heptane under alternating electric field of 24.33, 9.25 and 3.00 GHz at 25°C are shown in Figure 1, together with the experimental points on them. The straight line equations of methanol and ethanol in benzene at 9.84 GHz are :

$$\frac{\varepsilon_{0ij} - \varepsilon'_{ij}}{\varepsilon'_{ij} - \varepsilon_{\infty ij}} = 198.2809 \frac{\varepsilon''_{ij}}{\varepsilon'_{ij} - \varepsilon_{\infty ij}} + 5.4003$$

and $$\frac{\varepsilon_{0ij} - \varepsilon'_{ij}}{\varepsilon'_{ij} - \varepsilon_{\infty ij}} = 288.7386 \frac{\varepsilon''_{ij}}{\varepsilon'_{ij} - \varepsilon_{\infty ij}} - 4.5211 \quad \text{respectively.}$$

The experimental data of $(\varepsilon_{0ij} - \varepsilon'_{ij})/(\varepsilon'_{ij} - \varepsilon_{0ij})$ for methanol and ethanol are so high that they can not be plotted in Figure 1. In absence of reliable values of ε_{0ij} and $\varepsilon_{\infty ij}$ for methanol, it is not possible to show the applicability of simple mixing rule in determining relaxation data for this system. But the method has been applied to ethanol and it is found that the τ value is 3207.57 p Sec which is in good agreement with the measured data as presented in Table 1. The weight fractions w_j's of the respective solutes have been obtained from mole fractions x_i and x_j of the solvent and solute of molecular weights M_i and M_j respectively by a relation [21]

$$w_j = \frac{x_j M_j}{x_i M_i + x_j M_j}. \tag{17}$$

The linearity of all the straight lines, as illustrated in Figure 1; is, however, tested by evaluating their correlation coefficient r. They are found to lie within the range of 0.9638 to 0.6195 as shown in Table 1. The corresponding percentage of errors in the fitting technique, can be had from the correlation coefficients. They are all shown in the 5-th and the 6-th columns of Table 1 respectively. The errors, are, however, large in magnitudes in the hf electric field of 24.33 GHz for 1-hexanol, 1-heptanol and 1-decanol respectively, probably due to unavoidable uncertainty in measurements of relaxation parameters for such higher frequency.

τ_2 and τ_1 for each alcohol are estimated from the slope and the intercept of straight line eq. (8) and are placed in the 7-th and the 8-th columns of Table 1 respectively. All the monoalcohols show τ_2 and τ_1 at all the frequencies with an exception for methanol which exhibits the monorelaxation behaviour [12].

The monorelaxation behaviour [12] can easily be evaluated on the basis of the relaxation parameters by putting $c_1 = 0$ in eqs. (2) and (3). The resulting equation becomes :

$$\frac{\varepsilon_{0ij} - \varepsilon'_{ij}}{\varepsilon'_{ij} - \varepsilon_{\infty ij}} = \omega\tau_2 \frac{\varepsilon''_{ij}}{\varepsilon'_{ij} - \varepsilon_{\infty ij}}. \tag{18}$$

τ_2 for methanol is found to be 5254.3 p Sec in approximate agreement with τ_2 as obtained by double relaxation method (Table 1). τ_2's and τ_1's as obtained from the double relaxation method are then compared with the most probable relaxation time τ_0 where $\tau_0 = \sqrt{\tau_1 \tau_2}$ and the measured relaxation time τ_s's from the slope of the given relation :

$$K''_{ij} = K_{\infty ij} + \frac{1}{\omega \tau_s} K'_{ij}, \qquad (19)$$

where $K_{\infty ij}$ is the constant conductivity at infinite dilution. Both τ_0 and τ_s are shown in the 10-th and the 9-th columns of Table 1, respectively. τ_2 and τ_1 for the double relaxation processes show low values at 24.33 GHz and increase gradually at the lower frequencies of

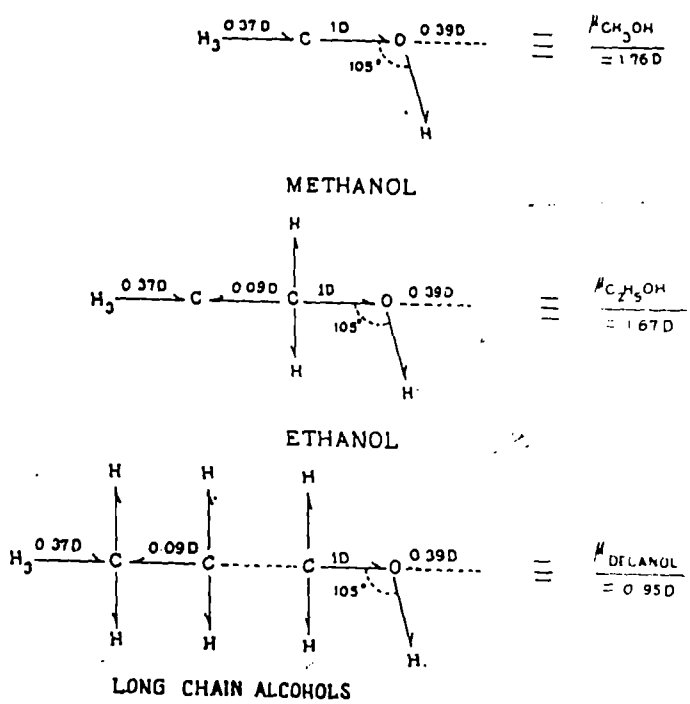

Figure 5. Conformational structures of methanol, ethanol and decanol.

9.25 and 3.00 GHz respectively. This is explained on the basis of the fact that at higher frequency, the rate of hydrogen bond rupture in long chain alcohols may be maximum to reduce τ for each rotating unit. This sort of behaviour is also observed in the estimated τ_1 and τ_0 respectively. Although, the measured τ_s and τ_0 are smaller in magnitudes, τ_1 agrees excellently with τ_s (Table 1). This is perhaps due to the fact that the hf conductivity measurement always yields the average microscopic relaxation time whereas the double relaxation phenomena offers a better understanding of microscopic as well as macroscopic molecular relaxation times.

The relative contributions c_1 and c_2 towards dielectric relaxations for each alcohol have been evaluated from Bergmann's eqs. (2) and (3) for fixed values of τ_1 and τ_2 as predicted by eq. (8), with the estimated x and y from graphical technique as well as from Fröhlich's eqs. (9) and (10) respectively. c_1 and c_2 thus obtained by Fröhlich's method are placed in the 6-th and 7-th columns of Table 2. In the 10-th and the 11-th columns of the same Table 2 are shown c_1 and c_2 values with the fixed values of x and y at infinite dilutions of Figures 2 and 3. The variations of x and y with w_j are concave and convex in nature as illustrated graphically in Figures 2 and 3 in accordance with Bergmann's eqs. (2) and (3) respectively. Ethanol is an exception whose y value changes in a similar way as x. This anomaly is perhaps due to nonavailability of the accurate ε_{0ij} and $\varepsilon_{\infty ij}$ [11], and it thereby yields abnormally high τ value like methanol, although the latter one exhibits monorelaxation behaviours as shown in Table 1. However, the estimated value of c_2 is greater than c_1 for each alcohol, under investigation, in Fröhlich's method, while the reverse is true for the graphical method. Eventually, c_2 is –ve for most of the cases except 1-hexanol at 24.33 GHz and ethanol at 9.84 GHz respectively in the latter case. This –ve value of c_2 is due to inertia of the flexible part [10]. This type of behaviour may be explained on the basis of the fact that the latter one ascertains the nature of the flexible part in comparison to Fröhlich's method. It is also interesting to note that unlike Fröhlich's method, the latter method yields $c_1 + c_2 < 1$ except for 1-decanol at 24.33 GHz where $c_1 + c_2 < 0$, although $|c_1 + c_2| > 1$ signifying more than two relaxation processes may be possible in them [14].

The dipole moments μ_1 and μ_2 of all the alcohols, as enlisted in Table 3, were estimated in terms of dimensionless parameters b_1 and b_2 and slopes β of K_{ij} *versus* w_j equations by using eq. (15). The linear variation of uhf conductivities K_{ij} of all the alcohols as a function of w_j's are shown in Figure 4. The correlation coefficient r and the corresponding percentage of error in the estimation of the slope β and hence all the μ's together with b's are shown in Table 3. From Table 3, μ_2's are, however, found to be large at 24.33 GHz while in comparatively lower frequencies like 9.25 and 3.00 GHz, they are gradually smaller for each polar alcohol under our investigation. But μ_1's, on the other hand, show the opposite trend. It is also interesting to note that the values of μ_2's for all the alcohols decrease with the increase of C-atoms in them. This type of behaviour may be explained by the fact that the long chain polymer type molecules having a large number of carbon atoms, in a nonpolar solvent, tend to break up in the hf electric field in order to reduce or even eliminate the absorption attributable to them. The proportion of smaller molecular species, on the other hand, have comparatively smaller number of C-atoms and the corresponding absorption will increase [14]. This is also confirmed by the fact that as τ decreases with increasing ω, the term $\omega^2\tau^2$ is higher and therefore, eq. (16) yields smaller b values to increase μ's according to eq. (15).

μ_1, μ_2 and μ_0 are finally compared with μ_{theo} for the orientational polarisation of all the associated liquids containing a large number of dipolar groups like $H_3 \rightarrow C$, $C \leftarrow O$ and $O \leftarrow H$ when their individual monomeric moments are added vectorially as shown in Figure 5. μ_{theo} may also be inferred from Fröhlich's equation having correlation factor which bears structural information for such liquids. But to a fair approximation, the structural conformation of such liquids, as shown diagrammatically in Figure 5 and placed in Table 3, from the bond moments of $H_3 \rightarrow C$, $C \leftarrow O$ and $O \leftarrow H$ and the bond angle of 105° made by –OH groups with the main bond axis, have the major contributions in yielding the theoretical dipole moment, μ_{theo}. All the μ's are displayed in Table 3 with those of μ_1, where $\mu_1 = \mu_2\left(\frac{c_1}{c_2}\right)^{1/2}$, assuming the two relaxation processes are equally probable. These μ_1's are slightly larger in magnitudes in comparison to μ_{theo}, μ_1 and μ_0 which are in close agreement among themselves.

4. Conclusion

The methodology so far advanced for double and single broad dispersions of the polar-nonpolar liquid mixtures seems to be much simpler, straightforward and significant one to detect the existence of double and monorelaxation behaviours of polar liquids in nonpolar solvents. The correlation coefficients between the desired parameters as given in eqs. (8) and (18) could, however, be estimated to find out the percentage of errors entered in the dielectric relaxation data, to yield τ_1 and τ_2 of the polar liquids, because the relaxation times τ's are claimed to be accurate within ± 10%. The monohydric alcohols so far studied always yield, both τ_1 and τ_2 at all frequencies of the electric field. The corresponding dipole moments μ_1 and μ_2 can then be estimated from eq. (15) in terms of b_1 and b_2 (which are, however, related to τ_1 and τ_2 as estimated) to arrive at their conformations as shown in Figure 5.

Acknowledgment

The authors are thankful to Mr. A R Sit, BE (Electrical) for his interest in this work.

References

[1] A K Chatterjee, U Saha, N Nandi, R C Basak and S Acharyya *Indian J. Phys.* **66** 291 (1992)

[2] U Saha and S Acharyya *Indian J. Pure Appl. Phys.* **31** 181 (1993)

[3] U Saha and S Acharyya *Indian J. Pure Appl. Phys.* **32** 346 (1994)

[4] S K Garg and C P Smyth *J. Phys. Chem.* **69** 1294 (1965)

[5] M Magat *Hydrogen Bonding* (New York : Pergamon) p 309 (1959)

[6] D J Denny and J W Ring *J. Chem. Phys.* **39** 1268 (1963); M Moriamez and A Lebrun *Arch. Sci. (Geneva)* **13** 40 (1960)

[7] R Misra, A Singh, J P Shukla and M C Saxena *Indian J. Pure Appl. Phys.* **24** 536 (1986)

[8] K Bergmann, D M Roberti and C P Smyth *J. Phys. Chem.* **64** 665 (1960)

[9] J Bhattacharyya, A Hasan, S B Roy and G S Kastha *J. Phys. Soc. Jpn.* **28** 204 (1970)

[10] U Saha, S K Sit, R C Basak and S Acharyya *J. Phys.* **D27** 596 (1994)

[11] M D Magee and S Walker *J. Chem. Phys.* **50** 2580 (1969)

[12] S K Sit, R C Basak, U Saha and S Acharyya *J. Phys.* **D27** 2194 (1994)

[13] S K Sit and S Acharyya *Indian J. Pure Appl. Phys.* (accepted) (1995)

[14] L Glasser, J Crossley and C P Smyth *J. Chem. Phys.* **57** 3977 (1972)

[15] H D Purohit and H S Sharma *Indian J. Pure Appl. Phys.* **8** 107 (1970)

[16] A K Ghosh *PhD Dissertation* (University of North Bengal, India) (1981)

[17] H Fröhlich *Theory of Dielectrics* (Oxford : Oxford University Press) p 94 (1949)

[18] A Budo *Phys. Z.* **39** 706 (1938)

[19] F J Murphy and S O Morgan *Bull. Syst. Techn. J.* **18** 502 (1939)

[20] C P Smyth *Dielectric Behaviour and Structure* (New York : McGraw-Hill) (1955)

[21] A K Ghosh and S Acharyya *Indian J. Phys.* **52B** 129 (1978)

Appendix

List of nomenclature used :

ε'_{ij}, ε''_{ij}	real and imaginary parts of the complex dielectric constant ε^*_{ij} of a solution,
$\varepsilon^*_{ij} = \varepsilon'_{ij} - j\varepsilon''_{ij}$	where $j = \sqrt{-1}$ is a complex number,
ε_{0ij}, $\varepsilon_{\infty ij}$	static and optical dielectric constants of the solution,
$\omega = 2\pi f$	angular frequency of the applied electric field, f being the frequency in Hertz,
K'_{ij}, K''_{ij}	real and imaginary parts of the complex electrical conductivity K^*_{ij} of a solution,
$K^*_{ij} = K'_{ij} + jK''_{ij}$	where $j = \sqrt{-1}$ is a complex number,
$K_{\infty ij}$	constant conductivity of the solution at $w_i \to 0$.
μ_j	dipole moment of the j-th type of solute,
μ_1, μ_2	dipole moments of the flexible part and the whole molecule,
τ_i	relaxation time of the solute,
τ_1, τ_2	relaxation times of the flexible part and the whole molecule,

τ_0	most probable relaxation time of the solute,
$A = \ln(\tau_2/\tau_1)$	the Fröhlich parameter,
w_j	weight fraction of the solute,
c_1, c_2	relative contributions due to τ_1 and τ_2 respectively,
M_j	molecular weight of the j-th type of solute,
β	slope of the $K_{ij} - w_j$ curve.

Double relaxations of some isomeric octyl alcohols by high frequency absorption in non-polar solvent

S K Sit, N Ghosh & S Acharyya

Department of Physics, University College, P O Raiganj, Dist Uttar Dinajpur, 733 134, W Bengal

Received 29 March 1996; revised 18 June 1996; accepted 7 November 1996

The double relaxation behaviour of some isomeric octyl alcohols in n-heptane at 25°C under the electric field frequencies of 24.33, 9.25 and 3.00 GHz is studied to get the relaxation times τ_1 and τ_2 for their flexible parts and whole molecules by a method of single frequency measurements of dielectric relaxation parameters. The isomers are long, straight chain, hydrogen bonded, polymer type molecules having methyl and hydroxyl groups attached to their C-atoms which may bend, twist or rotate internally under *hf* electric field each with a characteristic τ. The relative contributions c_1 and c_2 towards dielectric relaxations due to τ_1 and τ_2 are also estimated by using Fröhlich's equations and the graphical technique. The dipole moments μ_1 and μ_2 in terms of τ_1 and τ_2 of flexible part and the whole molecules are again found out from slope β of the total *hf* conductivity K_{ω} as a function of weight fractions ω_2's of the solute indicating μ_1 for the rotation of their −OH groups about C−C bonds only. μ_1 and μ_2 are finally compared with the theoretical dipole moments μ_{theo} arising out of the structures with bond-angles and bond-moments of their substituent groups to establish the conformations of these isomers which are justified like normal alcohols observed earlier.

Table 1—The estimated relaxation times τ_2 and τ_1 from the slope and the intercept of straight line Eq. 18 with errors and correlations (r) together with measured τ_1 from $K''_{\omega} - K''_{0}$ curve and most probable relaxation time $\tau_m = \sqrt{\tau_1 \tau_2}$ for six isomeric octyl alcohols at 25°C under different frequencies of electric fields

System with Sl. No. & Mol. wt M_1	Frequency in GHz	Intercept & slope of Eq.18		Correlation coefficient (r)	% Error in regression technique	Estimated values of τ_2 & τ_1 in p Sec.		Measured τ_1 in p Sec.	Most probable relaxation time $\tau_m = \sqrt{\tau_1 \tau_2}$ in p Sec.
I 2-methyl-3-heptanol in n-heptane M_1 = 130 gm.	(a) 24.33	2.3718	5.0952	0.9011	29.96	29.96	3.39	1.84	10.08
	(b) 9.25	0.6871	3.1205	0.9700	1.90	49.61	4.10	3.58	14.26
	(c) 3.00	0.1408	1.5830	0.9771	1.50	73.31	5.41	6.74	19.91
II 3-methyl-3-heptanol in n-heptane M_1 = 130 gm.	(a) 24.33	0.9087	2.6282	0.9294	4.59	14.52	2.68	2.19	6.24
	(b) 9.25	0.6389	2.7714	0.9709	1.93	41.34	4.37	3.70	13.76
	(c) 3.00	0.1611	1.5018	0.9985	0.10	73.55	6.17	5.58	21.30
III 4-methyl-3-heptanol in n-heptane M_1 = 130 gm.	(a) 24.33	1.9653	4.3873	0.8851	7.30	25.40	3.31	1.90	9.17
	(b) 9.25	0.6411	2.8636	0.9682	2.11	42.08	4.21	3.13	13.78
	(c) 3.00	0.2008	1.7153	0.9206	5.14	84.34	6.71	11.98	23.79
IV 5-methyl-3-heptanol in n-heptane M_1 = 130 gm.	(a) 24.33	0.6929	2.9788	0.5684	26.36	17.83	1.65	1.71	5.44
	(b) 9.25	0.7445	3.2866	0.9846	1.19	52.36	4.21	5.39	14.85
	(c) 3.00	0.2362	2.0308	0.9371	4.74	101.22	6.58	13.11	25.81
V 4-Octanol in n-heptane M_1 = 130 gm	(a) 24.33	0.9572	3.4750	0.8569	10.34	20.77	1.97	1.83	6.40
	(b) 9.25	0.3810	2.6361	0.9470	4.02	42.74	2.64	5.46	10.62
	(c) 3.00	0.1428	1.6929	0.9846	1.18	85.13	4.72	12.76	20.05
VI 2-Octanol in n-heptane M_1 = 130 gm	(a) 24.33	1.3664	5.0208	0.6336	23.60	30.00	1.89	1.83	7.65
	(b) 9.25	1.5853	5.6407	0.9888	0.96	92.00	5.11	6.26	21.68
	(c) 3.00	0.4458	3.1697	0.9780	1.69	160.41	7.83	18.70	35.44

Table 2—Fröhlich parameter A, relative contributions c_1 and c_2 due to τ_1 and τ_2, theoretical values of x and y from Fröhlich's Eqs (9) and (10) and from graphical extrapolation technique at $\omega = 0$

System with Sl. No.	Frequency, GHz	Fröhlich parameter $A = \tau_2/\tau_1$	Theoretical values of x & y from Eqs (9) and (10)		Theoretical values of τ_1 & τ_2		Estimated values of x & y at $\omega = 0$		Estimated values of c_1 and c_2	
I 2-methyl-3-heptanol in n-heptane	(a) 24.33	2.1790	0.3457	0.4028	0.3686	1.2101	0.295	0.366	0.0226	0.2476
	(b) 9.25	2.4932	0.5637	0.4023	0.4886	0.9434	1.025	0.29	0.2674	0.2324
	(c) 3.00	2.6063	0.7973	0.3232	0.6144	0.8500	1.025	0.074	0.1133	0.0508
II 3-methyl-3-heptanol in n-heptane	(a) 24.33	1.6797	0.5195	0.4490	0.4542	0.7733	0.295	0.32	0.0226	0.1120
	(b) 9.25	2.2943	0.8792	0.4115	0.4922	0.8573	1.025	0.256	0.2674	0.0810
	(c) 3.00	2.4781	0.7865	0.349	0.6028	0.8600	1.025	0.074	0.1133	0.0579
III 4-methyl-3-heptanol	(a) 24.33	2.0378	0.3747	0.4173	0.3857	1.0812	0.295	0.37	0.0226	0.2510

n-heptane	(c) 3.00	2.7313	0.7543	0.3490	0.5902	0.6112	1.015	0.094	1.0177	−0.0805
V 5-methyl-3-heptanol in	(a) 24.33	2.7741	0.5644	0.4088	0.4862	0.9057	0.645	0.274	0.6389	0.3763
n-heptane	(b) 9.25	2.5207	0.5499	0.4020	0.4814	0.9805	0.95	0.172	1.0297	−0.2211
	(c) 3.00	2.7332	0.7222	0.3529	0.5833	0.6848	1.065	0.042	1.1326	−0.2341
V 4-octanol in n-heptane	(a) 24.33	2.3555	0.5080	0.4131	0.4553	1.0030	0.72	0.22	0.7840	0.0126
	(b) 9.25	2.4506	0.4750	0.5163	0.5372	0.895	0.716	0.9254	−0.0654	
	(c) 3.00	2.8924	0.7813	0.3197	0.6210	0.5900	0.99	0.052	1.0218	−0.0850
VI 2-octanol in n-heptane	(a) 24.33	2.7964	0.4507	0.3967	0.4257	1.3507	0.67	0.208	0.7223	0.0764
	(b) 9.25	2.8925	0.4292	0.3795	0.4125	1.4780	0.895	0.214	0.9850	−0.3026
	(c) 3.00	3.0198	0.6201	0.3658	0.5361	0.9672	1.04	0.102	1.0810	−0.1813

Table 3—Estimated intercept and slope of $K_{ij} - \omega_i$ equation, dimensionless parameters b_2, b_1 (eq. (16)), estimated dipole moments μ_2, μ_1 (eq. (15)), μ_{theo} from bond angles and bond moments together with μ_1 from $\mu_1 = \mu_2(c_1/c_2)^{1/2}$ in Debye

System with Sl. No	Mol. Wt.	Frequency GHz	Intercept & slope of $K_{ij} - \omega_i$ equation		Dimensionless parameter		Estimated dipole moments (in Debye)		μ_{theo} in D	Estimated μ_1 in D from $\mu_1 = \mu_2(c_1/c_2)^{1/2}$
			$\alpha \times 10^{-10}$	$\beta \times 10^{-10}$	b_2	b_1	μ_2	μ_1		
I 2-methyl-3-heptanol in n-heptane	130 gm	(a) 24.33	2.3632	0.6974	0.0455	0.7885	4.80	1.15	2.65	2.65
		(b) 9.25	0.8998	0.3126	0.1075	0.9463	3.39	1.14	1.76	2.44
		(c) 3.00	0.2911	0.1224	0.3439	0.9897	2.08	1.23		2.20
II 3-methyl-3-heptanol in n-heptane	130 gm	(a) 24.33	2.3630	0.7490	0.1689	0.8564	2.58	1.15		1.98
		(b) 9.25	0.8959	0.3554	0.1363	0.9395	3.21	1.22	1.76	2.43
		(c) 3.00	0.2910	0.1130	0.3423	0.9867	2.18	1.26		2.26
III 4-methyl-3-heptanol in n-heptane	130 gm	(a) 24.33	2.3635	0.7213	0.0923	0.7963	4.17	1.17		2.49
		(b) 9.25	0.8984	0.3278	0.1273	0.9436	3.19	1.17	1.76	2.39
		(c) 3.00	0.2911	0.1283	0.2837	0.9843	2.35	1.26		2.31
IV 5-methyl-3-heptanol in n-heptane	130 gm	(a) 24.33	2.3646	0.6415	0.1187	0.9396	2.85	1.01		2.09
		(b) 9.25	0.9021	0.2771	0.0975	0.9436	3.35	1.08	1.76	2.35
		(c) 3.00	0.2922	0.1138	0.2157	0.9849	2.54	1.19		2.34
V 4-octanol in n-heptane	130 gm	(a) 24.33	2.3561	0.6492	0.0903	0.9169	3.29	1.03		2.22
		(b) 9.25	0.8965	0.2618	0.1396	0.9770	2.72	1.03	1.08	2.20
		(c) 3.00	0.2919	0.1044	0.2799	0.9922	2.13	1.13		2.19
VI 2-octanol in n-heptane	130 gm	(a) 24.33	2.3533	0.6572	0.0428	0.9230	4.80	1.03		2.69
		(b) 9.25	0.8980	0.2753	0.0538	0.9190	5.67	1.09	1.08	3.00
		(c) 3.00	0.2897	0.1221	0.0487	0.9787	3.88	1.23		2.89

Fig. 1—Plot of $(\varepsilon_{\infty ij} - \varepsilon'_{ij})/(\varepsilon'_{ij} - \varepsilon_{\omega ij})$ against $\varepsilon''_{ij}/(\varepsilon'_{ij} - \varepsilon_{\omega ij})$ of some isomeric octyl alcohols in n-heptane at 25°C. Curves of I (a), I (b), I (c) for 2-methyl-3-heptanol at 24.33, 9.25 and 3.00 GHz. (○, △, □). Curves of II (a), II (b), II (c) for 3-methyl-3-heptanol at 24.33, 9.25 and 3.00 GHz (●, ▲, ■). Curves of III (a), III (b), III (c) for 4-methyl-3-heptanol at 24.33, 9.25 and 3.00 GHz (◇, ◬, ◫). Curves of IV(a), IV (b), IV (c) for 5-methyl-3-heptanol at 24.33, 9.25, 3.00 GHz (◆, ◭, ◨). Curves of V (a), V (b), V (c) for 4-octanol at 24.33, 9.25 and 3.00 GHz (⊖, ▽, ⊘). Curves of VI (a), VI (b), VI (c) for 2-octanol at 24.33, 9.25 and 3.00 GHz (◉, ▼, ⊗).

Fig. 2—Plot of $(\varepsilon_{\infty ij} - \varepsilon'_{ij})/(\varepsilon_{\omega ij} - \varepsilon'_{ij})$ against weight fraction ω_i of some isomeric octyl alcohols in n-heptane at 25°C. Curves of I (a), I (b), I (c) for 2-methyl-3-heptanol at 24.33, 9.25 and 3.00 GHz. (○, △, □). Curves of II (a), II (b), II (c) for 3-methyl-3-heptanol at 24.33, 9.25 and 3.00 GHz (●, ▲, ■). Curves of III (a), III (b), III (c) for 4-methyl-3-heptanol at 24.33, 9.25 and 3.00 GHz (◇, ◬, ◫). Curves of IV(a), IV (b), IV (c) for 5-methyl-3-heptanol at 24.33, 9.25, 3.00 GHz (◆, ◭, ◨). Curves of V (a), V (b), V (c) for 4-octanol at 24.33, 9.25 and 3.00 GHz (⊖, ▽, ⊘). Curves of VI (a), VI (b), VI (c) for 2-octanol at 24.33, 9.25 and 3.00 GHz (◉, ▼, ⊗).

Fig. 3—Plot of $\varepsilon''_{ij}/(\varepsilon_{\omega ij} - \varepsilon_{\infty ij})$ against weight fraction ω_i of some isomeric octyl alcohols in n-heptane at 25°C. Curves of I (a), I (b), I (c) for 2-methyl-3-heptanol at 24.33, 9.25 and 3.00 GHz (◇, ◬, □). Curves of II (a), II (b), II (c) for 3-methyl-3-heptanol at 24.33, 9.25 and 3.00 GHz (●, ▲, ■). Curves of III (a), III (b), III (c) for 4-methyl-3-heptanol at 24.33, 9.25 and 3.00 GHz (◇, ◬, ◫). Curves of IV(a), IV (b), IV (c) for 5-methyl-3-heptanol at 24.33, 9.25, 3.00 GHz (◆, ◭, ◨). Curves of V (a), V (b), V (c) for 4-octanol at 24.33, 9.25 and 3.00 GHz (⊖, ▽, ⊘). Curves of VI (a), VI (b), VI (c) for 2-octanol at 24.33, 9.25 and 3.00 GHz (◉, ▼, ⊗).

Fig. 4—Conformations of some isomeric octyl alcohols

1 Introduction

The dielectric relaxation of a polar-nonpolar liquid mixture is a very convenient and useful tool in ascertaining the shape, size and structure of a polar molecule[1]. The process is generally involved with the estimation of dipole moment μ in terms of the relaxation time τ for a polar molecule in a non-polar solvent under different high frequency (*hf*) electric field of Giga hertz (GHz) range at a fixed or different temperature. There exist several methods[2] to estimate τ of a polar liquid in a non-polar solvent. They offer a deep insight into the intrinsic properties of a polar molecule because of the absence of dipole-dipole interactions in polar-nonpolar liquid mixtures.

Highly non-spherical polar molecules, on the other hand, possess more than one τ in the electric field of GHz range for the rotations of different substituent groups attached to the parent molecule and the whole molecule itself. Budo[3], however, proposed that complex dielectric constant ε^* of a polar liquid may be represented as the sum of a number of non-interacting Debye type dispersions each with a characteristic τ. The method was then made simpler by Bergmann *et al.*[4] by assuming that the dielectric relaxation is the sum of two Debye type dispersions characterised by the intramolecular and molecular τ_1 and τ_2 respectively. The corresponding relative contributions c_1 and c_2 towards dielectric relaxations could then be estimated. They used a graphical analysis which consists of plotting normalised values of $(\varepsilon' - \varepsilon_\infty)/(\varepsilon_0 - \varepsilon_\infty)$ against $\varepsilon''/(\varepsilon_0 - \varepsilon_\infty)$ on a complex plane in terms of the measured real ε', imaginary ε'' parts of ε^*, static dielectric constant ε_0 and high frequency dielectric constant ε_∞ of a polar liquid for different frequencies of the electric field. A number of chords were then drawn through the points on the curve until a set of parameters was found out in consistency with all the experimental points. Bhattacharyya *et al.*[5] subsequently modified the above procedure to get τ_1, τ_2 and c_1, c_2 different frequencies of the electric field.

A procedure was devised[6] to get τ_1 and τ_2 from the slope and intercept of a derived straight line equation involved with the single frequency measurements of the dielectric relaxation parameters like $\varepsilon_{\infty ij}$, $\varepsilon_{\infty ij}$, ε'_{ij} and ε''_{ij} for different weight fractions ω_j's of a polar solute (j) in a non-polar solvent (i) at a given temperature. The technique had already been applied on disubstituted benzenes and anilines[6] at 9.945 GHz electric field as well as mono-substituted anilines[7] at 22.06, 3.86, 2.02 GHz electric fields respectively. All these investigations reveal that they often showed the double relaxation behaviour at certain frequency of hf electric field.

The aliphatic alcohols are long straight chain, hydrogen bonded polymer type molecules having possibility of their bending, twisting and rotation under *hf* electric field each with a characteristic τ, besides the average macroscopic distribution of τ. The alcohols have high dipole moments owing to their strong intermolecular forces exerted by them like polymers in solution. Onsager's equation may be a better choice for such associative liquids, but it is not so simple like Debye's equation because of the presence of quadratic term ε^*_{ij}. The relaxation behaviour of aliphatic alcohols is very interesting because they show more than two τ's in pure state, but for a polar-nonpolar liquid mixture *hf* process becomes increasingly important on dilution[8,9]. An extensive study to detect the frequency dependence of double relaxation behaviour of four long chain normal aliphatic alcohols like 1-butanol, 1-hexanol, 1-decanol in solvent n-heptane[10] including methanol and ethanol at 9.84 GHz in benzene[11,12] at 25°C was already made[13]. All the alcohols showed τ_1 and τ_2 at all frequencies of the electric field except methanol which is a simple molecule to possess the expected τ_2 only.

The method was applied on six isomeric octyl alcohols like 2-methyl-3-heptanol, 3-methyl-3-heptanol, 4-methyl-3-heptanol, 5-methyl-3-heptanol, 4-octanol and 2-octanol at 24.33, 9.25 and 3.00 GHz electric fields, as reported in Tables 1-3 respectively, because of the availability of ε'_{ij}, ε''_{ij}, $\varepsilon_{\infty ij}$ and $\varepsilon_{\infty ij}$ measured by Crossley *et al.*[14] in n-heptane at 25°C. The straight line equations between $(\varepsilon'_{\omega_j} - \varepsilon'_{ij})/(\varepsilon'_{ij} - \varepsilon_{\infty ij})$ and $\varepsilon''_{ij}/(\varepsilon'_{ij} - \varepsilon_{\infty ij})$ for all the octyl alcohols at different ω_j's are linear as shown in Fig. 1 only to establish the applicability of Debye model in such isomeric alcohols like normal alcohols[13] once again. Moreover, all the long chain octyl alcohols are structural isomers with the molecular formulae $C_8H_{18}O$ having greater number of C-atoms in their structures. They are, therefore, expected to possess two relaxation processes at audio and radio frequencies of electric field at low temperature in pure state[14].

The paper presents the frequency dependence of τ_1 and τ_2 at all frequencies of 24.33, 9.25 and 3.00 GHz electric field for all the octyl alcohols like normal alcohols too. The measured τ_2 from the slope of the linear equation consisting of imaginary K''_{ij} and real K'_{ij} parts of the total complex *hf* conductivity K^*_{ij} and the most probable relaxation time τ_0 from $\tau_0 = \sqrt{\tau_1 \tau_2}$ are placed in Table 1 together with the estimated τ_1 and τ_2 in order to see their trends with frequency of the applied electric field. The relative contributions c_1 and c_2 towards dielectric relaxations in terms of intramolecular relaxation time τ_1 and molecular relaxation time τ_2 are then estimated as Figs 2 and 3. The estimated c_1 and c_2 are placed in Table 2.

The dipole moments μ_1 and μ_2 due to flexible parts as well as the whole molecules in terms of the estimated τ_1 and τ_2 and the slopes β of the linear variation of *hf* conductivity K_{ij} with ω_j are shown in Table 3. The slopes β and the intercepts α of the linear variation of K_{ij} with ω_j, as placed in Table 3, at each frequency for all the isomers in n-heptane are almost the same probably due to their same polarity[10]. This fact is also supported by their conformations as shown in Fig. 4. It was, therefore, very difficult to plot K_{ij} against ω_j. The computed μ_2's for most of the isomeric alcohols show larger values at 24.33 GHz and gradually decrease with lower frequencies unlike μ_1. In order to compare μ_2 and μ_1 with theoretical dipole moments μ_{theo}, a special attention is to be paid on the conformational structure of each isomer from the available bond angles and bond moments. They are shown in Fig. 4. Using the usual C–C bond moment of 0.09 D from methanol and ethanol[15] μ_{theo} for four methyl substituted octanols are found to show slightly larger values (see Fig. 4 and Table 3) than 1-heptanol[13] except the desired values for 2-octanol and 4-octanol perhaps due to bond moments of C–CH$_3$ and –O–H groups in their structures. The calculated value of μ_1 from $\mu_1 = \mu_2 / c_1 c_2$[1,2] assuming two relaxation processes are equally probable, are also placed in the last column of Table 3 with all the estimated μ's for comparison.

2 Theoretical Formulations to Estimate Relaxation Parameters

The complex dielectric constant ε^*_{ij} of a polar-nonpolar liquid mixture can be represented as the sum of a number of non-interacting Debye type dispersions in accordance with Budo's[3] relation.

$$\frac{\varepsilon^*_{ij}-\varepsilon_{\infty ij}}{\varepsilon_{oij}-\varepsilon_{\infty ij}}=\sum\frac{c_k}{1+j\omega\tau_k} \quad \ldots(1)$$

where $j=\sqrt{-1}$ is a complex number and $\Sigma c_k=1$. The term c_k is the relative contribution for the kth type of relaxation process[4]. When the ε^*_{ij} consists of two Debye type dispersions, Budo's relation reduces to Bergmann's equations[4]:

$$\frac{\varepsilon'_{ij}-\varepsilon_{\infty ij}}{\varepsilon_{oij}-\varepsilon_{\infty ij}}=\frac{c_1}{1+\omega^2\tau_1^2}+\frac{c_2}{1+\omega^2\tau_2^2} \quad \ldots(2)$$

and

$$\frac{\varepsilon''_{ij}}{\varepsilon_{oij}-\varepsilon_{\infty ij}}=c_1\frac{\omega\tau_1}{1+\omega^2\tau_1^2}+c_2\frac{\omega\tau_2}{1+\omega^2\tau_2^2} \quad \ldots(3)$$

such that $c_1+c_2=1$. Now with

$$\frac{\varepsilon'_{ij}-\varepsilon_{\infty ij}}{\varepsilon_{oij}-\varepsilon_{\infty ij}}=x, \qquad \frac{\varepsilon''_{ij}}{\varepsilon_{oij}-\varepsilon_{\infty ij}}=y$$

$\omega\tau=\alpha$ and using $a=1/1+\alpha^2$ and $b=\alpha/1+\alpha^2$ the Eqs (2) and (3) can be written as:

$$x=c_1a_1+c_2a_2 \quad \ldots(4)$$

$$y=c_1b_1+c_2b_2 \quad \ldots(5)$$

where suffixes 1 and 2 with a and b are related to τ_1 and τ_2 respectively. From Eqs (4) and (5), since $a_2-a_1\neq 0$ and $a_2>a_1$ we have

$$c_1=\frac{(xa_2-y)(1+a_1^2)}{a_2-a_1} \quad \ldots(6)$$

$$c_2=\frac{(y-xa_1)(1+a_2^2)}{a_2-a_1} \quad \ldots(7)$$

Since $c_1+c_2=1$, we get the following equation with the help of Eqs (6) and (7):

$$\frac{1-x}{y}=(a_1+a_2)-\frac{x}{y}a_1a_2$$

which on substitution of the values x, y and a yields:

$$\frac{\varepsilon_{oij}-\varepsilon'_{ij}}{\varepsilon'_{ij}-\varepsilon_{\infty ij}}=\omega(\tau_1+\tau_2)\frac{\varepsilon''_{ij}}{\varepsilon'_{ij}-\varepsilon_{\infty ij}}-\omega^2\tau_1\tau_2 \quad \ldots(8)$$

Eq. (8) is thus a straight line equation between $(\varepsilon_{oij}-\varepsilon'_{ij})/(\varepsilon'_{ij}-\varepsilon_{\infty ij})$ and $\varepsilon''_{ij}/(\varepsilon'_{ij}-\varepsilon_{\infty ij})$ with slope $\omega(\tau_1+\tau_2)$ and intercept $-\omega^2\tau_1\tau_2$ respectively where ω is the angular frequency of the applied electric field of frequency f in GHz. With the measured dielectric relaxation data of ε'_{ij}, ε''_{ij}, ε_{oij} and $\varepsilon_{\infty ij}$ for different weight fractions ω_i's of each octyl alcohol in n-heptane at 25°C under 24.33, 9.25 and 3.00 GHz electric fields[14] we get slope and intercept of Eq. (8) to yield τ_1 and τ_2 as shown in Table 1.

The relative contributions c_1 and c_2 towards the dielectric relaxation in terms of x, y and τ_1, τ_2 for each octyl alcohol are found out and placed in Table 2. The theoretical values[15] of x and y are, however, calculated from Fröhlich's Eqs:

$$x=\frac{\varepsilon'_{ij}-\varepsilon_{\infty ij}}{\varepsilon_{oij}-\varepsilon_{\infty ij}}=1-\frac{1}{A}\ln\left(\frac{e^{2A}\omega^2\tau_1^2+1}{1+\omega^2\tau_1^2}\right) \quad \ldots(9)$$

$$y=\frac{\varepsilon''_{ij}}{\varepsilon_{oij}-\varepsilon_{\infty ij}}=\frac{1}{A}[\tan^{-1}(e^A\omega\tau_1)-\tan^{-1}(\omega\tau_1)] \quad \ldots(10)$$

where A= Fröhlich parameter $=\ln(\tau_2/\tau_1)$ and τ_1 is called the small limiting relaxation time as obtained from the double relaxation method. A simple graphical extrapolation technique, on the other hand, was considered to get the values of x and y at $\omega_i\to 0$ from Figs 2 and 3 respectively. This is really in accordance with Bergmann's Eqs (2) and (3) when the once estimated τ_1 and τ_2 from Eq. (8) are substituted in the right hand sides of above Eqs (2) and (3).

The values of μ_1 and μ_2 of octyl alcohols in terms of τ_1, τ_2 and slope β of the concentration variation of the experimental *hf* conductivity K_{ij} were then estimated. The *hf* conductivity K_{ij} is, however, given by Murphy and Morgan[12]:

$$K_{ij}=\frac{\omega}{4\pi}(\varepsilon''^2_{ij}+\varepsilon'^2_{ij})^{1/2} \quad \ldots(11)$$

as a function of ω_i of polar solute. Since $\varepsilon''_{ij}\ll\varepsilon'_{ij}$ in the *hf* electric field, the term ε''_{ij} offers resistance to polarisation. Thus the real part K'_{ij} of the *hf* K^*_{ij} of a polar-nonpolar liquid mixture at TK can be written according to Smyth[16] as:

$$K'_{ij}=\frac{\mu_i^2 N\rho_{ij}F_{ij}}{3M_ikT}\left(\frac{\omega^2\tau}{1+\omega^2\tau^2}\right)\omega_i \quad \ldots(12)$$

which at $\omega_i\to 0$ yields that:

$$\left(\frac{dK'_{ij}}{d\omega_i}\right)_{\omega_i\to 0}=\frac{\mu_i^2 N\rho_iF_i}{3M_ikT}\left(\frac{\omega^2\tau}{1+\omega^2\tau^2}\right) \quad \ldots(13)$$

where M_i is the molecular weight of a polar solute, N the Avogadro number, k the Boltzmann constant, the local field $F_{ij}=1/9\,(\varepsilon_{ij}+2)^2$ (F_{ij} between $F_i=1/9\,(\varepsilon_i+2)^2$ and the density $\rho_{ij}\to\rho_i$ the density of solvent at $\omega_i\to 0$.

Again, the total *hf* conductivity $K_{ij}=(\omega/4\pi)\varepsilon''_{ij}$ can be written as:

$$K_{ij}=K_{ij\infty}+\frac{1}{\omega\tau}K''_{ij}$$

or

$$\left(\frac{dK'_{ij}}{d\omega_i}\right)_{\omega_i\to 0}=\omega\tau\left(\frac{dK'_{ij}}{d\omega_i}\right)_{\omega_i\to 0}=\omega\tau\beta \quad \ldots(14)$$

where β is the slope of $K'_{ij}-\omega_i$ curve at infinite dilution. From Eqs (13) and (14) we get:

$$\mu_i=\left[\frac{27M_ikT}{N\rho_i(\varepsilon_i+2)^2}\cdot\frac{\beta}{\omega b}\right]^{1/2} \quad \ldots(15)$$

as the dipole moment of each octyl alcohol in terms of b, where b is a dimensionless parameter given by:

$$b = \frac{1}{1+\omega^2\tau^2} \qquad \ldots(16)$$

The computed μ_1 and μ_2 together with b_1, b_2 and β of $K_{ij} - \omega_j$ equations for all the octyl alcohols are placed in Table 3.

3 Results and Discussion

The least square fitted straight line equations of $(\varepsilon_{\omega_j} - \varepsilon'_{ij})/(\varepsilon'_{ij} - \varepsilon_{\infty_j})$ against $\varepsilon''_{ij}/(\varepsilon'_{ij} - \varepsilon_{\infty_j})$ for six isomeric octyl alcohols like 2-methyl-3-heptanol, 3-methyl-3-heptanol, 4-methyl-3-heptanol, 5-methyl-3-heptanol, 4-octanol and 2-octanol in solvent n-heptane at 25°C under 24.33, 9.25 and 3.00 GHz electric field at different ω_j's of polar solutes are shown in Fig. 1 together with the experimental points on them. ω_j's are, however, calculated from the mole fractions x_i and x_j of solvent and solute with molecular weights M_i and M_j respectively according to the relation[19]:

$$\omega_j = \frac{x_j M_j}{x_i M_i + x_j M_j}$$

All the straight line equations are almost perfectly linear as evident from the correlation coefficients r lying in the range 0.9985-0.5684. The corresponding % of errors in terms of r in getting the slopes and intercepts of all the straight lines are placed in the 6th and 5th columns of Table 1. The errors are, however, large at 24.33 GHz indicating departure from the linear behaviour as evident from low values of r perhaps due to inherent uncertainty in measured data for such higher frequency which no differentiation with respect to ω_j and for

The estimated values of τ_2 and τ_1 for all the isomeric octyl alcohols from the slopes and the intercepts of straight line equations are of smaller magnitude at 24.33 GHz and increase gradually to attain maximum value at 3.00 GHz under the present investigation. This may be due to the fact that at higher frequency the rate of hydrogen bond rupture in long chain alcohols is the maximum thereby reducing τ for each rotating unit[13]. τ_2 and τ_1 are then compared with the measured τ_s from the relation:

$$K''_{ij} = K_{ij\infty} + \frac{1}{\omega\tau_s} K'_{ij}$$

and τ_0 where $\tau_0 = \sqrt{\tau_1 \tau_2}$. As evident from Table 1 although $\tau_0 > \tau_1$; τ_s agrees well with τ_1 for most of the solutes except slight disagreement at 3.00 GHz for 4-methyl-3-heptanol, 5-methyl-3-heptanol, 4-octanol and 2-octanol. This is explained on the basis of the fact that conductivity measurement may be applicable in higher frequency in yielding microscopic τ only whereas the double relaxation method offers a better understanding of molecular relaxation phenomena showing microscopic as well as macroscopic τ as observed earlier[13]. Unlike normal aliphatic alcohols, $-OH$ groups are screened by the substituted $-CH_3$ group, broad dispersion characterised by relatively short relaxation times were thus observed[14]. The respective positions of $-CH_3$ and $-OH$ groups also greatly affect the static dielectric constant, correlation factor, their temperature dependence and type of hydrogen bonding in them.

The relative contributions c_1 and c_2 towards dielectric relaxations are also estimated in terms of $(\varepsilon'_{ij} - \varepsilon_{\infty_j})/(\varepsilon_{\omega_j} - \varepsilon_{\infty_j})$, $\varepsilon''_{ij}/(\varepsilon_{\omega_j} - \varepsilon_{\infty_j})$ with the estimated τ_1, τ_2 as shown in Table 2 by Fröhlich and graphical methods. $x = (\varepsilon'_{ij} - \varepsilon_{\infty_j})/(\varepsilon_{\omega_j} - \varepsilon_{\infty_j})$ and $y = \varepsilon''_{ij}/(\varepsilon_{\omega_j} - \varepsilon_{\infty_j})$ were, however, evaluated from Fröhlich's Eqs (9) and (10) in the first case. The actual variations of $(\varepsilon'_{ij} - \varepsilon_{\infty_j})/(\varepsilon_{\omega_j} - \varepsilon_{\infty_j})$ and $\varepsilon''_{ij}/(\varepsilon_{\omega_j} - \varepsilon_{\infty_j})$ with ω_j are concave and convex as found in Eqs. 2 and 3 in accordance with Hermann Eqs (2) and (3), except 5-methyl-3-heptanol at 24.33 GHz whose $(\varepsilon'_{ij} - \varepsilon_{\infty_j})/(\varepsilon_{\omega_j} - \varepsilon_{\infty_j})$ curve is convex in nature due to its non-accurate ε_{ω_j} and ε_{∞_j} values like ethanol as observed earlier[13]. x and y were also obtained graphically from Figs (2) and (3) in the limit $\omega_j = 0$.

In Fröhlich method c_1 and c_2 are all positive as evident from 6th and 7th columns of Table 2 with $c_2 > c_1$. In graphical method $c_1 > c_2$ with negative c_2 for most of the systems probably due to inertia of the flexible parts under *hf* electric field, as shown in 10th and 11th columns of same Table 2. c_2 are, however, positive for the systems 5-methyl-3-heptanol, 4-octanol and 2-octanol at 24.33 GHz as well as 3-methyl-3-heptanol at 9.25 GHz. Both the methods in most cases, yield $|c_1 + c_2| \geq 1$, signifying thus the possibility of occurrence of more than two relaxation processes in them[13].

The dipole moments μ_1 and μ_2 of all the isomeric alcohols due to their flexible parts and the whole molecules are estimated in terms of dimensionless parameters b_1, b_2 and slope β of $K_{ij} - \omega_j$ curves by using Eq. (15). The variations of K_{ij} with ω_j are all linear having almost the same intercepts α and slopes β at each frequency of electric field. It was, therefore, difficult to plot them as they almost coincide. The values of α and β of K_{ij}s are little different and comparatively large at 24.33 GHz (Table 3). This sort of behaviour is perhaps due to same dipole moments[16] possessed by the polar molecules under investigation as evident from μ_2 and μ_1 placed in 7th and 8th columns of Table 3. μ_2 for most of the polar molecules shows values at 24.33 GHz and decrease gradually with lower frequencies except 3-methyl-3-heptanol, 5-methyl-3-heptanol and 2-octanol whose μ_2's are found greater at 9.25 GHz electric field. This type of behaviour may be explained on the basis of the fact that such alcohols behaving almost like polymer molecules have long chain of C-atoms and tend to break up in a non-polar solvent in order to reduce or even eliminate the absorption under *hf* electric field. The proportion of smaller molecular species having comparatively small number of C-atoms and their corresponding absorption will increase thereby[16]. The values of μ_1's on the other hand, are almost constant exhibiting a trend to increase a little towards low frequency. They are finally compared with bond moment of 1.5D of $-O-H$ group making an angle 105° with the $-C-C-$ bond axis according to the preferred conformations of all the isomers as sketched in Fig. 4. This confirms that μ_1 arises due to the rotation of $-OH$ group around $C-O$ bond in the long chain alcohols studied so far[13]. The slight difference is due to difference in steric hindrances as a result of structural configurations at different frequencies. μ_1 also estimated from $\mu_1 = \mu_2 \cdot c_1/c_2$[13] assuming two relaxation processes are equally probable as shown in the last column of Table 3. The other bond moments 0.77, 0.3, 1.0 and 0.00 D for $C-H_3$, $C-H$, $C-O$ and $C-C$ bonds are also involved to justify then

conformations. The resultant of all these bonds by vector addition method yields μ_{theo} of 1.76 D and 1.08 D for four methyl substituted heptanols and two octanols respectively. The derived result should decrease with increase in the number of C-atoms and μ_{theo} for them should be less then that for 1-heptanol[13]. But for μ_{theo} in Fig. 4 three isomers are only displayed due to typical positions of $=CH_3$ and $-OH$ groups. This may probably be the reason of having slightly larger values of μ_{theo} from 1-heptanol as observed earlier[13].

4 Conclusion

The methodology so far advanced for the double broad dispersions of the polar-nonpolar liquid mixtures based on Debye's model seems to be much simpler, straightforward and significant one to detect the very existence of τ_1 and τ_2 of a polar liquid in a nonpolar solvent. The correlation coefficients between the desired dielectric relaxation parameters involved in the derived equations of Eq. (8) could, however, be estimated to find out % of errors entered in the estimated τ_1 and τ_2 of a polar liquid, because τ is claimed to be accurate within ± 10%. The isomeric octyl alcohols like normal aliphatic alcohols are found to yield both τ_1 and τ_2 at all frequencies of the electric field of GHz range. The corresponding μ_1 and μ_2 can then be estimated from Eq. (15) in terms of b_1 and b_2 which are, however, involved with τ_1 and τ_2 as estimated, to arrive at their preferred conformations as shown in Fig. 4.

Acknowledgement

The authors are thankful to Mr A R Sit, B E (Electrical) for his interest in this work.

References

1 Saha U & Acharyya S, *Indian J Pure & Appl Phys*, 32 (1994) 346.

2 Gopalakrishna K V, *Trans Faraday Soc*, 53 (1957) 767.

3 Budo A, *Phys Z*, 39 (1938) 706.

4 Bergmann K, Roberti D M & Symth C P, *J Phys Chem*, 64 (1960) 665.

5 Bhattacharyya J, Hasan A, Roy S B & Kastha G S, *J Phys Soc Japan*, 28 (1970) 204.

6 Saha U, Sit S K, Basak R C & Acharyya S, *J Phys E Appl Phys*, 27 (1994) 596.

7 Sit S K, Basak R C, Saha U Acharyya S, *J Phys D: Appl Phys*, 27 (1994) 2194.

8 Denney D J & Ring J W, *J Chem Phys*, 39 (1963) 1268.

9 Moriamez M & Lebrun A, *Arch Sci (Geneva)*, 13 (1960) 40.

10 Glasser L, Crossley J & Symth C P, *J Chem Phys*, 57 (1972) 3977.

11 Purohit H D & Sharma H S, *Indian J Pure & Appl Phys*, 8 (1970) 10.

12 Ghosh A K, PhD Dissertation (NBU), 1981.

13 Sit S K & Acharyya S, *Indian J Phys B*, 70 (1996) 19.

14 Crossley J, Glasser L & Smyth C P, *J Chem Phys*, 55 (1971) 2197.

15 Fröhlich H, *Theory of Dielectrics* (Oxford University Press, Oxford) 1949.

16 Chatterjee A K, Saha U, Nandi N, Basak R C & Acharyya S, *Indian J Phys*, 66B (1992) 291.

17 Murphy E J & Morgan S O, *Bell Syst Techn J*, 18 (1939) 502.

18 Symth C P, *Dielectric behaviour and structure*, (McGraw-Hill, New York) 1955.

19 Ghosh A K & Acharyya S, *Indian J Phys*, 52B (1978) 129.

SADHANA P-8388

Indian J. Phys. 71B (4), (1997)

NOTE

IJP
– an international journal

Structural and associational aspects of binary and single polar liquids in non polar solvent under high frequency electric field

S K Sit, N Ghosh, U Saha and S Acharyya
Department of Physics, Raiganj College, Raiganj, Uttar Dinajpur-733 134, West Bengal, India

Received 17 April 1996, accepted 19 December 1996

Abstract : The structural and associational aspects of binary (*jk*) polar mixtures of N,N dimethyl formamide (DMF) and dimethyl sulphoxide (DMSO) together with a single (*j* or *k*) N, N diethyl formamide (DEF) and DMSO in nonpolar solvents (*i*) are studied in terms of their high frequency (*hf*) conductivities. The relaxation times τs and dipole moments μ's of the solutes under Giga hertz electric field at various temperatures are estimated from the measured real and imaginary parts of *hf* dielectric constants at different weight fractions of polar solutes. The variation of τ_{jk}'s with mole fractions x_k's of DMSO in DMF and C_6H_6 reveals the probable solute-solute molecular association around $x_k = 0.5$ of DMSO. The solute-solvent molecular association begins at and around 50 mole% DMSO in DMF and continues upto 100 mole% DMSO. The concentration and temperature variations of τ_{jk} of these protic liquids are in accord with the information of variation of τ_{jk} of *jk* polar mixtures with x_k's of DMSO. Thermodynamic energy parameters are also obtained from Eyring's rate process equation with the estimated τs to support the molecular associations. The slight disagreement between the theoretical dipole moments μ_{theo}'s from the bond angles and bond moments is noticed with the measured μ's in terms of slopes of concentration variation of *hf* conductivity curves at infinite dilutions and τs. This indicates the temperature dependence of mesomeric and inductive moments of different substituent groups of the molecules.

Keywords : Dipole moment, relaxation time, associational aspects

PACS Nos. : 31.70.Dk, 33.15.Kr

The dielectric relaxation mechanism of a polar-nonpolar liquid mixture under the microwave electric field is of special interest [1,2] for its inherent ability to predict the associational aspects of polar solutes in nonpolar solvents. An investigation was, however, made on ternary solution of binary polar liquids in which both or even one of them are protic [2,3] to study various types of weak molecular associations by polar liquids in

nonpolar solvents. We are, therefore, tempted further to consider more mixtures of binary protic polar liquids like N,N dimethyl formamide (DMF) and dimethyl sulphoxide (DMSO) together with a single protic polar liquid like N,N diethyl formamide (DEF) and DMSO in C_6H_6 and CCl_4 [4–6] respectively. DMSO, DMF and DEF are very interesting liquids for their wide application in medicine and industry. They also act as building blocks of proteins and enzymes. The concentration variation of the measured real ε'_{ijk}, ε'_{ij} or ε'_{ik} and imaginary ε''_{ijk}, ε''_{ij} or ε''_{ik} parts of *hf* complex dielectric constants ε^*_{ijk}, ε^*_{ij} or ε^*_{ik} of *jk*, *j* or *k* polar solutes in nonpolar solvents are used to detect the weak molecular interactions among the molecules [7] at a single or different temperatures under nearly 3 cm wavelength electric field. The t_{jk} of *jk* polar mixtures as well as τ_j's or τ_k's of *j* or *k* polar solutes in a nonpolar solvent were estimated from :

$$K''_{ijk} = K_{\infty ijk} + \frac{1}{\omega\tau_{jk}} K'_{ijk}, \tag{1}$$

where $K''_{ijk} = \frac{\omega}{4\pi}\varepsilon'_{ijk}$ and $K'_{ijk} = \frac{\omega}{4\pi}\varepsilon''_{ijk}$ are the imaginary and real parts of complex *hf* conductivity K^*_{ijk} [8]. The other terms carry usual significance as presented elsewhere [2]. The τ_{jk}'s are estimated from the slopes of the linear variations of K''_{ijk} against K'_{ijk} of eq. (1). The linearity of eq. (1) is tested by the correlation coefficients and the errors involved in the measurement of τ's are within 5%. τ_{jk}'s are then plotted with different mole fractions x_k's of DMSO at various experimental temperatures as shown in Figure 1.

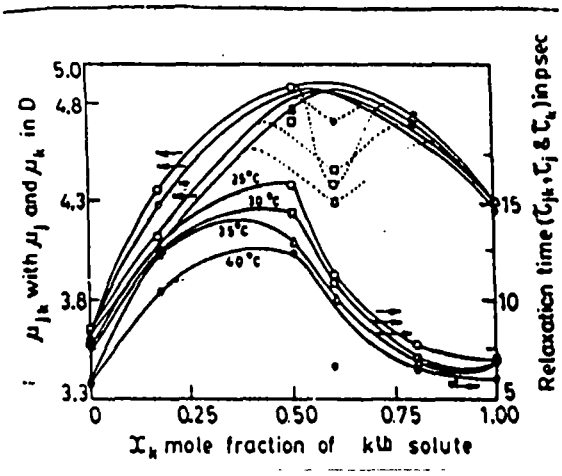

Figure 1. Variation of t_{jk} and μ_{jk} of DMF–DMSO mixture in C_6H_6 against mole fraction x_k of DMSO with t_j and t_k and μ_j and μ_k of DMF and DMSO respectively at different temperatures : (○) at 25°C, (□) at 30°C, (△) at 35°C and (●) at 40°C.

The formation of dimer is responsible for the gradual rise of τ_{jk} from τ_j of DMF at $x_k = 0$ to $x_k = 0.5$ and then its rapid fall to τ_k due to rupture of dimerisation and self association [4]. The estimated τ's are slightly larger than those of Gopalakrishna's method [9]. But τ's from conductivity measurement are much more reliable as they provide microscopic relaxation times [10].

The energy parameters due to dielectric relaxation process were then obtained in terms of measured τ from the rate process equation of Eyring *et al* [11]:

$$\tau_S = \frac{A}{T} e^{\Delta F_\tau / RT},$$

or
$$\ln(\tau_S T) = \ln A' + \frac{\Delta H_\tau}{RT}, \qquad (2)$$

where $A' = Ae^{-\Delta S_\tau / R}$.

Eq. (2) is a straight line of $\ln(\tau_s T)$ against $\frac{1}{T}$ as seen in Figure 2 having intercepts and slopes to yield the entropy of activation ΔS_τ, enthalpy of activation ΔH_τ and free energy of activation ΔF_τ due to dielectric relaxation. The values of $\gamma \left(= \frac{\Delta H_\tau}{\Delta H_\eta} \right)$ for all the liquids

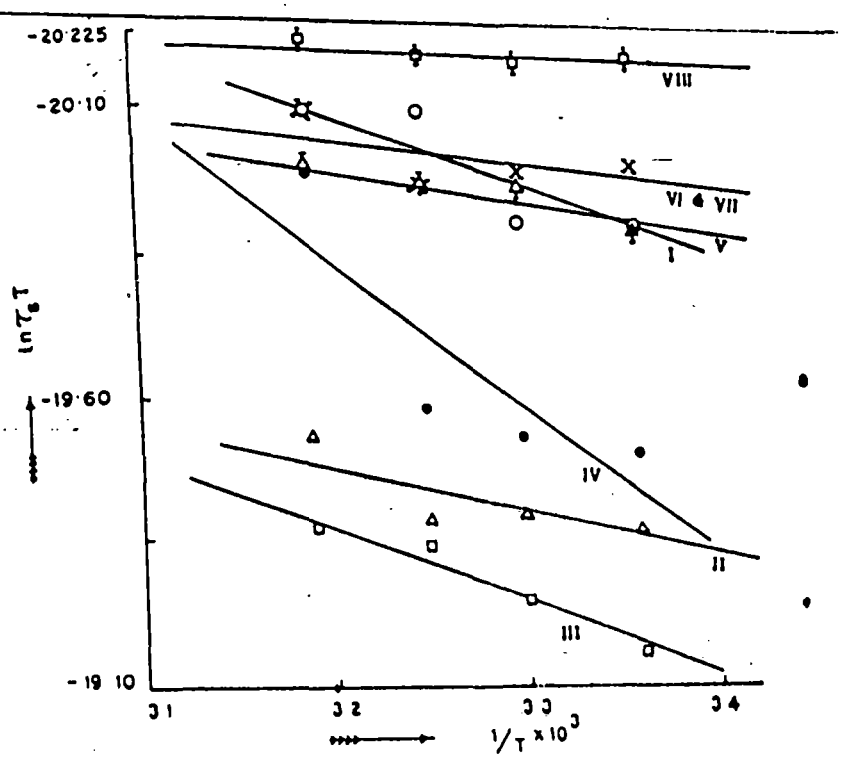

Figure 2. Variation of $\ln(\tau_s T)$ against $\frac{1}{T}$ of binary and single polar solutes in nonpolar solvent. I–DMF + 0 mole% DMSO in C_6H_6 (O), II–DMF +17 mole% DMSO in C_6H_6 (Δ), III–DMF + 50 mole% DMSO in C_6H_6 (□), IV–DMF + 60 mole% DMSO in C_6H_6 (•), V–DMF + 80 mole% DMSO in C_6H_6 (Δ), VI–DMF +100 mole% DMSO in C_6H_6 (X), VII–DMSO in C_6H_6, (X), VIII–DMSO in CCl_4 (□).

except DMSO in CCl_4 are greater than 0.55, as obtained from the slope of the linear relation of $\ln(\tau_s T)$ with $\ln h$ indicating them as solid phase rotators in solvent environment. h is the

coefficient of viscosity of solvent. ΔH_τ due to viscous flow of the solvent is obtained from slope of $\ln(\tau, T)$ against $\frac{1}{T}$ and known g. Again, ΔH_η are greater than ΔH_τ for all the mixtures except 0, 50 and 60 mole% DMSO in DMF and C_6H_6. The difference in ΔH_τ and ΔH_η is due to the involvement of various types of bondings which are either formed or broken to some extent, depending on the temperature and concentration of the system. The negative values of ΔS_τ's for all the systems except 0 and 60 mole% DMSO in DMF and C_6H_6 indicate the existence of cooperative orientation of the molecules arising out of steric forces to yield more ordered states while the reverse is true for positive ΔS_τ's. Although, ΔF_τ's in all cases are almost constant at all temperatures, they increase with x_k of DMSO from $x_k = 0.0$ to $x_k = 0.5$ and then decrease gradually to $x_k = 1.0$ signifying the maximum dimerisation of DMF–DMSO mixture around $x_k = 0.5$. The formation of dimer causes larger molecular size and hence, the energy needed for rotation in the relaxation process is higher.

The *hf* conductivity K_{ijk} as a function of weight fraction W_{jk} is given by

$$K_{ijk} = \frac{\omega}{4\pi}\left(\varepsilon'_{ijk} + \varepsilon''_{ijk}\right)^{\frac{1}{2}}. \tag{3}$$

Since $\varepsilon'_{ijk} \gg \varepsilon''_{ijk}$ eq. (1) can be written as

$$K_{ijk} = K_{\infty ijk} + \frac{1}{\omega\tau_{jk}} K'_{ijk},$$

$$\left(\frac{dK'_{ijk}}{dW_{jk}}\right)_{W_{jk}\to 0} = \omega\tau_{jk}\beta. \tag{4}$$

Here, β's are the slopes of $K_{ijk} - W_{jk}$, $K_{ij} - W_j$ of $K_{ik} - W_k$ curves respectively, which are linear with almost identical intercepts probably due to same polarity of the molecules [2]. The real part of *hf* conductivity, K'_{ijk} is again related to W_{jk} of *jk* polar solute dissolved in a nonpolar solvent (i) at temperature T°K [12] as

$$K'_{ijk} = \frac{\mu_{jk}^2 N P_{ijk} F_{ijk}}{3M_{jk}kT}\left(\frac{\omega^2\tau_{jk}}{1+\omega^2\tau_{jk}^2}\right)W_{jk}. \tag{5}$$

Differentiating eq. (5) with respect to W_{jk} and comparing the result at $W_{jk} \to 0$ to eq. (4), one obtains the following relation

$$\mu_{jk} = \left[\frac{27M_{jk}kT}{NP_i(\varepsilon_i+2)^2}\cdot\frac{\beta}{\omega b}\right]^{1/2} \tag{6}$$

to estimate μ_{jk}, μ_j or μ_k of the respective solutes. b is a dimensionless parameter in terms of estimated τ_{jk}, τ_j or τ_k given by :

$$b = \frac{1}{1+\omega^2\tau_{jk}^2}. \tag{7}$$

The other terms in eq. (6) carry usual significance [2]. All the μ's are then plotted against different x_k's of DMSO at each temperature as shown in Figure 1. It shows the gradual rise of μ_{jk} in the range $0 < x_k \leq 0.5$. It then decreases slowly in order to exhibit the convex nature of each curve with an abnormally low value of μ_{jk} around $x_k = 0.6$. This sort of behaviours of $\mu_{jk} - x_k$ curves (Figure 1) is explained by the fact that dimers are being formed from $x_k \geq 0$ to $x_k = 0.6$ causing increase of μ. The rupture of dimerisation *i.e.* self association occurs in higher concentrations in the range $0.6 \leq x_k < 1.0$ to yield lower values of μ's. But around $x_k = 0.6$, all μ_{jk}'s are minimum indicating the possible occurrence of double relaxation phenomena in such mixtures to be studied later on. μ_{jk} together with μ_j and μ_k for each mixture of a fixed concentration are shown graphically only to observe their temperature dependence like $\mu_{jk} = a + bt + ct^2$ with coefficients a, b and c as seen in Figure 3. The variation is concave with maximum depression at 17 mole% DMSO in DMF mixture. The depression gradually decreases upto $x_k = 0.6$ of DMSO in DMF and C_6H_6 probably due to solute-solute molecular association in the range $0 < x_k < 0.6$. The maximum

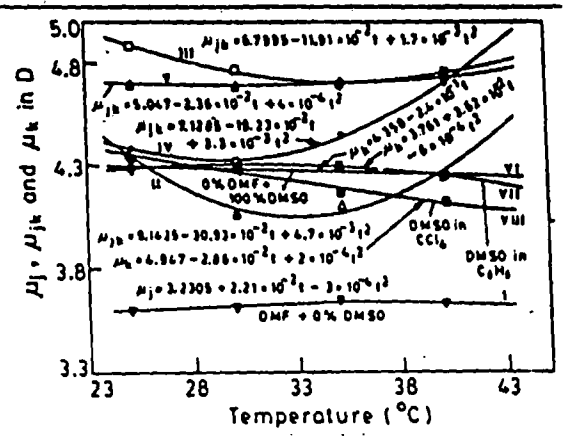

Figure 3. Variation of μ_j, μ_{jk} and μ_k of binary and single polar solutes in nonpolar solvent with temperature t in °C.
I–DMF + 0 mole% DMSO in C_6H_6 (▼), II–DMF + 17 mole% DMSO in C_6H_6 (Δ), III–DMF + 50 mole% DMSO in C_6H_6 (□), IV–DMF + 60 mole% DMSO in C_6H_6 (●), V–DMF + 80 mole% DMSO in C_6H_6 (▼), VI–DMF + 100 mole% DMSO in C_6H_6 (▽), VII–DMSO in C_6H_6, (X), VIII–DMSO in CCl_4 (■).

dimerisation is however, inferred from low μ's because of the larger molecular sizes as confirmed by high values of $\tau_s T/\eta^\gamma$ (being proportional to volume of the rotating unit) for 60 mole% DMSO in DMF and C_6H_6. As temperature increases the dipole-dipole interaction is weakened and the absorption of *hf* electric energy increases resulting in the rupture of dimer to yield high μ's for smaller molecular species [10]. The slight convex nature of curves for 0 mole% DMSO in DMF and C_6H_6 and DMSO in C_6H_6, along with almost straight line variation of 100 mole% DMSO in DMF and C_6H_6 and DMSO in CCl_4 (Figure 3) is probably due to solute-solvent molecular interaction of either DMF with C_6H_6 or DMSO with C_6H_6 and CCl_4 respectively as illustrated in Figure 4. The associations of DMF, DEF and DMSO in C_6H_6 can arise due to interactions of fractional positive charges of N and S atoms of the molecules with the π delocalised electron cloud of C_6H_6 ring as seen in Figure 4(i), (iii) and (iia) respectively. Again, one of C–Cl dipoles of CCl_4, owing to more –ve charge on Cl atom, interacts with the fractional

+ve charge of S-atom of DMSO (Figure 4 (iib)). The μ_{theo} = 4.55 D of DMSO is however, computed from available bond moments of 2.350 D and 1.55 D for S ← CH_3 and O ⇐ S respectively, assuming the molecule to be planar one. The major contributions to μ_{theo} for DMF and DEF are due to 0.64 D and 0.78 D for N ← CH_3 and N ← C_2H_5 since the other common bond moments in them are the same with values of 0.3 D, 0.45 D and 3.10 D for C ← H, C ← N and C ⇐ O respectively. Figure 4 (iv) however, shows a certain angle ϕ (= 106°) between monomeric μ's of DMF and DMSO to have μ_{theo} = 4.77 D of dimer below x_A = 0.6.

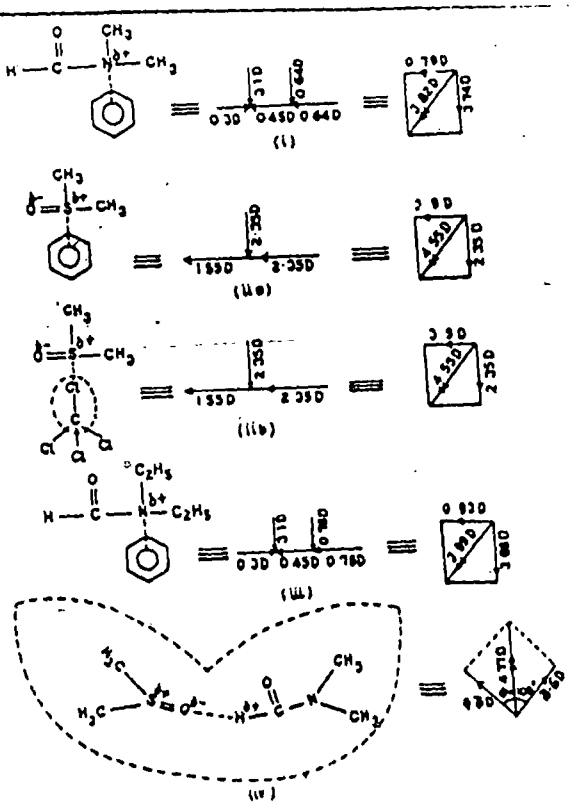

Figure 4. Conformational structures along with solute-solvent and solute-solute interaction of molecules. (i) –DMF in C_6H_6, (iia) –DMSO in C_6H_6, (iib) –DMSO in CCl_4 (iii) –DEF in C_6H_6, (iv) –DMSO–DMF dimer.

The slight deviations of the μ's from the μ_{theo}'s occur probably due to the presence of inductive and mesomeric moments of such molecules. This is also observed elsewhere [13]. The corrected μ's obtained from the reduced bond moments of the substituent groups by factors μ_{cal}/μ_{theo} establish the above facts at different temperatures, too. Thus the dielectric relaxation parameters from *hf* conductivity measurements offer a useful tool to arrive at the structural and associational aspects of the nonspherical polar liquids.

Acknowledgments

The authors are thankful to Sri R C Basak for his interest in this work.

References

[1] C R Acharyya, A K Chatterjee, P K Sanyal and S Acharyya *Indian J. Pure Appl. Phys.* **24** 234 (1986)
[2] A K Chatterjee, U Saha, N Nandi, R C Basak and S Acharyya *Indian J. Phys.* **66B** 291 (1992)
[3] U Saha and S Acharyya *Indian J. Pure Appl. Phys.* **31** 181 (1993)
[4] A Sharma, D R Sharma and M S Chauhan *Indian J. Pure Appl. Phys.* **31** 841 (1993)
[5] A Sharma and D R Sharma *J. Phys. Soc. Jpn.* **61** 1049 (1992)
[6] A R Saksena *Indian J. Pure Appl. Phys.* **16** 1079 (1978)
[7] U Saha and S Acharyya *Indian J. Pure Appl. Phys.* **32** 346 (1994)
[8] F J Murphy and S O Morgan *Bull. Syst. Tech. J.* **18** 502 (1939)
[9] K V Gopalakrishna *Trans. Faraday Soc.* **53** 767 (1957)
[10] S K Sit and S Acharyya *Indian J. Phys.* **70B** 19 (1996)
[11] H Eyring, S Glasstone and K J Laidler *The Theory of Rate Process* (New York : McGraw-Hill) (1941)
[12] C P Smyth *Dielectric Behaviour and Structure* (New York : McGraw Hill) (1955)
[13] R C Basak, S K Sit, N Nandi and S Acharyya *Indian J. Phys.* **70B** 37 (1996)

Author : Pl check the proof critically, specially the mathematics.
K. K Dalta.
23. 6. 97.